ISSN 0386-5878

Technical Memorandum of PWRI No. 1908

PROCEEDINGS OF THE SYMPOSIUM ON EROSION CONTROL IN VOLCANIC AREAS

July 6—9, 1982
at Seattle and Vancouver, Washington

February 1983
Sabo(Erosion Control) Division
Erosion Control Department
Public Works Research Institute
Ministry of Construction
Government of Japan

Copyright © 1983 by P.W.R.I.

All rights reserved. No part of this book may be reproduced by any means, nor transmitted, nor translated into a machine language without the written permission of the Director of P.W.R.I.

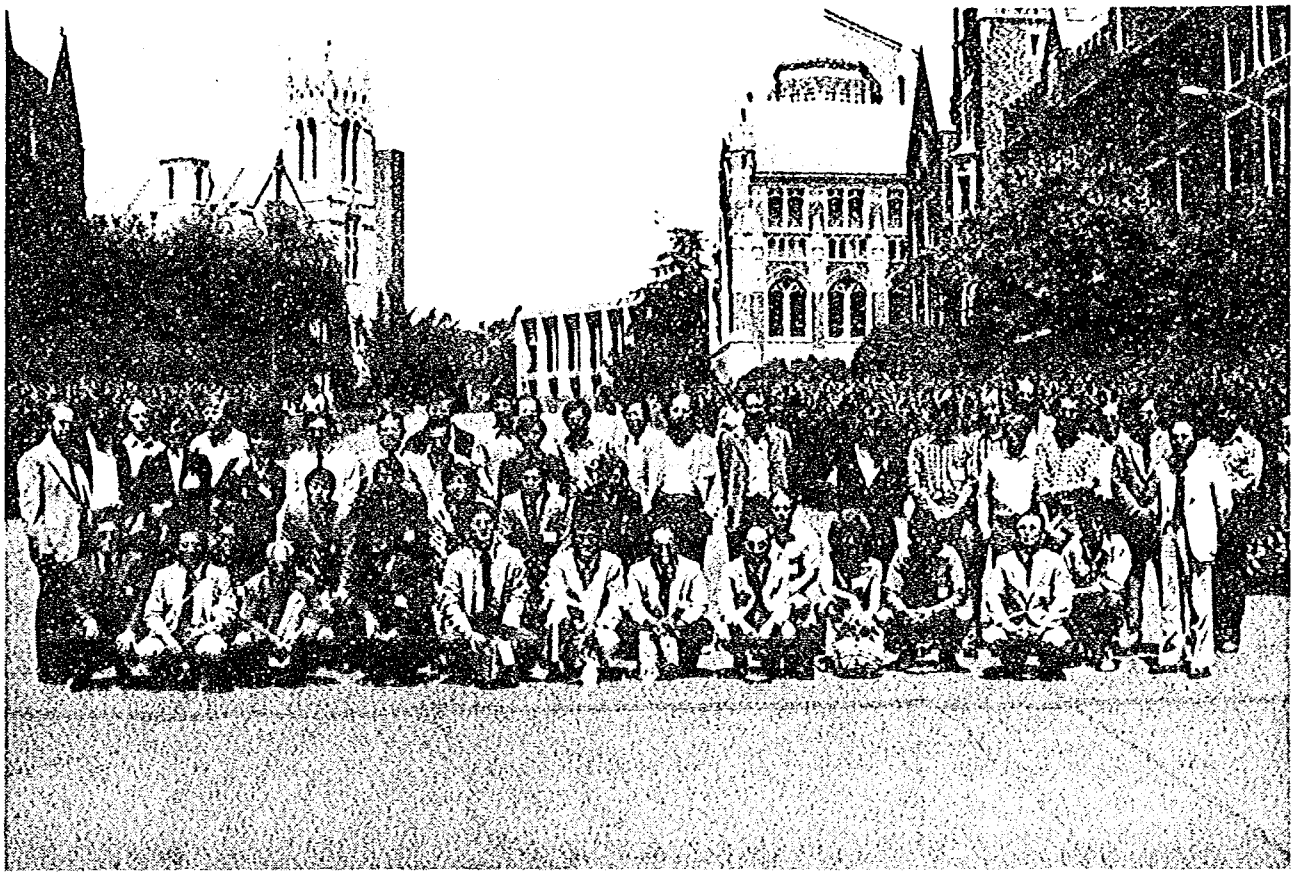
この報告書は，土木研究所長の承認を得て刊行したものである。したがって，本報告書の全部又は一部の転載，複写は土木研究所長の承認を得ずしてこれを行なってはならない。

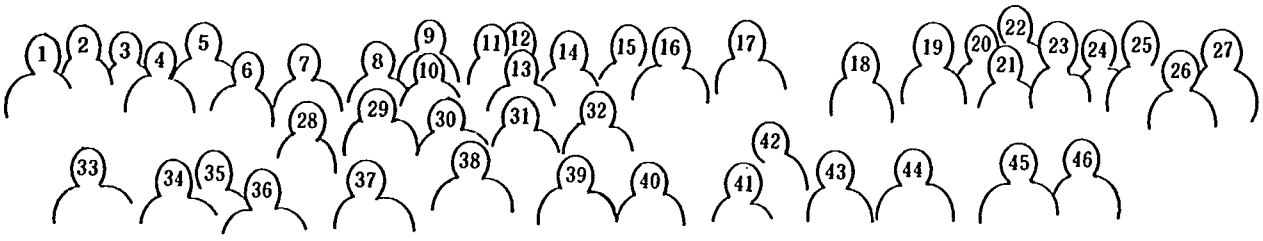
PROCEEDINGS
of the
SYMPOSIUM ON EROSION CONTROL IN VOLCANIC AREAS

July 6 – 9, 1982
at Seattle and Vancouver, Washington

February 1983

Sabo (Erosion Control) Division
Erosion Control Department





1 Jeff Bradley
2 Tom Lisle
3 Richard Janda
4 Shoichi Do (堂 聖 一)
5 Barry Voight
6 Etsuro Shimokawa(下 川 悦 郎)
7 Hiromichi Onodera(小野寺 弘道)
8 Cheng-lung Chen
9 Olav Slaymaker
10 Shinji Nagaoka (長 岡 信 司)
11 Tom Pierson
12 Chris Newhall
13 Shigeru Ono (小 野 茂)
14 Harry Glicker
15 Takashisa Mizuyama (水山 高久)
16 Rick Smith
17 Dave Meyer
18 Holly Martinson
19 Lee Fairchild
20 Brian Collins
21 Don Tubbs
22 Fred Swanson
23 Mark Wigmosta
24 Randy Sweet
25 Steven L. Stockton
26 Hiroshi Ikeya (池 谷 浩)
27 Jim Graham
28 Akito Nakasuji (中 筋 章 人)
29 Osamu Iida (飯 田 修)
30 Takahumi Tanaka(田 中 隆 文)
31 Takaaki Amada (天 田 高 白)
32 Tohru Araya (新 谷 融)
33 Kiyoshi Tanaka (田 中 清 司)
34 Masahito Ohira (大 平 征 人)
35 Atsuyuki Daido (大 同 淳 之)
36 Fukuzo Kobayashi(小 林 福 造)
37 Masashige Hirano(平 野 昌 繁)
38 Nobuo Anyoji (安養寺 信 夫)
39 Hiroshi Omura (大 村 寛)
40 Jun Kataoka (片 岡 順)
41 Aritsune Takei (武 居 有 恒)
42 Mike Nolan
43 Leslie Reid
44 Thomas Dunne
45 Yoshinori Tsukamoto(塚本良則)
46

Preface

This publication contains the papers and discussions presented at the US-Japan Symposium on Erosion Control in Volcanic Areas, held at Seattle and Vancouver, Washington USA, on July 6-9, 1982. The symposium was organized and sponsored by US Geological Survey, US Forest Service, US Corps of Engineers and Erosion Control Society of Japan.

The meeting was planned to discuss erosion problems around active volcanoes, especially Mount St. Helens which erupted on May 18, 1980. Through the free exchanges of information on erosion problems, mechanism of mud-debris flow and measures, much wider knowledge can be obtained, thus resulting in future more cooperation in this field between these two countries.

A total of about 50 engineers, geologists and others from US and Japan, one from Canada and one from France attended the symposium. A list of attendance is included in these proceedings.

Dr. T. Dunne, University of Washington, Dr. F. P. Swanson, Forest Service, Dr. R. J. Janda, Geological Survey and J. Kataoka, Nagoya University were organizers of the symposium.

These American organizers and some other attendants assisted in many ways, including local arrangements for conference meeting room, 2-day field trip to Mount St. Helens, hotel reservations, transportation, and other facilities.

Tomomitsu Yasue
Director, Erosion Control Dept.
Public Works Research Institute

Preface

In recent years issues concerning debris flows are gaining greater social concern more than ever. This may largely be due to the expansion and complication of human activities. Japan is no exception with yearly increase in damages to lives and property by debris flows triggered by localized torrential downpours. Of various measures to prevent and minimize the damages, the one of essential importance would be the research into the genesis and mechanism of debris flows. For this purpose we have devoted ourselves in observatory effort with such electro-visual aids as video cameras and so on set up in areas haunted by debris flows. A special emphasis has been made on volcanic areas where the occurance of debris flows is significantly high.

The size and magnitude of the debris flow resulting from May '80 eruption of Mt. St. Helens was overwhelming even in comparison with the Mt. Bandaisan debris flow. Thus Mt. St. Helens called not only Japanese volcanologists' attention but also debris flow researchers'. Also felt in need within the Erosion Control Engineering Society Japan was an opportunity for exchange of views with U. S. researchers working on Mt. St. Helens with a special emphasis on measures against debris flows, and accordingly a Japan - U. S. symposium on this subject was held in Seattle, Washington in the summer of 1982. The beginning of the symposium was marked by presentation of six papers each by Japanese and American researchers on July 6, followed by a field trip to the north slope of Mt. St. Helens on July 7 and to the south slope on July 8 both of which included spontaneous discussions in the field to the benefit of Japanese participants. The entire session was closed on July 9 when a tour was made to the Cascade Volcano Observatory followed by the general meeting. Japanese participants were very much impressed by the magnitude and scale of the Mt. St. Helens debris flow which had dwarfed any Japanese counterparts. The difference in size, however, did not prevent participants from feeling necessity for further accademic and technical exchange between Japan and the U. S. to tackle jointly such problems as stabilization of volcanic ash, control of subsequent mud flow and etc.

It is our pleasure to express our gratitude here to the U. S. representatives, Dr. R. J. Janda of U. S. G. S., Dr. F. P. Swanson of U. S. F. S. and Dr. Danne of the University of Washingtion for their devoted efforts of arranging the symposium. The success of the symposium is also indebted to Mr. H. Ikeya of the Ministry of Construction who devoted himself to preparatory arrangement in Japan, Dr. T. Mizuyama of Public Works Research Institute who did all the negotiation with the U. S. representatives, and Dr. M. Hirano of Osaka Municipal University who then was visiting the University of Washigton and helped us in many ways throughout the sysposium session.

Jun Kataoka
Professor
Nagoya University

Contents

OPENING SESSION

Introduction and welcome – T. Dunne 1

SYMPOSIUM

Emplacement and subsequent erosion of the debris avalanche associated with the May 18, 1980 erupti of Mt. St. Helens –
R. J. Janda ..... (not included in this volume)

Debris movement in torrential rivers of volcanic areas –
T. Araya (新谷融) and S. Higashi (東三郎) 5

Stream Channel Adjustments After the 1980 Mount St. Helens Eruptions
T. E. Lisle, A. K. Lehre, H. A. Martinson, D. F. Meyer,
K. M. Nolan and R. Smith 31

Mechanics of the initiation and movement of mud-debris flows –
A. Daido (大同淳之) 73

Flow Behavior of Two Major Lahars Triggered by the May 18, 1980 Eruption of Mount St. Helens, Washington
T. C. Pierson 99

Dynamic and volumetric characteristics of the 18 May 1980 lahars on the Toutle River, Washington
L. H. Fairchild and M. Wigmosta 131

Sediment yield from hillslopes on active volcanoes –
E. Shimokawa (下川悦郎) and Y. Taniguchi (谷口義信) 155

Erosion of hillslopes affected by volcanic eruptions –
F. P. Swanson, B. Collins, T. Dunne and B. P. Wicherski 183

Erosion control works in Nikko volcanic area –
Y. Tsukamoto (塚本良則), K. Komori (小森幸造)
and M. Kawabata (川端正夫) 223

Engineering responses to flood hazards created by the eruptions of Mt. St. Helens – S. Stockton 249

Countermeasures for debris-flow disasters in volcanic areas –
N. Anyoji (安養寺信夫), Y. Tomomatsu (友松靖夫) and H. Suzuki (鈴木宏) 273

Anticipating volcanic hazards at Mount St. Helens, Washington
C. G. Newhall 295

Study of volcanic disasters and forecasting of hazard areas –
A. Nakasuji (中筋章人) and H. Ikeya (池谷浩) 329

Summary of discussion – T. Dunne 355

FINAL DISCUSSIONS

Summary of final discussions –
F. J. Swanson and R. J. Janda 361

(Appendix) List of the Symposium Participants

INTRODUCTION AND WELCOME

On behalf of Dr. Janda of the U.S. Geological Survey and Dr. Swanson of the U. S. Forest Service, with whom I organized this meeting, I welcome you to the Symposium on Erosion Control in Volcanic Areas. I want to welcome with particular enthusiasm the participants from the Erosion Control Engineering Society of Japan led by Professor Takei, President of the Society and Professor of Kyoto University.

We look forward to the participation of the Japanese group because they have more experience with erosion control in volcanic areas than any other national group of scientists. Because of the number and variety of active and recently-active volcanoes in Japan, and the density of population in those islands, Japanese scientists must confront the problem of how to avoid, control, and modify a wide range of erosion processes, including landslides, avalanches, debris flows, sheetwash, and channel erosion. In doing so, they have developed Disaster Prevention Science, or Sabo, which constitutes a major effort by government and university scientists. An important characteristic of this effort is its inter-disciplinary nature, involving geologists, engineers, foresters, and other professionals.

In the United States, our experience with erosion control in volcanic areas is limited, but is developing. Of course, this development is largely a consequence of the eruption of Mt. St. Helens, which left billions of cubic meters of sediment in a highly erodible form, including: the debris slide and avalanche deposit in the Toutle Valley; and debris flow (lahar) deposits in the Toutle, Muddy River, and Pine Creek valleys; and the tephra deposits, mainly north and east of the volcano. Since the eruption, these sediments have been eroded rapidly by sheetwash, rilling, landsliding, debris flows, and the undermining of channel banks. Lehre et al. (1982) estimated that 56×10^6 m^3 of sediment were eroded from 775-km^2 of hillslopes in the North Fork Toutle River during the first post-eruption year, and that approximately two-thirds of this amount left the North Fork drainage basin during that year. The debris avalanche deposit provided 75 percent of the eroded sediment through the extension of channels and slumping of channel walls; 32% originated through rill and sheet erosion of tephra; and the remainder was supplied by undermining of lahar deposits by the main stream.

High rates of sediment transport and of deposition in the main channels of the region (Meier et al, 1981) caused much concern about maintaining flood-control capacity and navigation, about the recovery of fish habitat, as well as the probable effect on erosion of land management methods such as salvage logging and replanting. Only preliminary analyses of these issues have been completed to date (Collins et al, 1982; Dunne and Leopold, 1981; Lehre et al, 1982). Other results will be reported during this symposium.

Beyond the immediate effects of the 1980 eruption, we are concerned with high rates of erosion and sediment transport from several volcanic regions along the Pacific Rim of the United States. Several of these volcanoes have erupted frequently for long periods during the recent part (Crandell and Mullineaux, 1974; Beget, 1982). Other volcanoes in the range are considered dormant, but on all of them the combination of steep slopes, heavy precipitation, and mechanically weak materials is responsible for rapid erosion, expressed in the form of persistently high sediment yields, occasional catastophic mass wasting, or both. For example, Mills (1976) determined long-term average erosion rates of 3-6 mm/yr (7800-15600 $t/km^2/yr$) from the cone of Mt. Rainier, Washington. The generally erosive nature of stratovolcanoes further affects the rates of sedimentation in reservoirs and the susceptibility of hillslopes to landsliding after forest cutting or roadbuilding.

We need to improve our ability to predict and control these sedimentation hazards during exploitation of the natural resources of volcanic areas for timber, power, or recreation. The accumulation of knowledge and of predictive skill in these tasks requires the combined work of geologists, hydrologists, foresters, and engineers. It will also benefit from the exchange of ideas and information between scientists working in regions with similar forms of volcanism and erosion. It is the purpose of this symposium to initiate and develop the process of exchanging information between sedimentation specialists from Japan and the United States.

We want to emphasize that the theme of the symposium is erosion control, and therefore discussion should focus as much as possible on the various options which exist for reducing erosion and downstream sedimentation. Those of us who are geologists usually enjoying describing erosion features or processes without having to address the problem of whether or how these processes can be slowed. During the symposium and in future

exchanges between the participants, we are asking the geologists to cooperate with the engineers and foresters in discussing potential solutions to some of these problems.

Thomas Dunne
University of Washington

References

Beget, J. E. (1982) Recent volcanic activity at Glacier Peak; Science, 215, 1389-1391

Collins, B.D., Dunne, T., and Lehre, A.K. (1982) Sediment influx to the Toutle River from erosion of tephra, May 1980-May 1981; Proc. Conf. on Mt. St. Helens: Effects on Water Resources, Washington State University Press, Pullman, Washington, 82-97.

Crandell, D. R. and Mullineaux, D.R. (1974) Technique and rationale of volcanic-hazards appraisals in the Cascade Range, Northwestern United States; Environmental Geology, 1, 23-32.

Dunne, T. and Leopold, L. B. (1981) Flood and sedimentation hazards in the Toutle and Cowlitz valleys as a result of the Mt. St. Helens eruption. Federal Emergency Management Agency, Region X, Seattle, 141 pp.

Lehre, A. K., Collins, B. D., and Dunne, T. (1982) Preliminary post-eruption sediment budget for the North Fork Toutle River drainage June 1980-June, 1981; Proc. Conf. on Mt. St. Helens: Effects on Water Resources, Washington State University Press, Pullman, Washington, 215-234.

Meier, M.F., Carpenter, P.J., and Janda, R. J. (1981) Hydrologic effects of Mt. St. Helens 1980 eruptions; EOS American Geophysical Union Transactions, 52, 625-626.

Mills, H.H. (1976) Estimated erosion rates on Mt. Rainier, Washington; Geology, 4, 401-406.

DEBRIS MOVEMENT IN TORRENTIAL RIVERS OF VOLCANIC AREAS

by

Touru Araya and Saburo Higashi

Laboratory of Erosion Control Engineering,
Faculty of Agriculture,
Hokkaido University

INTRODUCTION

In Japan, natural disasters have occurred every year, being caused by mass movement as debris flow or landslide, and followed by heavy losses of life and property. These are mostly of drastic progressive developments in the mountainous areas, combined with geophysical and meteorological characteristics. Therefore, torrent and hillside control works are usually needed in wide area of Japan for protecting them from disasters.

It is therefore very important when planning erosion control to clarify the principles of debris movement, especially in volcanic areas which have a high frequency of mass movements, many of which are large scale due to the devastation in the area.

The principles of disaster prevention due to movements are to clarify the movement laws, to make hazard maps and to predict the occurrences. Then, the hazard zones can be made safe by setting the control works. Solution to these problems depends on understanding the characteristics of the watershed, so initially the individual characteristics of the watershed should be investigated in the field.

Debris movements has mainly two types, landslide on the hillside and debris flow due to bed load movement in the channel. The purpose of this paper is to introduce the process of bed load movement in the upstreams of the volcanic torrential rivers in Hokkaido, Japan.

METHOD OF STUDY

This study was carried out with geomorphological and dendrochronological aspects to clarify the process of movement by field investi-

gations.

The volcanic river channels were investigated, especially the distribution and shape of the deposits which were formed by the past debris flows.

The forest composition and ages were surveyed and tree rings were measured to estimate the years of movement or deposit formation by dendrochronological analysis.

The deformation of the deposits was surveyed continuously from 1972 to 1981 by profile and cross sectional levelling with fixed point surveying in the three areas at Mt. Tokachi.

INVESTIGATED WATERSHED

Hokkaido, northern Japan, has many active volcanoes, which erupted in 20th century, such as Mt. Tokachi, Usu, Tarumae and Komagatake. The location of Hokkaido and these volcanoes, which are situated in lat.42°-44° and long.140°-146°, are shown in Fig.1. The history of certain volcanic activities during the past one hundred years is shown in Table 1. Especially on May 1926, the debris flow occurred by eruption of Mt. Tokachi, which flowed along the Furano and Biei River courses and destroyed 650 ha of the forest, 1200 ha of the farmland, 617 houses and killed 144 persons.

Main investigated watersheds of Mt. Tokachi are generally described in Table 2. The Furano River and Nukkakushi-furano River flow down from the craters of Mt. Tokachi(2077m), Mt. Kamihorokamettoku(1887m) and Mt. Furano(1912m) as shown in Fig.2. In this district, the precipitation registered 211 mm as daily maximum experienced, 39 mm as hourly maximum

and 900-1200 mm as anual. Annual mean temperature is 6°C and maximum snow depth is 170 cm.

Furano River has the main stream length of 40 km, the area of 296 km^2 and the mean slope of 1/200. In this river, disasters have occurred 42 times in the past 100 years, especially on May 1926 the eruption of Mt. Tokachi gave rise to serious damages to the Furano Town.

Nukkakushi-furano River has the main stream length of 32 km, the area of 74 km^2 and the slope of 1/180, and 19 times of disasters in the past 100 years.

In upstreams of these rivers, SABO(erosion control) works such as check dams, consolidation dams, debris barriers, retardation basins and channels have been constructed since 1966.

GEOMORPHOLOGICAL SURVEY

The site, length, width, depth and volume of the deposits were surveyed in these rivers.

The deposit forms were classified into two types as terrace and tongue-shaped; terrace deposits were formed at the wide area of channel course, while tongue-shaped deposits are formed at the wider area, as shown in Fig.3.

DENDROCHRONOLOGICAL SURVEY

In the channel course of torrential rivers, one can find a natural even aged forest formed on the deposits. It is mainly composed of pioneer trees such as Salix, Populus, Alnus and Betula spp..

Fig.4. shows typical forest types on the terraced deposit. The left figure shows the type of natural even aged forest formed after one

deposition. The middle figure is the storied forest formed with new deposit on the old one. The right figure is the forest formed on three steps of recent, new and old deposit.

It was clarified that the ages of these trees were all the same, suggested the years of occurrence of deposition and might be useful as plant indicator.

Furthermore the branches and roots can be defined as indicators. Fig.5. shows the bent, injured and buried trees. When the deposit was destroyed by scouring, the bent trees began to grow new compression wood, and new shoots straightly to upward direction. If the deposit was overflowed, trees were injured and started to grow new sprouts. If the deposit was buried, trees started to grow adventitious roots.

The ages of compression wood, new sprouts and adventitious roots indicate the years of movements, so that the ages of the movements can be defined by the annual rings. From these facts it was assumed that it was useful to estimate the years of movements by tree rings analysis.

ANALYSIS OF THE DEPOSITS AND THE AGES

Distribution of the deposits and the ages were surveyed and process of the past movements were clarified by geomorphological and dendrochronological analysis, at the hillside of Mt. Tarumae and Tokachi.

Fig.6. shows an example of terraced deposit and the forest, plane figure and cross section figures, in Furano River. Numbers in the plane figure are the years after the terraced deposits were formed. On the higher terrace in the two cross sections, trees were higher and ages of trees were older. Distribution of each year's deposits in the river

channel and the past movements' years are shown in Fig.7. This figure shows that flood marks with tree rings analysis are made in some deposition areas, and especially discontinuity of these deposition areas is existing along the channel. Each movement has own scale and 1962's was the largest among all.

Results of these analysis are shown in Table 3. The frequencies of the movements were 1/17 at Mt. Tarumae and 1/6-1/10 at Mt. Tokachi.

The distribution of deposits was investigated along the channel. Fig.8. shows four typical types of the distribution such as Alternative, Progressive, Regressive and Identical types. Among these the most typical type is the Alternative which shows the deposition occurrence alternatively in place at the same movement and in time alternatively between the one and the next. Progressive is the one in which movement occurrence develops toward downstreams. On the other hand the Regressive is the one which shows gradual movement to the direction of upstream. Identical is the one which shows the same process of movement among the various movements. These types indicate the process of the movement in the channel which is very important character of the channel for planning of erosion control works.

CONTINUED SURVEY ON DEFORMATION OF DEPOSIT

Survey on deformation

Three areas of Nukkakushi-furano River and Furano River were surveyed on the deformations of the deposits at the each movement from 1972 to 1981 as shown in Table 4. Nukkakushi-furano River has two areas(A and B). The A has 660m length, 13.2-66.0m width and slope of 1/8. The B is the

upper area which has 450m length, 14-38m width and slope of 1/10. The C is the upper area of Furano River having the length of 4500m, width of 8-70m and slope of 1/8. The A had 7 times of movement in 8 years from 1974 to 1981, the B; 8 times in 10 years from 1972 to 1981, the C; once every year.

Debris movement deformed the channel bed, raising the one by deposition and descending the one by scouring. The deformations of channel bed were measured just after the each movement in the surveying period, as area and volume in cross section, by profile and cross sectional levelling. An example of the deformations was drawn in Fig. 9.

The deformation volume of the each cross section was calculated as D.V. (volume of deposition) and S.V. (volume of scouring), which signified the scale of movement, as shown in Table 4. The maximum volume in each movement reached to $48m^2$ in the A, $84m^2$ in the B and $48m^2$ in the C. The maximum value of average height of each movement was 2.9m in the C.

In Table 5, an example of the results was shown on deformed cross section area(D.A.), average height of bed(D.A./W) and deformation volume of the section(L • D.V.), in the two areas(A and B)which had each 12 cross sections, in the case of A in 1972 and of B in 1974-1975. The maximum values of D.A. were $32m^2$ of deposition and $10m^2$ of scouring in the A, $84m^2$ of deposition and $47m^2$ of scouring in the B. The maximum values of average height were 0.4 m by deposition in the A and 2.2 m by scouring in the B. The maximum values of deformation volume of the section were $800m^3$ by deposition and $380m^3$ by scouring in the A, $4200m^3$ by deposition and $2720m^3$ by scouring in the B.

Alternation of deposition and scouring

It was clarified that typical shapes were existing in the figures.

Fig. 10 shows the results of four movements on deformation area and volume of the section. The left figure shows two small movements in the A and right figure shows two larger movements in the B. These four figures show the fact that deposition occurs in one section, while the neighboring section had scouring at the one movement. This inclination which had been assumed by distribution analysis of the ages of deposition with dendrochronological analysis, was recognized at the movements. This regularity was named as alternation in place.

Fig.11 shows the regularity that at the same section deposition and scouring occurred alternatively in time. This regularity was named as alternation in time. In Fig.12, the most typical case of alternation of two movements was drawn as wave shape and five movements were drawn in wave shape in Fig.13.

The surveyed sections were classified into deposited section and scoured one. Fig.12 shows typical example of changes in deformation volume at each section that is shown by two movements. In the sections deposition and scouring occurred alternatively. Then the alternation of deposition and scouring should be expressed as something like wave.

Supposing that alternation of deposition and scouring can be expressed as wave, repetition of deformation that occurred in the area C may be represented as the aggregation of various types of wave as shown in Fig.13.

WIDTH OF DEBRIS FLOW

Distribution of deposit volume, width and cross section area of the debris flows on July 1980 and August 1981 in the area C were surveyed. The results were drawn in Fig.14 which showed an alternation in

the area C, where these occurred longer than those observed in the A and B. And this figure shows an assumption that deposition is connected to channel width, because in the both movements deposit volume became larger in the wider area of channel and width of debris flow was due to channel width.

Auto correlation function of the deposit volume change on July 1980 in Furano River was drawn in Fig.15. In this figure, a peak of wave was recognized near 350m lag. The fact suggests that deposition occurrs at interval of 350 meters.

Moving average and moving translation ratio of channel width were calculated and drawn in Fig.16. Though channel width was measured variable at each section, moving average of channel width seems to be one kind of wave that has a certain cycle and moving translation ratio also seems to have its own cycle. Therefore, it was assumed that deposition occurred depending on the spreading of channel width and its occurrence had some cycles.

MODEL OF ALTERNATION

Model of alternation in place and in time was drawn as shown in Fig. 17. In this figure, left picture was drawn as an alternation model of deformation volume of deposition and scouring, and right picture shows the alternation in plane picture of the channel. The deposited section in a movement will be scoured in the next movement and the scoured section will be deposited when the next debris flow will occur in the same area.

WAVE SHAPE OF MOVEMENT TO THE SCALE

Supposing that each deformation could be dealt as wave, repetition

of deformation is considered as aggregation of various waves which have their own cycles.

Wave shape of movement varies in accordance with the movement scale. In a small scale movement, the shape has a short wavelength and low amplitude, in large scale the shape has a long wavelength and high amplitude as shown in Fig.18.

DEBRIS FLOW VOLUME AT EACH SECTION

Until now the alternation as wave was discussed in detail. In this part we will deal with debris flow. Debris flow volume is impossible to be measured directly, but can be assumed by calculating the balance of deposited and scoured volume as shown in Fig.19. In this figure D.V. is the deposition volume and S.V. is the scouring volume. Also, V is the debris volume passed through the section.

By above mentioned calculation debris flow volumes were assumed in the areas A nad B of Nukkakushi-furano River as shown in Fig.20. On July 1974, September 1974 and August 1975, debris flows occurred in both areas. It was clarified that the peak volume was very different from each other area in the same movement and discontinuity of debris movement was existing.

Debris flows were classified into two types; one is the flow from the upper area(the area A: July and September 1974, the area B: September 1974) and the other is the flow that occurred by bed loas movement in the area(the area A: August 1975, the area B: July 1974 and August 1975).

The relation between the debris flow volume(V) and the return period (T) was shown in Fig.21, with the data taken by the continued survey on the deformations of channel bed and by the investigation on the volume and the ages of the past deposits.

From this figure, the formula ($V = aT^b$; a:300-900, b:1.4-1.6) was followed. This formula can be used in the prediction of the volume of debris flow which will occur in the future period of erosion control planning.

CONCLUSION

Processes of debris movements in the torrential rivers were studied by means of geomorphological, dendrochronological surveys on the past movements and continued survey on the new deformations of the deposits. The results are as follows,

1) Surveying the deposits and the forests, it was clarified that tree ring's method was useful for estimating the years of past movements.
2) By this method, it is possible to recognize the frequency and scale of the past movements(as in Table 3) and inclination of movement process in the channel(Fig.7).
3) Distribution of the deposits and the ages resulted in an assumption that deposition occurred alternatively(Fig.8).
4) Continued deformation survey of the deposits derived a regulation which had an alternation of deposition and scouring.
5) Alternation in time and place can be drawn as wave shape(Fig.13).
6) Distribution of deposit volume is depending on channel width.
7) Wave shape has a cycle whose length is decided to the channel width and the movement scale.
8) Model of alternation can be drawn to the each scale which has own wavelength and amplitude as shown in Fig.17.

REFERENCES

1) Araya,T.: Morphological study of bed load movement in torrential rivers. Res.Bull.Coll.Exp.For.Hokkaido Univ., Vol.28 No.2 pp.193-258, 1971.

2) Higashi,S.: A method of the watershed research for forest working. Res.Bull.Coll.Exp.For.Hokkaido Univ., Vol.30 No.1 pp.69-101, 1973.

3) Sakamoto,T. and Araya,T.: Stream bed deformation and discontinuity of debris flow. A voluntary paper at the 17th IUFRO World Congress 1981.

Table 1. Main active volcanoes in Hokkaido

Volcanic mountain	Altitude (m)	History of volcanic activity
Tokachi	2077	1887 1926-28 1962
Komagatake	1133	1888 1905 1919 1922-24 1928-29 1935 1937 1939 1942
Usu	727	1910 1943-45 1977
Tarumae	1024	1883-87 1894 1909 1917-23 1926 1928-29 1931 1933 1936 1944 1947 1951 1953-54
Shiretoko-iou	1563	1889-90 1936
Meakan	1499	1954-60 1962 1964-66

Table 2. General description of the surveyed rivers

River	Area (km^2)	Main stream length (km)	Slope	Times of disaster	Sabo works
Nukkakushi furano	74	32.4	1/180	19	7
Furano	295.6	40.2	1/200	42	3

Table 3. Results of field investigation on the past movements in the rivers at Mt.Tarumae and Tokachi

Volcanic mountain	River	Investigated length (km)	Times of movement	Time intervals of movements	Frequency of movement	Distance between the same age deposits (km)
Tarumae	Oboppu-karasawa	6.5	3	4,5	1/17	0.4 - 3.4
	Shishanonai	4.0	3	8,3	1/17	0.2 - 2.3
Tokachi	Nukkakushi-furano	5.3	8	10,5,5,5,5,6,5	1/6	0.1 - 3.4
	Nukkakushi-furano-sashi	3.4	5	4,4,5,6	1/10	0.1 - 1.6
	Furano	5.2	5	7,5,4,5	1/10	0.2 - 2.1

Table 4. Results of the continued survey on the deformation of the deposits

Area	Surveyed period	Length (m)	Width (m)	Slope	Times of movement (times/years)	Deposited Length (m)	Deposited Volume (D.V.) (m)	Scoured Length (m)	Scoured Volume (S.V.) (m)	Maximum area of deformation in cross section (m)	Maximum of deformed height (m)
A	1972	450	14.0	1/10	8/10	25	400	25	500	6	0.2
	≀		≀			≀	≀	≀	≀	≀	≀
	1981		38.5			290	6000	165	1000	48	1.4
B	1974	660	13.2	1/8	7/8	40	900	40	200	12	0.3
	≀		≀			≀	≀	≀	≀	≀	≀
	1981		66.0			270	20000	470	10000	84	2.2
C	1980	4500	8.0	1/8	2/2	400	12000	400	3300	20	2.9
	≀		≀			≀	≀	≀	≀	≀	≀
	1981		70.0			500	24400	800	14800	48	2.2

Table 5. An example of mesurement on deformation

Area	Cross section		1	2	3	4	5	6	7	8	9	10	11	12
A	SP. (m)		25	50	75	100	125	150	200	230	265	305	360	420
	Length of section (Lm)		37.5	25	25	25	25	37.5	40	32.5	37.5	47.5	57.5	60
	Width of cross section(Wm)		66.0	59.4	39.6	26.2	24.6	28.2	22.4	16.6	17.6	17.4	13.2	29.8
	D.A.(m^2)	Aug. 1972	-10	32	-9	4		-4	-6	0	1	2	2	-2
		Oct. 1972	18	-5		-4		5	3	-3		-4	-2	5
	D.A/W(m)	Aug. 1972	-0.2	0.4	-0.2	0.2		-0.1	-0.3	0	0.1	0.1	0.2	-0.1
		Oct. 1972	0.3	-0.1		-0.2		0.2	0.1	-0.2		-0.2	-0.2	-0.2
	L·D.A.(m^3)	Aug. 1972	+380	800	-230	150		-200	-240	0	40	100	120	-120
		Oct. 1972	680	-190		-200		250	120	-160		-260	-120	300
B	SP. (m)		1215	1265	1315	1365	1415	1446	1496	1544	1633	1710	1784	1835
	Length of section (Lm)		40	50	50	50	50	40.5	40.5	49	83	75.5	62.5	51
	Width of cross section(Wm)		36.0	38.5	38.0	36.5	29.0	30.0	32.5	32.5	14.0	16.5	17.0	21.0
	D.A.(m^2)	Sep. 1974			84	79	27	30	-47	42	23	27	0	4
		Aug. 1975	37	30	81	26	-22	-7	-23	-30	-24	-36	-13	-4
	D.A/W(m)	Sep. 1974			2.2	2.2	0.9	1.0	-1.4	1.3	1.6	1.6	0	0.2
		Aug. 1975	1.0	0.8	2.1	0.7	-0.8	-0.2	-0.7	-0.9	-1.7	-2.2	-0.8	-0.2
	L·D.A.(m^3)	Sep. 1974			4200	3950	1090	1210	-2300	2880	1910	2040	0	210
		Aug. 1975	1480	1500	4050	1300	-890	-280	-1130	-2060	-1990	-2720	-810	-200

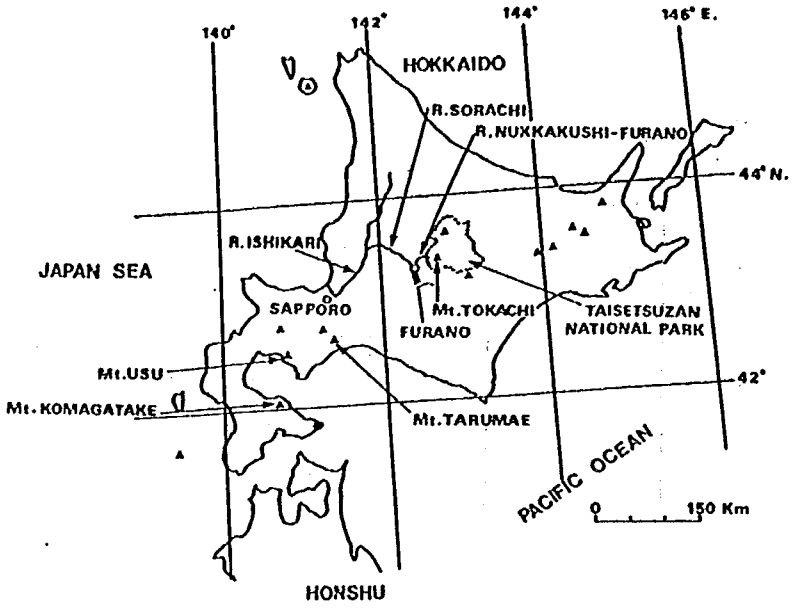


Fig.1. Location of active volcanoes in Hokkaido

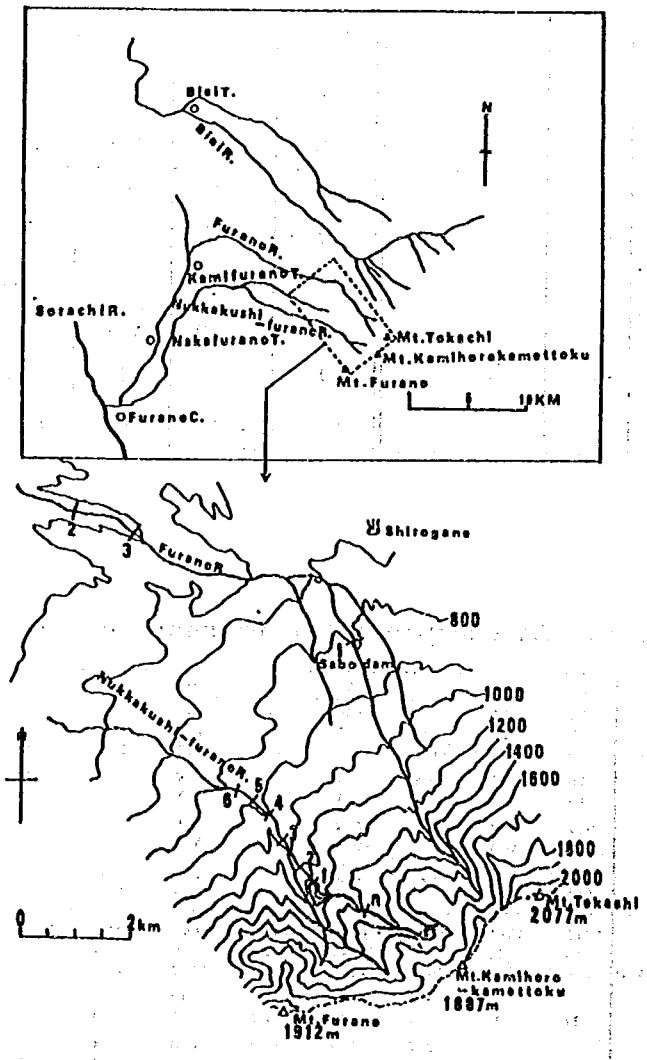


Fig.2. Surveyed rivers on deformation of the deposits (R,1-6:SABO dam).

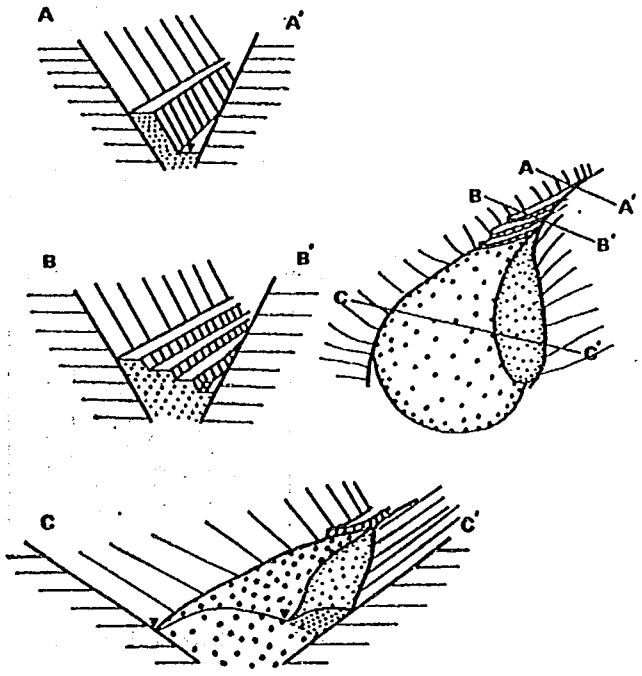


Fig.3. Typical forms of deposit in the torrential rivers

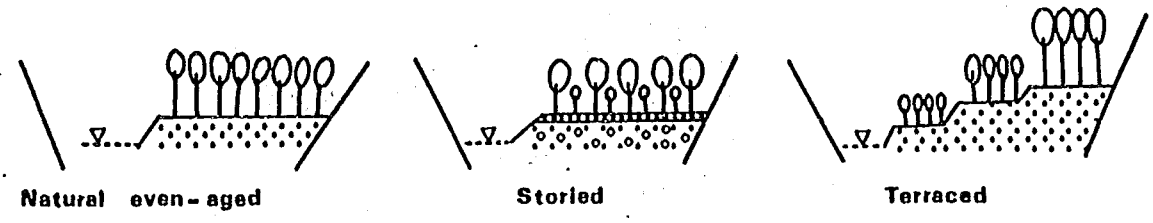


Fig.4. Typical forests on the terraced deposit

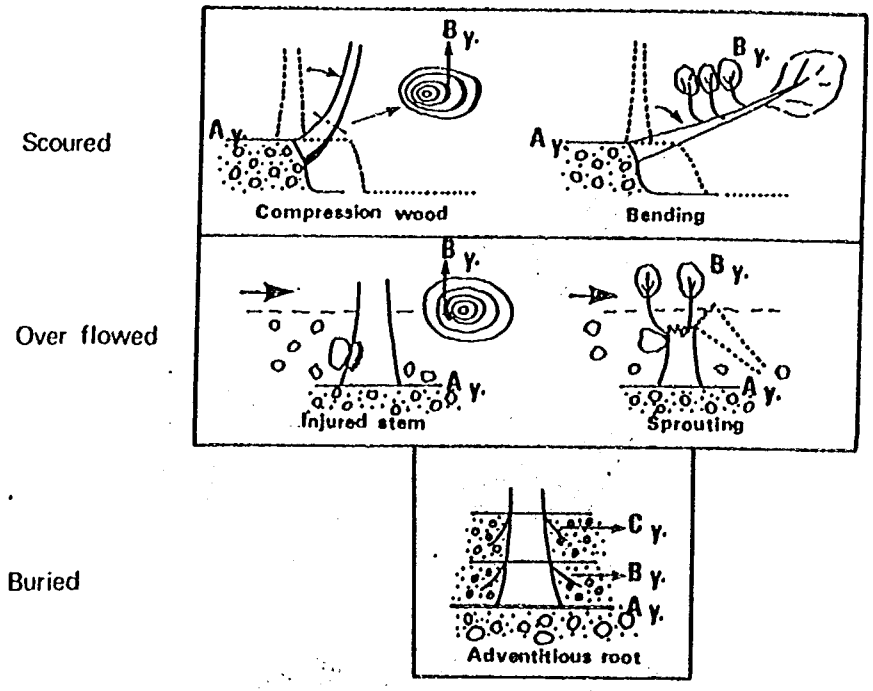


Fig.5. Bending, injured and buried trees as indicator

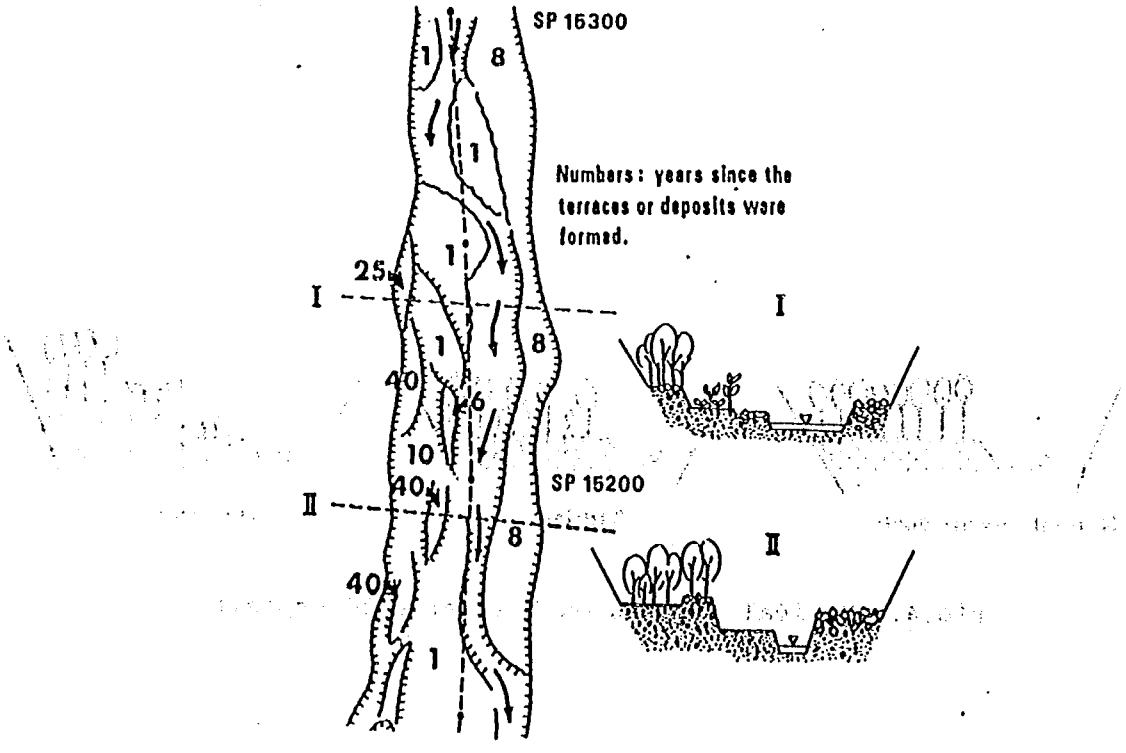


Fig.6. Terrace deposits and forests formed by debris movements

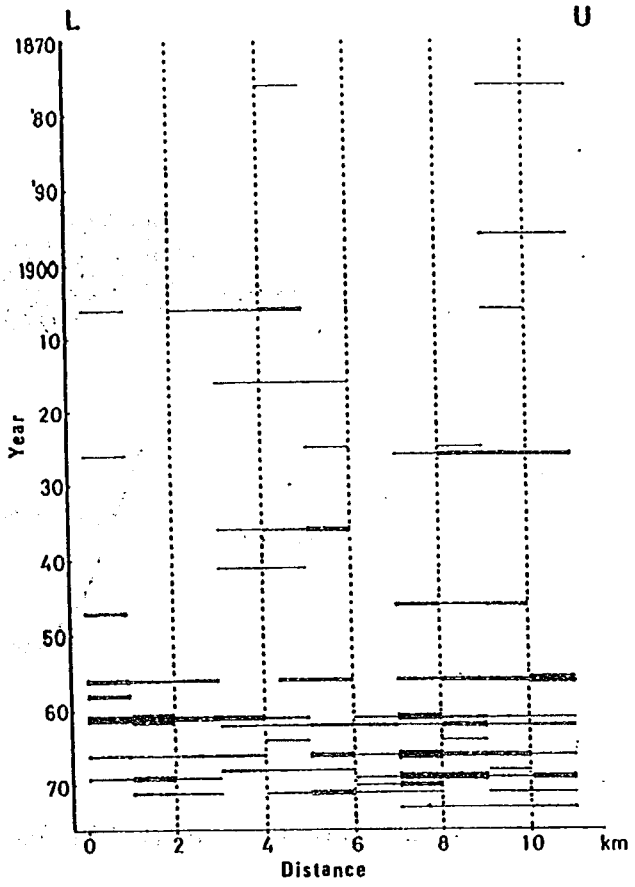


Fig.7. Distribution of the deposits' ages by dendrochronological analysis

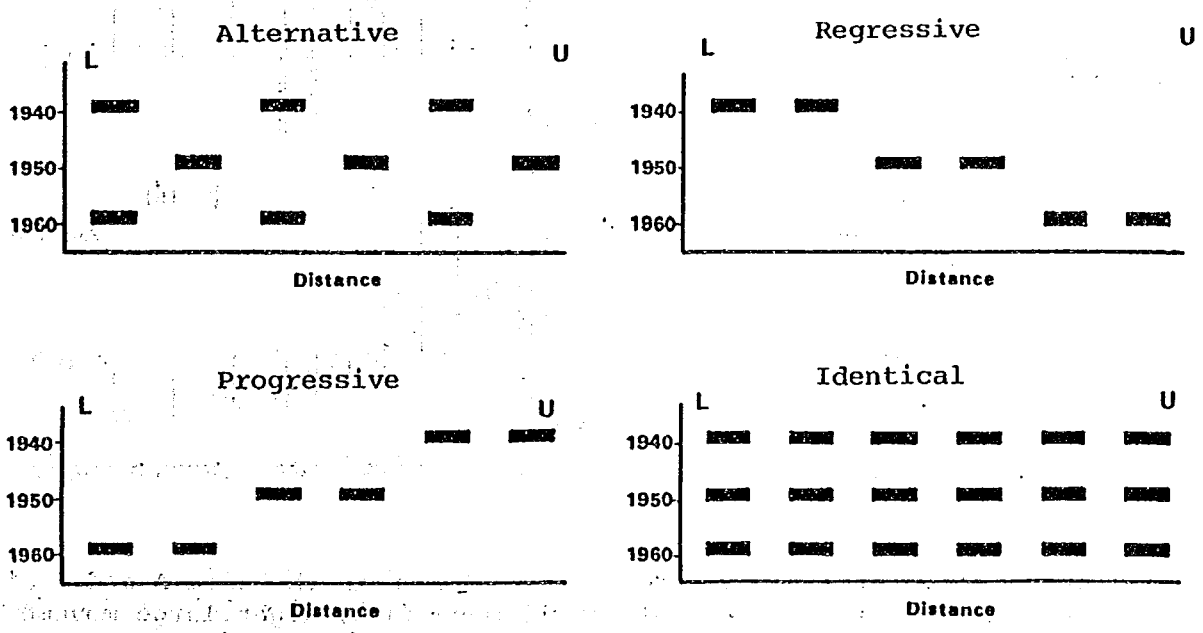


Fig.8. Typical types of the distribution of depoists' ages

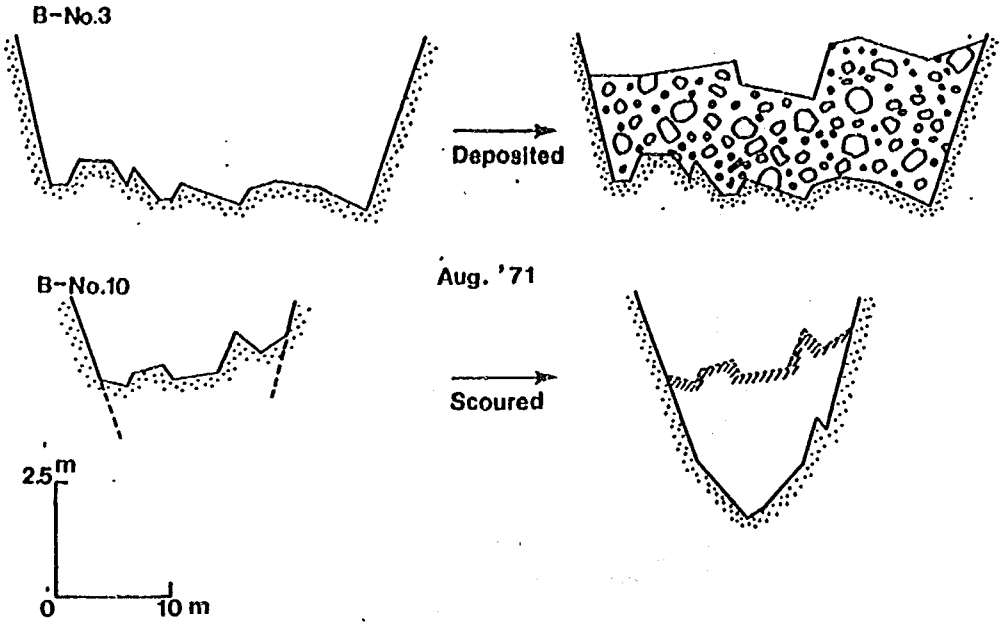


Fig.9. River bed deformed by deposition and scouring

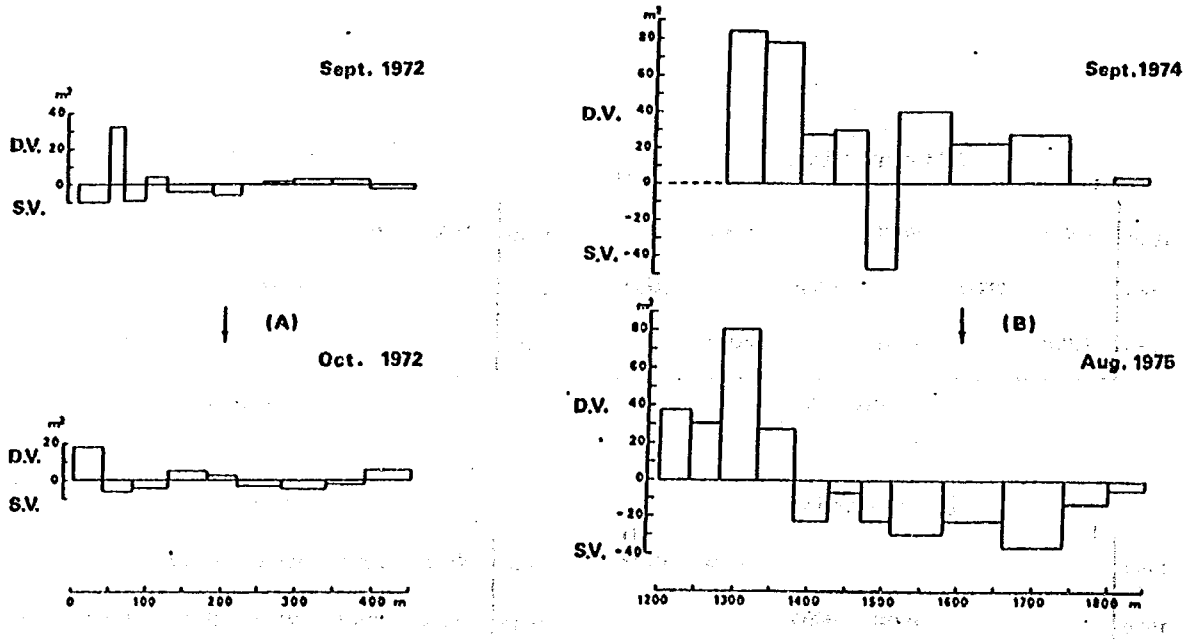


Fig.10. Deformation area and volume of the section in the area A and B of Nukkakushi-furano River(Left:small movements, Right:large movements)

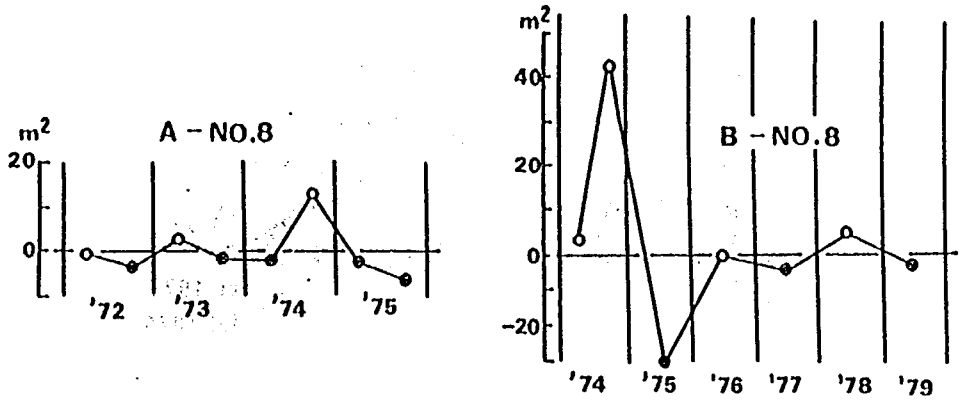


Fig.11. Alternation in time of deposition and scouring in the same section

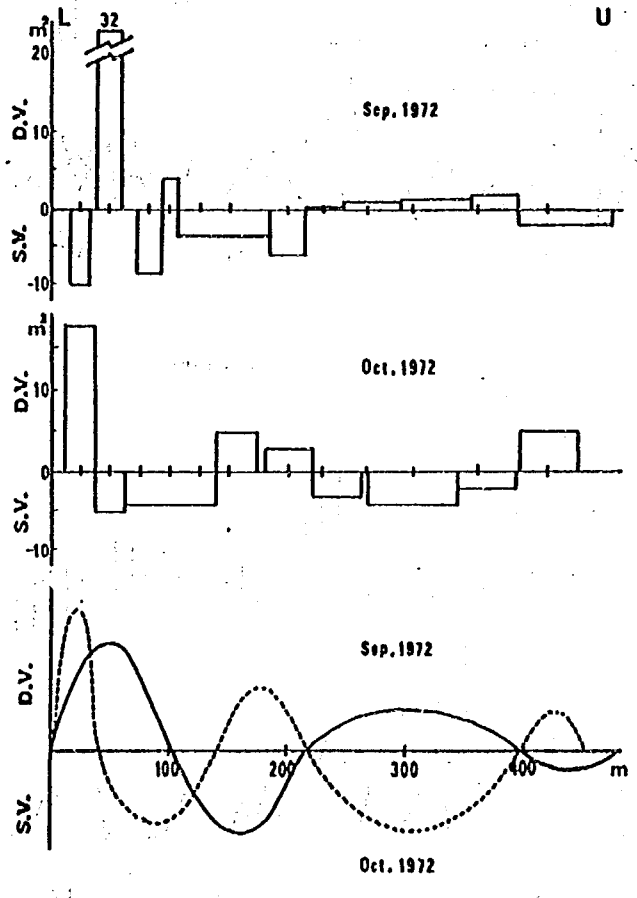


Fig.12. Typical example of a wave shape due to alternation of deposition and scouring in the area A

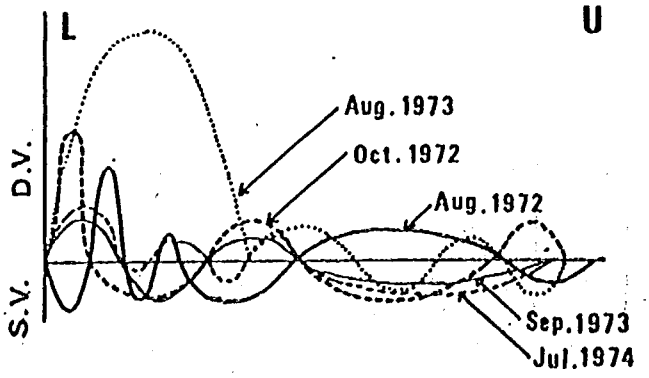


Fig.13. Movements expressed as wave shapes in the area A

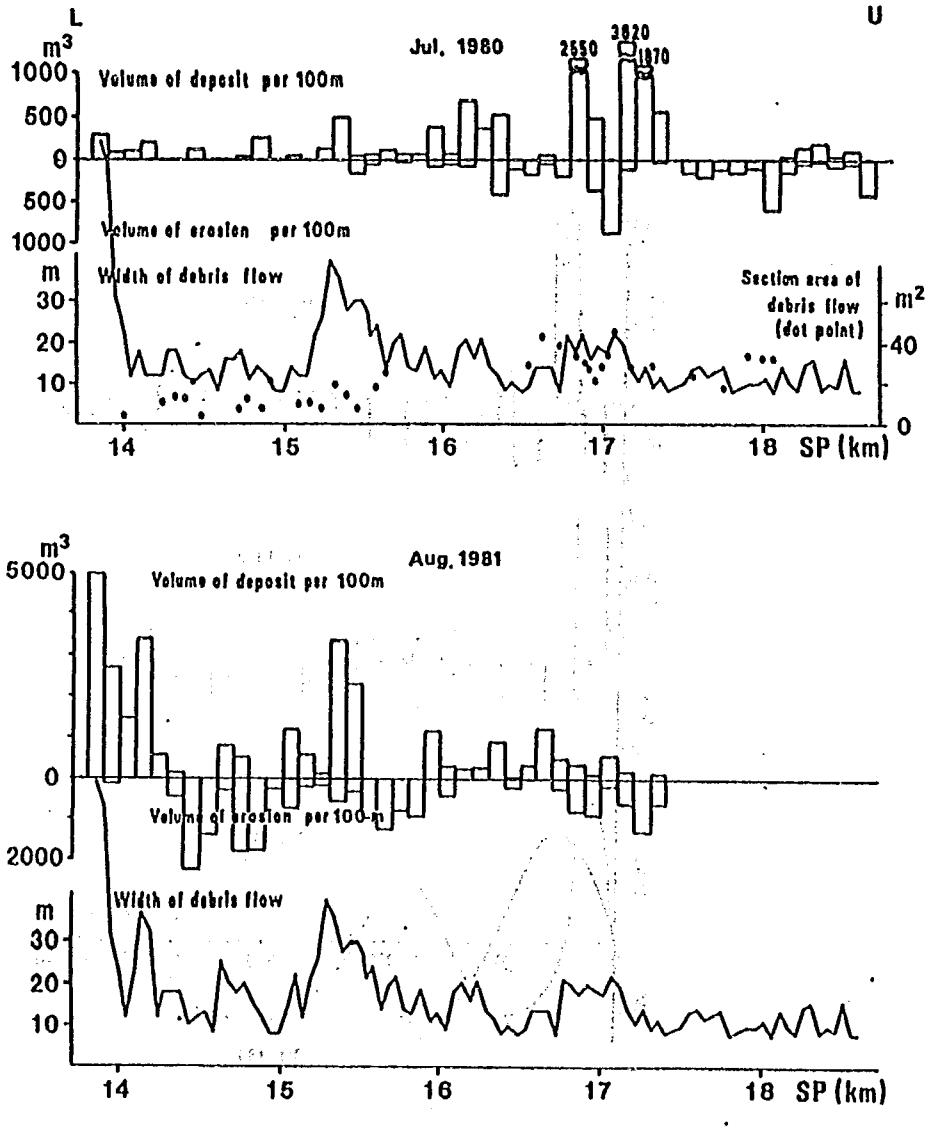


Fig.14 Distribution of deposit volume and width of the debris flows in the area C (Furano River)

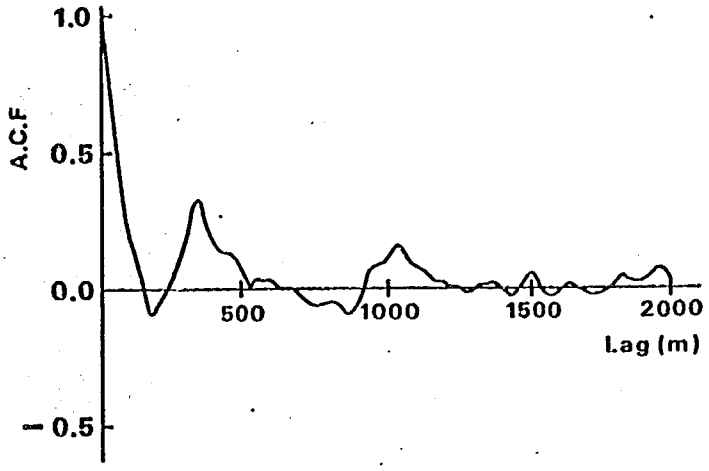


Fig.15. Auto correlation function of the deposit volume changed on July 1980 in the area C (Furano·River)

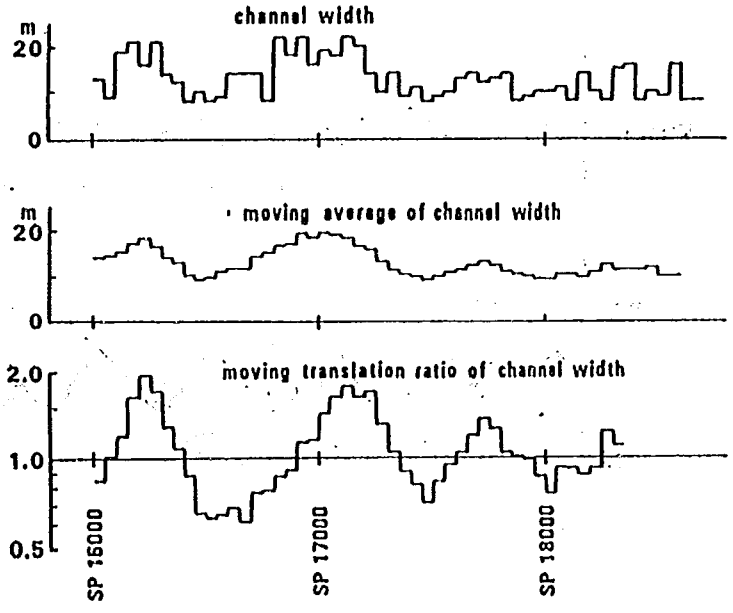


Fig.16. Moving average and moving translation ratio of channel width in the area C

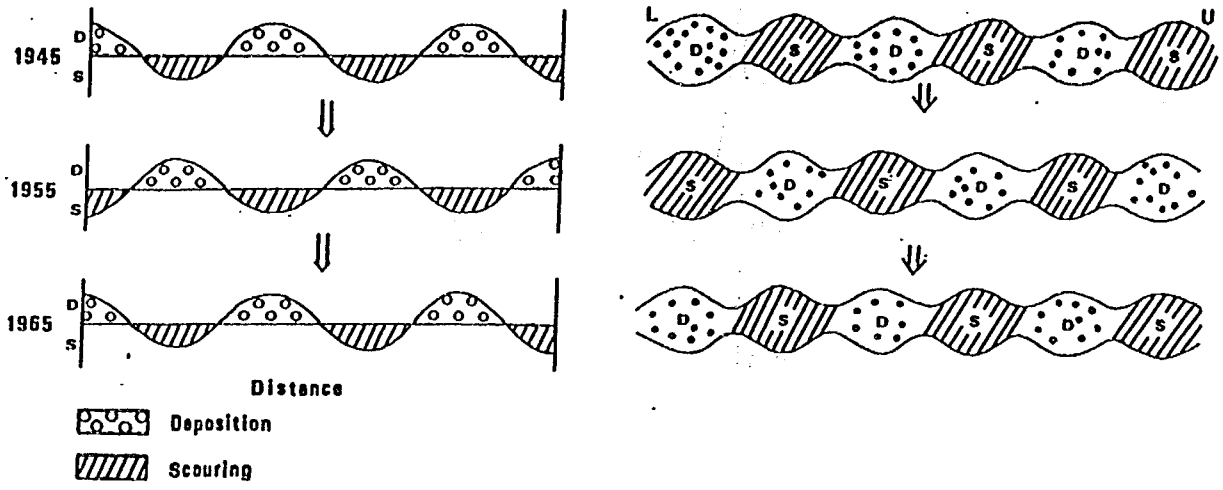


Fig.17. Model of alternation in deposition and scouring

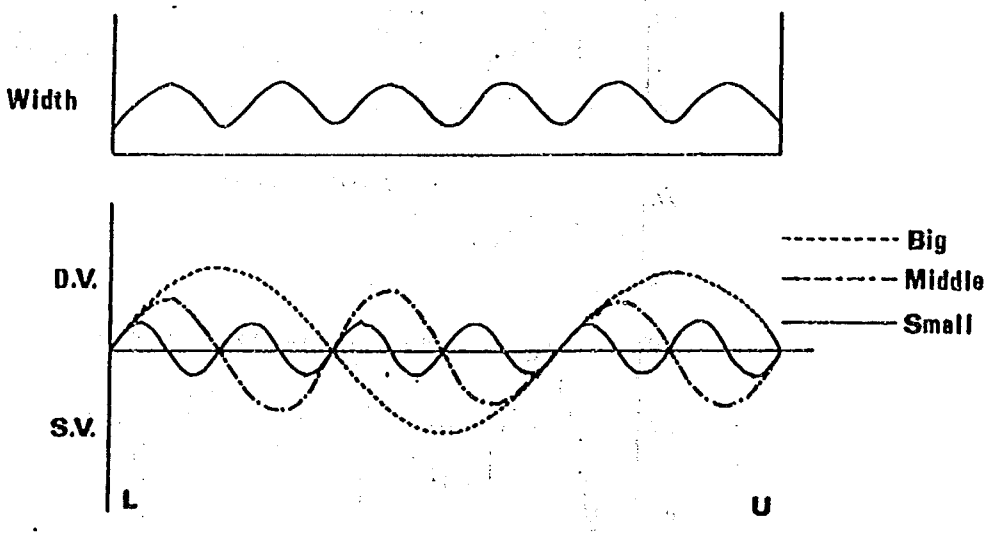
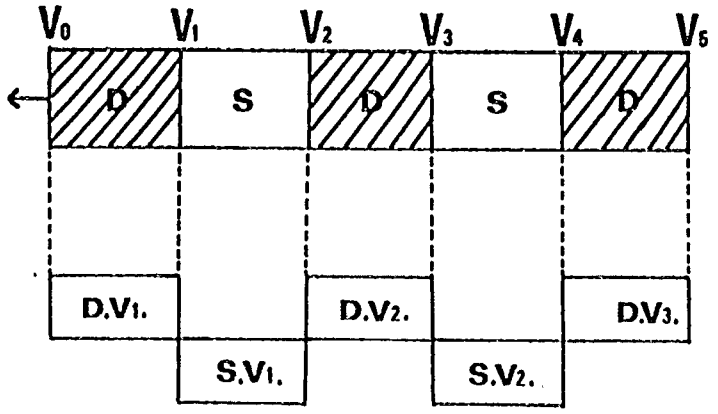


Fig.18 Wave shape model due to movement scale



$$V_n = V_0 + \sum_{n=1}^{n} D\,V_{A(n)} - \sum_{n=1}^{n} V_{B(n)}$$

$$A(n) = \frac{1}{2}(1-\cos n\pi) + \frac{n}{2}$$

$$B(n) = \frac{1}{2}(1+\cos n\pi) + \frac{n}{2}$$

D:Deposited
S:Scoured
D.V.:Deposited volume
S.V.:Scoured volume

Fig.19. Calculation of debris flow volume through the section

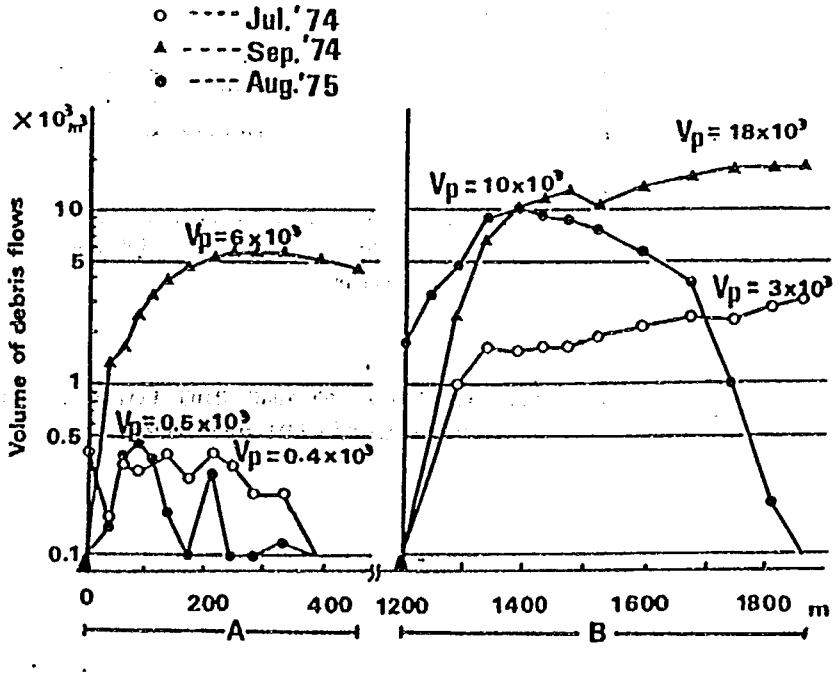


Fig.20. Changing of debris flows' volume and their peaks in the area A and B

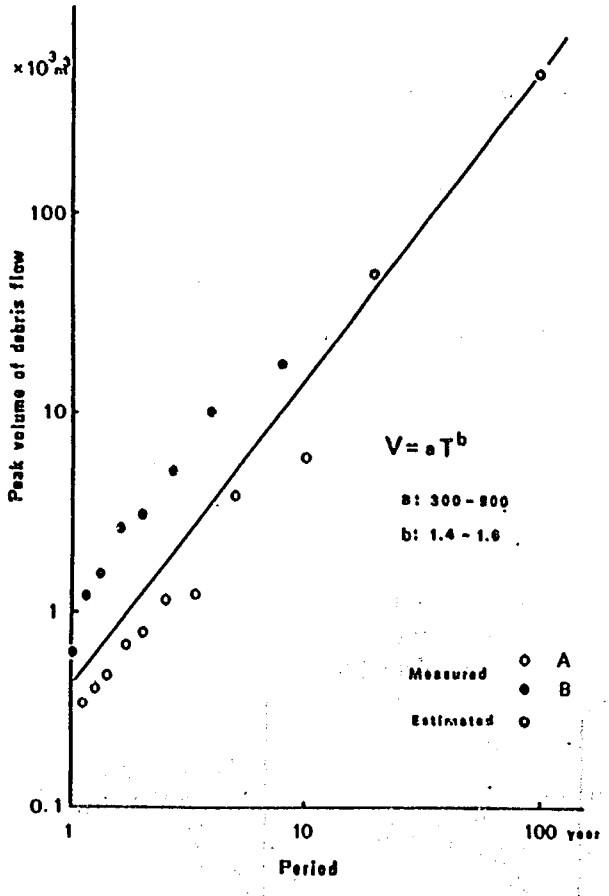


Fig.21. Debris flow volume and return period in Nukkakushi-furano River

Stream Channel Adjustments After the 1980 Mount St. Helens Eruptions

by

Thomas E. Lisle, Andre K. Lehre, Holly A. Martinson, David F. Meyer, K. Michael Nolan, and Richard D. Smith

Proceedings of a Symposium on Erosion Control in Volcanic Areas. Seattle, Mt. St. Helens, Vancouver, Washington, July 6-9, 1982.

Stream Channel Adjustments After the 1980 Mount St. Helens Eruptions

by

Thomas E. Lisle, Andre K. Lehre, Holly A. Martinson, David F. Meyer, K. Michael Nolan, and Richard D. Smith

ABSTRACT

Stream channel response to the 1980 eruption of Mount St. Helens has varied widely. Stream channels that received only airfall deposits have shown no significant sedimentation following the eruption. In drainage basins that received both blast and airfall deposits, localized channel modification has been observed. However, as the blast/airfall deposits are predominately sand-sized, they have been quickly removed from the steep low-order channels surrounding the mountain with little net effect on pre-eruption channel morphology. Some subsequent channel modification has resulted in lowered gradient reaches downstream as sediment eroded from upstream hillslopes and stream channels has been redeposited in these reaches. Long-term effects in blast/airfall-affected streams appear limited to channel subjected to debris torrents resulting from shallow-seated landsliding and breakup of in-channel debris jams.

Channels and floodplains affected by lahars were covered by as much as 1 to 5 meters of material and were initially reduced substantially in size. Subsequent flow has increased channel width, often as much as 100 percent, and caused a complex sequence of scour and fill over a range of several meters in bed elevation. Even in reaches characterized by up to several meters of aggradation, the net volume of sediment stored in valley bottoms has decreased due to large increases in channel width. In the North Fork of the Toutle River, the integration of stream systems on the surface of the 2.5-km^3 debris-avalanche deposit has resulted in the fluvial reworking of large volumes of sediment. Transport of this sediment dominates fluvial processes otherwise influenced by blast, airfall, and lahar deposits, causing ubiquitous channel widening and complex sequences of channel scour and fill.

INTRODUCTION

The 1980 eruptions of Mount St. Helens, Washington, had a major impact on the hydrology and sediment load of all streams in a 600-km^2 area around the mountain (fig. 1). The lateral blast destroyed vegetation and deposited sand, silt, and gravel over a large area north of the mountain. A massive debris avalanche filled the bottom of the North Fork Toutle valley. Lahars (volcanic mud flows) flowed down all major streams that drain the mountain, and fine-grained airfall ash blanketed an area beyond the blast zone.

The effects of these events on fluvial systems depend upon (1) thickness, grain size, and distribution of volcanic deposits, and (2) preeruption topography of valleys and stream channels. On the basis of these characteristics two types of channel are blast area channels and lahar-affected channels. Irregular longitudinal profiles of blast area channels (fig. 2) create local tendencies for either transport or deposition of sediment. The primary sediment source for blast area channels is sandy tephra (the lateral blast deposit, ash, and pumice) that blankets the landscape. Sediment is produced mainly by hillslope erosion. The complex drainage networks that transport the sediment extend nearly to drainage divides. Lahar-affected channels contain thick (1-5 m) deposits that range in size from clay to boulders. Such deposits from the 1980 eruption as well as from previous eruptions have created channels with distinctively smooth concave longitudinal profiles (fig. 2). Important channel changes have resulted from reworking of May 18, 1980 and older lahar deposits.

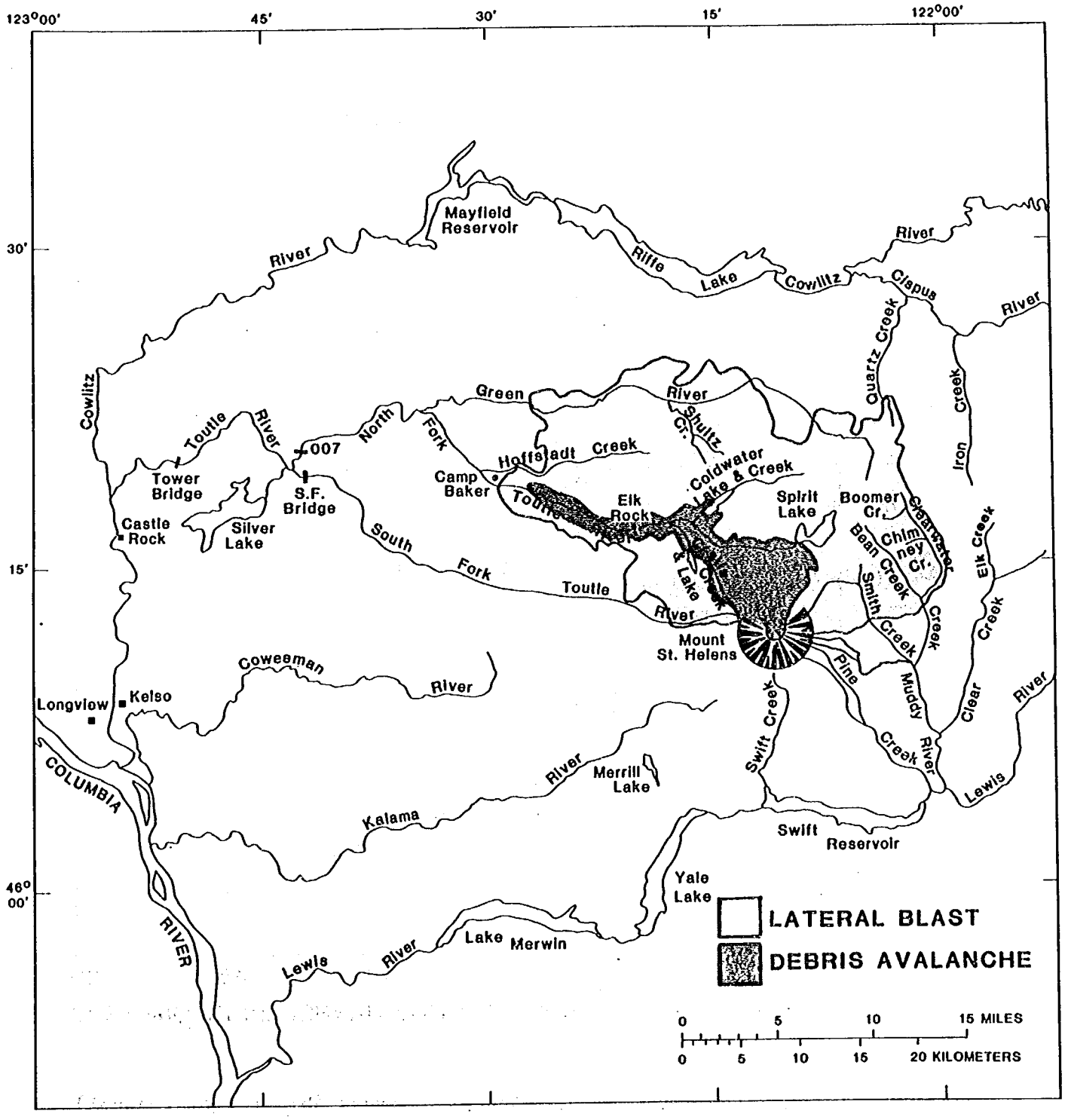


Figure 1. Mount St. Helens area, major drainage systems, lateral blast-affected area, and debris avalanche deposit.

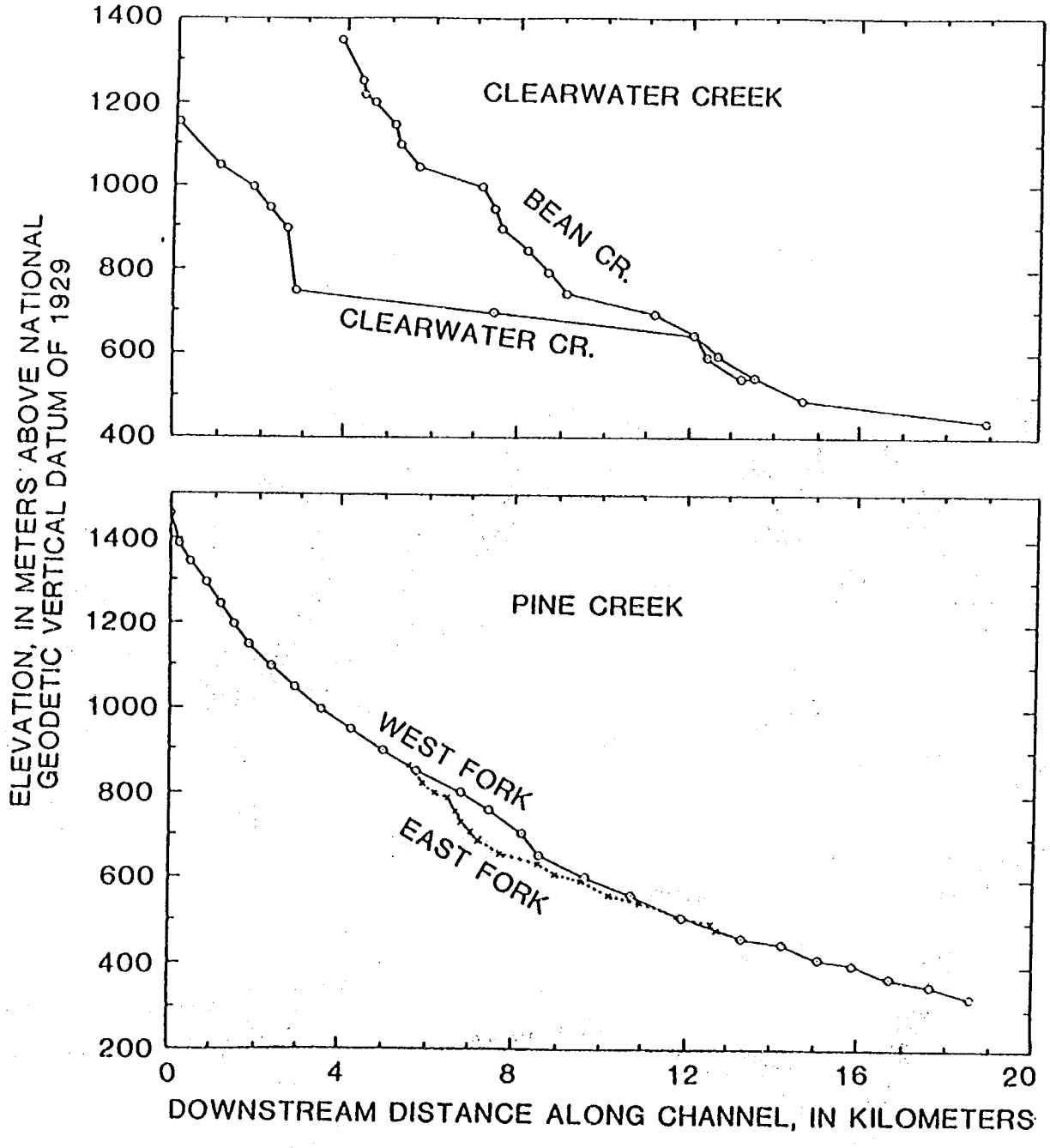


Figure 2. Longitudinal profiles of Clearwater Creek (blast area channel) and Pine Creek (lahar-affected channel), constructed from topographic maps.

This paper reports qualitative and semiquantitative post-eruption changes in drainage basins altered by the blast--to include those of the Green River, Shultz Creek (tributary to the Green River), and Clearwater Creek--and by lahars--to include those of the Toutle River, Muddy River, and Pine Creek (fig. 1). Each basin received different types and amounts of deposits during the 1980 eruptions, and the dominant processes involved in erosion and transport of these deposits in part depend on these differences.

Other investigators report on channel development on the debris avalanche in North Fork Toutle River (see Janda, this volume); problems of the lower Toutle and Cowlitz Rivers (see Stockton, this volume); and erosion on hillslopes (see Swanson and others, this volume).

Study Sites and Methods

Cross sections and longitudinal profiles in all major channels that drain the blast area were established in 1980-1981 to monitor post-eruption changes in the morphology of channels and valley bottoms, net changes in sediment storage, and the amount and rate of bank erosion. Aerial photographs (1:9600, October, 1981) provided an overview of channel change.

Blast-Area Channels

Emplacement of volcanic deposits in blast-area channels and subsequent erosion, transport, and storage of sediment vary with topography and rates of sediment input at points along drainage

networks. These processes are discussed below in order of occurrence and distance downstream.

Volcanic Events and Hillslope Deposits of 1980

The lateral blast of May 18, 1980, removed or toppled all vegetation in a 550-square kilometer area north of Mount St. Helens. Especially in the periphery of the blast-affected area, the blast shock wave and hot gases were channeled away from the general blast direction down major valleys that lead west, north, and east (Kieffer, 1981). The blast deposited from 0.025 m to more than 1 m of lithic particles and woody debris on hillslopes throughout the devastated area. In the North Fork Toutle and Green River drainages the blast deposit contains about 15 percent gravel, 63 percent sand, and 21 percent silt and clay, as well as various amounts of woody debris (Collins and others, 1982).

Tephra (airfall) deposited on May 18 and during five subsequent eruptions (May 25, June 12, July 22, August 7, and October 16-18, 1980) ranges in thickness from more than a meter on the volcano's flanks to only a few millimeters 20 km away (Waitt, 1981; Waitt and Dzurisin, 1981; Waitt and others, 1981). Prevailing winds on May 18 carried most of the ash to the north-northeast. Drainage basins adjacent to this side of the volcano were covered with up to 0.33 m of tephra having large proportions of pumiceous gravel. Ash deposits in other directions around the volcano were insignificant. May 18 airfall deposits to the north of the mountain consist largely of silt and very fine sand; to the east along the path of the plume they include pebble- and gravel-sized pumice fragments.

Subsequent eruptions (particularly that of May 25) locally deposited a thin layer of coarse sand (Waitt and others, 1981).

A few examples depict the variation between drainage basins in thickness and size composition of deposits on hillslopes. In Shultz Creek basin (fig. 1), 12-20 km northwest of the volcano, 0.1-0.5 m of sandy blast deposit is topped by 0.02-0.06 m of silty airfall ash; in Boomer Creek basin (fig. 1), 12 km northeast of the mountain, 0.18 m of sandy blast deposit is topped by 0.14 m of gravelly pumice and 0.01 m of silty ash. Basins more than 20 km northeast and east of the summit, such as those of Quartz Creek, Iron Creek, and Clear Creek (fig. 1), were outside of the blast, but received up to 0.15 m of sandy/silty ash. Elk Creek, 20 km northwest of the volcano, was largely unaffected by the blast and received only a few centimeters of silty tephra.

Blast deposits reduced infiltration of subsequent rainfall and increased runoff. These effects varied with both grain size and total thickness of tephra. Pumiceous tephra deposits northeast of the cone are more permeable than silty ash to the west. Infiltration rates of about 13 mm/hr in pumiceous tephra and 8 mm/hr in non-pumiceous tephra were measured in the summer of 1981 (Swanson and others, this volume). Infiltration rates in nonpumiceous tephra in Shultz Creek during the fall of 1980 ranged from 3 to 8 mm/hr (George Leavesley, U.S. Geological Survey, oral communication, 1981). Infiltration rates in unaffected forested watersheds in the Cascades are about 100 to 130 mm/hr (Johnson and Beschta, 1981). In areas where tephra is both fine grained and thin, the deposit may reduce infiltration and (or) act as mulch and reduce

evaporation from the soil. Erosion of relatively impermeable silty ash and exposure of more-permeable, sandy blast deposits in Shultz Creek basin have increased infiltration rates (Lehre and others, 1982).

Pre-eruption annual runoff averaged 1500 mm in the Toutle River (U.S. Geological Survey, 1981). Destruction of vegetation reduced water interception and transpiration, and may have increased runoff within the affected area by as much as 50 cm during the summer growing seasons after the eruption (Robert R. Ziemer, U.S.D.A. Forest Service, oral communication, 1982).

The post-eruption hydrologic record is too short for one to draw conclusions about changes in long-term, basin-wide hydrologic response to the lateral blast, but short-term changes are significant. Data from the Toutle River suggest that total runoff and peak discharges have increased. After the first hydrograph rises in the fall of 1980, peak runoff in the Toutle River was consistently higher and earlier than predicted by a model calibrated to historical precipitation-runoff relations (Orwig and Mathison, 1982). It is probable that reduced infiltration rates in the blast area, as well as on the debris avalanche, are responsible for the increase in peak runoff. A discharge equalled or exceeded 1 percent of the time in the Toutle River in water year (WY) 1981 was about 20 percent higher than that of a pre-eruption year, even though more than 8 percent of the Toutle River basin was not contributing runoff because tributaries were dammed by the debris avalanche. During WY 1982, the discharge of the North Fork Toutle River was significantly greater than that during the previous year due to greater precipitation and to expansion of the

contributing area by drainage integration on the debris avalanche deposit, upper North Fork Toutle River (Janda, this volume).

The blast and airfall deposits are readily erodible, because they deposited on steep terrain and are unconsolidated and contain predominantly pebble size or smaller material with little clay. Sheet and rill erosion delivered 100 to 400 m^3/ha of sediment to the streams that drain the affected watersheds in the first year after the May 18 eruption (Swanson and others, this volume). Much of the pre-1980 landscape was mantled by poorly weathered but vegetated deposits that are strikingly similar to those deposited during the 1980 eruptions. This is particularly true along the river valleys draining the cone. Banks of unweathered, pre-1980 deposits are easily undermined and large volumes of readily transportable sediment are continually introduced into streambeds. Rills and gullies forming in the 1980 tephra commonly incise into these pre-1980 deposits in areas where rill erosion had not previously occurred.

Erosion and Sediment Transport

Tephra deposits on slopes with gradients less than 70 percent have been eroded chiefly by sheetwash and rilling, while on steeper slopes (comprising 5.5 percent of the blast-affected area of the North Fork Toutle River basin), shallow slides have almost completely removed the tephra cover (Lehre and others, 1982). Much of the sediment eroded from hillslopes, particularly in clearcuts, is carried without intermediate storage to tributaries.

Low order channels in the blast-affected zone were initially choked with sandy and silty tephra (Waitt and others, 1981) and by sliding and avalanching of surge deposits from adjacent slopes during or immediately after their deposition. Blast deposits along streambanks and in fill terraces along Shultz and Hoffstadt Creeks (fig. 1) and their tributaries, for example, range in thickness from 0.05 m to more than 2 m; thickness averages 0.5 to 1 m. Mean particle size distribution of the blast deposit sampled at seven sites along Hoffstadt Creek indicate the material was 10 percent gravel, 75 percent sand, and 15 percent silt/clay.

Low-gradient reaches of low order channels in the blast-affected area, particularly above channel constrictions such as culverts, bridges, and blow-down timber, locally contain relatively thick (0.6 to 5 m) deposits of reworked coarse sandy ash with a total volume of 10^5 m^3 or less. These deposits show poorly to moderately well-defined stratification and commonly contain layers of logs or branches, particularly at the top or bottom of the deposit. The top of the deposit is generally flat to gently undulating and fairly smooth. A particularly thick deposit along West Fork Shultz Creek contains logs at its base and a convex downstream shaped log-jam embedded in its surface.

Large volumes of fresh sandy volcanic material introduced to small channels were transported up to a few kilometers by three types of flow and deposited in low gradient storage sites. In the Mount St. Helens area, muddy flows are relatively shallow Newtonian flows that contain high concentrations of sandy material and locally caused rapid aggradation. Debris flows are nonerosive slurries of sandy material

with greater sediment concentrations than muddy flows. Debris torrents are also sediment-rich slurries, but they also contain coarse channel and hillslope material and organic debris often eroded by the break-up of dams formed by blast-downed trees. Presumably, organic debris were overridden and buried or borne along in highest concentration at the top of the torrent fronts.

The processes responsible for generating these sediment-laden flows are not clear. Before the May 18 eruption, snowmelt was already contributing moderate runoff, and thick snowbanks probably persisted along steep streambanks of small, high elevation streams. Although evidence of overland runoff generated by rapid melting of snow on hillslopes is lacking (Fred Swanson, U.S.D.A. Forest Service, oral communication, 1982), the blast concentrated in valleys may have rapidly melted streamside snowbanks. Failure of unstable matrices of blown down timber that temporarily stored water and sediment apparently triggered compounding debris torrents in Shultz Creek, for example. In other cases, sediment transported by muddy flows and debris flows passed through log matrices without appreciably disturbing them.

Blast deposits were scoured from channel banks and bed in higher-gradient reaches and deposited in lower-gradient reaches where flows or torrents could spread out or pond. These deposits, first evident on the June 19, 1980, airphotos, were most likely emplaced during or shortly after the May 18 eruption. Although muddy flows and debris flows and torrents were not inventoried, it is likely that they were relatively common in steep, low-order channels in the blast zone immediately after the May 18 eruption. Muddy flows and debris torrents

have been more common than debris flows during the following high runoff seasons, but less frequent than shortly after the May 18 eruption. In view of the changing nature of deposits, sediment loads have generally declined in low order channels, except where hillslope and channel failures have released debris torrents.

Chimney Creek, a third order tributary which flows over an alluvial fan before entering Clearwater Creek, exemplifies sediment transport and deposition in low order tributaties during the first 2 years after the eruption. On May 18 a muddy flood of predominantly sand-sized volcanic material moved down Chimney Creek as far as the midpoint of the alluvial fan. Near the flow terminus, sediment was deposited as far as 30 m from the channel over the fan surface (fig. 3). Subsequently incision down to a series of steps formed over organic debris in the summer of 1980 left fill terraces as high as 3 m (fig. 4) and added more sediment to the flow terminus, but negligible amounts of sediment reached the mouth of Chimney Creek. Another muddy flow traversed the entire length of Chimney Creek during the winter of 1980-1981, depositing as much as 0.5 m of sediment over the fan as far as 100 m from the channel (fig. 3). High flow levels were less than 0.3 m above the highest terrace, as indicated by preservation of airborne ash on logs above the channel. This suggests that rapid aggradation caused a relatively shallow flow to overtop the banks and to deposit a large volume of sediment over the alluvial fan. Subsequent flows re-incised the channel down to organic steps or to a preexisting armor layer and exposed preexisting streambanks, as most of the unconsolidated sediment recently stored in the channel was removed (fig. 4).

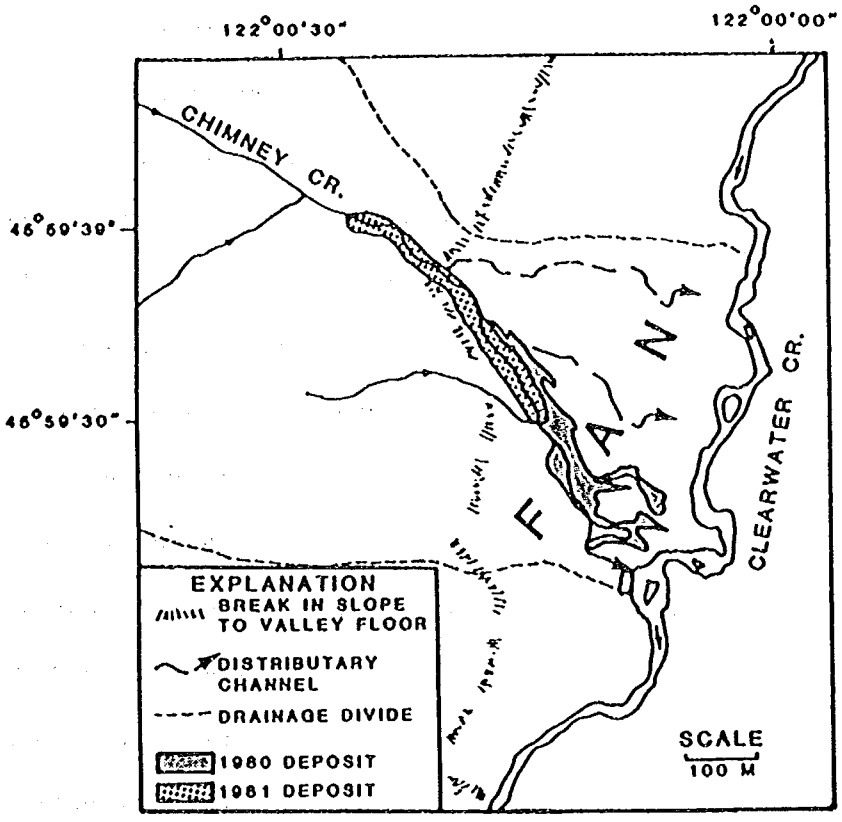


Figure 3. Deposits of 1980 and 1981 in lower Chimney Creek. Deposits are thickest near the main channel. The terminus of the 1980 muddy flow corresponds to a decrease in slope.

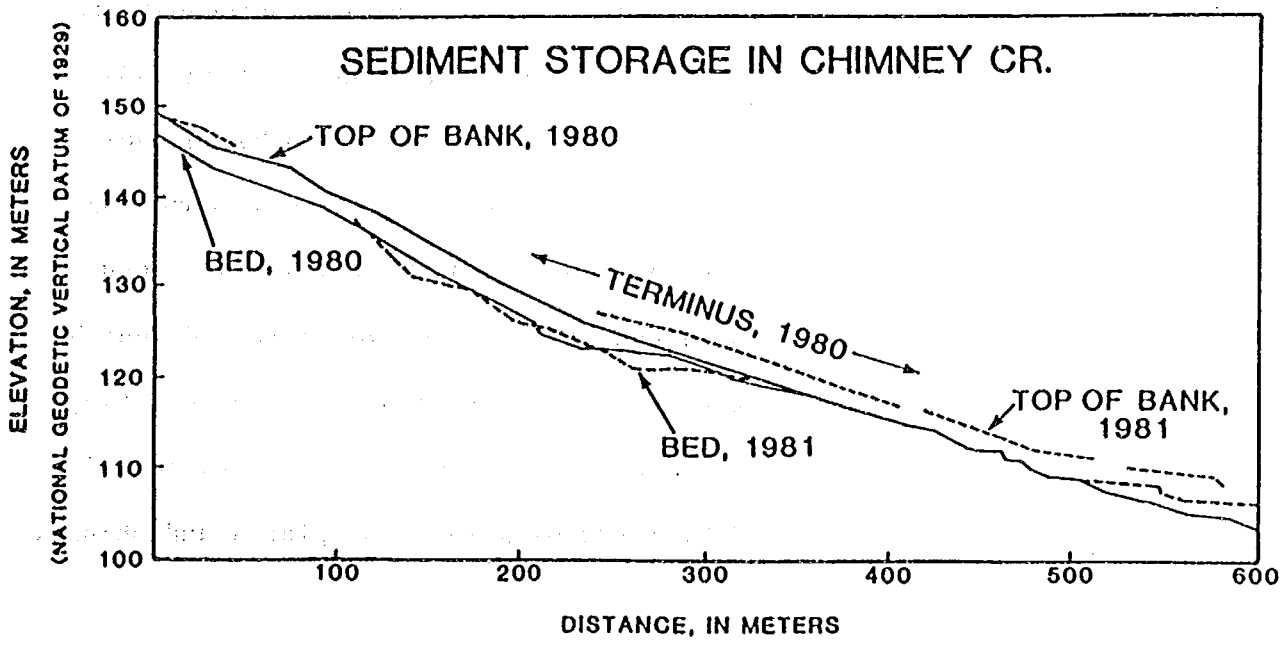


Figure 4. Longitudinal profile of Chimney Creek from the head of the alluvial fan to the mouth. Profiled banks are fill terraces composed of recent volcanic alluvium; gap in bank profile (for example, from 40 to 240 m, 1981) indicates absence or erosion of fill terraces.

Debris torrents produced by post-eruption winter storms have deposited organic debris and coarse sediment scoured from channels and adjacent hillslopes in downstream reaches. Shallow-seated debris avalanches, which often flow into channels and create debris torrents, have increased in number since the 1980 eruptions, as large storms have occurred and soil strength has declined due to rotting of roots in the area of blown-down trees (Swanson and others, this volume). For example, storms of November 1980 produced the first major runoff events after the eruption; sections of Main Fork Shultz Creek (fig. 5A) filled as a result of a debris torrent. The sandy-gravelly post-eruption bed was replaced by coarse gravel, cobbles, and small boulders. Large logs up to 1.3 m in diameter were moved. In tributaries of Shultz Creek, post-eruption debris torrents have left trim lines as high as 6 m above the channel bottom. Torrents in this case were probably generated when dams of logs and branches in narrow channel reaches suddenly broke and released a flood wave capable of transporting logs, cobbles, and boulders. Scour during subsequent storms has gradually removed some of these torrent/flood deposits (fig. 5B).

Land managers have been concerned that flow diversion by unstable organic debris may cause extensive bank erosion and channel wandering across valley flats. However, such channel instability has not been observed in the blast area. Although fine-grained volcanic sediment has been readily removed from bank storage, in most cases the pre-existing streambanks have eroded little. They are apparently cohesive, largely due to shear strength provided by roots of herbaceous plants and shrubs,

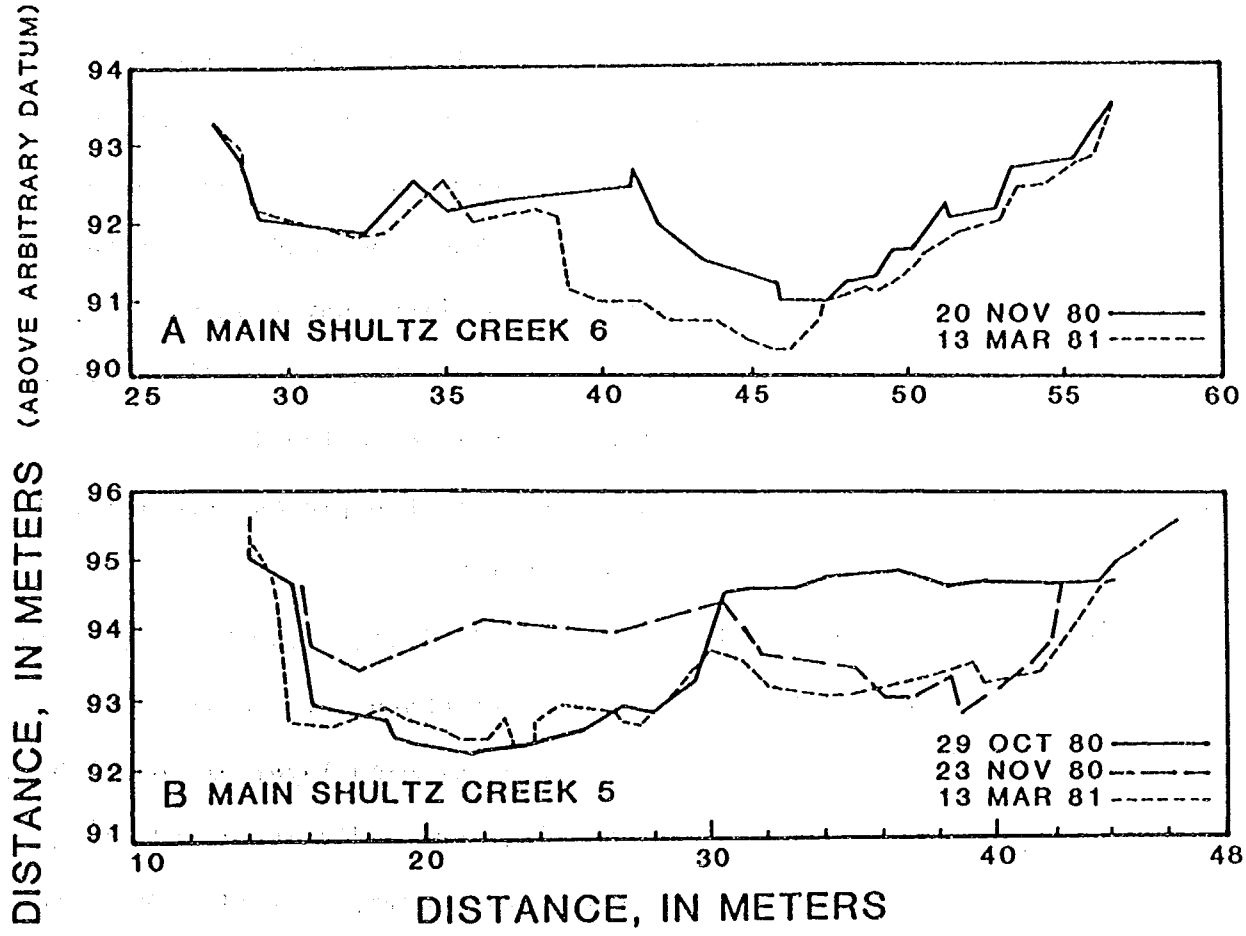


Figure 5. Posteruption changes in sediment stored in the channel of Main Fork Shultz Creek: A. Main Shultz Creek, cross section 6. Post-eruption debris torrents filled channel with coarse gravelly deposits in October and November 1980; winter flows have progressively removed these and reduced channel gradient. Channel bed is now near its preeruption position.
B. Main Shultz Creek, cross section 5. Between October 29 and November 23, 1980, high flows removed tephra deposits 1.5 m-thick on right bank; during same period debris torrent filled left half of channel with 1 m of coarse gravelly debris. Winter high flows have since degraded channel to nearly its original (preeruption) depth.

which have resprouted and grow vigorously because shade was eliminated and volcanic material was quickly removed from steep streambanks exposed to channel flow. Trees blown down from old-growth riparian areas were large (commonly 1 m in diameter and 40 m or more in height), their stems remain attached to root wads, and thus they are relatively stable. Blown down trees that move are usually anchored on one bank by their root wads or long stems. They tend to rotate about their root wads and form acute angles with the streambank, thus diverting the flow away from the streambank. Submerged logs extending across the channel can direct flow into the opposite bank, but more often only part of a log diverts the flow. Logs often broke over the channel so that two pieces were rotated by the flow and formed acute angles on either bank.

In drainage basins affected by the lateral blast, scour has generally progressed downstream to third or fourth order channels. In most low order channels the bed has scoured down to an armored layer or to bedrock, except where sediment is retained by debris; most sediment stored along the preeruption streambanks was removed by the summer of 1981. For example, at about half of the monitored cross sections in Hoffstadt Creek, Shultz Creek, and upper Green River, the channel had eroded down to bedrock or to large bed material by the summer of 1981. Subsequent erosion in these reaches has removed unconsolidated volcanic material from streambanks. Most of the remaining stored sediment resides in fill terraces and over adjacent valley flats and alluvial fans. In some places a storage reach has been depleted while an adjacent downstream site has filled. For example, during the winter of 1981, a large amount of sediment stored behind an open

framework of large organic debris in the upper Green River (cross sections 60.05-60.25, table 1) was removed and redeposited in a downstream reach (cross sections 60.40-60.50). Without further large sediment contributions, sand- and silt-sized material comprising the bulk of volcanic sediments that were in contact with winter flow have been removed. Scour to stable levels by channels that have not been affected by lahars is generally followed by bank erosion of unconsolidated volcanic material deposited during and after May 18. For example, the reach of the upper Green River that filled in 1981 has scoured downward, but had not yet widened by summer 1982.

Table 1. Changes in cross-sectional area of Green River channel, summer 1980 to summer 1982. Total change in cross-sectional area was divided by bankfull width to facilitate comparing the magnitude of changes observed.

Cross section No.	Distance from mouth of Green River (km)	Area change 1/ (m^2/m)
60.05	47.75	+0.52
60.10	47.70	+0.22
60.15	47.66	+0.39
60.20	47.61	+0.49
60.25	47.57	+0.51
60.40	46.00	-0.38
60.50	45.95	-0.33

1/ Negative value, channel aggradation; positive value, channel scour

Although large volumes of sand remain in storage above the high water levels for the winters of 1980 and 1981, much of the material eroded from hillslopes has probably been carried out to major rivers (Lehre and others, 1982). This hypothesis is supported by time-sequential photographs of stream reaches taken from monumented points. The photographs show progressive coarsening of the bed, removal of tephra deposits on banks, and no systematic buildup of sediment around logs and stumps on footslopes. Fine sediment, which makes up the bulk of the material in storage sites, is rapidly transported through the drainage systems into high order channels. Sediment concentrated in storage reaches may be expected to disperse as it moves downstream.

Sediment Storage

Sediment storage in blast-area channels depends on (1) rate of sediment delivery to potential storage sites (sediment delivery is apparently most rapid where thick tephra deposits initially covered steep channels and hillslopes); (2) storage potential (length and width of valley flats, amount of large organic debris, and channel gradient); and, (3) coarseness of deposits.

Green River and Clearwater Creek, the two major basins affected mainly by the blast, have been sculpted not so much by recent volcanism as by fluvial erosion, mass wasting, and glaciation. These processes, operating on materials of varying resistance, have produced breaks in slope in stream channels (for example, Clearwater Creek, fig. 2) and of adjacent hillslopes. Low gradient stream reaches, alluvial fans, and valley flats

downstream from steep reaches and at the base of steep hillslopes are common storage sites for fluvially worked volcanic sediment.

Although most sand-sized volcanic sediment has been removed from the channel of Chimney Creek, sediment deposited over the alluvial fan may be expected to remain in storage for centuries because overbank flows are very infrequent. The channel of Chimney Creek presently bounded by high fill terraces appears large enough to carry the highest flows except for perhaps a debris torrent. Important volumes of sediment thus appear to be in long-term storage on alluvial fans and floodplains of low-order tributaries. In Boomer Creek, a tributary to Clearwater Creek and similar in size, morphology, and aspect to Chimney Creek, 34 percent (12,500 m^3) of the storage of recent volcanic sediment is in two alluvial fans. The long residence of sediment on tributary fans is further evidenced by their construction in glaciated valleys since the last major ice advance (about 12,000 yr before present) and their support of a mature forest before the May 18 eruption.

In Boomer Creek, northeast of the crater, much sediment (0.21 m^3/m sampled channel) remains in storage on the beds of low order tributaries (table 2). Relatively low rates of runoff over coarse pumice airfall and many down trees are most likely responsible for greater amounts of sediment remaining in storage in Boomer Creek than in streams to the west, such as Shultz Creek.

Coarse clasts deposited by outburst floods or debris torrents from behind debris dams appear to be the most persistent deposits. For example, alluvial fan deposits dominated by cobbles and boulders at the

Table 2. Sediment in storage components of Boomer Creek. For each storage component, values for sediment volume per unit length of sampled channel are listed above values for the percentage that volume represents of the total stored sediment in each stream order. The volume of sediment per unit length of sampled channel is determined by dividing the volume of sediment in the sampled reach, in cubic meters, by the length of sampled reach, in meters A fourth order channel in this analysis is classified as a third order channel in table 3.

Stream order	Sampled Channel Length (m)	Storage components						Total Channel Length[2] (m)	Total Volume Sediment in Storage[3,4] (m^3)
		Alluvial fans (m^3/m) (%)	High flow terraces (m^3/m) (%)	Debris related (m^3/m) (%)	Bed (m^3/m) (%)	Other (m^3/m) (%)	Total[1] (m^3/m) (%)		
1	379	0.004 1	0.053 15	0.118 32	0.152 42	0.036 10	0.363	15,460	5,610
2	464	.237 26	.104 11	.162 18	.401 44	.005 1	.909	6,600	6,000
3	384	0 0	.500 19	1.39 53	.114 4	.604 23	2.61	2,340	6,110
4[4]	1190	1.35 37	.553 15	1.59 43	.129 4	.043 1	12.90	2,240	8,200
All channels[5]		.175 18	.147 15	.364 37	.209 21	.079 8	.974	26,640	

	Storage components					
	Alluvial fans	High flow terraces	Debris related	Bed	Other	
Total volume of stored sediment (m^3)[5]	4,670	3,920	9,700	5,560	2,100	25,900

1/ Percentages may not sum to 100% exactly because of rounding errors.
2/ Sampled length plus unsampled length of channel.
3/ Volume of sediment per unit length of sampled channel multiplied by total storage length for all storage components.
4/ A large alluvial fan deposited over the broad central valley of Clearwater Creek is not included in this analysis. This fan contains an additional 11,000 m^3 of stored sediment.
5/ Values calculated by extrapolation of sampled channel data over total channel lengths for all stream orders in the basin.

mouth of Shultz Creek were only moderately modified by flows during the winter of 1981. This stands in marked contrast to the rapid removal of sandy deposits from the active channels of most upstream reaches.

Trees blown into channels by the lateral blast, as well as preexisting large organic debris in streams, cause significant sediment storage in channels as large as fourth order streams (order determined for blue line streams on 7.5 minute topographic quadrangles). Large organic debris (more than 0.1 m in diameter) cause sediment deposition by locally raising the streambed base level, by creating protected eddies in complex matrices that trap sediment, and by increasing the frequency of sediment-laden overbank flows. As observed in other areas (Keller and Swanson, 1979), debris-stored sediment is proportionately greatest in low order channels.

Unless a debris torrent occurs, large organic debris in small channels are not readily moved until they rot away. Sand-sized volcanic sediment may be transported through a framework of large organic debris, but debris on channel bottoms and sealed log jams may cause upstream deposits several meters thick. In Boomer Creek basin, debris accounts for 53 percent of all storage in third order channels and 37 percent of all storage in the entire drainage network, disregarding the alluvial fan at the mouth of Boomer Creek (table 2).

In fourth order channels, debris may be redistributed by high flows and concentrated into debris jams. This may increase the storage effectiveness of organic debris, as in upper Clearwater Creek where a series of debris jams created sediment storage sites that resemble a

string of pearls (Fred Swanson, U.S.D.A. Forest Service, oral communication, 1982). In Bean Creek (fig. 1), a tributary of Clearwater Creek, large jams which have formed behind bedrock constrictions at the downstream end of low gradient reaches have ponded large volumes of sediment.

Large organic debris commonly occupy as much as 30 percent of the bankfull cross-sectional area of Clearwater Creek. By thus reducing channel capacity while increasing flow resistance, the debris increases the frequency of overbank flows. A reach with little organic debris in the channel nearly reached bankfull stage during WY 1981. In adjacent reaches with much debris, flows overtopped the banks and deposited sediment over the flood plain in some areas and eroded airfall and blast deposits in others.

Lahars, or the debris avalanche, in the North Fork Toutle River blocked the mouths of tributaries and created 12 large storage sites for sediment eroded from blast-affected drainage basins. Dammed tributary mouths form the largest storage sites in channels that did not carry lahars. For example, 9.2×10^5 m^3 of sediment was stored within 1.3 km of the mouth of Clearwater Creek, which was dammed by a lahar in the Muddy River. This volume, which is probably less than that contained in similar storage sites along the North Fork Toutle River, is greater than that in any other storage reach unaffected by lahar damming. Flow at the mouth of the Green River was impounded behind the North Fork Toutle River lahar, causing deposition of up to 2 m of fine-grained, thixotrophic sediment.

Channel gradient appears to be a determining factor in the storage of sediment since the May 18 eruption. Channel reaches storing significant amounts of sediment in Clearwater Creek, the mainstem Green River, and Shultz Creek were mapped from aerial photos taken in the fall of 1981. In a plot of cartographic slope versus drainage area for channel reaches (fig. 6), a function derived from discriminant analysis separates fields of points that correspond to storage and nonstorage reaches. As expected, the tendency for sediment storage increases with decreasing gradient and increasing drainage area.

Relatively low gradient reaches where sediment has been stored are still steeper than most stable sand-bed streams. Rough estimates of maximum stream gradients of coarse sand-bed channels with zero transport, on the basis of Shield's criteria and estimated flow depths at low flow, range from 0.001 to 0.0003 m/m well below the minimum slope (0.005 m/m) of the reaches represented in figure 6. Before the May 18 eruption, most channels were armored with gravel; these streams will probably become armored again as erosion rates decrease and fine-grained sediment passes out of the drainage systems.

The total length of storage reaches (mapped from aerial photographs) is proportionately greatest in third and fourth order channels (table 3). In lower order channels, storage is less because channel slopes are steeper, valley flats are less prevalent, and upstream channel storage has been depleted. Fifth order channels store sediment along proportionately less of their length, presumably for the following reasons: 1) sediment pulses from upstream reaches have been depleted by deposition and dispersed as they moved downstream, 2) maximum loads may not yet have reached some mainstem channels, and 3) fifth order channels are too large for large organic debris to store sediment.

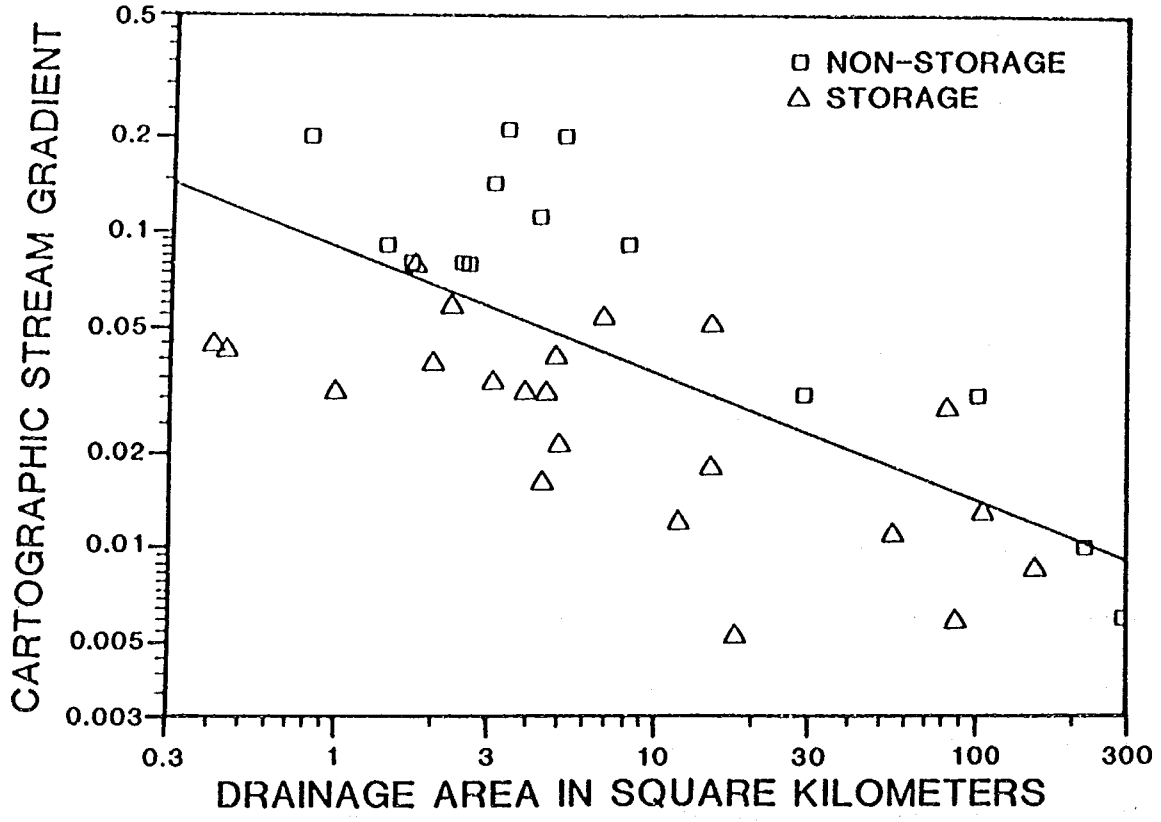


Figure 6. Cartographic slope versus drainage area of reaches of Shultz Creek, Clearwater Creek, the mainstem of Green River showing sediment storage in banks and valley flats in October 1981, and of reaches showing no storage. A discriminant function separates storage and nonstorage reaches.

Lahar-Affected Channels

Volcanic Events and Deposits

On May 18 lahars flowed down upstream reaches of all streams flanking Mount St. Helens. Major lahars flowed the entire length of the Toutle River and entered the Cowlitz River, while others flowed down Smith Creek, Muddy River, Pine Creek, and Swift Creek, eventually entering

Table 3. Distribution of sediment storage reaches by stream order in Clearwater Creek, mainstem of Green River, and Shultz Creek. (Mapped from aerial photographs, U.S. Geological Survey series 24327, October 20, 1981.)

Stream order[1/]	Percent length of channels[2/]			Total channel length (km)
	No storage	Storage limited to one channel width from banks	Storage extending beyond one channel width from banks	
2	65.4	32.0	2.7	20.6
3	29.9	61.4	8.6	19.8
4	14.8	47.4	37.9	19.9
5	62.7	20.8	16.5	25.8

1/ From blue line streams on 7.5 minute quadrangles.

2/ Each reach of channel classified as only one of the three storage categories.

Swift Reservoir (fig. 1). Grain size, composition, and thickness of lahar deposits are highly variable, both down-valley and cross-valley (Janda and others, 1981). Lahar deposits on major streams range from one to several meters thick near the channel and generally thin to zero as they spread across the floodplain or terraces. Where lahars ponded, as on the lower North Fork Toutle River, overbank deposits may locally be thicker than near-channel deposits (Janda and others, 1981). Lahar deposits are poorly sorted and commonly appear similar in grain size and composition to older lahars exposed in stream banks. Mean particle size distributions ranged from 21 percent gravel, 59 percent sand, and 20 percent silt/clay to 74 percent gravel/boulders, 19 percent sand, and 7 percent silt/clay for lahar deposits on the North Fork Toutle River (Lehre and others, 1982).

Lahar deposits are limited primarily to the valley bottoms of the major streams that flank the volcano and thus directly affect main-channel processes. The relative importance of lahars to posteruption channel adjustments depends on the presence of other volcanic deposits in the basins. Basins of Smith Creek and North Fork Toutle River lie mostly in the blast area; basins of Pine Creek and South Fork Toutle River are mostly outside the areas of the blast and the high airfall (fig. 1). In the North Fork Toutle River, fluvial reworking of the debris avalanche deposit has dominated fluvial processes that are otherwise influenced by effects of the blast, airfall, and lahars (Janda, this volume).

The poorly sorted lahar and debris avalanche deposits tend to be nearly impermeable and thus, similar to blast and airfall deposits,

tend to increase storm runoff. Although lahars affected a much smaller percentage of the total devastated area than did the lateral blast, runoff from lahars is contributed directly to mainstem channels. The anticipated increase in peak runoff in rivers, however, has not been well documented.

Although lahar deposits are coarser than blast and airfall deposits, they also have low cohesion and are easily eroded by lateral channel migration. They directly contribute a large volume to the sediment load of the major rivers that drain Mount St. Helens.

Sediment Transport and Channel Changes

May 18 lahars in North and South Fork Toutle Rivers, Smith Creek, Muddy River, and Pine Creek apparently transported more sediment than subsequent individual hydrologic events. Because lahars completely or partly buried pre-existing channels, subsequent low flows were contained in reduced channels or incised into the surface of the lahar deposit. Channel roughness was reduced by loss of sinuosity, by disruption or burial of the pre-existing cobble-boulder bed, and by obliteration of bar-pool topography. Winter floods have extensively reshaped lahar-affected channels. High flows have incorporated large sediment loads by enlarging channels formed during recession of lahars and by migrating laterally against highly erodible banks. Channels have simultaneously widened and either aggraded or degraded. In alluvial reaches, volumes of sediment produced by channel widening exceed

volumetric changes in storage caused by bed aggradation or degradation. Channel widening thus strongly influences net sediment storage.

Sediment transport and channel adjustment in the mainstem and North Fork Toutle River occur chiefly during high discharge events. This timing is attributed to an increase in peak runoff and to accelerated erosion of the debris avalanche in the North Fork Toutle River during storm runoff. During Water Year (WY) 1981, suspended sediment load of the Toutle River was about 26.8×10^6 megagrams (Mg). About 46 percent of this was discharged in four days in two storm-induced floods (fig. 7).

In reaches bounded by banks or terraces of erodible alluvium or lahar deposits, channels were surveyed only between flood events. Frequent surveys at the South Fork County Bridge, North Fork Toutle River at 007, and Elk Rock (within the debris avalanche) from February 1981 to January 1982 showed little change during this period of low peak discharge (fig. 8). At North Fork Toutle River at 007 and Elk Rock, flood-related deposition and erosion after January 1982 were 5 to 10 times greater than during the preceding period of lower flows. The section near Camp Baker showed substantial erosion from May 1981 to January 1982 but also showed pronounced erosion and deposition during the storm period beginning in January 1982.

Channel integration, incision, and widening in the debris avalanche deposit was a major source of sediment during WY 1981 (Janda, this volume). Most eroded material downstream of the debris avalanche consists of older lahar and alluvial deposits. For example, at Camp Baker (fig. 9) material eroded from the right bank consisted of more than

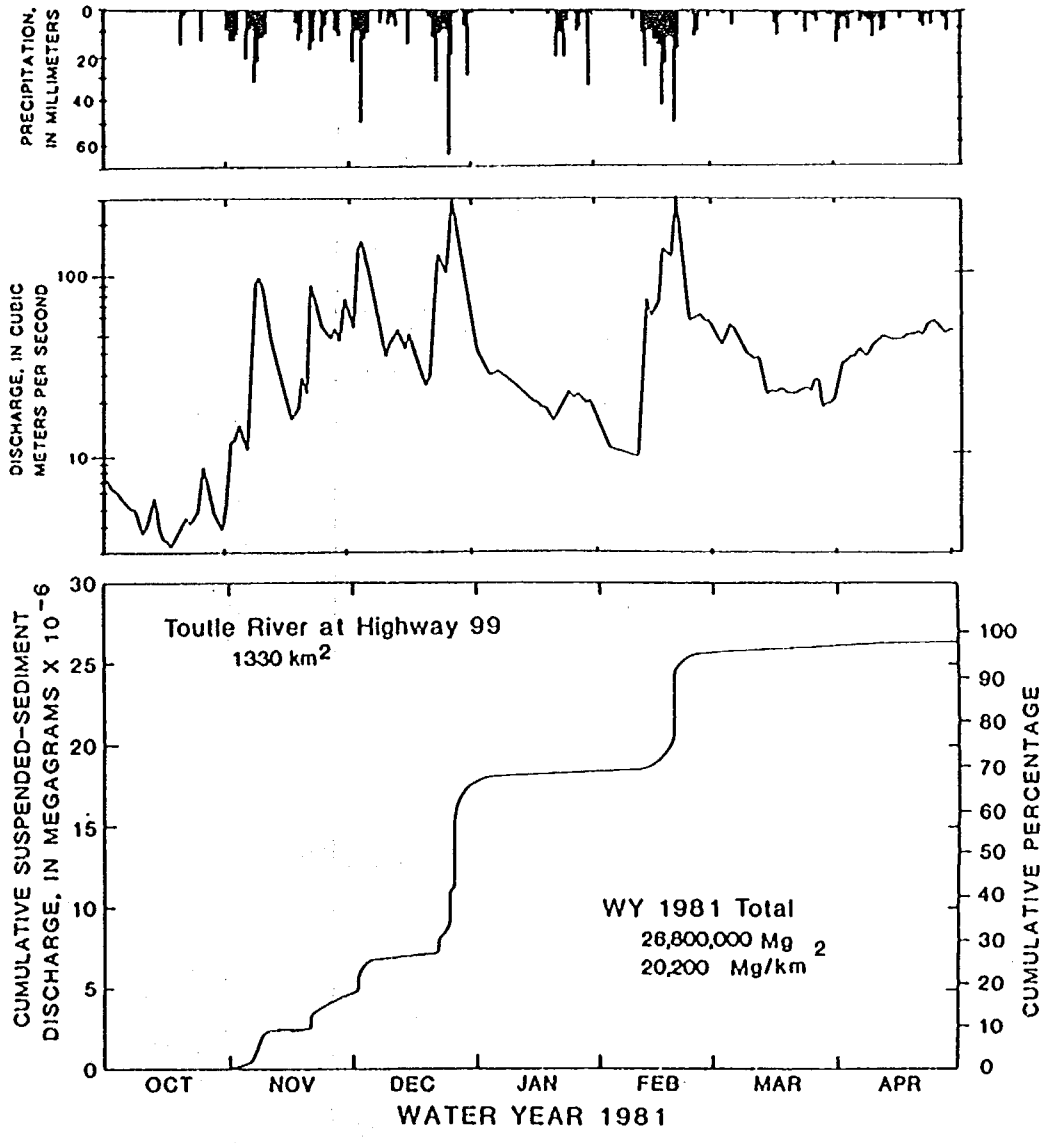


Figure 7. Daily precipitation and daily mean discharge of the North Fork Toutle River near Kid Valley, and cumulative suspended sediment discharge of the Toutle River at Highway 99, WY 1981.

7 m of older lahars and alluvium, mantled by less than 0.5 m of May 18 lahar deposits. Although much of the total load of the Toutle River was derived from the debris avalanche deposit, the portion of the load contributed in the downstream reaches greatly exceeded that deposited by the 1980 lahars (Meyer and others, 1981; Martinson and others, 1981).

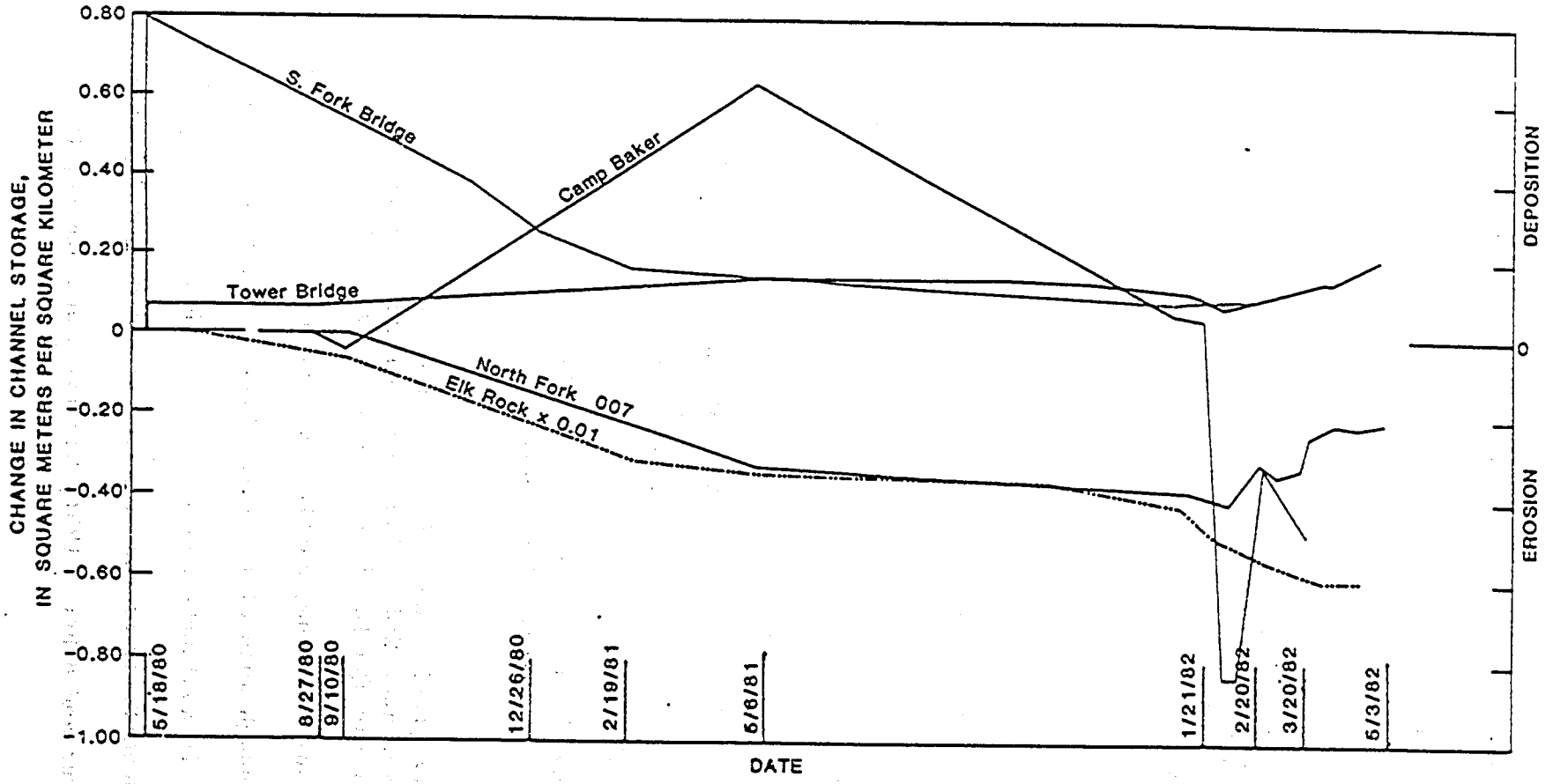


Figure 8. Changes in channel storage, normalized by dividing cross-sectional area by drainage area, at sites on the Toutle River (Tower Bridge), North Fork Toutle River (Camp Baker, 007, and Elk Rock), and South Fork Toutle River (S. Fork Bridge).

As observed with other volcanoes (Davies and others, 1978; Japan International Cooperation Agency, 1980) bed particle size decreases downstream in the Toutle River, presumably due to selective transport of small particles and the disintegration of large ones. The largest boulders in a given reach are generally a lag deposit derived from lahars or eroded banks of older lahars and alluvium, and thus maximum bed material size does not necessarily reflect local competence. Therefore, somewhat finer grains were examined in active bars for an indication of local competence. On the North Fork Toutle River, the size of D_{85} (the grain size of which 85 percent of the sediment in a given sample is finer) decreases downstream. Downstream of the toe of the debris avalanche near Camp Baker, the size of D_{85} is about 100 mm, whereas at the Kid Valley gaging station, 16 km downstream, it is only about 50 mm. En echelon bars, where grain size was measured, are commonly covered by medium- to fine-grained sand deposited during low flows. Below Tower Bridge in the lower Toutle River, channel deposits rarely contain particles larger than coarse sand, and although the channel braids, en echelon bars do not form.

Large volumes of sediment produced during storms have apparently been mainly responsible for channel adjustments downstream. Post-eruption channels were overwhelmed by greatly increased sediment loads. In the Toutle River, channel width commonly increased 150 to 200 percent during the winters of WY 1981 and WY 1982 (fig. 9, for example), and the channel became braided wherever it was unrestricted by bedrock or man-made constrictions. Braiding and aggradation occurred as en echelon bars spread and accreted. Although most braided channels aggraded, net

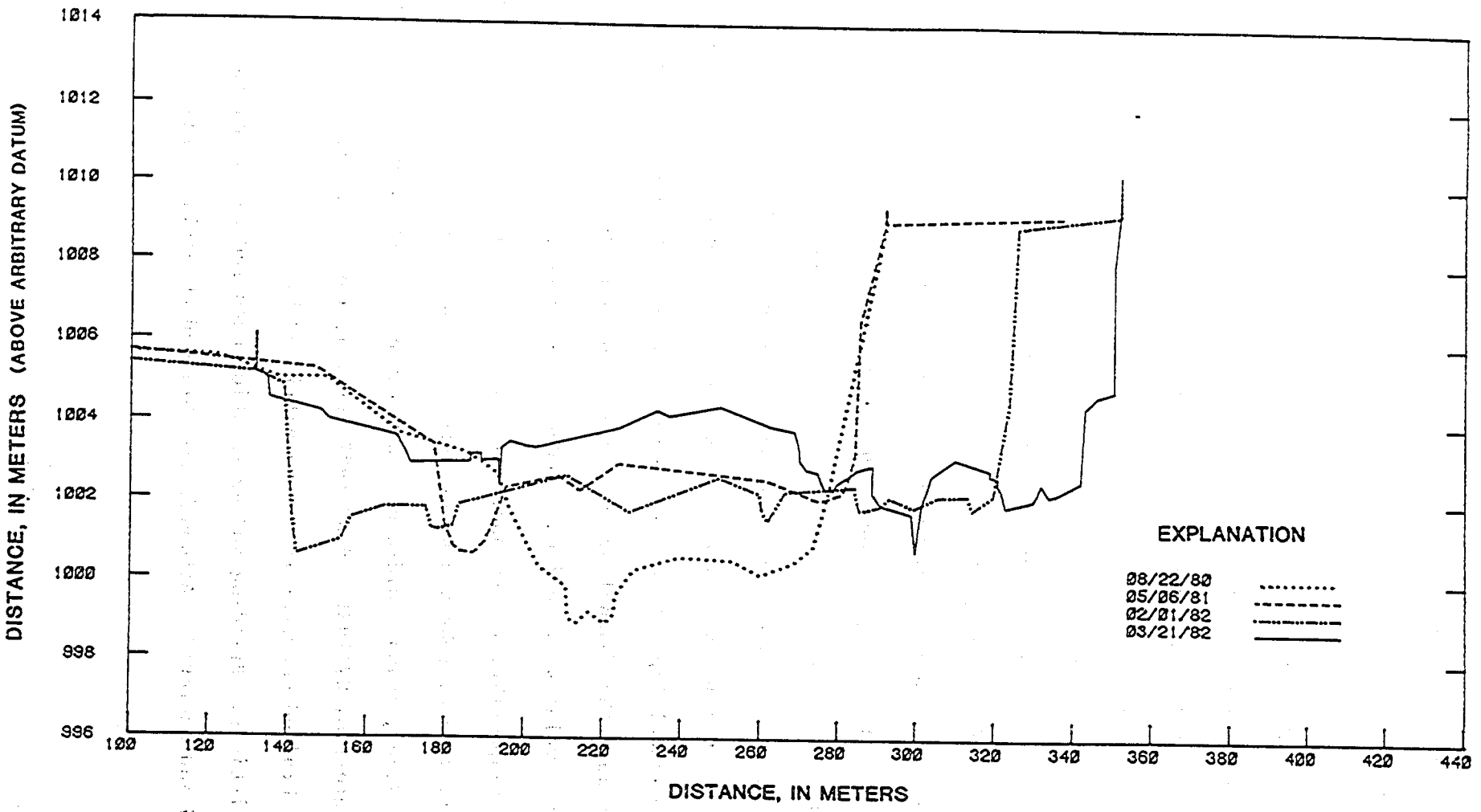


Figure 9. Cross section of the North Fork Toutle River near Camp Baker. Lahars deposited as much as 1 m of sediment on the flood plain. Channel changes during the following low flow season were negligible. During the winter of water year 1981, sediment-laden floods aggraded the channel about 2 m, and the channel pattern shifted from straight to braided. Although the channel widened by about 50 percent, net sediment storage increased. The channel aggraded similar amounts during water year 1982, but massive bank erosion occurred. The decrease in sediment storage caused by bank erosion exceeded the increase in storage by channel aggradation.

sediment storage decreased as larger volumes of material were removed from banks than were deposited in the widening channel. Note, for example, the decrease in sediment storage in cross sections on alluvial reaches at North Fork Toutle River at Camp Baker (fig. 8 and 9) and at North Fork Toutle River 007 (fig. 8).

As in the North Fork and mainstem, changes in the South Fork Toutle River have generally resulted from lateral channel migration with little change in average bed elevation (table 4). Cross sections along the South Fork Toutle River were surveyed less frequently than at many sites on the North Fork and mainstem, but a series of cross sections were surveyed during the summers of 1981 and 1982. Average changes at 20 cross sections were as follows: channel width +12.5 m, bed elevation -0.02 m, sediment storage -35.6 m^2. Changes in average bed elevation in the middle and lower reaches varied randomly, but the upper-most reaches showed consistent incision (less than 0.5 m). All cross sections but two showed significant widening, generally more than 20 percent in the lower 5 km of the channel.

Sediment removal from the South Fork Toutle River channel is similar to that in the North Fork at Camp Baker and 007. Channel widening is nearly ubiquitous. Although changes in average bed elevation are commonly negligible or positive, sediment storage has decreased due to erosion of channel banks composed predominantly of pre-May 18 alluvium and lahar deposits.

In contrast to alluvial reaches, low gradient reaches with narrow valley walls of bedrock (for example, Tower Bridge, fig. 8) have filled discontinuously, resulting in sediment storage. Changes in geometry during floods have been monitored only at nonalluvial reaches where river

Table 4. Changes in channel width, average bed elevation, and sediment storage during Water Year 1982 at selected sites along the South Fork Toutle River.

Cross section No.	Change in channel width (m)	Change in channel width (%)	Change in avg. bed elevation (m)	Change in sediment storage (m^3/m)1	Distance upstream from mouth (km)
20-2	9.9	17	-0.31	-40.2	1.3
20-5	1.4	2	-0.29	-25.1	2.2
20-6	25.8	18	-0.45	-182.	2.4
20-7	60.3	91	0.35	-152.	2.6
20-9	42.0	81	0.65	-34.6	3.0
20-13	21.8	41	-0.25	-58.2	4.1
20-15	11.3	29	0.55	11.0	4.5
20-17	38.6	37	0.84	27.2	5.1
20-24	0.9	1	-0.17	-16.9	7.4
20-43	5.3	11	-0.03	-4.91	13.0
20-44	0.8	1	-0.04	-12.8	13.3
20-46	0.6	1	0.14	12.6	13.8
20-47	0	0	0.04	2.23	15.8
20-49	8.7	21	0.27	-0.95	16.4
20-103	4.4	4	0	-9.12	29.5
20-105	10.8	16	-0.56	-61.7	30.6
20-108	3.8	2	-0.23	-46.4	31.8
20-109	1.2	2	-0.44	-60.8	32.1
20-111	0.1	0	-0.26	-12.9	32.6
20-131	2.1	2	-0.26	-47.2	37.8

1/ Positive values, deposition; negative values, erosion.

banks are stable or artificial, such as at gaging stations or bridges. At these sites, channels have scoured during the rise and peak of a flood, then have aggraded during the recession. Some sections along the lower Toutle and Cowlitz Rivers have continued to aggrade for weeks or months after a flood. Downstream transport of fine sediment eroded from the debris avalanche and from upstream bank erosion is probably responsible for persistent aggradation during low flow after floods.

Summary and Conclusion

Post-eruption adjustments of stream channels that drain the area around Mount St. Helens show some significant differences between channels that carried lahars and those that carried only sediment eroded from lateral blast deposits, airfall, and pre-existing soils. The debris avalanche in the North Toutle River and lahars in mainstem channels around Mount St. Helens are ready sources of relatively coarse sediment along major channels. In contrast, blast and airfall deposits are finer (mostly sand-size) and are distributed throughout these drainage basins. Sediment derived from these deposits is transported and stored by sequences of processes operating from hillslopes to tributaries to mainstem channels. The impact of blast and tephra deposition has been manifested primarily in changes in hillslope and low order tributaries, with relatively minor effects on mainstem channels, whereas the debris avalanche and lahars have directly affected channel form and processes on larger streams. Stream channels in basins that received only airfall (no blast) have shown no significant sedimentation.

Changes in blast area channels have generally been shorter term, smaller scale, and more localized than changes in lahar-affected channels. Predominantly sand-sized blast and airfall material introduced into these mostly steep mountain streams has been quickly removed, unless upstream sediment inputs periodically overwhelmed the transport capacity. Large volumes of this material pass through channels without substantially modifying them. Intricate matrices of blown down timber, pre-existing vegetated streambanks, and armor layers appear to be little disturbed during voluminous fill-scour sequences. However, the frequency of erosive debris torrents seems to have increased since the 1980 eruptions, probably due to sudden large impulses of sediment triggered by surficial landslides of volcanic material and by the breakup of debris jams in steep, low order channels. Debris torrents have created long-term changes by scouring channels and depositing coarse debris in low gradient reaches. Deposition at levels high above streambeds by debris torrents and debris flows has placed material in long-term storage over alluvial fans and valley flats. The distribution of sediment storage areas shows a stream gradient threshold decreasing with drainage area. The areal extent and volume of sediment storage increases with stream order, although highest order channels store relatively little sediment due to upstream storage. Blown down trees form many storage sites, particularly in low order channels.

Lahar-affected channels and flood plains were covered by as much as 1 to 5 m of material as large as boulders, and the size of channels was initially reduced. Subsequent high flows have widened alluvial channels

and caused complex sequences of scour and fill over a range of several meters in bed elevation. In the South Fork Toutle River, which was affected only by lahars, upstream reaches have been incised, and middle and downstream reaches have changed little in elevation. In the North Fork and mainstem Toutle Rivers, which receive large amounts of sediment from the debris avalanche and blast area, channels have aggraded intermittently.

Ubiquitous channel widening, commonly by over 100 percent, has decreased the volume of sediment stored in lahar-affected channels, in spite of several meters of aggradation. Most of the sediment removed has been derived from pre-1980 lahar and alluvial deposits. Unlike blast area channels, there are no pronounced low gradient reaches in the lahar-affected channels to preferentially store sediment. Sorting and disintegration of sediment in fluvial transport has reduced the size of bed material by one half over a distance of 16 km in the North Fork Toutle River.

Acknowledgments

Critical reviews from D. Hagans, H. M. Kelsey, W. Weaver, and G. P. Williams aided considerably in the preparation of the final manuscript. The National Science Foundation provided funding for some of the field research.

REFERENCES

Collins, B.; Dunne, T.; and Lehre, A. K. 1982. Sediment influx to the Toutle River from erosion of tephra, May 1980-May 1981. In Proceedings: Mt. St. Helens: Effects on Water Resources. Jantzen Beach, Oregon, Oct. 7-8, 1981, Pullman, State of Washington Water Research Center, p. 82-97.

Davies, D. K.; Vessell, R. K.; Miles, R. C.; Foley, M. G.; and Bonis, S. B. 1978. Fluvial transport and downstream modifications in an active volcanic region. In Fluvial sedimentology, A. D. Miall (ed.), Can. Soc. Petrol. Geol., Calgary, Alberta, p. 61-84.

Janda, R. J. (this volume) Emplacement and subsequent erosion of the debris avalanche associated with the May 18, 1980 eruption of Mount St. Helens.

Janda, R. J.; Scott, K. M.; Nolan, K. M.; and Martinson, H. A. 1981. Lahar movement, effects, and deposits: U.S. Geol. Surv. Prof. Paper 1250, p. 461-478.

Japan International Cooperation Agency. 1980. Master plan for land erosion and volcanic debris control in the area of Mt. Merapi. Supporting 1, Republic of Indonesia.

Johnson, M. G.; and Beschta, R. L. 1981. Seasonal variation of infiltration capacities of soils in western Oregon: USDA Forest Service Res. Note PNW-373.

Keller, E. A.; and Swanson, F. J. 1979. Effects of large organic material on channel form and fluvial processes: Earth Surf. Proc., v. 4., p. 361-380.

Kieffer, S. W. 1981. Fluid dynamics of the May 18 blast at Mount St. Helens. U.S. Geological Survey Professional Paper 1250, p. 379-400.

Lehre, A. K.; Collins, B.; and Dunne, T. 1982. Preliminary sediment budget for the North Fork Toutle River drainage, Washington. In Proceedings: Mt. St. Helens: Effects on Water Resources. Jantzen Beach, Oregon, Oct. 7-8, 1981, Pullman, State of Washington Water Research Center, p. 215-234.

Martinson, H.; Meyer, D.; and Janda, R. 1981. Storm-induced changes in channel morphology of mudlfow-impacted streams (abst.). Proceedings, Mt. St. Helens: Effects on Water Resources. Jantzen Beach, Oregon, Oct 7-8, 1981, Pullman, State of Washington Water Research Center, p. 215-234.

Meyer, D.; Janda, R.; and Martinson, H. 1981. Initial and subsequent stream responses to the 1980 eruption of Mount St. Helens (abst.). American Geophysical Union, Pacific Northwest Section 1981 Meeting, Sept. 17-18, Ellensburg, Washington.

Orwig, C. E.; and Mathison, J. M. 1982. Forecasting considerations in Mount St. Helens affected rivers. In Proceedings, Mt. St. Helens: Effects on Water Resources, Jantzen Beach. Oregon, Oct 7-8, 1981, Pullman, State of Washington Water Research Center, p. 215-234.

Stockton, S. (this volume) Engineering responses to the eruptions of Mt. St. Helens.

Swanson, F. J.; Collins, B.; Wicherski, B. P.; and Dunne, T. (this volume) Erosion of hillslopes affected by volcanic eruptions.

U.S. Geological Survey. 1981. Water data report WA-80-1, Water resources data for Washington, v. 1, Western Washington. 432 p.

Waitt, R. B., Jr. 1981. Devastating pyroclastic density flow and attendant air fall of May 18--stratigraphy and sedimentology of deposits. U.S. Geological Survey Professional Paper 1250, p. 439-460.

Waitt, R. B., Jr.; and Dzurisin, D. 1981. Proximal air-fall deposits from the May 18 eruption--stratigraphy and field sedimentology. U.S. Geological Survey Professional Paper 1250, p. 601-616.

Waitt, R. B. Jr.; Hansen, U. L.; Sarna-Worjcicki, A. M.; and Wood S. H. 1981. Proximal air-fall deposits of eruptions between May 24 and August 7, 1980 - stratigraphy and field sedimentology. U.S. Geological Survey Professional Paper 1250, p. 617-628.

The mechanism of occurence and its flow of the mud-debris flow

ATSUYUKI DAIDO*

ABSTRACT

This paper treats the introduction of the study on the mechanism of the occurence and its flow of the mud-debris mainly in Japan. The mud-debris flow is devided into two groups. One is caused by the fluidization of deposit in agully. The second is caused by extrusion of the volcanic ashes. For the fluidization of the deposit, the threshold condition of the fluidization in which it will be started is explained by an equilibrium of the force. The flow mechanism of the material discussed is based on the consideration of the interparticle shearing stress for the debris flow and is explained based on the character of the plastic fluid containing plenty of clay. The forecast method of the danger digree is proposed in the last part.

For the effect of the volcanic ashes, the threshold condition of the creep of saturated ashes is treated with an equilibrium of the force. Next, the critical shearing stress of the gravel in the muddy stream is discussed. The transport mechanism of the gravel in the muddy stream is discussed with the experiment at last.

*Faculty of the Science and Engineering Department, Ritsumeikan University

1. INTRODUCTION

In Japan regional mountain disasters are often caused by the moving of the deposit in a gully. At heavy rainfall a mountainside is covered by volcanic ashes, those deposits will start moving and flow down hundreds of meters or even kilometers over comparatively gentle slopes transporting a great number of huge stones.

Mud-debris flow, as it is called, is a high concentration of sediment that often moves at surprisingly high speed and therefore has very strong destructive power. Establishment of the countermeasures to prevent the debris flow needs knowledge of the mechanism of its occurence and the characteristic of the flow such as the total amount of the mud-debris transport, flow velocity, depth, destructive power, etc. The mud-debris flow are divided into groups by the cause of occurance. The first is caused by the fluidization of the deposit in a gully. This type is most common in Japan. The second is caused by an extrusion of the volcanic eruption, especially causing the volcanic ashes.
The third is caused by the fall or the landslide on the valley sides. However, there is not allways the relation between the mud-debris flow.

This paper introduced the study for the mechanism of the occurence and the characteristics of the mud-debris flow mainly in Japan.

2,MECHANISM FOR OCCURENCE OF MUD-DEBRIS FLOW CAUSED FLUIDIZATION OF DEPOSIT IN A GULLY,

2-1, Outline and Actual Example

The deposit in a gully on the mountainside is not transported by streams but also slides down or falls down from both sides of the mountain. At the downstream of the gully were the stream appears on the deposit

surface, the sediment is transported by the stream and the deposit is made by the force of the stream being balanced with the nature of the sediment. Whereas when the surface stream is slow, the sediment supplied by mass transport accumulates as it is not being carried down stream. The gradient can not be matained when acted upon by a running stream. The above idea is shown by a sketch in Fig.1 .

There was a heavy rain in and around Ashiwada village, Yamanashi Pref. , Japan, in Sep. 1966, then the run-off of a large amount of the sediment took place[1)]. This was almost all of the deposit in a gully with no participation of the fall in the mountainslope, Fig.2 shows the classification of the topographic features at equivalent gradient, and Fig.3 shows the area where scours and deposits took place at this time. Comparison between Fig.2 and Fig 3 indicates that the fall in the slope is limited within places having the 30° for the gradient, 20° for the scour and 10° for the deposit. The distribution of the occurence coincides well with that of the equivalent gradient map. Places having a gradient of 20° have a nature resembling a talus,the deposits having such a mixture of soil as afforestation was at work, which seems to have suffered from no shift from water flow.

From the traces of flowing water over the deposit, it inferred that water ran over the deposit brought by the mass transport and induced the run-off of the large quantity of the sediments in the process of shifting to the aqueous gradient.

Considering it in this way, the volume of the deposit in a valley that has not suffered any shift of water flow comes to have a relation with the scale of the mud-debris flow. As to this deposit in the neighbourhood of Ashiwada village with reference to the topographic map, the biggest was Nishi-irazawa followed by Motozawa and Misawa

river in that order of size. The sediment discharge investigated by the prefectural government was in the same order verifying this inference.

As the deposit is small in the areas outside the neighbourhood of Ashiwada village which is included in the Fig.3, it is understandable that there was no large mud-debris flow in those outer areas in so much as Fig.3 shows.

Fig.4 is for the lateral change of the bed elevation before and after the occurence of the mud-debris flow in the valleys around Ashiwada village, Fig.5(a) shows the longitudinal change in the bed elevation taken from Fig.4 . At the positions of both of the two channel bottoms in Fig.5 where the old-time gradients were bigger than the aqueous gradient, it is observed that the grades have been getting slower.

2-2. Critical Angles for Occurence of Debris Flow

Bagnold[2] has studied this kind of grain flow by introducing an idea of dispersive stress. The author[3] confirmed the idea of the experimential study for the mud-debris flow. Takahashi[4] makes the definition of the occurence following Bagnold's idea. It is as follows.

Suppose a uniform layer of loose granular materials of negligible cohesive strength, of depth D, and of slope angle θ. When the surface flow depth approaches h_0, the pore spaces are saturated, and infiltration flow is parallel, i.e., excessive pore pressure is zero, the characteristic shear stress distributions in the bed should be shown in Fig.6, in which τ is the applying tangential stress, and τ_L is the internal resisting stress. If the bed is very thick, case 2 and case 3 in Fig.6 are finally the same. So, for simplicity, only cases 1and 3 will be considered.

When the applying stress is larger than the resisting stress, in case 1 the whole bed starts moving and in case 3 the part of the bed above the depth a_L begins to flow. The a_L is the depth where the applying stress is equal to the resisting stress, and is deeper than the single particle diameter. Pore spaces in the moving grain layer should increase, because grains are strongly fluidized that might be enough to flow several kilometers.

Mathematical description of the mechanics of occurence is as follows. The static tangential stress τ due to the wholly parallel flow and the resisting shear stress τ_L at depth a are respectively,

$$\tau = g \sin\theta \left[C_* (\sigma - \rho) a + \rho (a + h_0) \right] \quad \cdots 1)$$

$$\tau_L = g \cos\theta \left[C_* (\sigma - \rho) a \right] \tan\theta \quad \cdots 2)$$

in which σ, ρ: the densities of grains and fluid respectively, g: the gravity acceleration, C_*: the grain voluminal concentration of the sediment, θ: the internal friction angle.

Case 1 in Fig.6 occurs under condition $d\tau/da \geqq d\tau_L/da$, which condition is, from Eqs.1 and 2, by Bagnold [2]

$$\tan\theta \geqq \left\{ \frac{C_* (\sigma - \rho)}{\left[C_* (\sigma - \rho) + \rho \right]} \right\} \tan\phi \quad \cdots 3)$$

A slope which satisfies Eq.3 might slip even though the infiltration flow would not reach the surface, but in the layer above $\tau_L = \tau$ the structure of the bed would be maintained. This phenomenon should be called landslip rather than debris flow. Conversely speaking, on the slope that does not satisfy Eq.3, without surface flow, no slip would occur. Consequently, one can assume the debris flow may occur only when the surface flow on the debris accumulation appears.

Case 3 in Fig.6 occurs under the conditions, $d\tau/da < d\tau_L/da$ and $a_L \geqq d$, and its condition is, by Eqs.1 and 2,

$$\frac{C_*(\sigma-\rho)}{C_*(\sigma-\rho)+\frac{1+h_0}{d}} \tan\phi \leqq \tan\theta \leqq \frac{C_*(\sigma-\rho)}{C_*(\sigma+\rho)+\rho} \qquad \cdots 4)$$

in which d: a representative grain diameter, because, if a_L is shallower than d, no grain layer should be moved, and if any grains of surface move, the movement is called bed load transportation. Accordingly, a critical slope angle is,

$$\tan\theta_1 = \frac{C_*(\sigma-\rho)}{C_*(\sigma-\rho)+\rho\left(\frac{1+h_0}{d}\right)} \tan\phi \qquad \cdots 5)$$

θ_1 in Eq.5 is smaller as h_0 is larger, and is smaller than tan θ_1 of actual experiences (tan $\theta_1 \simeq 0.3$ leads $h_0/d < 0.6$ from Eq.5). But, now, considering that a_L should be large enough to be able to make grains uniformly dispersed throughout the whole depth of the flow, the little colliding dispersivility demands $a_L \geqq \kappa h_0$, and κ is determined by experiments but would be nearly equal to unity. This speculation leads to the following critical slope,

$$\tan\theta_1 = \frac{C_*(\sigma-\rho)}{C_*(\sigma-\rho)+\left(\frac{1+1}{\kappa}\right)} \tan\phi \qquad \cdots 6)$$

For example, for $C_*=0.7$, $\sigma=2.6 g/cm^3$, $\rho=1.0 g/cm^3$, $\kappa=0.75$, and $\tan\phi=0.8$, Eqs.4 and 6 lead $14.5° < \theta < 22.9°$. Many actual debris flows occur between these values. The two criteria, Eqs. 5 and 6, reveal that massive transportation occurs at the slope between these slopes.

2-3. Flow Properties of Mud-Debris Flow

i) Debris Flow

The mud-debris flow is that of full-fluidized solids, and has a surge at the stream front. The flow phonomena are different from that of the clear water. The solids disperse uniformly in the stream, and the dispersion is supported by inter particle contact force.

Bagnold[5] made pioneer studies in this field, and proposed a semi-experimental equation on the basis of the experiment and used a double cylindrical rotational shearing meter, as follows,

$$\sigma_{zx} = a \sin\alpha_B \sigma d^2 \{ (\frac{C_*}{C})^{1/3} - 1 \}^{-2} (\frac{du}{dz})^{-2} = \sigma_{zz} \tan \alpha_B \quad \cdots 7)$$

in which a: constant, λ: the linear concentration, α_B: the angle of dynamic internal friction, and du/dz: the velocity gradient that is normal to the shear plane.

Recently, theoretical studies on the stress of the interparticle for the solid without liquid were performed. Mctigue[6] proposed that the shear stress is proportional to the second power of the velocity gradient, concidering elastic collision between solids. Kanatani[7] researched the theoretical relationship between macroscopic and microscopic mechanical properties of ideal granular materials, and found the macroscopic constitutive equation, which indicated that the shear stress is propotional to the second power of the velocity gradient, similar to Mctigue. In this study, he used freely many physical methodology, and it will be more developed, but experimental verifications of the hypothesis in the theory remain.

The author[8] measured the shear stress and normal stress vs. the shear strain rate for the full-fluidized granular material with paraffin wax grains and alcohol, and proposed the following equation,

$$\sigma_{zx} = \frac{1}{6} K^2 \sigma d^2 \{ (\frac{C_*}{C})^{1/3} - 1 \}^{-1} (\frac{du}{dz})^2 \tan\phi = \sigma_{zz} \tan\phi \quad \cdots 8)$$

and for $C<0.5$, $K=0.38$ $\tan\phi=0.7$, and for $C>0.5$, K and $\tan\phi$ are equal to bagnold's result (in Fig.7).

The author introduced the velocity of the complex phase flow consisting of sediments and water according to Eq.8 . In the steady flow in an open

channel, the static tangential stresses due to the wholly parallel flow at the depth a is expressed by Eq.1 . Putting Eq.1 into Eq.8, the mean velocity Um is obtained. For example, if h_0 is relatively small or negligible, for the steady flow condition,

$$\frac{Um}{u_*\sqrt{\Psi_0}} = \frac{2}{5}(K\sin\alpha)^{1/2}\left(\frac{D}{d}\right), \quad \Psi_0 = \frac{4}{9}\frac{\rho(1-C)+\sigma C}{\lambda^2\sigma} \qquad \cdots 9)$$

in which u_*: shearing velocity, α: mean collision angle of the solids, d: particle diameter. To find the constant of Eq.8, the experiment was done in an open channel for various sediments. The results were shown in Fig.8. Fig.8 shows that Eq.9 is valid. From Fig.8, it can be read as K=0.5, at sinα adopted 0.32, the wide range of the complex phase floow consisted of sediment and water. Eq.9 can be applied to the quasi-uniform flow.

Takahashi[4] introduced the mean velocity from Eq.7, for the surge part of flow.

$$\frac{Um}{u_*} = \frac{2}{5\sqrt{a\sin\alpha}}\left(\frac{D}{d}\right)\left\{C+(1-C)\frac{\sigma}{\rho}\right\}^{1/2}\left\{\left(\frac{C_*}{C}\right)^{1/3}-1\right\} \qquad \cdots 10)$$

then, $a\sin\alpha = 0.02$ by his experiment.

Tsubaki et. al.[9] observed the collision process of solids in fluid. They concluded that the collisions of the solids were not elastic, and those solids kept the contact flow without repeling the complex phase flow consisting of sediment and water. They divided interparticle stress into the collision stress and the isotropic friction stress. They proposed the equation of the interparticle stress by the aid of the kinetic model which expressed the transpotation mechanics of the momentum. By Tsubaki, the shearing stress was introduced as follows,

$$\sigma_{zx} = (0.0762+0.102\mu)\frac{\pi}{6}\beta^2 k_M \sigma d^2 \frac{C_*}{1-C/C_*}\left(\frac{du}{dz}\right)^2 \qquad \cdots 11)$$

in which β: constant. If k_M was employed 7.5, then Eq.11 coincided well with Eq.7 . The mean velocity was expressed, considering the distribution

of concentration,

$$\frac{Um}{u_*} = \{\frac{\sigma}{\rho} k_M (\frac{\Psi}{x} C_*)^{1/3} \frac{D}{d} \int_{C_s}^{C_*} \frac{2C - C_s}{C - C_a} (\int_{C}^{C_*} F(C)\, dC)\, dC \qquad \ldots 12)$$

in which the integral term explained the effect of concentration distribution, Ψ: the constant related the internal friction angle, x: the coefficient related the bulk modulus in regard to the continuum body. In Fig.9 is shown the comparison of Eq.12 with the experimental data.

ii) Muddy flow

a) Viscosity μ_B and yield value τ_y for the muddy flow

Independently, as above explained, the author studied the velocity and the friction factor of the muddy stream containing plenty of clay. In the fluid having a composition of clay particles, the relation of the shear stress to the strain rate $d\gamma/dt$ is frequently expressed by the following equation ,

$$\tau = \tau_y + \mu_B (d\gamma / dt) \qquad \ldots 13)$$

in which τ_y: the shearing yield stress, μ_B: the plastic viscosity. τ_y and μ_B related the particle concentration, but cannot be correlated by real particle only. The clay particle made an aggrigation in the liquid. The aggrigation is called floc in the later part. The author[10] employed the floc volume as a significant particle volume in clay-contained fluid in order to correlate the viscosity and the yield value of the shearing stress. The result of the reserch is expressed as follows,

$$\mu_B = \mu_0 (1 + \frac{3}{1/\phi_F - 1/\phi_{FC}}) \quad , \quad \phi_F = C_{FS}\, \phi_S \qquad \ldots 14)$$

in which μ_0:the viscosity of the clear water, ϕ_F: the floc volume concentration, ϕ_{FC}: the floc volume concentration at close packing, C_{FS}: the coefficient. The comparison between the measuered value and Eq.13 shows in Fig.10. Similarly, the yield value is expressed as,

$$\tau_y = A_1 \left(\phi_F - \phi_{F0} \right)^3 + A_2 \phi_F^2 \qquad \ldots 15)$$

in which A_1: the constant which showed the strength counter to break the network binding floc, ϕ_2: the constant which showed the magnitude of the structual viscosity, ϕ_{F0}: the threshold concentration where the network binding between flocs appears. Fig.11(a),(b) shows the relation of Eq.13 and the measured value.

b) Frictional coefficient f for the muddy flow

The author proposed the frictional coefficient f for the muddy stream in an experiment,

$$Um = \sqrt{2/f}\,\sqrt{g\,R} \qquad \ldots 16)$$

To be accurate, the measurement was performed in the pipe flow. For the plastic flow, even when the mean velocity is constant, the velocity gradient on the boundary changes with variation of τ_y and μ_B. Therefore, the friction factor f does not depend only on the mean velocity. Instead of Um, we employ the specified velocity U which is expressed by

$$U^2 = \frac{2\pi}{\pi R^2} \int_{r_y}^{R} ru^2\, dr = Um^2\, F(a) \qquad \ldots 17)$$

The usual equation of head loss is given by

$$I_f = f \frac{1}{D} \frac{Um^2}{2g} = f_B \frac{1}{D} \frac{U^2}{2g}, \quad f_B = \frac{2g\,D\,h_f}{Um^2\,F(a)\,\Delta x} \qquad \ldots 18)$$

On the other hand, Reynolds number, which is introduced in order to hold the similitude of the energy dispersion, is as follows,

$$Re_B = \frac{4a\,\alpha\,\sigma\,D\,Um\,F(a)}{\mu_B} \qquad \ldots 19)$$

The result of experiments on the friction factor for the flow containing plenty of clay are shown in Fig.12 . As shown in Fig.12, the resistance low of the flow containing plenty of clay is expressed by the same constant on the clear fluid through the muddy fluid as the Reynolds number holds

the similitude of the energy dispersion. It shows as follows,

$$1/\sqrt{f_B} = -0.8+2.0 \log_{10}(Re_B\sqrt{f_B}) \quad \ldots 20)$$

From Fig.13, the new parameter Re_B, more, divides clearly phenomena into the apparent laminar flow and the apparent turburent flow (in Fig.13). In order to consider the effect of roughness on the muddy fluid, an experiment was performed with a comparatively rough surface by natural sand. The result is shown in Fig.13, the Reynolds number Re_B which is employed here explains clearly the boundary between hydraulic smooth and rough regime. And Fig.13 shows, as the modified Reynolds number is increased, the friction factor depends on the relative roughness R/k rather than the modified Reynolds number, in which R is the hydraulic mean depth and k is the height of roughness, and the frictional coefficient in the hydraulic rough region is expressed as follows,

$$1/\sqrt{f_B} = 1.74 + 2.0 \log \frac{R}{k} \quad \ldots 21)$$

2-4. Forecast for the Danger Degree of Occurrence of Mud-Debris Flow caused by Fluidization of Gully Deposit.

A goal of the estimate of the danger degree is to forcast the degree of the disaster and to consider a counterplan in each place.

There are some studies for the forcast of the danger degree. Ashida et. al.[12] proposed the forecast method. In the condition (c)in Fig.6, the mud-debris flow occurs when the surface flow depth h is in excess of the critical value of h_0 given by Eq.5 . The surface flow depth h is

$$h = \left(\frac{f}{8\, g \sin \theta_1} \right)^{1/3} \left(\frac{Q}{B} \right)^{2/3} \quad \ldots 22)$$

in which Q: the discharge of surface flow, B: the width of stream, f: the frictional coefficient. The discharge Q is by rational equation

$$Q = \frac{1}{3.6} r_e A_d \quad \ldots 23)$$

in which r_e: effective rainfall intensity, Ad: the catchment area.

Then, Eq.22 is rewritten as follows,

$$\frac{h}{d} = \left(\frac{f}{8 \sin \theta} \right) \left(\frac{r_e A_d / 3.6 - Q_s}{g d^3 B^2} \right) \quad \ldots 24)$$

in which Qs: the infiltration discharge in the deposit. The necessary catchment area for the occurrence is expressed by the rearrengement of Eq.24 to the critical gradient θ_1

$$A_d = \frac{3.6}{r_e} \left\{ \left(\frac{8 \sin \theta_1}{f_k^3} g d^3 B^2 \right)^{1/2} + Q_s \right\} \quad \ldots 25)$$

in which f_k: friction coefficient of the surface flow. The danger area can be determined by Eq.25 . They proposed the decision method of the danger degree with the information of the sediment volume.

The forecast of the danger degree of occurrence required the ranking of the danger degree of each gully in general. The author[13] tried to decide the ranking of the danger degree. The method can be built up to compare the resistance strength for the occurrence in each gully. h_0 is calculated by Eq.5 as the constant distance through the gully. It is taken up as the relative frequency for any value of h_0. If the relative frequency of the small value of h_0 is large, then the gully is highly dangerous. If it is supposed that the rational equation on run-off is held, h_0 is translated into the rainfall intensity r_0 by Eq.22, Eq.23 . And the distribution of h_0 is translated into r_0, in which the mud-debris flow will occur. Then the ranking of the danger degree can be employed by the comparison between the ratios occupied by relative frequency of any value of h_0 for each gully. In Fig.14, the topography in the upper region of the Joganji is shown. The relative frequency of r_0 in each gully from the map is gotten. Fig.15 shows the relative frequency of r_0 which is approximately a normal distribution in the logarithmic scale. The relative frequency of rainfall intensity near the spot shows in Fig.15. A ranking of the danger

degree for gullies is decided when the comparison of the non-excess frequency of r_0 is below that of the rainfall intensity. It can be concluded No.3 in Fig.15 is most dangerous.

3. EFFECT ON THE OCCURENCE DUE TO ACTION OF VOLCANIC ASHES.

3-1. Out Line

The effect on the occurence of the mud-debris flow due to the action of volcanic ashes are expressed as follows;

(a) Effect for the mud-debris flow is caused by the fluidization of deposit in a gully. i) Increase of run-off due to the decrease of the infiltration is caused by the coat of ashes. ii) Increase of the density or viscosity of the fluid by the fluid containing plenty of clay particles.

(b) Effect for the mud-debris flow is caused by the developement of the creep of shear layer.

The effect on (a) can be estimated by the given condition. As the mud-debris flow of the eruptive ashes is caused by a very low rainfall intensity, the process for the occurrence is not always caused by the stream on the deposit in a gully. As the second type, there is a possibility that the creep of ashes which is saturated by water developes into mud-debris flow or that the concentration of ashes in the snrface flow increases according to how much it picks up. It clears the possibility to research the transport mechanism of the ashes in the water. But the mechanism of the ashes is transported into the clear water. But the mechanism of the ashes transported into the clear water may not be changed as it is compared with the past studies. Therefore, the author studied the threshold condition of the creep of ashes, the critical shearing stress for gravels in muddy stream, as basic research for the study of the second type.

3-2. The Threshold Condition of the Creep of Ashes Layer.

The volcanic ashes have a property that the liquid limit is high when compared with another sediment, and the shearing stress is not so strong. Actualy,traces of creep on the mountainside can be found. The rainfall infiltrates into the ashes layer from the surface and reaches some depth y, the creep will occur on the thickness y. The shearing strength τ is expressed as follows, as it is seemed that the behavior of the saturated ashes with water shows a character as the plastic body. The relation between the shear stress and shearing rate is expressed by Eq.13. The balance of the shear stress at the depth y (in Fig.16) is expressed as,

$$(\gamma_w \, g \, h_0 + \gamma_s' \, g \, y) \sin \theta = \tau_y + \mu \, d\varepsilon/dt \qquad \cdots 27)$$

in which γ_w,γ_s': specific gravity of water and the saturated sediment respectively, h_0: the depth of surface stream. The threshold gradient at which the creep will be starting

$$\sin \theta = \tau_y \, / \, \{ \gamma_s' \, g \, h \, (1 + \frac{\gamma_w}{\gamma_s'}) \} \qquad \cdots 28)$$

The shearing yield value τ_y for the saturated ashes is expressed by Eq.5, as well as clay. In a little while after the creep starts, it is very seldom that the charactor depends on the creeping time of the materials, so $d\varepsilon/dt$ in Eq.27 is changed into du/dz. The fluidity behavior is divided into the non-fluidity layer (= $\tau<\tau_y$) and the fluidity layer (= $\tau>\tau_y$) in Fig.16 . If the surface flow depth h_0 is negligible, the velocity distribution for the fluidity layer is,

$$\frac{u_1}{u_*} = \frac{\gamma_s' \sqrt{g \sin \theta}}{\sqrt{h + h_0} \, \mu_B} (\frac{z_y \, z}{2} - z^2 + \frac{\gamma_w}{\gamma_s'} h_0 \, z) \qquad \cdots 29)$$

in which z_y: the hight exists the shearing yield stress. The velocity of the non-fluidity layer is,

$$u_2 \, / \, u_* = u_{zy} \, / \, u_* \qquad \cdots 30)$$

in which u_{zy}: the velocity at the yield plane (in Fig.16). Then the mean velocity Um is expressed as follows,

$$\frac{Um}{u_*} = \frac{\beta\, h^{1/2} \tau_y}{g\, i\, \mu_B} \quad , \quad \beta = \frac{a'^2 \left(1 - \frac{a'}{3} \right)}{2 \left(1 - a' \right)} \quad , \quad a' = \frac{z_y}{h} \qquad \cdots 31)$$

3-3. Critical Shearing Stress for Gravel in Muddy Stream.

For the flow mentioned 3-2, the mean concentration is,

$$\bar{C} = \frac{C_* \int_0^h u_1 \, dz}{\int_0^h u \, dz + \int_0^{h_0} u \, dz} \qquad \cdots 32)$$

in which C_*: the volume concentration is in the deposit.

When fluid containing clay or ashes flows down on the mountainside, it seems that there is a different mechanism of sediment transport between the clear and muddy stream. It is caused by the decrease of difference in density of the fluid and the gravel, by the change of the liquid viscosity, and by the change of the velocity of fluid. This difference is traced at the critical shearing stress in the stream containing plenty of clay particles in which the above difference is presumed to present itself most conspicuously. Many studies on the critical shearing stress of gravel in the clear water have been done.

When as shown in Fig.17, there is a grain of the diameter d on the rough bed,

$$R_T + W' \sin\theta = W' \cos\theta \tan\phi \qquad \cdots 33)$$

in which R_T: fluid resistance, W': submerged weight of grain, ϕ: frictional angle

$$R_T = \frac{\rho_s}{8} C_D u^2 \pi d^2 \quad , \quad W' = (\sigma - \rho_s) g \frac{\pi}{6} d^3 \qquad \cdots 34)$$

ρ_s: the density of muddy liquid, C_D: the drag coefficient, d: diameter, σ: density of grain. therefore, Eq.33 is,

$$\{(\sigma - \rho) g \frac{\pi}{6} d^3\} \cos\theta \, (\tan\phi - \tan\theta) = \frac{\rho_s}{8} C_D u^2 \pi d^2 \qquad \cdots 35)$$

The fluid velocity at the height d from bottom is expressed by Eq.29,

$$u = (u_*^2 \, d \, / \, \nu_B) \, a' \qquad \ldots 36)$$

Inserting the expressions for u into Eq.34,

$$u_{*c}^2 \, a'^2 / [\{ (\sigma - \rho_s) / \rho_s \} \, g \, d \tan\phi] = 1 / \{ \frac{3}{4} C_D (\frac{u_* \, d}{\nu_B})^2 \} \qquad \ldots 37)$$

The relation between $u_*^2 / \{ (\sigma/\rho - 1) gd \tan\phi \}$ and $u_{*c} d/\nu$, which was presented by shield, shows a good parameter for the critical shearing stress in the clear liquid. To hold the kinematic similarlity in the muddy stream, the author introduced the modified Reynolds number and non-dimentional critical shearing stress, respectively,

$$Re_* = (\frac{u_{*c} \, d}{\nu_B})^2 \, a' \, / \, [\, 1 + \{ (1/a') - 1 \} \, I_D \,] \qquad \ldots 38)$$

$$\frac{u_{*c}^2 \, a'}{\frac{\sigma}{\rho} gd \tan\theta} \{ 1 + (\frac{1}{a'} - 1) \, I_D \} \qquad \ldots 39)$$

Fig.18 shows Iwagaki's theory for the critical shearing stress in the clear water, with which equation a'=1 on the modified parameter. Taking 0.3 for the shadow coefficient as Iwagaki did, the measured value in the muddy fluid expressed by the modified parameter coincides with Iwagaki's equation. It concluded the Reynolds number held the similitude of the force act on the particle. The experiment formulas made on the bases of the above experiments are shown below by adopting the same coefficient with that on the clear water. For the $671 \leq R_*$, $162.7 \leq R_* \leq 671$, and $54.2 \leq R_* \leq 162.7$, respectivly, and R_* is,

$$u_{*c}^2 = 0.05 \, (\frac{\sigma}{\rho_s} - 1) \, g \, D \, a'^{-1} \{ 1 + (\frac{1}{a'} - 1) \, I_D \}^{-1}$$

$$u_{*c}^2 = \{ 0.015 \, g \, (\frac{\sigma}{\rho} - 1) \}^{25/22} D^{31/22} \nu_B^{-3/11} a' \{ 1 + (\frac{1}{a'} - 1) I_D \}^{-7/5.5}$$

$$u_{*c}^2 = 0.034 (\frac{\sigma}{\rho_s} - 1) \, g \, D \, a'^{-1} \{ 1 + (\frac{1}{a'} - 1) \, I_D \}^{-1}$$

$$R_* = (\frac{\sigma}{\rho_s} - 1)^{1/2} g^{1/2} D^{3/2} \nu_B^{-1} [a' \{ 1 + (\frac{1}{a'} - 1) \, I_D \}]^{-1/2} \qquad \ldots 40)$$

For the gravel placed on an inclined plane, Eq.40 must be devided by cos θ (tan φ - tan θ) / tan φ . For the big stone, the first one of the Eq.40 is applicable, but where Reynolds number is large, I_D approached zero so that Eq.40 would come to be expressed by,

$$u_{*c}^2 = 0.05 \left(\frac{\sigma}{\rho} - 1 \right) g d a' \qquad \cdots 41)$$

In this condition, the coefficient was the same with that on the clear water.

3-4. Effect on the Bed Load by the Muddy Flow.

The transport of the sediment shows the irregular and intermittent movement. The movement has a character as stochastic phenomena. The effect of the muddy flow on the movement of the sediment should be studied as the change of the stochastic phenomenon. It's stochastic character of the sediment transport mechanics is studied with the experiment number of colored gravel as tracers. The conciderable number of colored gravel is set in a spot on the movable surface which is formed by the same diameter measuring the travers length at unit time in each particle. From the measured data, the mean travers velocity and its variance are calculated. The sediment transport rate q_T is expressed as follows

$$\frac{q_T}{u_* d} = (\text{traversed layer thickness}) \times (\text{mean traverse velocity}) \times \frac{1}{u_*} \qquad \cdots 42)$$

Fig.19 shows the measured result. From the measured gravel transport rate, the traversed layer thickness does not so change as compared with that in a clear stream. It seems that the increase of the gravel transport rate is done by the increase of traverse velocity. By the study of Hubbell[15], the mean traverse velocity dx/dt and variance σ^2 are expressed as follows,

$$dx/dt = \lambda_2/\lambda_1 \quad , \quad \sigma^2 = 2 \lambda_2 t/\lambda_1^2 \qquad \cdots 43)$$

in which $1/\lambda_1$: the mean traversed length at one step, λ_2: the transport

probability at unit time. The measured results show that $1/\lambda_1$ and λ_2 increase in the muddy stream and the clear stream respectively, and, especially, the transport probability is very hight.

4. CONCLUSION

As substantially proved, the theoretical and the experimental consideration on the occurrence and the flow of the mud-debris flow is explained. The major results are as follows:

a) The major of the mud-debris flow in Japan is caused by the fluidization of the deposit in a gully. The mud-debris flow occurs when the surface flow is in excess of the critical depth, at given gradient. This is substantially proved in Fig.2 and Fig.3 .

b) The threshold condition of the fluidization of the deposit is explained by an equilibrium of the force in Eq.3 and Eq.5 .

c) The flow character is explained bv the consideration of the interparticle shearing stress. The many studies of the interparticle shearing stress have been done to clear the flow mechanism. These studies are shown in Fig.9, Fig.10, and Fig.12 .

d) The frictional coefficient f on the muddy stream is expressed in Fig.12,

e) The forecast method for danger degree on occurrence is explained. The forecast method is not only to indicate the danger area but to indicate the danger degree in each gully. The ordering goes on with the comparison of the relative frequency of the necessary rainfall intensity for the debris occur.

f) The threshold condition of the creep of the ashes layer is expressed in Eq.28 .

g) The critical shearing stress for the gravel in the muddy fluid discussed with the experimental study, and the experimental equation Eq.40

is proposed.

h) The sediment transport rate in the muddy stream increases compared with that in the clear stream. It results that the increase is done with the increase of the traversed velocity and that transport probability is very high.

ACKNOWLEDGEMENT

The paper introduced main studies on the mud-debris flow in Japan. But many studies are left, specially, the field study is not mentioned.

REFERENCE

1) Daido, A., On the Occurence of Mud-Debris Flow, Bul. of the Kyoto. Univ., Vol.21, Nov., 1971.

2) Bagnold, R. A., The Flow of Cohesionless Grain in Fluid, Philo. Trans. Royal Society of London, England, Vol.249, 1951.

3) Daido, A., Flow of Granular Materials, 12th Proc. of Natural Disaster Science pp.225-226, 1975. (In Japanese)

4) Takahashi,T., A Mechanism of Occurence of Mud-Debris Flow and Their Characteristics in Motion, No.20-B2, Annuals, Kyoto. Univ.,Apr., 1977. (In Japanese)

Takahashi, T., Mechanical Characteristic of Debris Flow, Proc. of ASCE Vol.104 HY 8 pp.1153-1169, 1978

5) Bagnold, R. A., Experiments on a Gravity-Free Dispersion of Large Solid Spheres in a Newtonian Fluid under Shear, Proc. Royal Society of London, London, England, Vol.225-A, Aug.,1954.

6) Mctigue, D. F., A Model for Stresses in Shear Flow of Glanular Materials, Proc. U.S.-Japan Sem. on Continuum-Mechanical and Statistical Approaches in the Mechanics of Granular Materials, pp.266-271, 1978.

7) Kanatani, K., Fandamental Study of Granular Materials 1.2., Proc. of JSME., Vol.45, 392, pp.507-514, pp.515-522, 1979. (In Japanese)

8) Daido, A., Flow Formula of Granular Materials, 16th Proc. of Natural. pp.215-218,1979.(In Japanese)

9) Tsubaki, T., Hashimoto, H., Suetsugu, T., Grain Stresses and Flow Properties of Debris Flow, Proc. JSCE, No.317, Jan., 1982.

10) Daido, A., Viscosity and Yield Value of Fluid Containing Clay, Theoret. and Appl. Mech. Vol.26 pp.461-472, 1976.

11) Daido, A., Friction Factor and Velocity Distribution in Turbulent Region for Bingham Plastic Fluid, Proc. of 14 Japan National Congress. for Appl. Mech., pp.192-196, 1965.

12) Ashida, K., Takahashi, T., Sawai, K., Estimation Method on the Danger Degree of Debris Flow Occurence, No.21 B-2, Annuals, Kyoto Univ., Apr.,1978.(In Japanese)

13) Daido, A., Ordering on the Danger Degree for Debris Flow Occurence, Proc. of Annuals Japan Erosion Control Soc., 55th, pp.90-91, 1980. (In Japanese)

14) Daido, A., Fundamental Study on Mud-Debris Flow, thesis, Kyoto Univ., 1970.(In Japanese)

15) Hubbell, D., Sand Transport Studies With Radioactive Tracers, Proc. ASCE, Vol.90, HY3, pp.36-68, 1964.

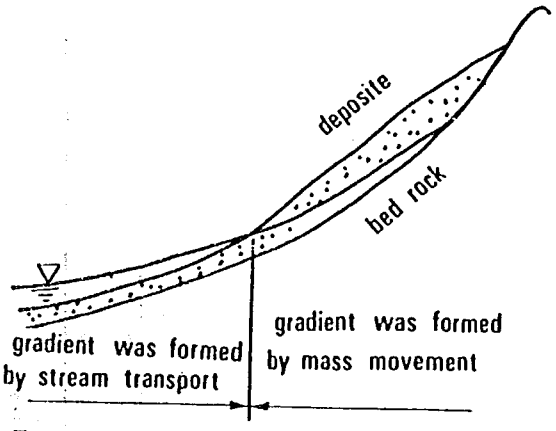


FIG.I SKETCH OF GRADIENT IN VALLEY

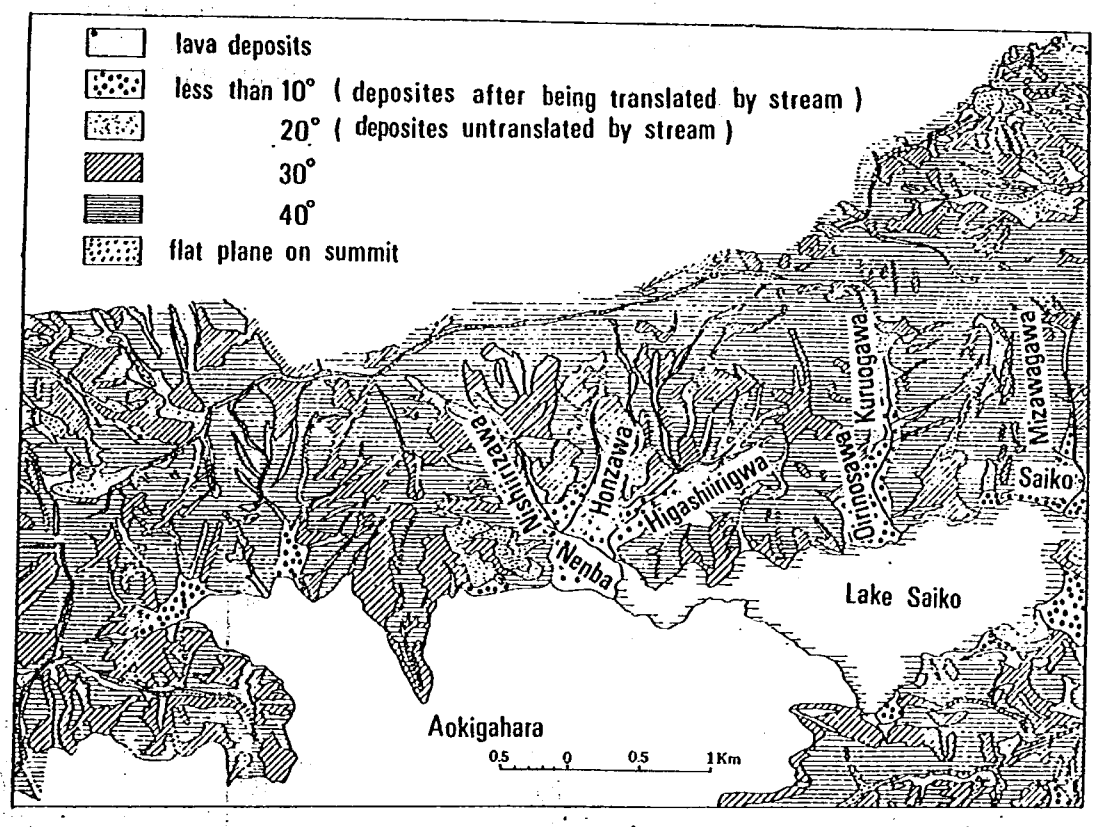


FIG.2 IDENTICAL GRADIENT MAP(ASHIWADA VILLAGE)

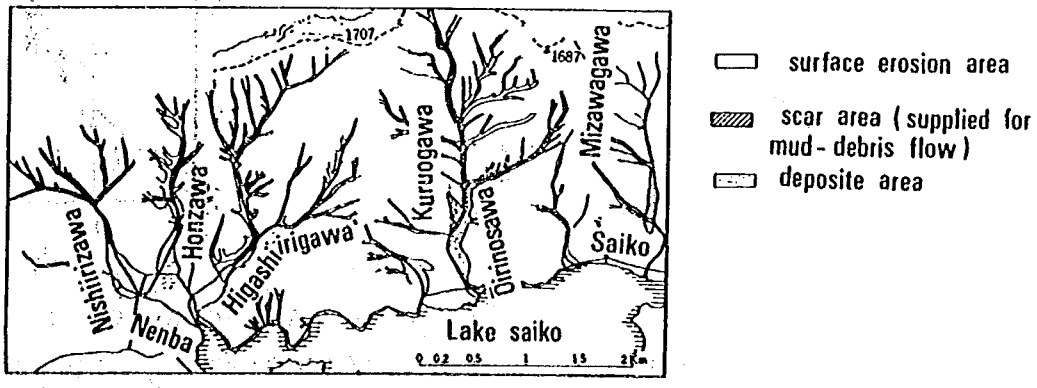


FIG.3 CLASSIFIED SEDIMENT MOVEMENT BY HEAVY RAIN(ASHIWADA VILLAGE)

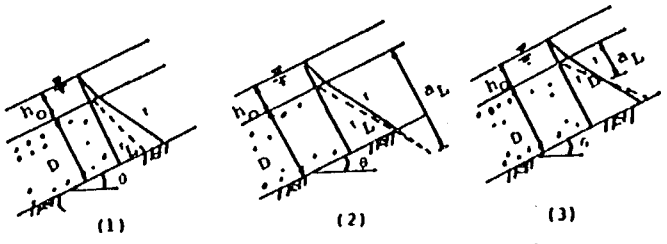


FIG.6 CHARACTERISTIC SHEAR STRESS DISTRIBUTION

$h = f(f \cdot Q \cdot B)$

$Q = f(r_e \cdot B_d)$

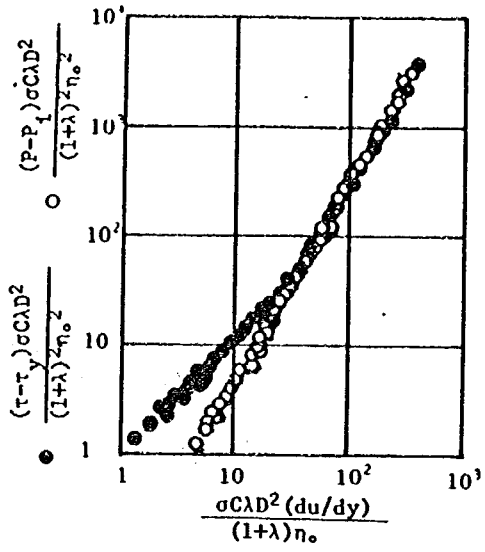


FIG.7 RELATION SHEAR STRESS, NORMALSTRESS AND SHEAR RATE

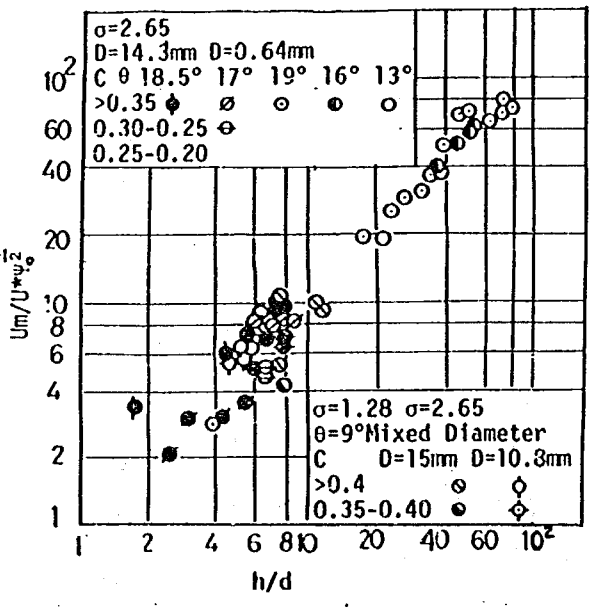


FIG.8 COMPARISION OF EQ.9 WITH EXPERIMENT VALUE

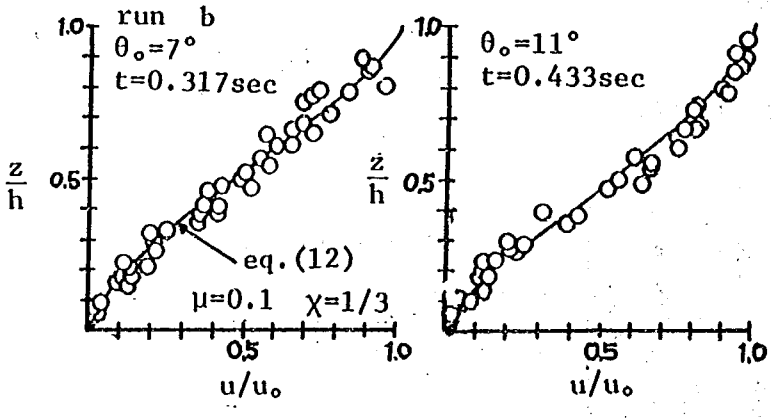


FIG.9 COMPARISION OF EQ.12 WITH EXPERIMENT VALUE

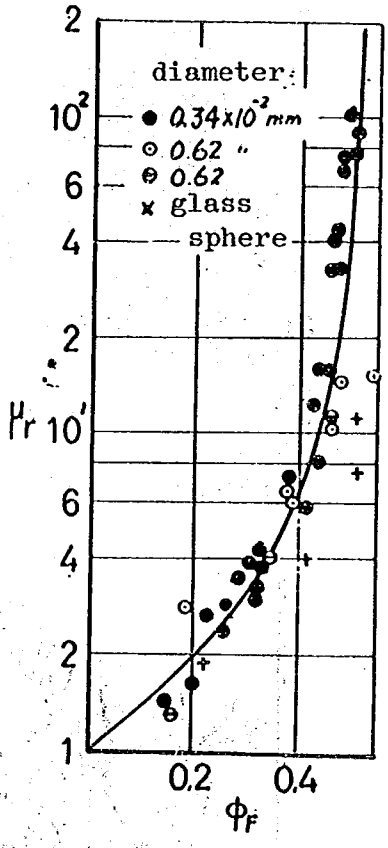


FIG.10 RELATION BETWEEN RELATIVE VISCOCITY μ_B AND VOLUME CONCENTRATION OF FLOC ϕ_F ABOUT MUDDY FLUID

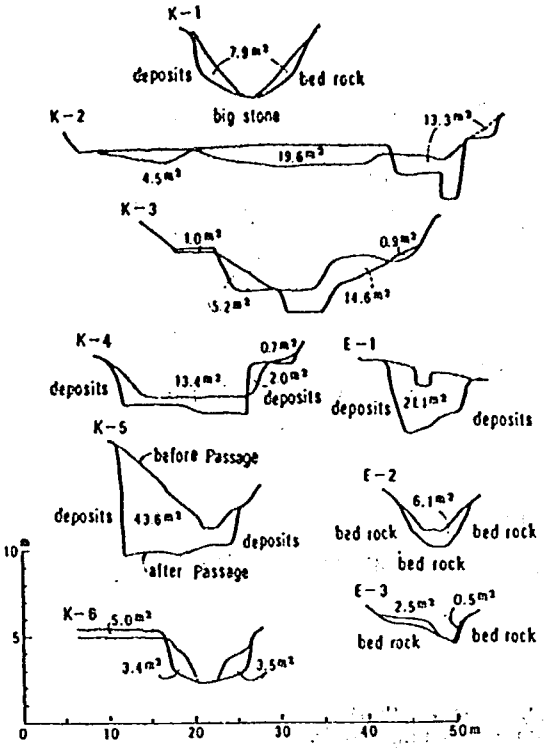


FIG.4(a) LATERAL VARIATION OF BED ELEVATION BY MUD-DEBRIS FLOW (ASHIWADA VILLAGE)

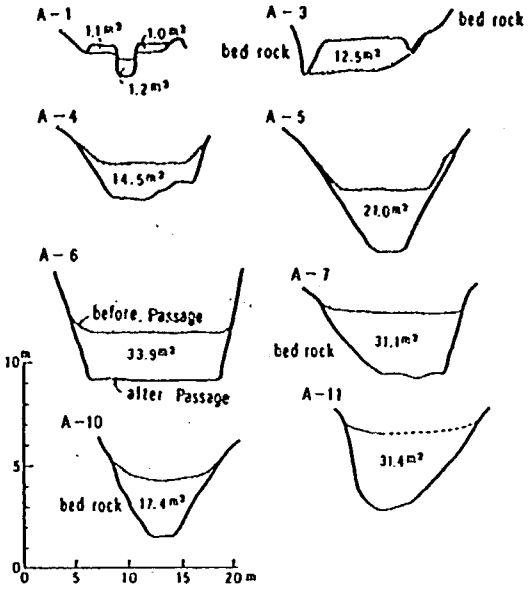
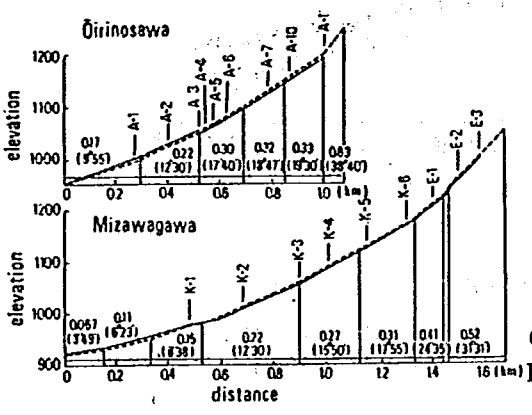


FIG.4(b) LATERAL VARIATION OF BED ELEVATION BY MUD-DEBRIS FLOW (MIZAWAGAWA)



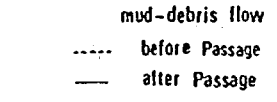


Fig.5(a)

LONGITUDINAL VARIATION OF BED ELEVATION BY MUD-DEBRIS FLOW(ASHIWADA VILLAGE)

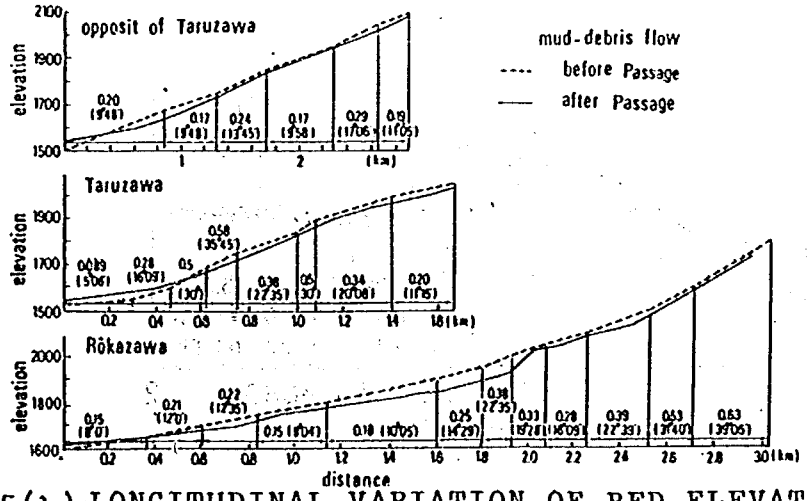


FIG.5(b) LONGITUDINAL VARIATION OF BED ELEVATION BY MUD-DEBRIS FLOW(KUROBE RIVER)

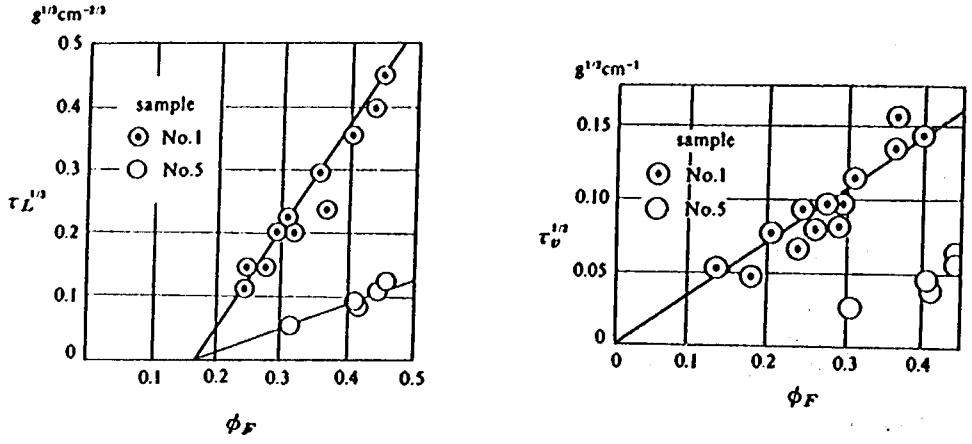


FIG.11 A_1 AND A_2 IN EQ.15
WHICH IS MEASURED ABOUT MUDDY FLUID

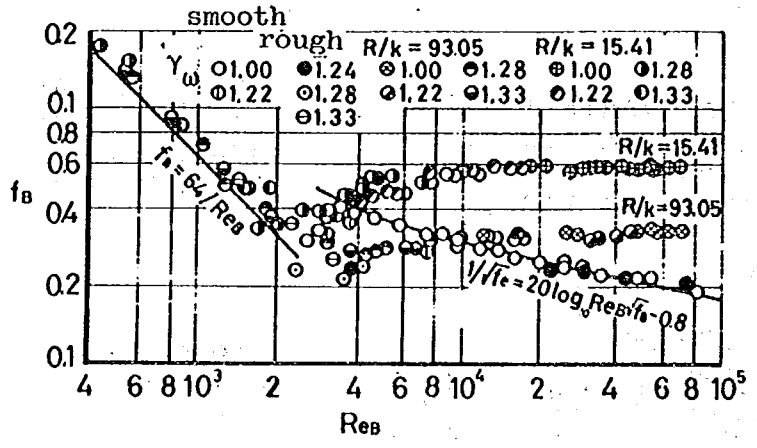


FIG.12 RELATION BETWEEN f_B AND Re_B
FOR THE MUDDY STREAM IN SMOOTH
AND ROUGH SURFACE ABOUT MUDDY FLUID

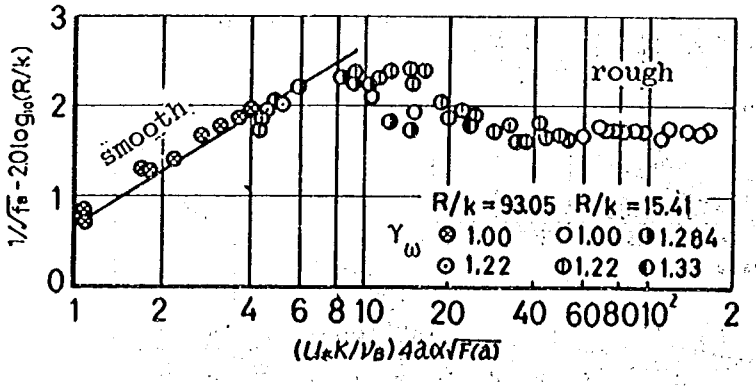


FIG.13 RELATION BETWEEN $1/\sqrt{f_B} - 2.0\ \log_{10}(R/k)$ AND
$(u_* k/\nu_B)4a\alpha\sqrt{F(a)}$ ABOUT MUDDY FLUID

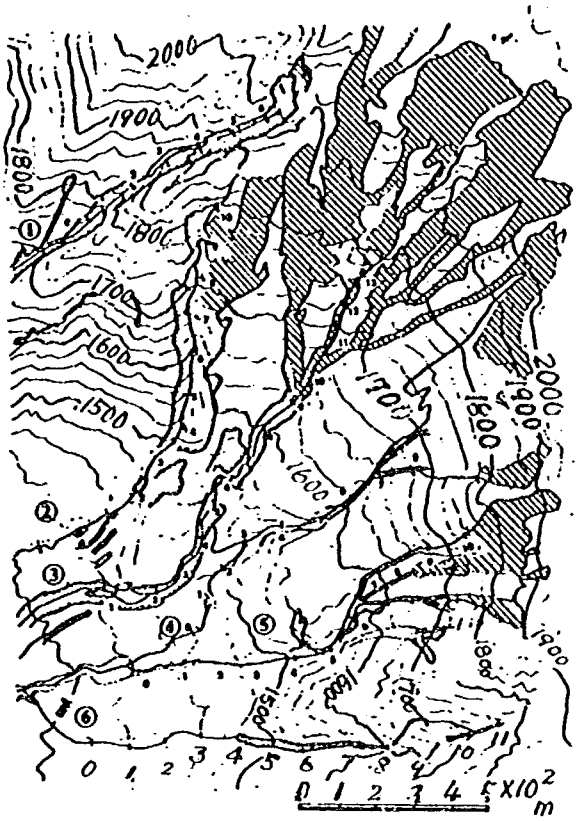


FIG.14 TOPOGRAPHY AT UPPER REGION OF THE JOGANJI

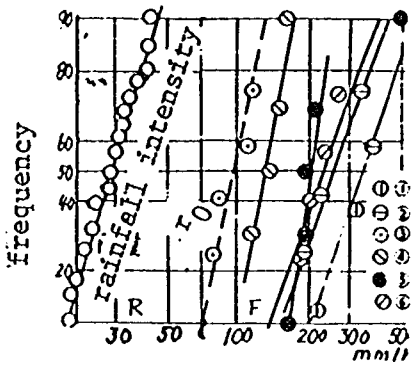


FIG.15 RELATIVE FREQENCY OF CRITICAL RAINFALL INTENSITY r_0 IN EACH GULLY AT SPOT IN FIG.13 AND RELATIVE FREQUENCY OF RAINFALL INTENSITY AT NEAR SPOT

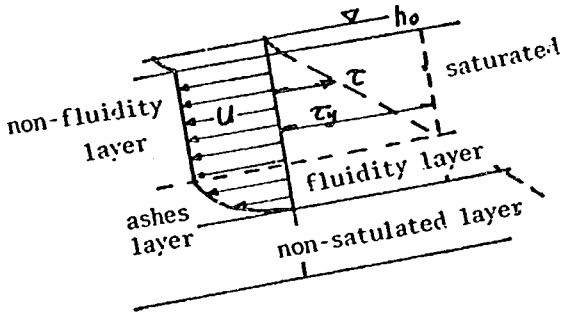


FIG.16 VELOCITY DISTRIBUTION

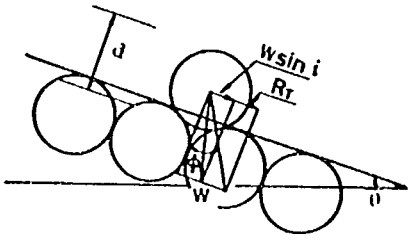


FIG.17 FORCE ACTED ON THE GRAVEL

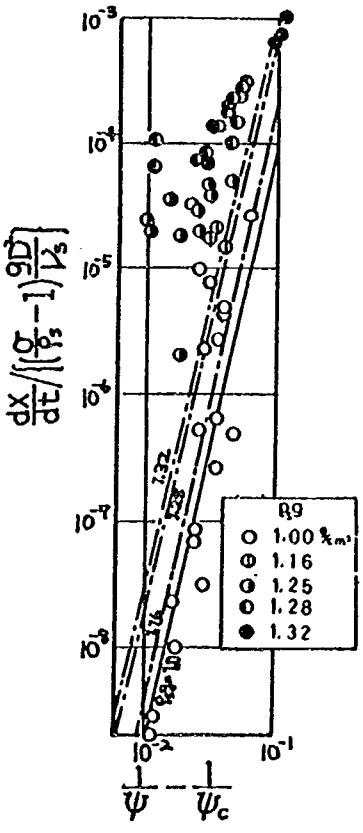


FIG.19 SEDIMENT TRANSPORT RATE IN MUDDY STREAM

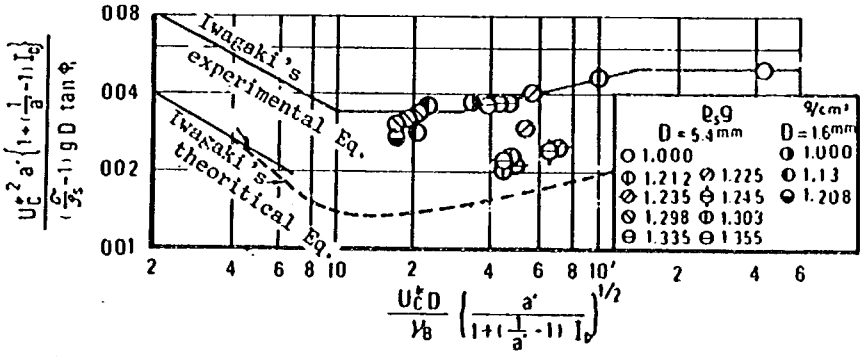
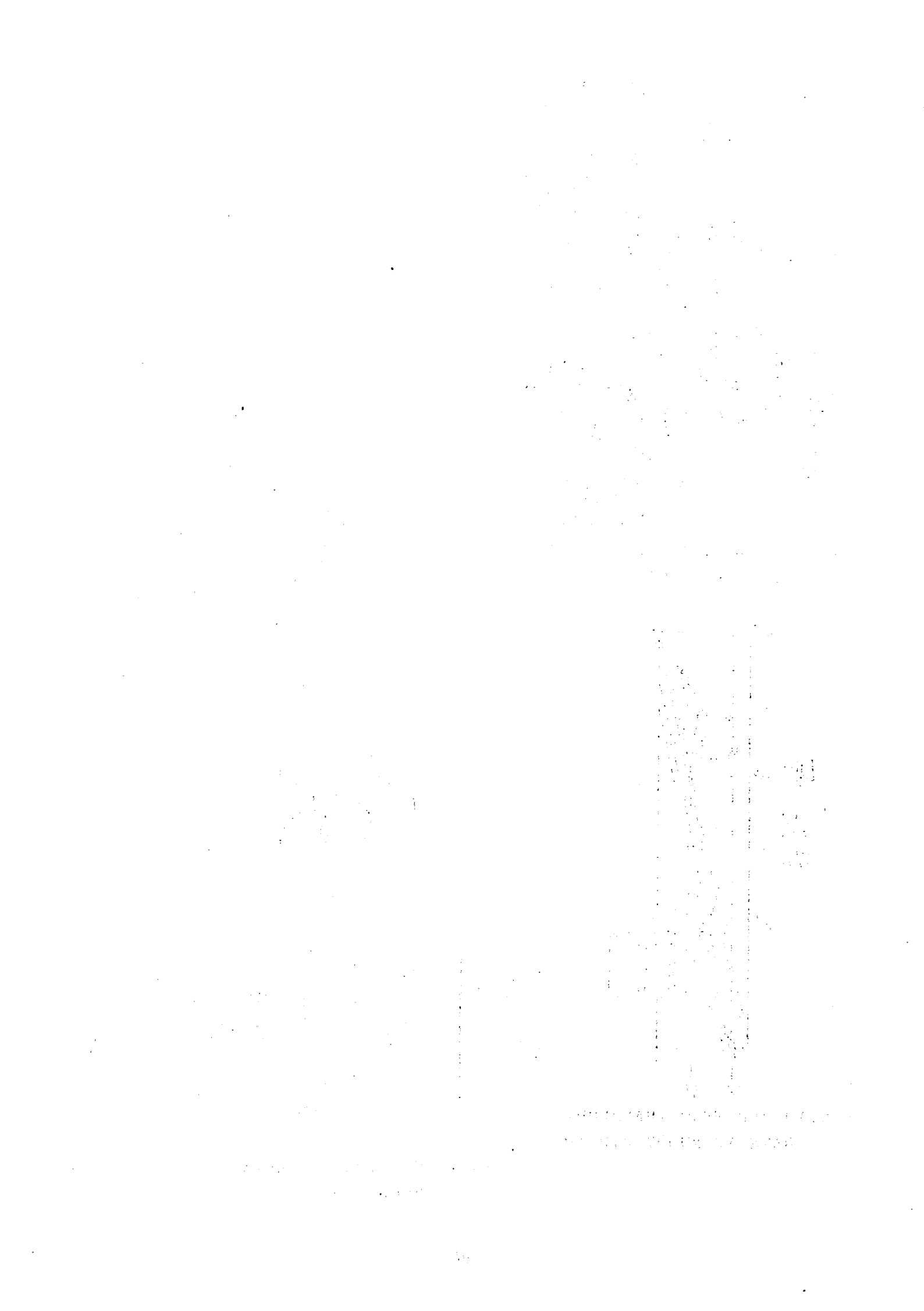


FIG.18 CRITICAL SHEARING STRESS IN THE MUDDY STREAM



FLOW BEHAVIOR OF TWO MAJOR LAHARS TRIGGERED BY THE MAY 18, 1980 ERUPTION OF MOUNT ST. HELENS, WASHINGTON

Thomas C. Pierson

U.S. Geological Survey, WRD
David A. Johnston Cascades Volcano Observatory
5400 MacArthur Boulevard
Vancouver, Washington 98661

This manuscript is submitted for publication with the understanding that the United States Government may reproduce and distribute reprints or may authorize the reproduction and distribution of reprints for governmental purposes.

INTRODUCTION

Within the first few minutes of the May 18, 1980 eruption, lahars of varying magnitude and composition were generated on the upper western, southern, and eastern flanks of Mount St. Helens. Two of the largest of these lahars were initiated on the eastern side (Fig. 1) and flowed down two parallel channels to Swift Reservoir. One flowed 23 km down the East Fork Pine Creek channel while other lahars moved down Smith Creek, Ape Creek, and Muddy River, joining to flow together down the flatter lower Muddy River channel (Fig. 2). Together they destroyed 16 bridges, buried several kilometers of road, and raised the level of the 14 km long reservoir 0.8 m (Cassidy and others, 1980; Schuster, 1981). The general sequence of events and descriptions of these flows and their deposits are given in Janda and others (1981) and Cummans (1981).

Lahars (volcanic mudflows or debris flows) are dense, viscous slurries of poorly sorted gravel, sand, mud, and water. The coarse fragments are suspended in a fluid matrix of silt- and clay-sized particles plus water and are held in suspension by varying combinations of frictional, buoyant, dispersive, and cohesive forces. Such slurries are non-Newtonian fluids, differing from Newtonian fluids, such as water, by having a finite yield strength. Although there are a number of well defined hydrodynamic equations that can be used to accurately compute how water flows under specific sets of idealized conditions, there is little quantitative information that will allow prediction of flow behavior for lahars.

The objectives of this paper are to characterize flow behavior of two large lahars that occurred at Mount St. Helens, to describe downstream and interchannel variation in flow behavior, and to identify possible controlling variables for this variation. It is not the purpose of this report to try to

derive flow equations for these lahars; the data set is limited, numbers are only refined estimates, and the criterion of uniform flow was not met. Nevertheless, empirical relations between variables are developed in order to provide some basis for predicting the timing and magnitude of a significant volcanic hazard.

METHODS

For the analysis of lahar dynamics, knowledge of mean flow velocity ($\bar{U}$) is essential, but it has not yet been measured directly. Two methods were used in this study to compute $\bar{U}$ from the elevations of mudlines left behind by flows on channel banks and tree trunks. These techniques have been widely applied to the study of mud and debris flows of both volcanic and nonvolcanic origin, including other 1980 lahars from Mount St. Helens (Fairchild, this volume; Fink and others, 1981; Janda and others, 1981).

The first method utilizes maximum runup of flow on hills or banks oriented perpendicular to the flow path (Fig. 3). It is derived by assuming that all kinetic energy (of peak flow) is converted to potential energy:

$$\tfrac{1}{2}\, m\bar{U}^2 = mgh \qquad [1]$$

which reduces to

$$\bar{U} = [2\, gh]^{\frac{1}{2}} \qquad [2]$$

where m = mass, g = gravitational acceleration, and h = amount of runup. Because frictional energy losses are not taken into account, velocities so calculated must be minimum values.

The second method is based on the principle of superelevation of open channel flow, i.e. the tilting of the free surface in a bend due to the action of centrifugal force (Fig. 3). The surface rises on the outside and lowers on

the inside of the bend in proportion to $\bar{U}$. The difference in elevations is defined as the superelevation, h. If it is assumed that all filamental velocities in the bend are equal to the mean velocity, that all streamlines have the same radius of curvature, and that flow is subcritical, application of Newton's second law of motion to the centrifugal action in the curve yields a simple equation for velocity (Chow, 1959, p. 448):

$$\bar{U} = \left(\frac{g \quad h \quad r_c}{w} \right)^{\frac{1}{2}} \qquad [3]$$

where r_c = centerline radius of curvature, and w = channel width. This same equation has been derived theoretically from the principle of radial acceleration of a unit mass, assuming that the free surface stays perpendicular to the radial component vector of the angular acceleration (Johnson and Hampton, 1969). Equation 3 can also be derived from the parabolic equation for the free surface of a rotating fluid, given the assumptions that the material is a perfect fluid, r_c is constant, and there is no relative motion between fluid particles (which may be approached in plug flow).

If flow is supercritical, cross waves should be generated in channel bends and in other localities of irregular channel alinement and shape. In bends, a disturbance pattern from intersecting wave fronts will form and cause multiple maximum and minimum mudline elevations at regular intervals on both channel banks. When maximum cross-wave height occurs on the outer bank, it is additive to superelevation and doubles the mudline elevation above the horizontal water-surface plane; when maximum cross-wave height occurs on the inner bank, it cancels the effect of superelevation and the resulting mudline coincides with the horizontal water-surface plane (Chow, 1959, p. 450).

Except for notable "cross valley slashing" of the lahar in upper Ape Canyon, no multiple mudline maxima were seen in Pine Creek or Muddy River bends, even though the bends were long enough. Either the lahars remained subcritical or else the flow was supercritical but with cross waves migrating because of unsteady flow conditions and leaving a relatively smooth trimline. In either case, equation 3 is valid for velocity computation. It is valid for the supercritical case because the "effective superelevation" measured would be the difference between the outside and inside cross-wave maxima, which is the same elevation difference caused by superelevation alone (Chow, 1959).

Neither this equation nor any others in use (Chow, 1959; Apmann, 1973; Davies and others, 1978) considers the effect of channel roughness or internal resistance of the fluid, and velocities determined by equation 3 must therefore also be considered minimum values. Frictional losses in flowing non-Newtonian slurries, however, can be very low; some industrial suspensions flow through pipes with less than half the friction loss of water (Hughes and Brighton, 1967). Although the accuracy of these equations has not been verified experimentally for non-Newtonian fluids, equation 3 did give nearly the same value of $\overline{U}$ as equation 2 at two sites in this study. If it is assumed that mean fluid velocity at peak flow is approximately equivalent to velocity of the leading edge of the lahar, preliminary data from the South Fork Toutle River lahar (L.H. Fairchild, University of Washington, written commun., 1982) suggests that these computed velocities are not far off the actual values.

THE LAHARS

Pine Creek Lahar

Analysis of the eruption's lateral blast by Rice and Watson (1981) indicates that the northward-propelled blast began at 08:34:50 PDT. The initial velocity of the blast pyroclastic surge was about 90 m/s (Moore and Rice, 1983) and the cloud reached the boundaries of the blast zone by 08:37. This rapid lateral expansion of the blast cloud was captured in frames 13 to 22 of a sequence of photos taken from Mount Adams by John V. Christiansen. In frame 14 of this photo sequence, a large dark, ground-hugging cloud assumed to be a pyroclastic surge (Wohletz and Sheridan, 1979), can be seen spilling over the crater rim and down the east and southeast sides of the volcano. From the dark color of the cloud and calculations that indicate high water content of the volcanic cone at the time of the eruption (Voight and others, 1981), it is assumed that this pyroclastic surge was wet. Between frames 14 and 15, it appears to have been moving very rapidly, faster at that moment than the northside blast cloud in fact, but on reaching the Pine-Muddy fan (Fig. 1), it slowed and appeared to stall near the middle of the fan by frame 22, approximately the same time as the northward-directed blast cloud halted (time assumed to be 08:37).

Assuming that the movement of the pyroclastic surge is bracketed by the times 08:34:50 and 08:37, and taking the distance from the crater rim to the middle of the fan, an average velocity of 38 m/s is obtained. This value compares reasonably well with 30 m/s calculated for the smaller, slower cloud descending the south flank (Moore and Rice, 1983). Another photographic sequence taken by Ken Seibert from the south shows that this pyroclastic surge was the only event to have affected the southeast flank between 08:32 and at least 10 a.m. Since lahars arrived at Swift Reservoir by about 9 a.m., this

must have been the initiating event. The high-velocity, turbulent cloud probably eroded and incorporated a large volume of snow and ice from the upper flank of the cone; it definitely eroded an unknown thickness of soil from the upper fan surface. Brugman and Meier (1981) report 6 m of scour on the Shoestring Glacier on May 18, but part of this could have been removed by smaller pumiceous pyroclastic flows that followed the same flow path later in the day.

At approximately the base of the volcano (3.8 km from the crater rim), a distinctly basal gravity flow of debris, approximately 3 m thick, had separated from the surge cloud. It ran 47 m up the side of a ridge, so from equation 2 a velocity of 30 m/s was computed (Fig. 1). Peak discharge here ($Q = A \times \overline{U}$) was roughly 110,000 to 120,000 m^3/s. Large-scale eddying along this flow margin was indicated by the angle of abrasion impacts to standing trees, which deviated from the main direction of flow by 90 to 180 degrees. This suggests that the flow was still partially inflated at this point. Two kilometers farther down the fan, depth and velocity were roughly the same, velocity had decreased to 28 m/s, and evidence of eddying was no longer visible. Therefore, it is assumed that complete transition from gas-supported pyroclastic surge to water-supported lahar was essentially completed between these two points on the upper Pine-Muddy fan. This transition zone is indicated on figure 1. Fink and others (1981) reported a velocity of 31 m/s where a branch of the flow entered West Fork Pine Creek from the upper fan just short of 4 km from the crater rim.

The main portion of the lahar entered East Fork Pine Creek at a velocity of at least 24 m/s after having traveled 10 km over the Pine-Muddy fan (Fig. 1). Once channelized, superelevation of the debris slurry around bends at such velocities was dramatic (Fig. 3). As the lahar entered the East Fork channel, peak discharge was approximately 29,000 m^3/s and flow depths were on the order of 10 to 15 m. In the upper channel where width was constricted,

flow depth remained at about 13 m for several kilometers and average velocity varied between 11 and 20 m/s. Sharp bends in the channel appear to have played an important role in providing hydraulic resistance and slowing the lahar. The lower half of the Pine Creek channel was wider than above; average flow depth decreased to 8 m and average velocity ranged from 9 to 12 m/s. At the mouth of Pine Creek, peak discharge had decreased to about 7300 m^3/s.

The first of the two major lahars to enter Swift Reservoir probably came down Pine Creek, the shorter and steeper route to the reservoir. A small lahar also entered the reservoir from Swift Creek, but its volume was not great enough to effect the sustained rapid rise in stage that was observed. A stage recorder at Swift Dam operated by Pacific Power and Light Co. recorded the arrival of the first wave between 09:05 and 09:15 (error in resolution of record and establishment of time base). Calculations indicate it would take about 10 minutes for a wave set up by the lahar entering the lake to travel the length of the reservoir; thus the initial lahar entered the lake between 08:55 and 09:05. Routing the lahar down Pine Creek using calculated $\bar{U}$ values and assuming a starting time of 08:35, the lahar should have arrived at Swift Reservoir at 08:58. This overlapping of times suggests that the simplified runup and superelevation formulas used to calculate mean velocities are reasonably accurate, given the interpolation errors of routing and the uncertainties on the observed and starting times.

Deposition by the lahar on the lower Pine-Muddy fan and along the Pine Creek channel was minimal. Typically, a thin (0-0.5 m) veneer of debris was accreted on the lower fan surface, on terrace surfaces, or was ponded together with organic debris along the channel margin. Boulders up to about 1 m in diameter are thickly scattered over the lower fan, and bouldery accumulations were noted on the insides of tight bends, but whaleback bars, such as those described for the lahars in the Toutle River (Janda and others, 1981), were not observed.

Muddy River Lahar

The same pyroclastic surge that swept down the Pine-Muddy fan also moved down the slopes above Ape Canyon and (apparently) the headwaters of Smith Creek, both tributaries to Muddy River (Fig. 1). The massive lahar that descended Ape Canyon exceeded 20 m in depth and had a peak discharge of approximately 67,000 m^3/s. Average velocities calculated were 32 m/s at the head of the canyon (Janda and others, 1981), 28 m/s in the canyon just above the mouth, and 27 m/s as it ran up the slope opposite the canyon mouth in Smith Creek. A large lahar also came down upper Smith Creek, (Fig. 1) although its velocity and discharge were not calculated. It is unclear whether this lahar was triggered by the directed blast or by the pyroclastic surge that initiated the Ape Creek lahar. Smith Creek below Ape Canyon (below 8 km point, Fig. 2) is a wide (250-300 m), flat (0.013 gradient) valley. Both the Ape Creek and the upper Smith Creek lahars deposited large volumes of debris in this reach. Another lahar with a peak discharge of about 20,000 m^3/s split from the Pine Creek lahar and came down the Muddy River canyon, parallel to and just downstream from Ape Canyon, joining the Ape Creek lahar (Fig. 1). Average velocity calculated at the head of this canyon was 20 m/s; halfway down the canyon it was 23 m/s (Cassidy and others, 1980). A fourth but relatively minor contribution to the Muddy River lahar descended an unnamed canyon immediately downstream from Muddy Canyon.

By the time these combined flows reached the confluence of Clearwater Creek (Fig. 1; 14 km point, Fig. 2), average velocity had decreased to 14 m/s. Velocity continued to decrease in the downstream direction (Fig. 1). One eyewitness account (testimony of Paul and Kathy Hickson) states that the highway bridge (Road 125) on the lower Muddy was gone and the river was still "in flood" at about 10:00 PDT. Below the bridge velocities fluctuated between 3 and 6 m/s and peak discharge varied between 2700 and 4900 m^3/s. After

entering the Lewis River, the lahar was still flowing at about 6 m/s (Cassidy and others, 1980) when it flowed into Swift Reservoir. Routing this lahar down the channel using calculated velocities and the same starting time as the Pine Creek lahar yields an arrival time at the head of Swift Reservoir of 09:39 PDT. The leading edge should have reached the bridge across the Muddy River by about 08:57.

PHYSICAL COMPOSITION OF LAHAR SLURRIES

Samples (1-2 kg) of lahar deposits were collected at different points along the channels from as high as possible on channel sides or terraces and were analyzed by dry sieving, in order to define composition of the lahars during peak flow. Sample sites were selected to avoid clasts larger than about 100 mm diameter, so the data are biased against the coarse fraction. It was felt, however, that large cobbles and boulders were not as important to the mechanics of flow as the finer matrix material. On the basis of Varnes (1978) classification, the Pine Creek and Muddy River lahar samples were close to the boundary between "mudflow" and "debris flow". However, if all unsampled coarse clasts were included, both lahars would be classified as debris flows.

Statistical grain-size parameters were calculated and are shown in table 1. Data from the North Fork and South Fork Toutle River lahars are shown for comparison. Texturally, the sampled deposits can be described as either muddy sandy gravels or gravelly muddy sands (Folk, 1965). Envelopes of cumulative particle-size curves are shown in figure 4.

The Muddy River samples were, on the average, coarser than those from Pine Creek, but both east-side lahars were considerably coarser than the North Fork and South Fork Toutle River lahars. All were very poorly sorted, the particle-size distributions of most were weakly skewed toward the fine fraction (with the exception of Pine Creek), and all were platykurtic (tails

better sorted than central portion of distribution). No downstream changes in grain-size parameters were evident for the Pine Creek lahar (Fig. 5). The Muddy River lahar, on the other hand, showed a distinct fining and improvement of sorting in the downstream direction. This could possibly be due to the slower velocities of the Muddy River flow, which allowed more time for sorting to take place.

VARIATION IN FLOW BEHAVIOR

These lahars, viewed over their entire flow paths, maintained neither steady nor uniform flow; peak velocities displayed dramatic deceleration and peak discharges attenuated rapidly downstream. Even over relatively short reaches, the state and type of flow was probably variable. No photographic record exists for the southeast-side lahars, but KING-TV (Seattle) obtained a very good videotape record of the North Fork Toutle River lahar on the irregular surface of the debris avalanche. Velocities, flow depths, slurry composition, and even flow direction of this mudflow were extremely varied as strands of flow diverged and coalesced. Mean velocities were in the range of 12 to 15 m/s in areas where flow was concentrated to a depth of at least several meters (Janda and others, 1981). Although the slurry appeared quite viscous, flow fronts appeared to be less than 1 m high and plug flow was not observed. The greater portion of the flow had a smooth surface and laminar flow was indicated in some areas by streamlines of light colored material on the flow surface, which remained undistorted and parallel to the flow direction for hundreds of meters. Numerous hydraulic jumps indicate that the boundary between subcritical and supercritical flow was frequently crossed, and turbulence at the jumps was extremely violent. Although the composition of the North Fork Toutle River lahar differed from the coarser Pine Creek and Muddy River flows, it would not be unreasonable to expect similar flow behavior there, especially at the higher velocities.

The magnitude and nature of the Pine Creek and Muddy River lahars changed drastically in the downstream direction (Fig. 6, 7, 8). Both had initial peak velocities on the order of 25 to 30 m/s near the base of the volcano on the open slopes and in the steep, confined canyons (Fig 6), but velocities dropped off relatively rapidly with distance away from the volcano, more so in Muddy River than Pine Creek. Below a point approximately 22 km downstream, flow velocity in Muddy River became roughly constant, whereas the Pine Creek lahar continued to decelerate all the way to Swift Reservoir. Peak discharge, calculated from the mean peak velocities and surveyed cross-sectional areas, decreased even more rapidly (Fig. 7) indicating a major attenuation of the peak (more than two orders of magnitude) over the approximately 20 and 30 km traveled by each flow. Discharge decrease fits a power curve in the form $Q = a\ L^{b}$ ($r^2 = 0.85$), where $a = 2.3 \times 10^6$ and $b = -2.0$. Froude numbers calculated for the surveyed cross-sections ($F = \bar{U}/(gD)^{\frac{1}{2}}$) indicate that flow in Pine Creek remained near or above critical velocities along the entire flow path, whereas the Muddy River lahar flowed subcritically though the lower channel reaches (Fig. 8). This suggests that if any cross waves did form during peak flow, their locations migrated.

Nearly 14 million m^3 of lahar slurry reached Swift Reservoir on the morning of May 18 (Cassidy and others, 1980), nearly all of it arriving via these two drainages. The leading edge of the higher velocity Pine Creek lahar arrived there within half an hour of the beginning of the eruption, and entry of the lahar into the standing water of reservoir generated a wave 0.4 m high (when it reached the dam). The combined hydrograph of the two lahars entering the reservoir (plus the small Swift Creek lahar) had relatively steep rising and falling limbs with a peak discharge of about 2700 m^3/s (Fig. 9). Time to peak was approximately 30 minutes and discharge within 90 percent of peak was sustained for about 45 minutes. Total flow duration was a little more than 4 hours.

Relationships between independent channel parameters and mean velocity have been investigated in order to identify the relative control exerted by easily measured variables on lahar peak velocity in two natural channels. Establishment of such empirical relationships can be of use in defining and predicting lahar hazards, at least in similar terrains. Although regression analyses have not been made, apparent correlation of some channel parameters with velocity appears better than others. None of the relationships are strong, however, suggesting that the interactions of flow-driving forces to resisting forces are complex.

A plot of mean velocity against channel gradient (Fig. 10) yields a moderately good nonlinear relationship with some scatter of data points. The two extreme outlying points above the main trend were taken from the mouth of Ape Canyon. There, the lahar had just cascaded down an extremely steep reach of channel and the flow had considerable momentum, maintaining a high velocity even though channel gradient had decreased. The average gradient for the kilometer upstream of the location of the superelevation calculation was 0.130. Using this value for the two Ape Canyon velocities, the points would fall on the main trend. Apparent dependence of mean velocity on average depth, on the other hand, is almost nonexistent for both Pine Creek and Muddy River (Fig. 11). This lack of influence may be partly due to a geomorphic factor--a number of the bends in these channels coincide with channel constrictions. At these locations depth increases as width is confined, and the natural tendency for flow velocity to increase in response to increased depth is countered by the resistence to flow offered by the bends themselves. Plotting mean velocity against radius of curvature of bends for lower reaches only (Fig. 12) suggests that, for Pine Creek at least, the tighter the bend, the lower the velocity.

CONCLUSION

Two very large, high velocity lahars were triggered by a pyroclastic surge during the first few minutes of the May 18, 1980 eruption of Mount St. Helens. Transition from gas-supported pyroclastic surge to water-supported lahar appears to have occurred at the base of the volcanic cone, approximately 4 to 5 km downslope from the crater rim. A combined initial peak discharge from the Pine-Muddy fan, upper Smith Creek, and Ape Creek probably exceeded 200,000 m^3/s but decreased exponentially in the downstream direction. Initial average velocities of about 30 m/s also decreased markedly downstream. During much of the route traveled, the velocity of lahar appears to have been supercritical. Channel gradient exerted considerably more control over mean velocity than did average depth, although the depth-velocity relationship appears to have been seriously affected by hydraulic resistance to flow at channel bends. Particle-size distribution of the lahar peak flow deposits covers a fairly wide range. Texturally, these lahars are debris flows.

The two formulas used to compute lower limits on average velocity yielded results that were internally consistent. When used to route the lahars down their respective channels to Swift Reservior, the computed velocities led to arrival times that were in agreement with the recorded arrival times. But the uncertainties posed by insufficiently accurate data on the recorded times do not permit a critical evaluation of equations 2 and 3. In the meantime, it would appear that these two simple velocity equations provide reasonable estimates of mean velocity for lahars.

REFERENCES

Apmann, R.P., 1973, Estimating discharge from superelevation in bends: J. Hydraul. Div., Proc. Amer. Soc. Civ. Eng., v. 99, p. 65-79.

Brugman, M.M. and Meier, M.F., 1981, Response of glaciers to the eruptions of Mount St. Helens, in Lipman, P.W. and Mullineaux, D.R. (eds.), The 1980 Eruptions of Mount St. Helens, Washington: U.S. Geol. Survey Prof. Paper 1250, p. 733-741.

Cassidy, J.J., Coombs, H.A., and Shannon, W.L., 1980, Study of effects of potential volcanic activity on Lewis River projects: unpublished report to Pacific Power and Light Co., Portland, Oregon, 91 p.

Chow, V.T., 1959, Open-Channel Hydraulics: New York, McGraw-Hill, 680 p.

Cummans, John, 1981, Chronology of mudflows in the South Fork and North Fork Toutle River following the May 18 eruption, in Lipman, P.W. and Mullineaux, D.R. (eds.), The 1980 Eruptions of Mount St. Helens, Washington: U.S. Geol. Survey Prof. Paper 1250, p. 479-486.

Davies, D.K., Quearry, M.W. and Bonis, S.B., 1978, Glowing avalanches from the 1974 eruption of the volcano Fuego, Guatemala: Geol. Soc. Amer. Bull., v. 89, p. 369-384

Fink, J., Malin, M. D'Alli, R.E., and Greeley, R., 1981, Rheological properties of mudflows associated with the spring 1980 eruptions of Mount St. Helens volcano, Washington: EOS Geophysical Research Letters, v. 8, no. 1, p. 43-46.

Folk, R.L., 1965, Petrology of sedimentary rocks: Hemphill's, Austin, Texas, 159 p.

Hughes, W.F. and Brighton, J.A., 1967, Theory and problems of fluid dynamics: New York, McGraw-Hill (Schaums Outlines),265 p..

Janda, R.J., Scott, K.M., Nolan, K.M. and Martinson, H.A., 1981, Lahar movement, effects, and deposits, in Lipman, P.W., and Mullineaux, D.R. (eds.), The 1980 Eruptions of Mount St. Helens, Washington: U.S. Geol. Survey Prof. Paper 1250, p. 461-478.

Johnson, A.M. and Hampton, M.A., 1969, Subaerial and subaqueous flow of slurries: Unpublished final report to the U.S. Geological Survey; available through the U.S. Geological Survey Library, Menlo Park, California, and Branner Library, Stanford University, Stanford, California.

Moore, J.G. and Rice, C.J., 1983, Chronology and character of the May 18, 1980 explosive eruptions of Mount St. Helens, in Boyd, F.R. (ed.), Explosive Volcanism: National Research Council [in press].

Rice, C.J. and Watson, D.K., 1981, Satellite observations of Mount St. Helens: EOS, Trans. Amer. Geophys. Union, v. 62, p. 577-578.

Schuster, R.L., 1981, Effects of the eruptions on civil works and operations in the Pacific Northwest, in Lipman, P.W. and Mullineaus, D.R. (eds.), The 1980 Eruptions of Mount St. Helens, Washington: U.S. Geological Survey Prof. Paper 1250, p. 701-718.

Varnes, D.J., 1978, Slope movement types and processes, in Schuster, R.L. and Krizek, R.J. (eds.), Landslides, Analysis and Control, Transportation Research Board: National Acad. of Sciences, Washington, D.C., Spec. Report 176, p. 12-33.

Voight, B., Glicken, H., Janda, R.J., and Douglass, P.M., 1981, Catastrophic rockslide avalanche of May 18, in Lipman, P.W., and Mullineaux, D.R., (eds.), The 1980 Eruptions of Mount St. Helens, Washington: U.S. Geological Survey Prof. Paper 1250, p. 347-377.

Wohletz, K.H. and Sheridan, M.F., 1979, A model of pyroclastic surge: Geol. Soc. Amer., Special Paper 180, p. 177-194.

Table 1. Summary of statistical grain-size measures for deposits at peak flow from the Pine Creek and Muddy River lahars. Measures are those defined by Folk (1965). Measures for North Fork and South Fork Toutle River lahars (K. Scott, USGS, written commun., 1982) are shown for comparison. Number of samples for each lahar are indicated.

	Mean grain Diameter M_Z (ø units)	Sorting Coefficient σ_I (ø units)	Skewness Sk_I	Kurtosis K_G
Pine Creek lahar n = 13	0.19 ± 0.68	3.19 ± 0.28	-0.15 ± 0.08	0.86 ± 0.07
Muddy River lahar n = 11	-0.36 ± 1.50	3.03 ± 0.35	0.20 ± 0.27	0.87 ± 0.13
North Fork Toutle River lahar n = 13	1.22 ± 1.13	3.58 ± 0.51	0.13 ± 0.18	1.04 ± 0.11
South Fork Toutle River lahar n = 7	1.20 ± 0.94	3.06 ± 0.62	0.04 ± 0.15	1.06 ± 0.15

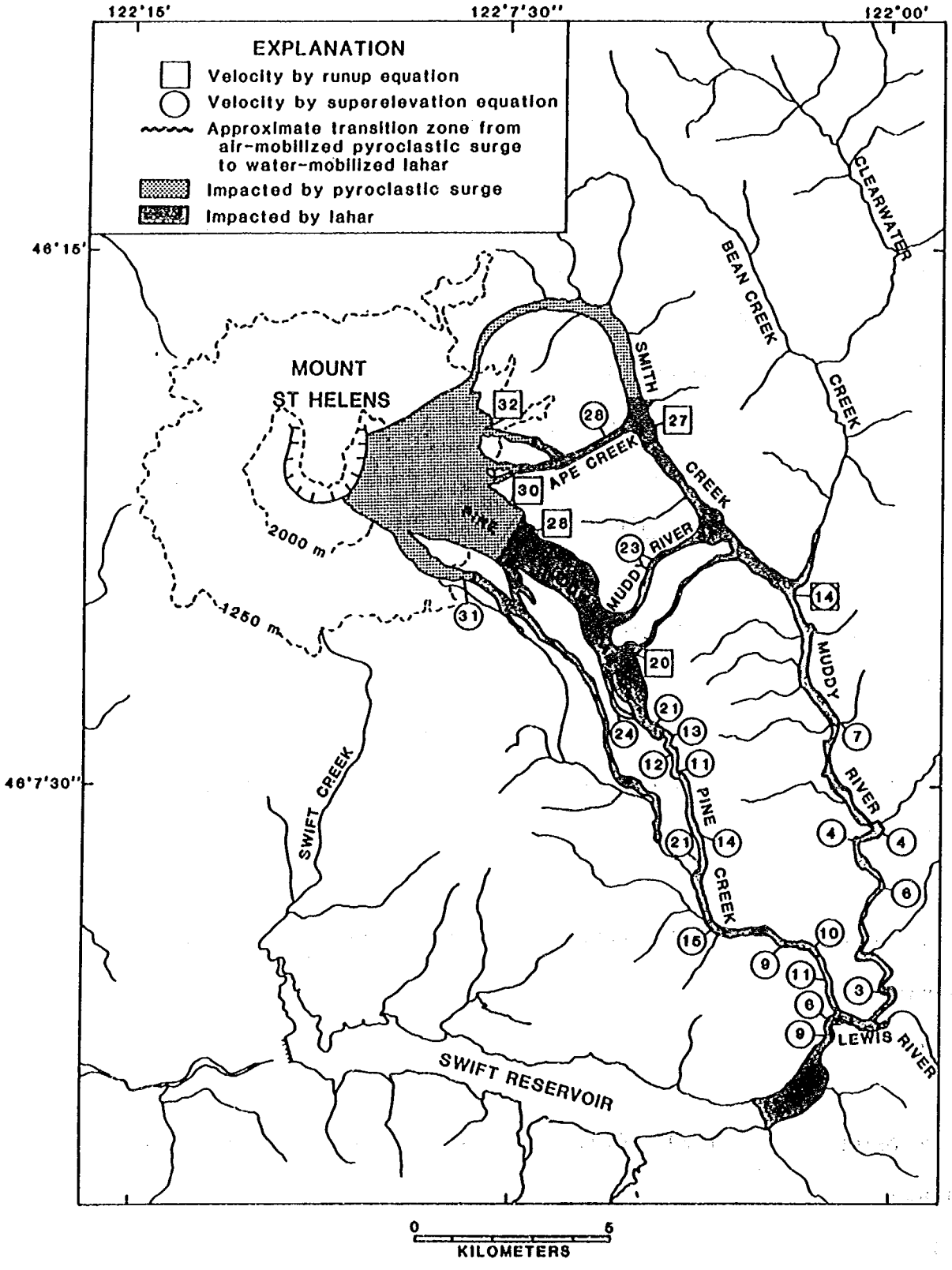


Figure 1. Slopes and channels impacted by pyroclastic surge and lahars on east flank of Mount St. Helens on May 18, 1980. Velocities indicated are in meters per second; values from Cassidy and others (1980), Fink and others (1981), and Janda and others (1981) are included.

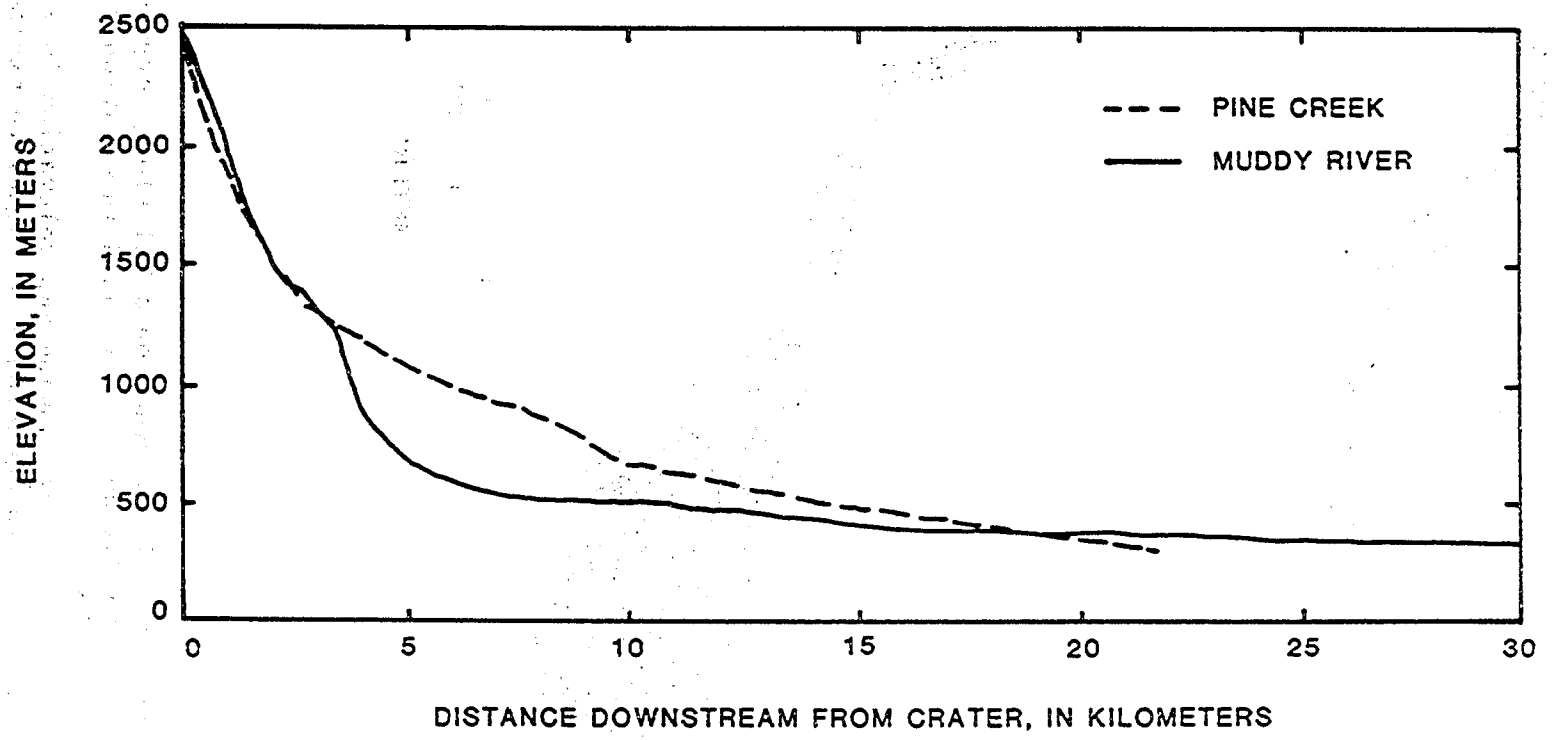


Figure 2. Longitudinal profiles of the Pine Creek and Muddy River (via Ape Creek) channels. Vertical exaggeration is 5.3 times.

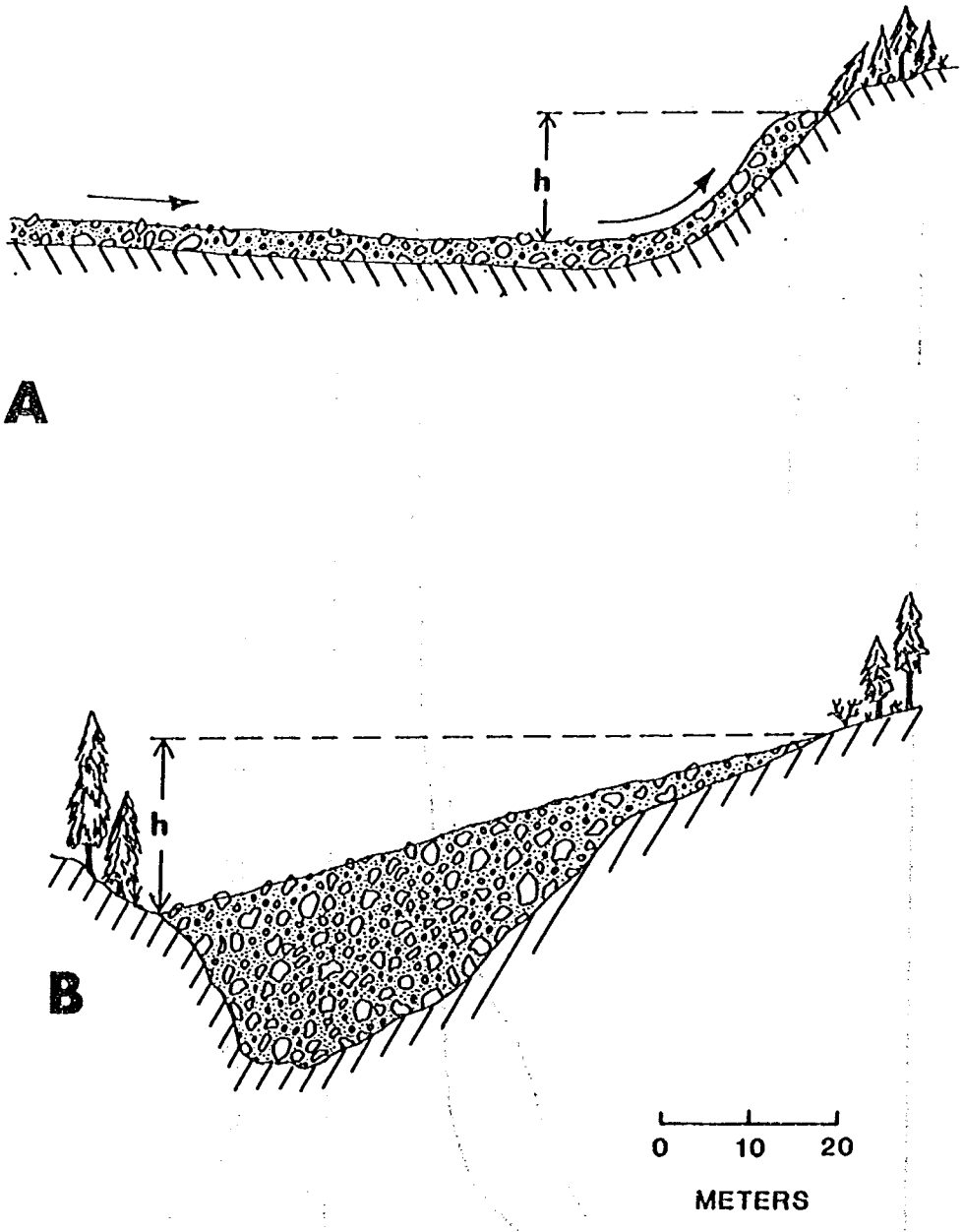


Figure 3. A. Longitudinal section of lahar runup on a hillslope perpendicular to the flow path. The distance, h, is used in equation 2 to calculate minimum velocity.
B. Transverse section of a lahar showing superelevation in a bend. The distance, h, is used in equation 3 to calculate minimum velocity. This is a scale drawing of a surveyed cross-section at the head of Pine Creek; h = 20 m.

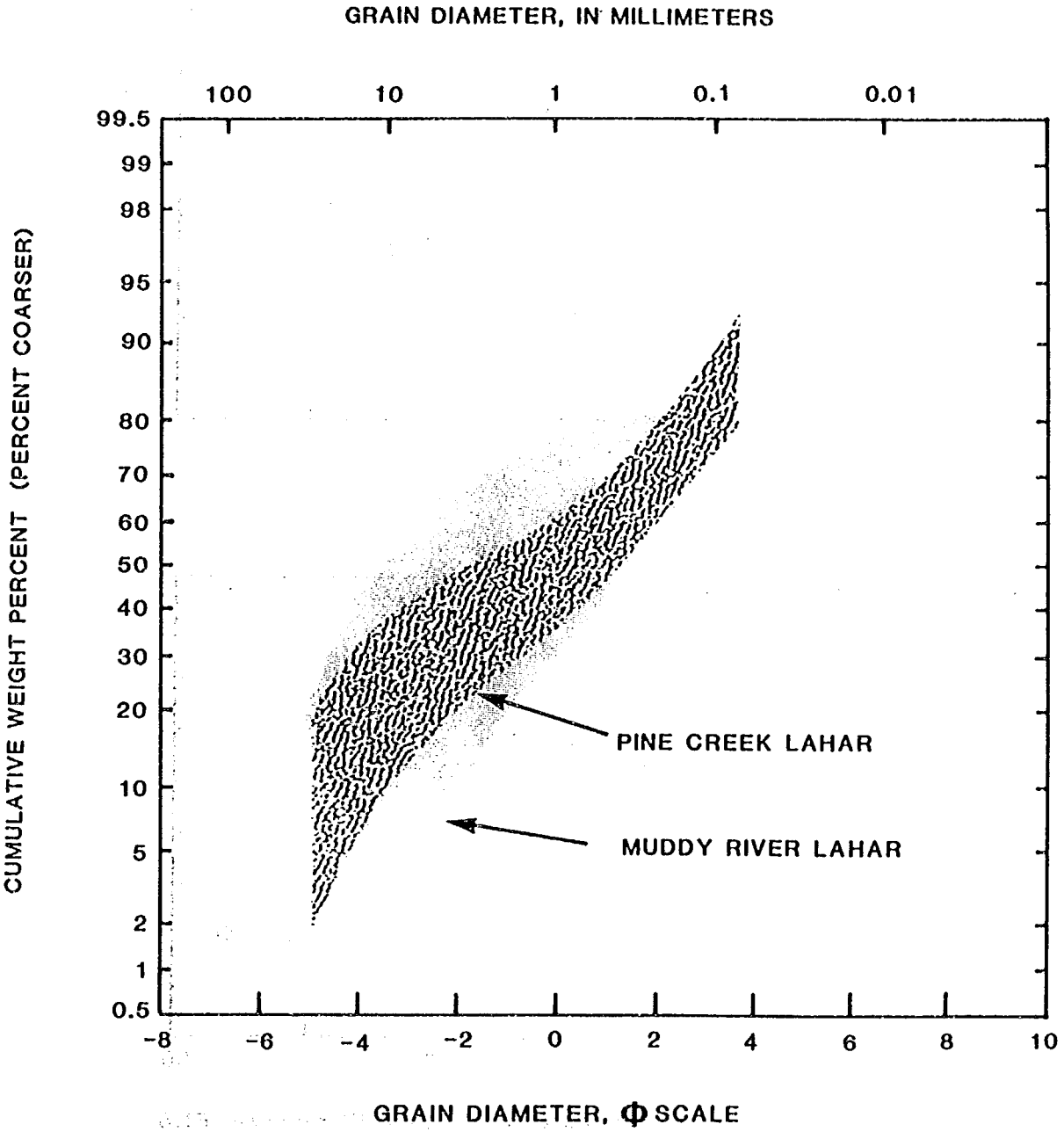


Figure 4. Envelopes of cumulative grain-size curves for the Pine Creek and Muddy River lahars. Sampling was limited to peak flow deposits and sites where clasts were finer than -6ϕ.

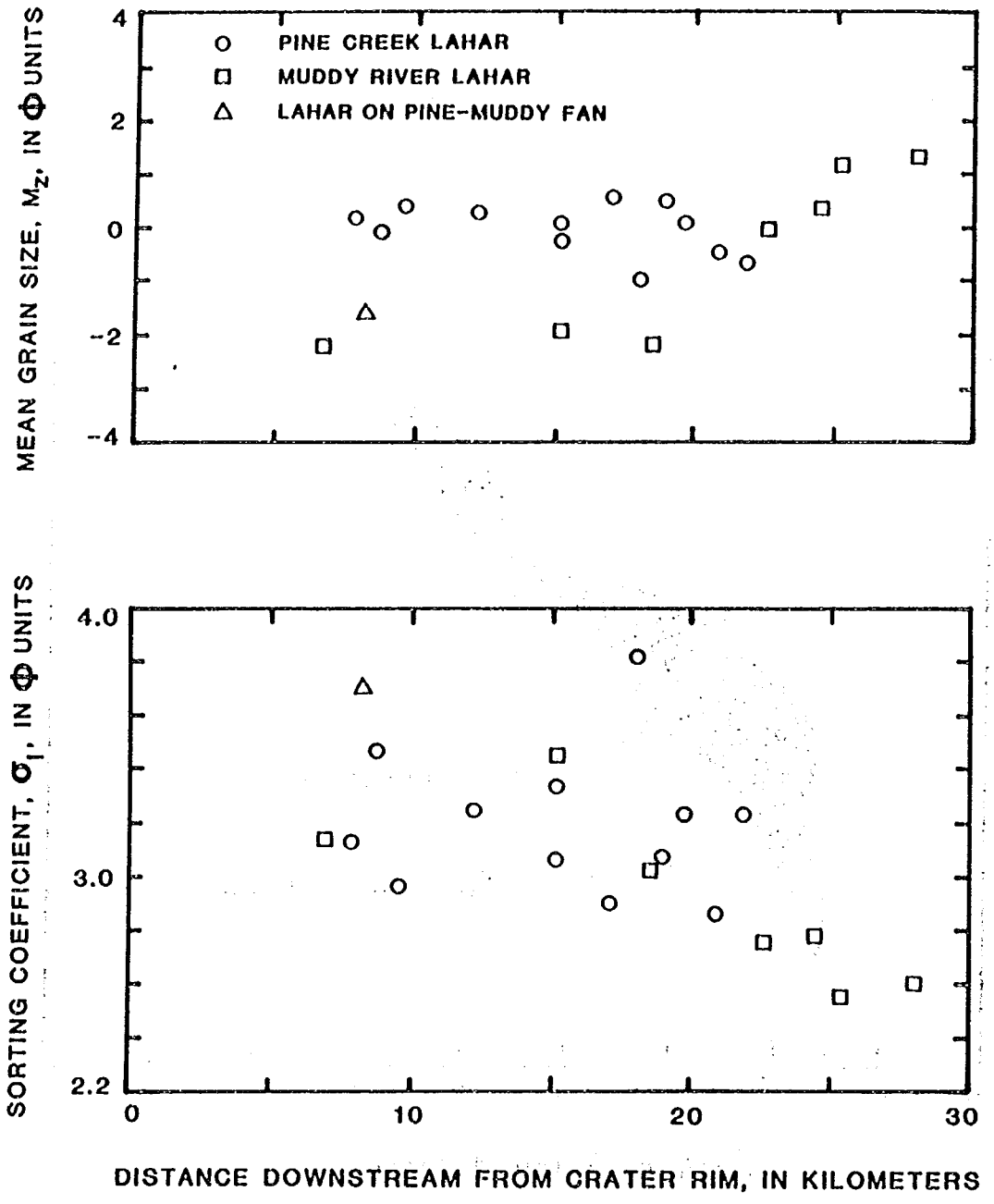


Figure 5. Downstream variation in mean grain size (graphic mean) and degree of sorting (inclusive graphic standard deviation) in peak flow lahar deposits. From Folk (1965).

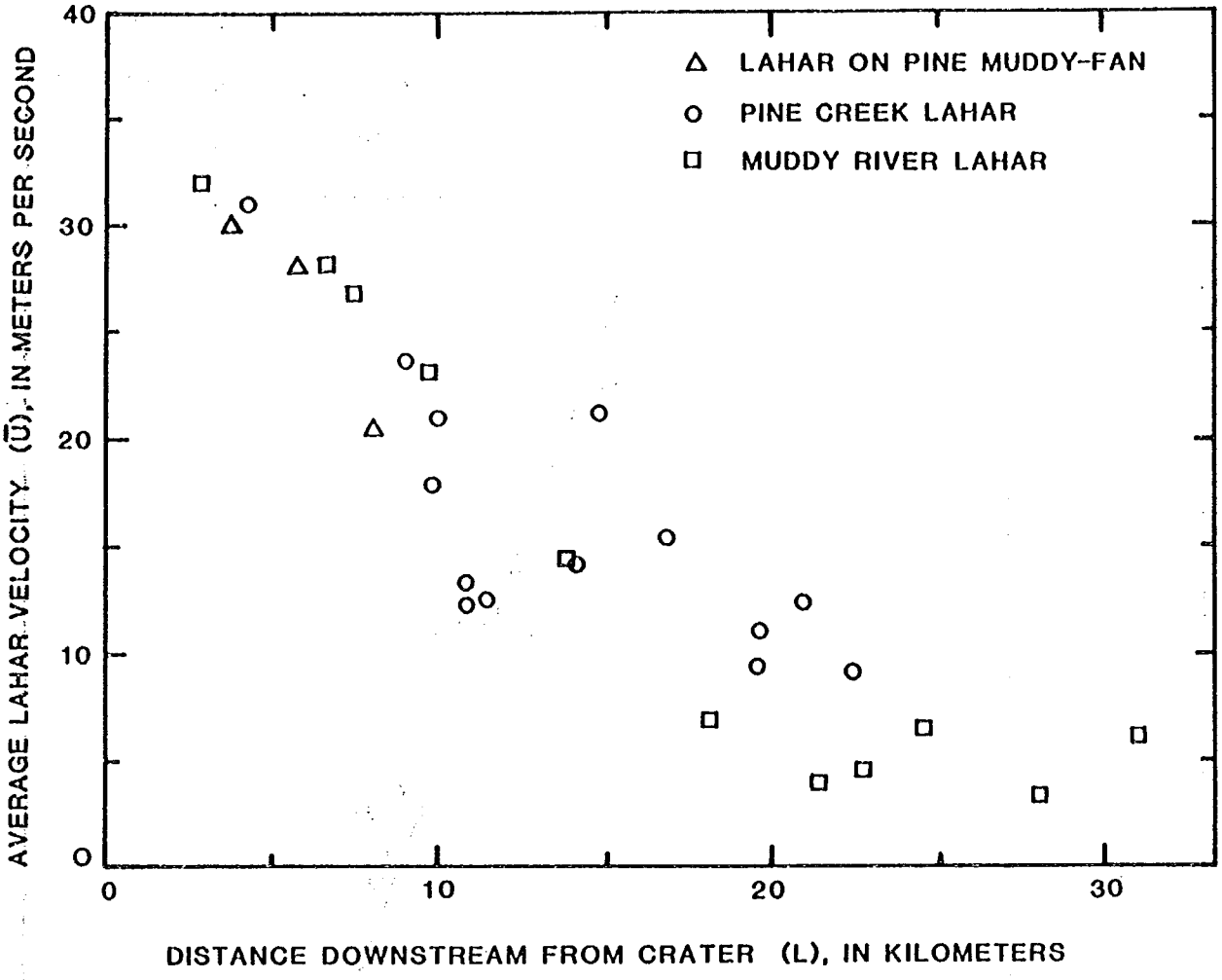


Figure 6. Downstream variation in calculated average lahar velocity on the Pine-Muddy Fan, in Pine Creek and in Muddy River.

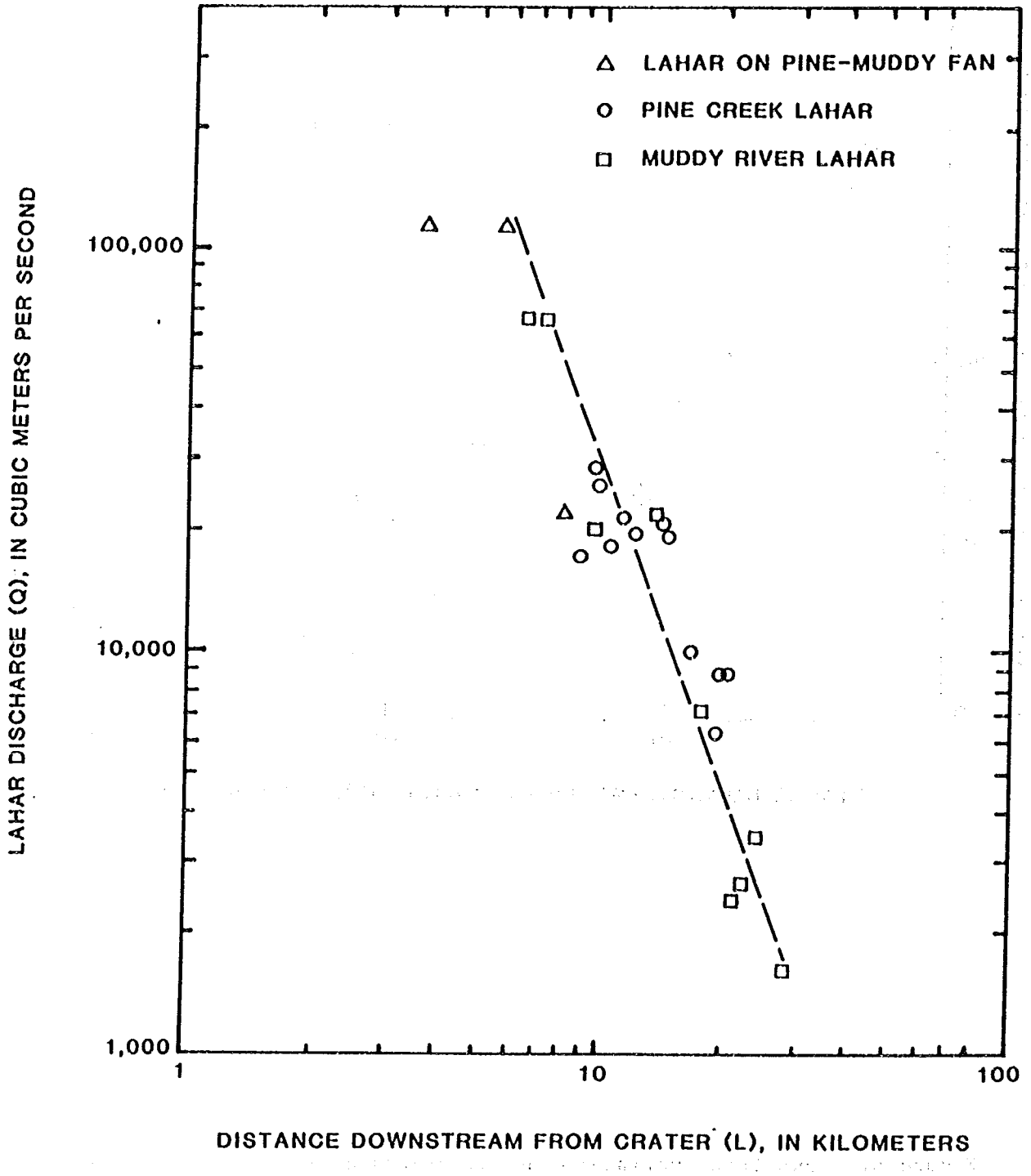


Figure 7. Downstream variation in calculated lahar discharge on the Pine-Muddy fan, in Pine Creek, and in Muddy River.

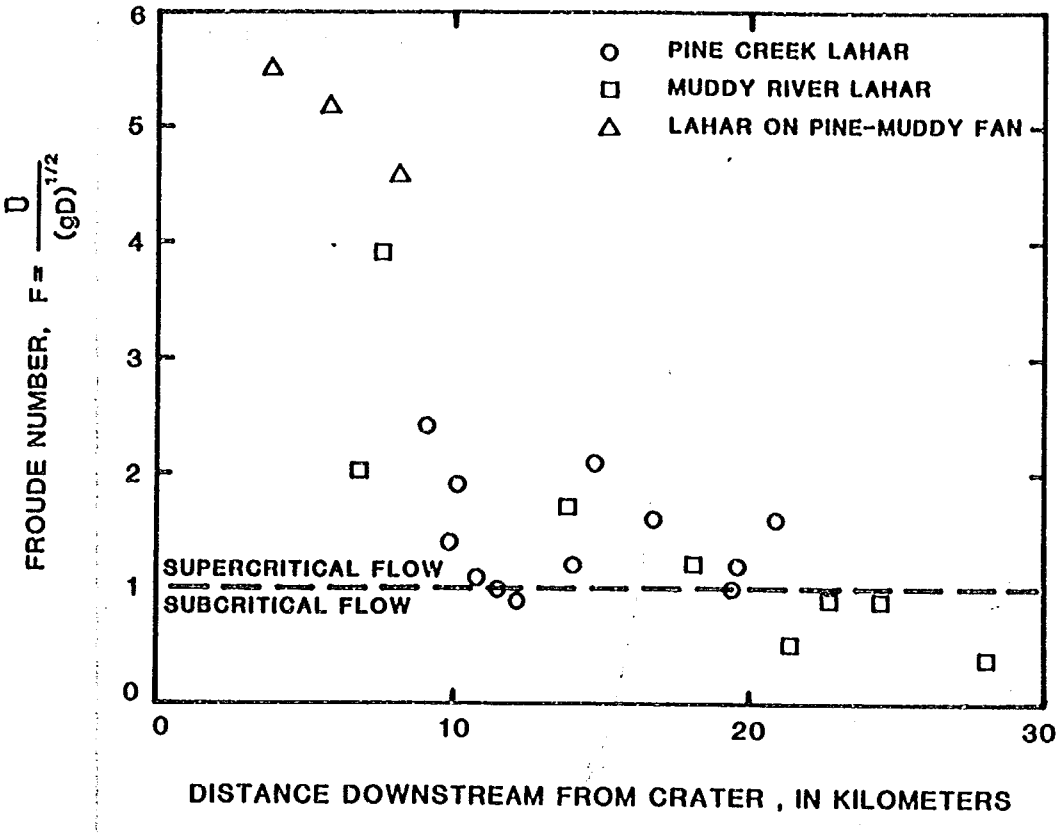


Figure 8. Downstream variation in Froude number of lahar flow on Pine-Muddy fan, in Pine Creek, and in Muddy River.

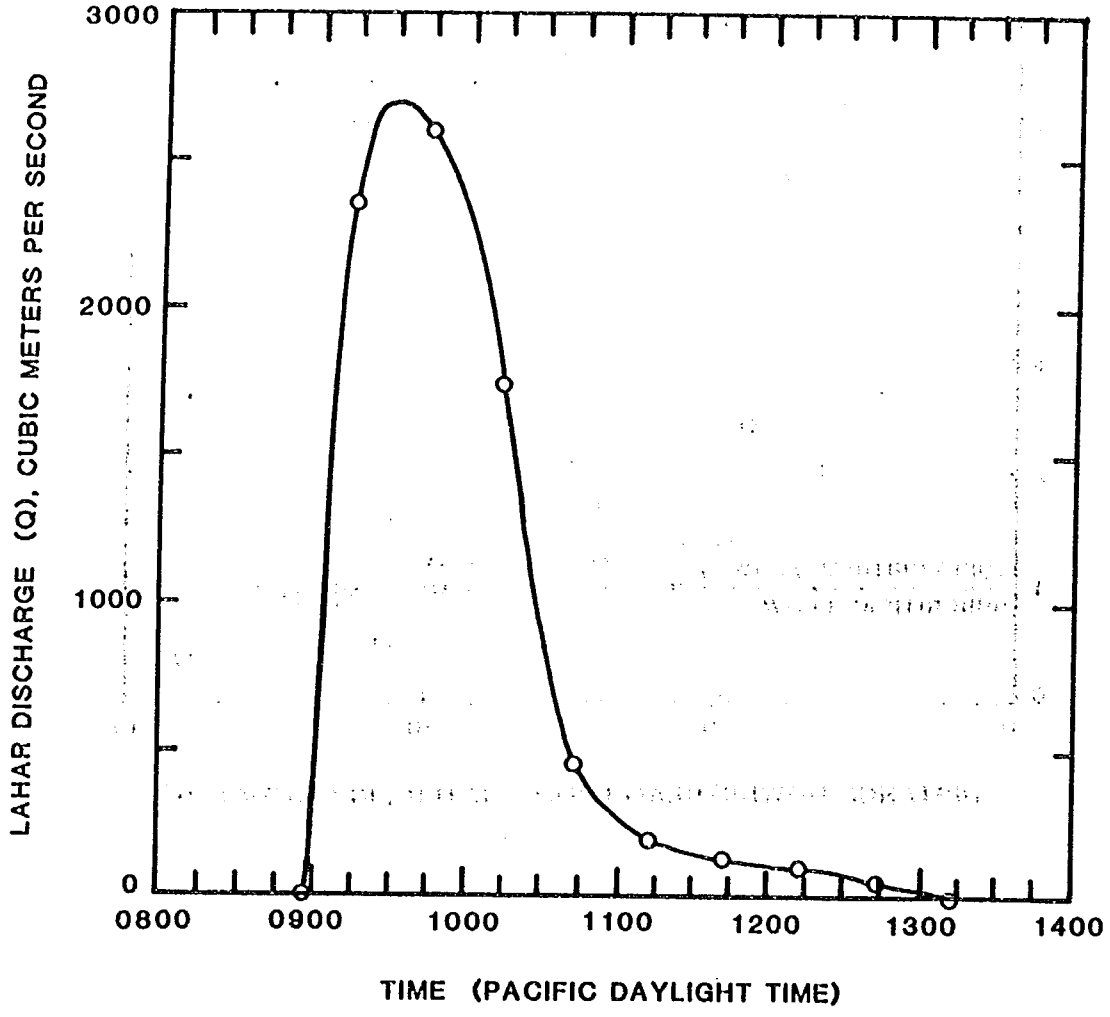


Figure 9. Reconstructed hydrograph of lahars entering Swift Reservoir, determined from water stage record at Swift Dam. Record courtesy of Pacific Power and Light Company.

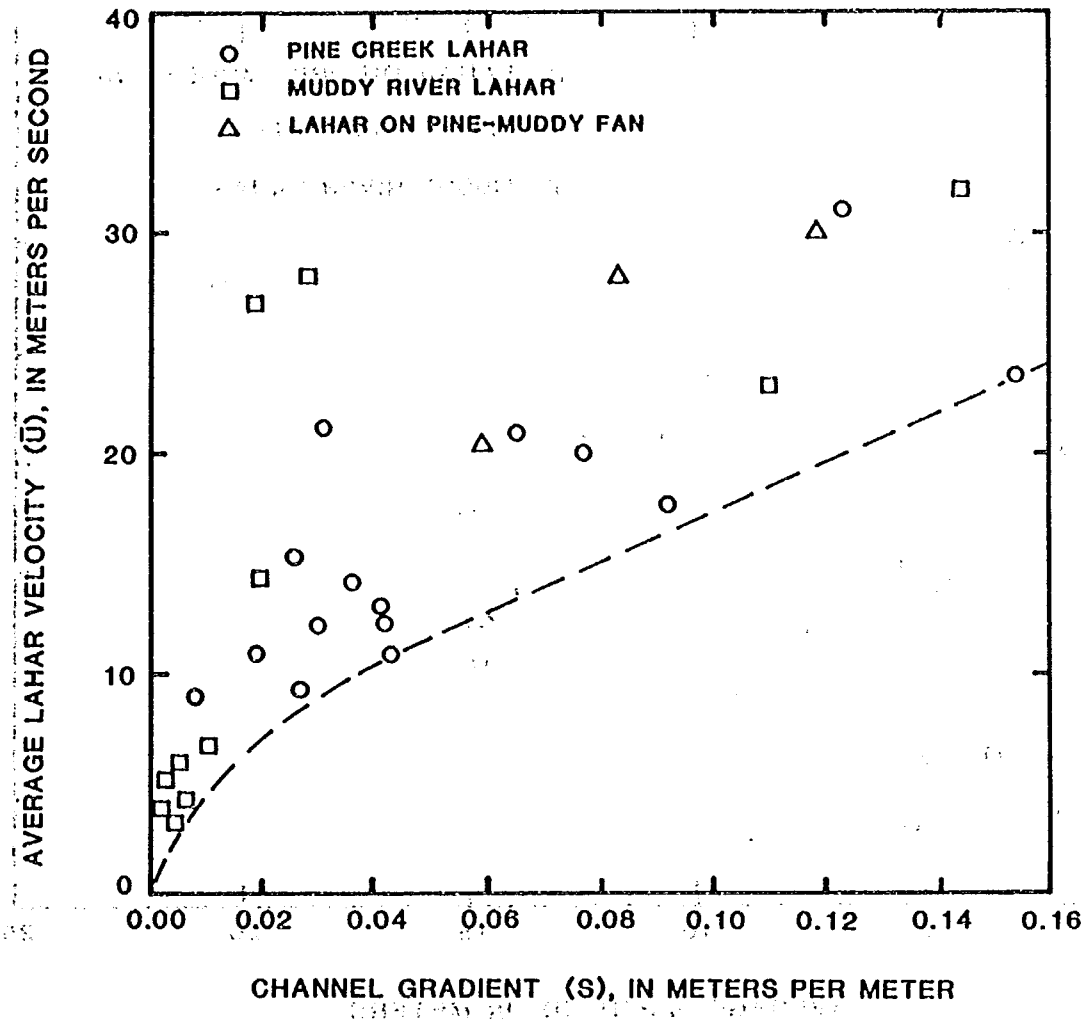


Figure 10. Average lahar velocity plotted as a function of channel gradient. Apparent lower limit is drawn.

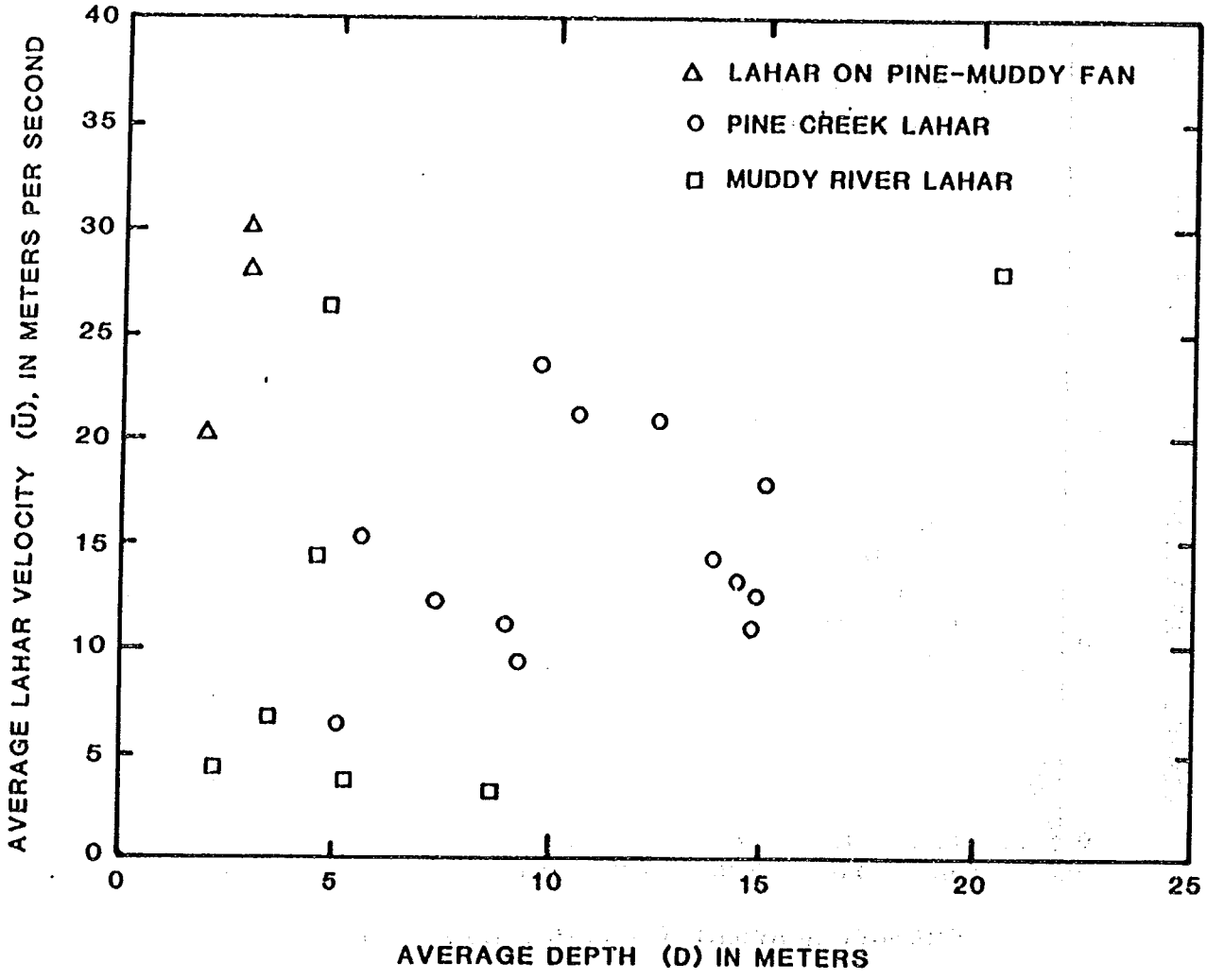


Figure 11. Average lahar velocity plotted as a function of average depth of flow (A/w).

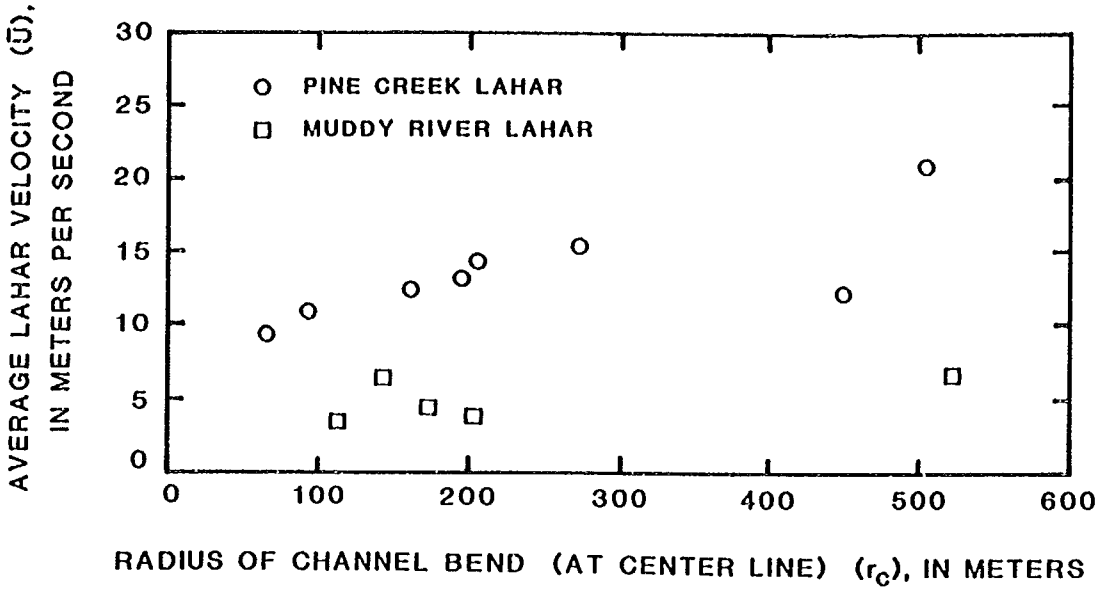


Figure 12. Average lahar velocity plotted as a function of channel bend radius. Sites where flow had large inertial forces (inherited from much steeper upstream reaches) were excluded.

DYNAMIC AND VOLUMETRIC CHARACTERISTICS OF THE 18 MAY 1980 LAHARS ON THE TOUTLE RIVER, WASHINGTON

Lee H. Fairchild
Mark Wigmosta
Department of Geological Sciences
University of Washington
Seattle, WA 98195
USA

Leon H. Rosenfeld
Mark Wilemski
Department of Geological Sciences
University of Washington
Seattle, WA 98195
USA

INTRODUCTION

The North and South Forks of the Toutle River flow westward from Mt. St. Helens, join near the town of Toutle Lake, and continue to the confluence with the Cowlitz River between 65 and 70 km from Mt. St. Helens (Figure 1). Both drainages were sparsely populated near Mt. St. Helens before 18 May 1980. The closest significant development on the South Fork was timber storage Camp 12 40 km from from the volcano. The valley of the South Fork between the camp and the confluence with the North Fork (44 km) was sparsely populated by permanent residents. The North Fork of the Toutle River was occupied by scattered small settlements between Maple Flats (Figure 1) and the confluence with the South Fork. Between the confluence and the junction with the Cowlitz River the valley bottom of the Toutle River was characterized by a moderate density of permanent residents. Castle Rock, Kelso, and Longview, three major population centers of relatively high population density, were established along the Cowlitz River (Figure 1).

Lahars were generated on both forks of the Toutle River during the 18 May 1980 eruption of Mt. St. Helens. Photographic and seismic evidence (S. C. Malone, personal communication) document that the South Fork lahar was initiated when a pyroclastic surge (correlative with surge of Moore & Rice, 1981) overtopped the summit of Mt. St. Helens and flowed rapidly into the drainage of the South Fork at approximately 0834 Pacific Daylight Time (PDT), two minutes after the eruption began. The North Fork lahar was probably initiated by liquefaction of avalanche deposits saturated by hydrothermal and ice-melt water. This lahar was first reported moving down channel from its source at approximately 1310 PDT. Both lahars reached the Cowlitz River; the South Fork lahar produced only a moderate rise in stage at Castle Rock and caused no damage, the North Fork lahar inundated the Cowlitz River valley and transported a large volume of sediment downstream to the Columbia River.

In this paper we will present results of detailed field measurements we have made that allow calculation of dynamic and volumetric characteristics of the Toutle River lahars. Work that is still in progress will only be introduced briefly; the paper will concentrate, instead, on the results of velocity calculations made from lahar superelevations around channel bends or at channel obstructions. Work done concurrently on the size characteristics of lahar deposits by Gilkey and Fairchild will not be presented; some results of this work are published in Gilkey (1982).

Measurements of the diameters of trees snapped by lahars and of the superelevation of the lahar surface on the up-flow sides of standing trees are being used by Wigmosta to calculate lahar velocity. Viscosity and vertically-averaged velocity can be calculated from the diameter of snapped trees for lahars with specified constitutive properties by balancing tree strength (a function of tree diameter and species) against the bending movement imposed by the lahar flowing past the tree. Field and experimental measurements provide constitutive properties necessary for the calculations. Velocities calculated in this manner are being applied in two ways. First, groves of snapped and standing trees are being used to determine a critical snapping diameter; trees with larger diameter were too strong to be snapped, trees with smaller diameters were snapped. Calculation using this critical diameter provides a lahar velocity averaged for the entire grove. Second, calculations for individual snapped trees provide a minimum, local, vertically-averaged velocity vector for the lahar. Local velocity vectors can also be calculated from measurements of the superelevation of the lahar surface on the up-flow side of standing trees. Both snapped and standing trees have been surveyed in four channel reaches. Calculated velocity vectors provide detailed three dimensional maps of the velocity field, which will be used to calibrate mechanical models of flow through these reaches (work in progress by Fairchild). Because this

work is in progress it will not be reported in detail in this paper.

Measurements of the superelevation of the lahar surface at channel bends or channel obstructions allow calculation of average velocity and discharge at peak flow. Calculated discharges have been used to construct hydrographs for both Toutle River lahars. These hydrographs have provided calibration for models routing potential future lahars down-channel (Dunne and Leopold, 1981). Calculated velocities and constructed hydrographs are discussed in detail in the remainder of the paper.

VOLUMETRIC AND DYNAMIC CHARACTERISTICS OF THE LAHARS

Where a flowing lahar traverses a channel bend, its average velocity can be calculated from measurements of the cross-channel slope of the lahar surface. This slope, represented by a "superelevation" of the mudline marking the mudflow surface on the outer bank relative to the mudline on the inner bank, is a function of flow velocity and channel radius. A relationship for average surface slope (equation 1) can be derived from the cross-channel equation of motion in curvilnear coordinates by assuming steady, uniform flow in which cross-stream basal deviatoric stresses and the derivatives of cross-channel deviatoric stresses are small relative to the cross-channel pressure gradient imposed by the sloping lahar surface (Smith and McLean, in prep.).

$$(1) \quad \text{slope} = \frac{\Delta h}{W} = \frac{(U^2)ave}{Rg}$$

Δh = elevation difference between outer and inner mudlines

W = channel width at the mudflow surface

R = channel radius

U = velocity

g = gravitational acceleration

If it is assumed that $(U^2)ave \approx (U)ave^2$, then this equation can be rearranged to permit solution for average velocity at peak flow:

$$(2) \quad (U)_{pk}^{ave} = \left(\frac{R\Delta hg}{W}\right)^{1/2}$$

At the four locations closest to Mt. St. Helens on the South Fork, velocity was calculated from the mudline rise measured on topographic obstructions directly in the path of flow. Because the channel is not curved at these locations, $R = \infty$ and equation (2) is inappropriate. We have instead used equation (3), which is derived by equating kinetic energy to the potential energy represented by the mudline rise (dh).

$$(3) \quad (U)_{pk}^{ave} = [2g(dh)]^{1/2}$$

Because this equation does not account for energy loss due to friction, it provides a minimum estimate of velocity.

Peak discharge (Qpk) can then be calculated from $(U)_{pk}^{ave}$ if the lahar cross sectional area (A) is known:

$$(4) \quad Qpk = (U)_{pk}^{ave} \cdot A$$

Hydrographs can be constructed at locations where four of the following five variables can be determined: (1) Qpk; (2) lahar volume; and the time of lahar (3) arrival, (4) peak, (5) termination (figure 2). Compilations of eye-witness observations by Cummans (1981, 1982), supplemented where necessary by Fairchild, provide times of lahar arrival, peak, and termination. In most locations, however, one of these times cannot be determined, so that lahar volume must be calculated independently to provide enough data for hydrograph construction. The measurements of the volume of material deposited and eroded by each lahar allow computation of the net change of lahar volume for any specified channel reach. Once lahar volume is established at one location, the sediment budget can be used to determine lahar volume at any other location.

South Fork Lahar

The South Fork lahar traversed three reaches of contrasting channel

geometry in the 44 km between the base of Mt. St. Helens and the confluence of the South and North forks of the Toutle River (subsequently simply called the confluence). The upper 16 km of the South Fork valley is characterized by a high-gradient (S = 0.04), flat-bottomed valley with an average width of 450 m (Figure 3a). At 18 km from Mt. St. Helens, the valley constricts to approximately 1/5 its former width. Below this is 21 km of sinuous bedrock channel, with an average gradient of 0.008, and widths typically between 50 and 180 m (Figure 3b). Between 37 km and 44 km, the channel widens again to an average width of 320 m and gradient of 0.008. Below the confluence, the North Fork lahar covered mudlines left by the South Fork lahar so that depth and velocity data on the South Fork lahar are not available.

The lahar depth in the upper reach of the South Fork was generally less than 10 meters because of the large channel width. At 18 km the channel constriction forced an increase in maximum flow depth to between 20 and 30 m in the narrow bedrock channel. The lahar then thinned in the wider lowest reach to between 4 and 9 meters.

The average peak velocities and peak discharges of the South Fork lahar, which were measured at locations in Figure 1, are plotted in Figure 4. Results at the four locations closest to Mt. St. Helens are based on mudline superelevations on topographic obstructions. Two values on the lower South Fork are based on cross sections measured at locations where there was no mudline superelevation. Instead, a probable range of average velocity was estimated based on channel depth, gradient, and on velocities estimated on the North Fork for comparable conditions. This velocity range was then used to calculate a predicted range of peak discharge. Both results are plotted as brackets in Figure 4. The remaining data are calculated from mudline superelevation at channel bends.

The initial velocity of the South Fork lahar as it moved off the steep slopes of Mt. St. Helens was clearly very high. Our closest measured velocity,

4 km from the base of St. Helens, is 33.3 m/s. The lahar slowed rapidly to approximately 20 m/2 at 18 km as it flowed down the wide upper reach. Though our calculations show a sharp velocity decrease at the channel constriction, a potentially high error of the velocity at 19 km makes such an interpretation insecure. In the bedrock channel below the constriction, lahar velocity fluctuated between 8.5 and 13 m/s, but no longer decreased downchannel. Once the lahar reached the wider lower channel, however, the decrease in average velocity resumed, until velocity reached a probable value between 4 and 8 m/s near the confluence. Peak discharge decreased along the entire length of the South Fork from 68,000 m^3/s at 4 km to approximately 18,000 m^3/s at 25 km, and between 2,000 and 5,000 m^3/s at 43 km. Our results also document a downchannel decrease in the rate of change of peak discharge per length of channel. Measurements of the net volume of deposition (Table 1) indicate that large volumes of debris were deposited in the wide upper and lower reaches where the lahar was comparatively shallow, but a much smaller volume was deposited in the deep, narrow bedrock reach.

Hydrographs constructed for the South Fork lahar graphically document the rapidly-changing character of the lahar (Fig. 5). Photographs taken by observers show that the South Fork lahar started within 2 minutes of the beginning of the eruption, suggesting that it reached our first measurement location 4 km down the South Fork at about 0838 PDT. There the peak discharge of the lahar was 68,000 m^3/s, its volume was 13 million m^3, but its duration was only approximately 6.5 minutes. Seventeen kilometers downchannel from Mt. St. Helens the flow duration had increased to 14 minutes despite a decrease in volume to approximately 12 million m^3. When the lahar reached the confluence about 108 minutes after the eruption began, its volume was approximately 8 million m^3 and duration was about 72 minutes. The flow peak traversed the 40 km between our first measurement location and the confluence in about 127 minutes, indicating an average celerity fo 5.2 m/s (see also Cummans, 1981).

The rapid downchannel decrease in Qpk is in part due to deposition by the lahar. Lahar volume, represented graphically by the area under each hydrograph, was reduced approximately 37% by deposition along the South Fork. But the downchannel increase in flow duration indicates that attenuation of the hydrograph and a commensurate decrease in Qpk was also important.

North Fork Lahar

The North Fork channel is characterized by wide valleys (gradient $\tilde{=}$ 0.005-0.01) with extensive high-level terraces (Figure 6a). Typical lahar depths of between 5 and 8 were enough to innudate the terraces. Interspersed between wide valley reaches are narrow, sinuous bedrock canyons similar to those on the South Fork, but commonly with more promenant terraces (Figure 6b). Lahar depth in these canyons typically varied between 10 and 18 m.

Thick rockfall-avalanche deposits filled the wide valley bottom between the source of the lahar and 9 km down valley (Figure 1). As the lahar flowed across these unconsolidated deposits it incised trapezoidal gullies, which then conveyed most of the discharge. The final dimensions of these gullies were on the order of 10-30 m deep and 20-70 meters wide.

Calculated velocities, which are restricted to bends in the narrow bedrock canyons, vary widely between 6 and 12 m/s (Figure 7a). Despite this variability, there appears to be a slight decreasing trend down-channel. A best fit linear function generated from regression analysis (equation 5) supports such a trend, but a small R^2 confirms that the scatter is large relative to the trend.

(5) $(U)_{pk}^{ave} = 13.69 - (.14)D$

$R^2 = 0.52$

D = distance downchannel from source

A reasonable conclusion is that any systematic downdhannel trend in $(U)_{pk}^{ave}$ is small.

Calculated peak discharge data display a visually well-defined, gradual

decrease down channel (Figure 7b). A nearly-linear exponential function provides the best fit to the data:

$$(6) \quad Qpk = 7660^{(-3.94 \times 10^{-3})D} \qquad R^2 = .49$$

R^2 is very low, again suggesting that the scatter is of the same order as any systematic down-channel variation. We conclude, therefore, that any downchannel variation is small, and that since flow volume did not increase downchannel (see below) Qpk must have either remained constant or decreased slightly.

The calculated sediment budget is shown in Table 2. As the lahar flowed across the avalanche debris it both eroded and deposited material. The sediment budget shows that erosion exceeded deposition by 4 million m^3 so that the lahar volume at the terminous of the avalanche deposits exceeded the lahar volume at 4 km from its source. Once beyond the avalanche terminous the lahar eroded little, but deposited large volumes of debris, primarily on terraces as 1-2 m thick flat-topped sheets of matrix-supported sediment. A net total of 16 million m^3 was deposited along the Toutle (Table 2).

Hydrographs for the North Fork lahar (Figure 8) were constructed at locations where eye-witness observations were available but calculated Qpk were not. Qpk was, therefore, calculated from equation 6, except at 4.5 km, where Qpk was deduced using estimates of the other variables necessary for hydrograph calculation. At 4.5 km from its source, the lahar lasted approximately 480 minutes, and discharge was maintained near its peak value of 7200 m^3/s for about 2.5 hours. The calculated lahar volume was 140 million m^3. Volume increased between 4.5 and 9 km as the lahar incised gullies in the avalanche debris. Beyond the terminous, the lahar experienced net volume loss, so that at 15 km the volume and Qpk were still 140 million m^3 and 7200 m^3/sec respectively, though flow duration had increased slightly to about 490 minutes. At the mouth of the Toutle River, 59 km downchannel, lahar volume had decreased to approximately 120 million m^3, and peak discharge had decreased to 6050 m^3/sec, while flow duration had increased to 660 minutes. Detailed hydrograph data are

presented in the appendix.

Peak discharge of the North Fork lahar decreased downchannel only 15%. This is in part attributable to the comparably small 11% reduction in flow volume due to deposition. The long, 1 to 2.5 hour duration of near-peak discharge also should have reduced the effect of flow attenuation on the magnitude of Qpk.

Eye-witness observations indicate that the North Fork lahar first started moving down-channel at approximately 1310 (PDT), and reached the first hydrograph location (4.5 km) at about 1325. The average celerity of the arrival of the peak discharge was 2.11 m/s between 4.5 km and the confluence (38 km), and 1.5 m/s between the confluence and the mouth of the Toutle River (59 km) (Cummans, 1981).

COMPARISION OF THE NORTH AND SOUTH FORK LAHARS

Both lahars were highly mobile, traveling 10's of kilometers on slopes of less than 1°, but it is here that the similarity ends. The South Fork lahar began as a brief, intense pulse. Its peak discharge decreased by a factor of 23 in response to flow attenuation and significant volume reduction by sedimentation. As a consequence, by the time the South Fork lahar had reached moderately-developed areas more than 40 km from Mt. St. Helens, peak discharge had decreased to approximately 6000 m^3/s and was continuing to drop (Figure 9). These discharges were sufficiently small that damage was relatively light, and primarily restricted to the reach between 40 and 44 km where peak discharge was between 6,000 and 3,800 m^3/s.

The North Fork lahar volume was more than an order of magnitude larger than the South Fork lahar, and the North Fork lahar deposited a volume of sediment along the Toutle that itself was larger than the initial volume of the South Fork lahar (Figure 9). The extremely long duration both of the flow and of near-peak discharge combined to maintain discharge of the North Fork lahar in populated areas. High peak stage resulting from high discharge

caused extensive damage, including innundation of two equipment and timber storage yards, destruction of eight major bridges, and damage or destruction of more than 100 houses. Deposition of sediment along the Cowlitz River caused extensive damage to floodplain developments and dramatically reduced the capacity of the Cowlitz (Lombard, et. al., 1982).

Because the celerity of both flows was low, sufficient time was available to evacuate developed areas. The South Fork lahar reached the first developed areas approximately 40 km from Mt. St. Helens 1.6 hours after initiation of the lahar (Cummans, 1981). The late initiation time and low celerity of the North Fork lahar delayed arrival of its peak at the nearest developed area (15 km) until approximately 6.5 hours, and at the mouth of the Toutle (59km) until 14.5 hours after the eruption began (Cummans, 1981).

REFERENCES

Cummans, J.(1981). Mudflows resulting from the May 18, 1980 eruption of Mount St. Helens, Washington: USGS Circular 850-B, 16 pp.

Cummans, J.(1982). Chronology of mudflows in the South Fork and North Fork Toutle River following the May 18 eruption. USGS Professional Paper 1250, p. 479-488.

Dunne, T. and L.B. Leopold(1981). Flood and Sedimentation Hazards in the Toutle and Cowlitz River System as a result of the Mt. St. Helens Eruption. Federal Emergency Management Agency, January, 1981, 92 pp.

Gilkey, K.E.(1982). Sedimentology of debris flows generated during the 1980 eruption of Mt. St. Helens. GSA Abstracts with Programs, 14, #4, 166.

Lombard, R.E., M.B. Miles, L.M. Nelson, D.L. Kresh, and P.J. Carpenter (1982). The impact of mudflows of May 18 on the lower Toutle and Cowlitz Rivers. USGS Professional Paper 1250, p. 693-700.

Moore, J.G. and C. J. Rice(1981). Chronology and character of Mt. St. Helens explosive eruptive phase of May 18, 1980. EOS, 62, #45, 1081-1082.

Smith, J.D. and S.R. McLean(unpublished manuscript). A Model for meandering streams.

TABLE I: Sediment Budget--South Fork Lahar

Channel Reach		Volume of Net Deposition	Compiled Volume of Net Deposition	Compiled % of original volum
0-4 km	upper reach	4.0×10^5	4.0×10^5	3.1%
4-8 km		1.0×10^5	5.0×10^5	3.8
8-17 km		9.0×10^5	1.4×10^6	10.7
17-37 km	middle reach	8.8×10^5	2.3×10^6	17.6
37-44 km	lower reach	2.6×10^6	4.9×10^6	37.4
44-68 km	below confluence	5×10^5 (estimate)	5.4×10^6	41

TABLE II: Sediment Budget--North Fork Lahar

Channel Reach		Volume of Net Deposition	Compiled Volume of Net Deposition	Compiled % of Volume at the Avalanche Terminous
4-9 km	avalanche deposits	(4×10^6)		
9-38 km	avalanche terminous to confluence	1.2×10^7	1.2×10^7	8.2
38-59 km	confluence to mouth of the Toutle	6.2×10^6	1.8×10^7	12.6

Appendix:

HYDROGRAPH DATA FOR THE SOUTH FORK LAHAR

Distance from Mt. St. Helens	Location	Arrival	Time of Peak	Conclusion	Duration (minutes)	Qpk (m^3/sec)	Volume (m^3)
4 km	Upper South Fork	0838	0841	0844.5	6.5	68,000	1.28×10^7
17	Constriction	0853	0859	0907	14	29,500	1.18×10^7
37	Above Camp 12	0932	0955	1020	48	7,700	1.09×10^7
44	Confluence	1020	1048	1132	72	3,800	8.3×10^6
65	Mouth of Toutle	1155	1240	1325	90	2,900	8×10^6

HYDROGRAPH DATA FOR THE NORTH FORK LAHAR

Distance from Source Area	Location	Arrival	Begin Peak	End Peak	Conclusion	Duration (minutes)	Qpk (m^3/sec)	Volume (m^3)
4 km	Elk Rock	1325	1421	1700	2121	476	7,200	1.4×10^8
15	Camp Baker	1358	1500	1730	2209	491	7,200	1.4×10^8
38	Confluence	1748	1920	2055	0333	591	6,600	1.3×10^8
59	Mouth of Toutle	2045	2305	0005	0750	665	6,050	1.2×10^8

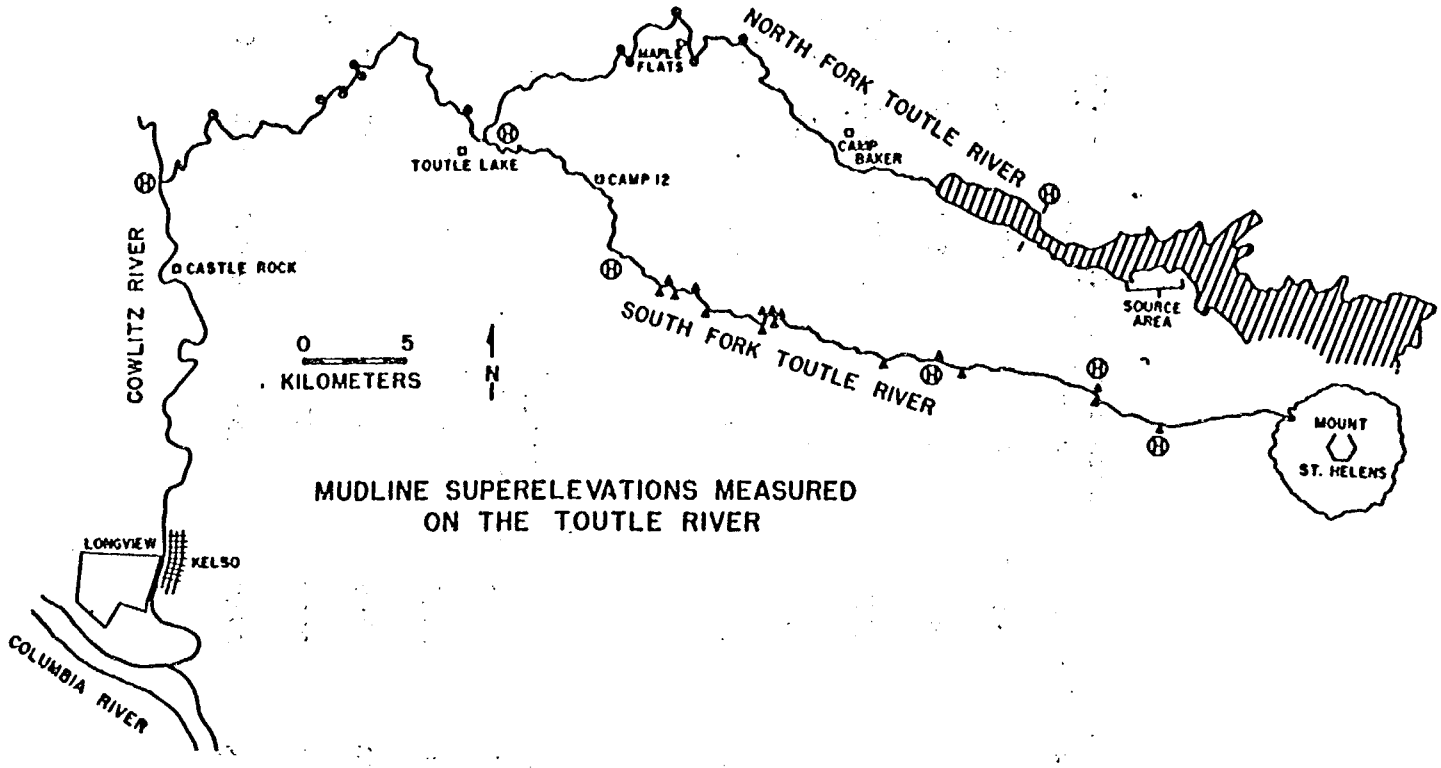


Figure 1: Simplified map of the Toutle River System. The South Fork lahar started on the slopes of Mount St. Helens and moved down the South Fork to the Cowlitz River. The North Fork lahar was generated from avalanche deposits(cross-hatched area) in the zone marked "source area" on the map(Fairchild, unpublished data) and moved down the Toutle to the Cowlitz and Columbia Rivers. Triangles mark superelevations measured on the South Fork, circles mark superelevations measured for the North Fork lahar. Circled "H" indicates the location of constructed hydrographs presented in figures 5, 8, and 9.

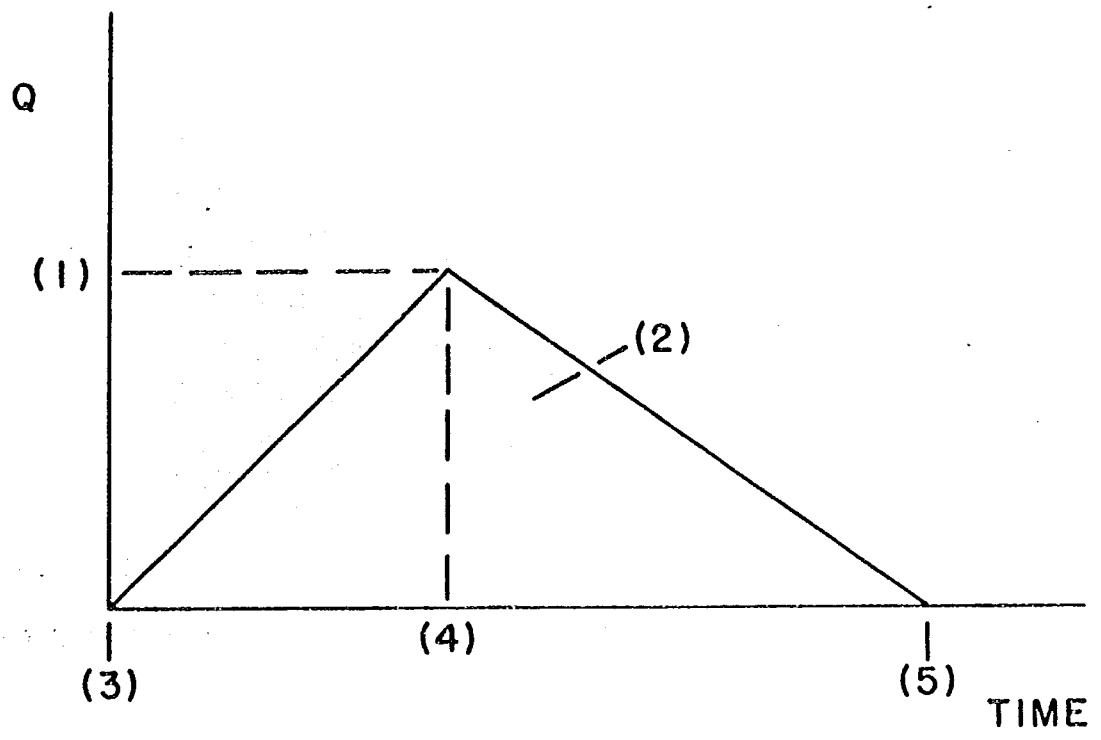
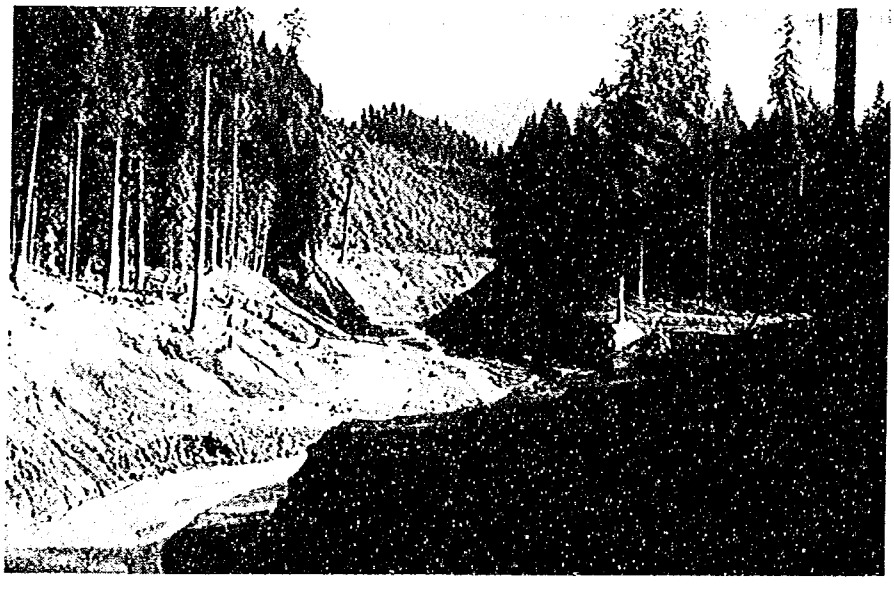


Figure 2: Schematic constructed hydrograph. Numbers correspond to variables needed for hydrograph construction discussed in the text.



Figure 3: a) Photograph of the wide upper reach of the South Fork Toutle River. The wide strip devoid of vegetation in the valley bottom is the path of the lahar.



b) Bedrock channel of the middle reach. The maximum depth of the lahar here was approximately 28 meters.

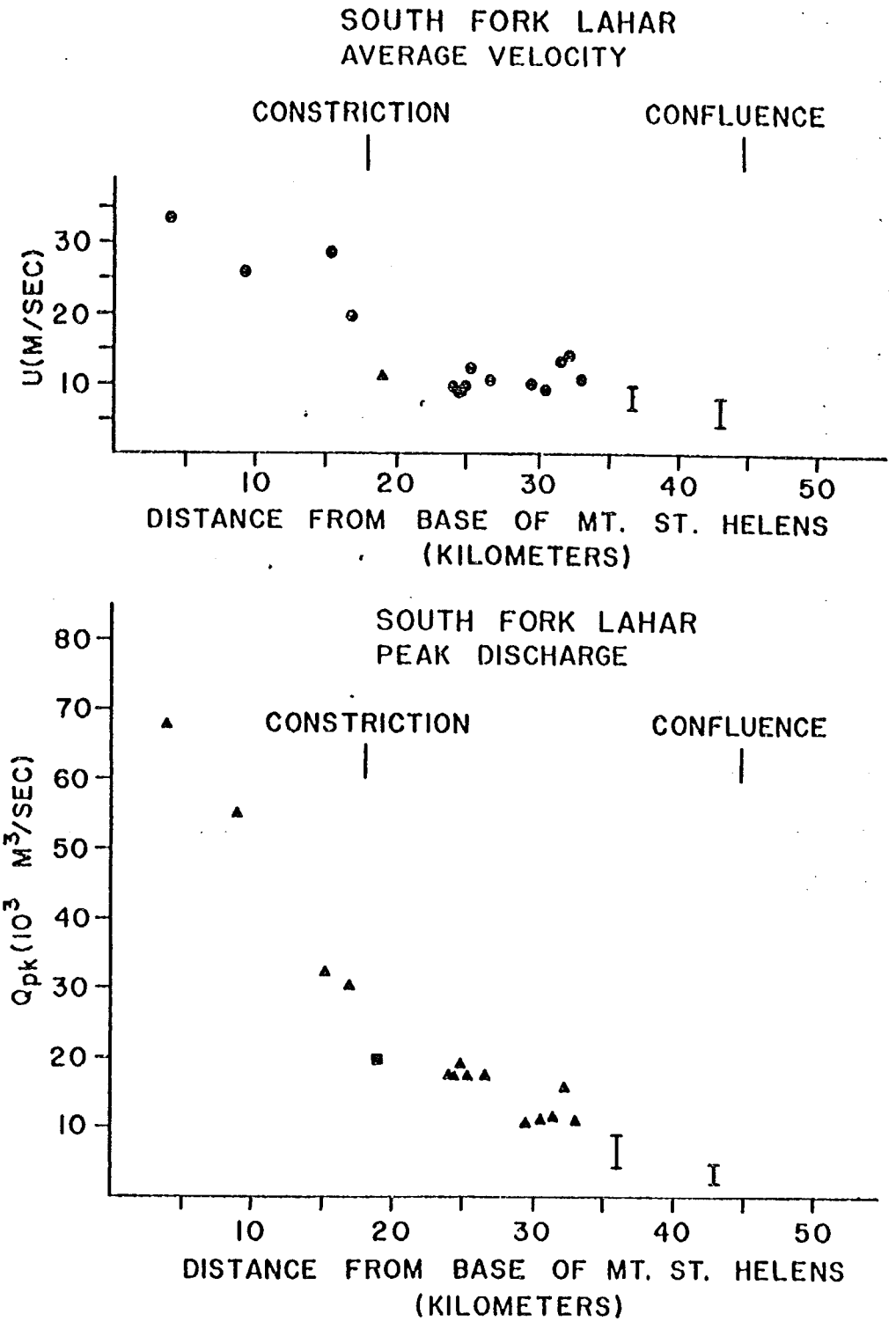


Figure 4: Average velocities and peak discharges for the South Fork lahar calculated from measurements made at locations plotted in Figure 1. Triangles identify bends with geometry that field observations suggest is sufficiently non-uniform that the potential error in U and Qpk is large.

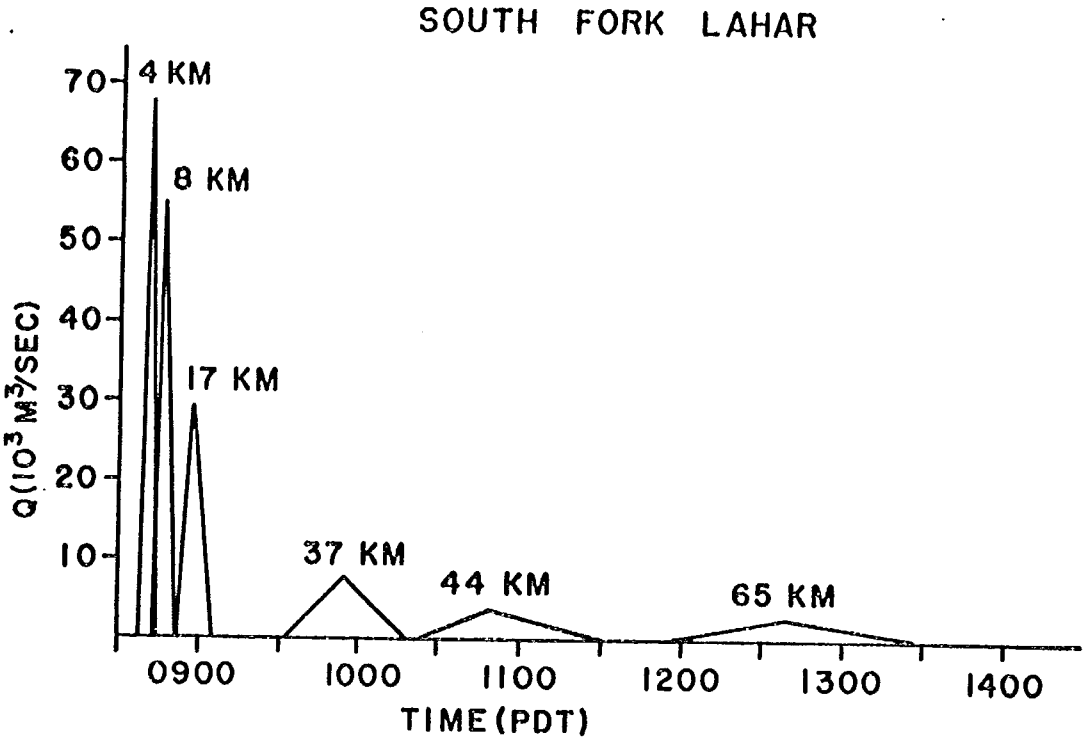


Figure 5: Hydrographs constructed for the South Fork lahar at locations plotted in Figure 1. Though the hydrographs are not likely to be strictly triangular, no data are available to further refine hydrograph shape, so triangular hydrographs have been drawn.

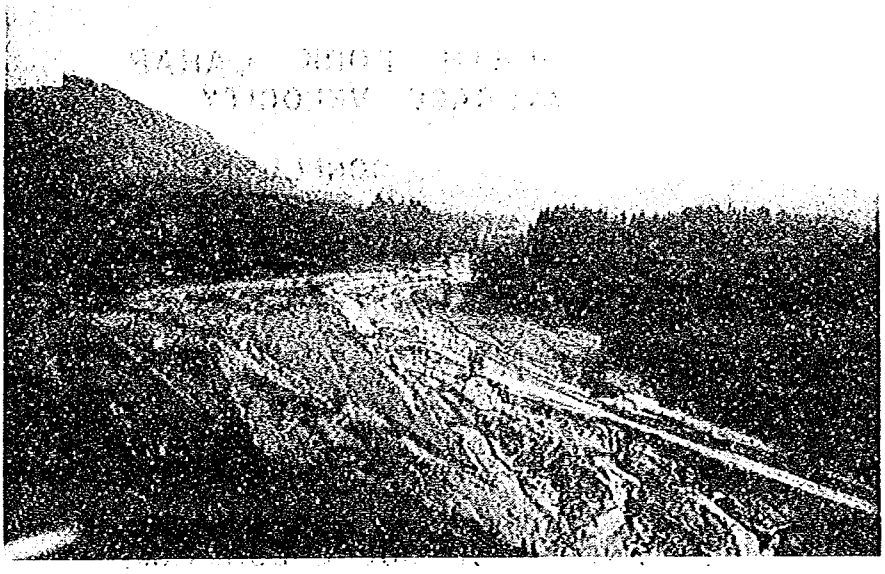
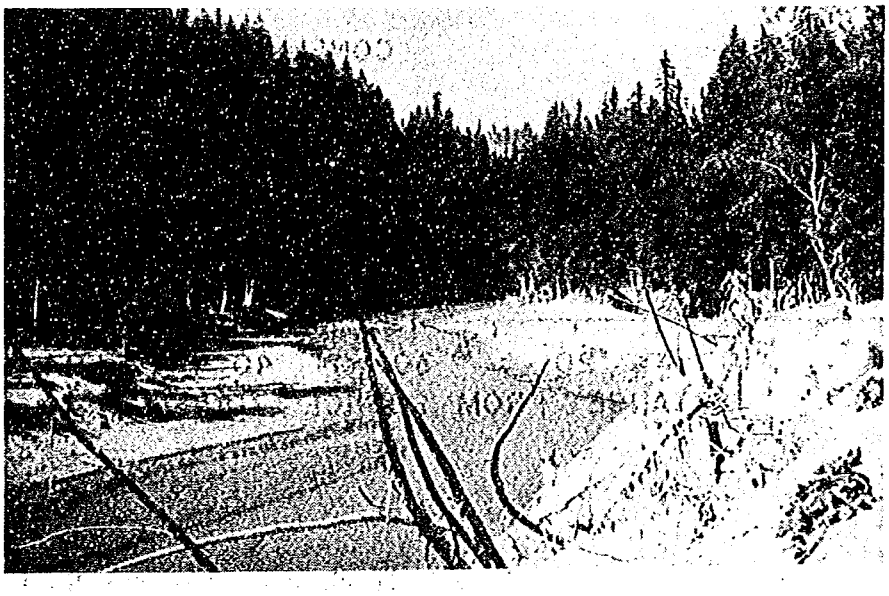
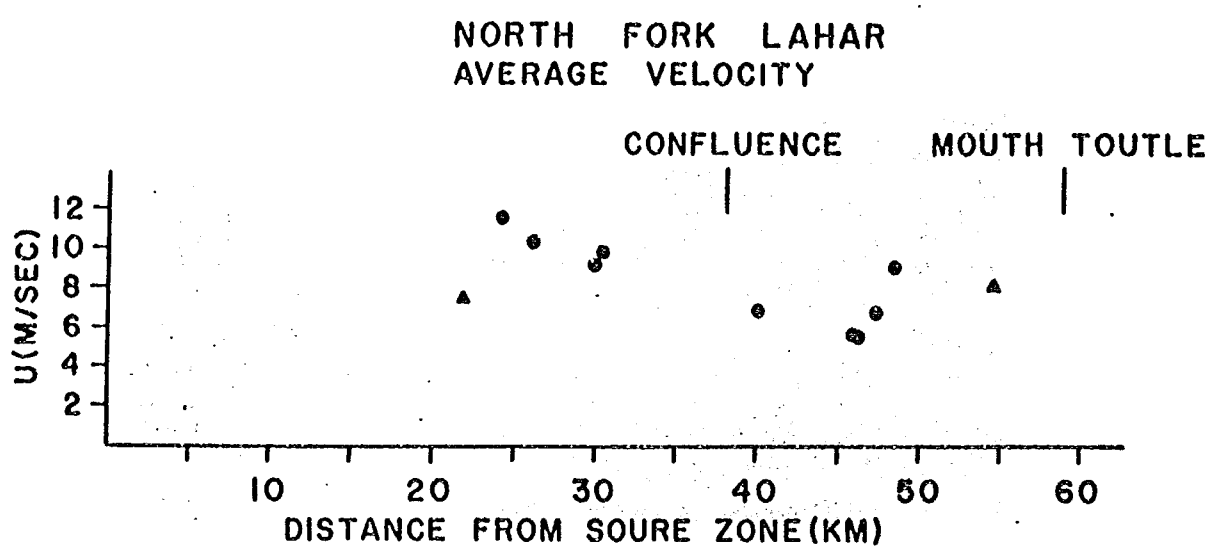


Figure 6: a) Typical wide valley reach on the North Fork Toutle River.



b) Bedrock canyon on the North Fork. High mudline is visible on trees.



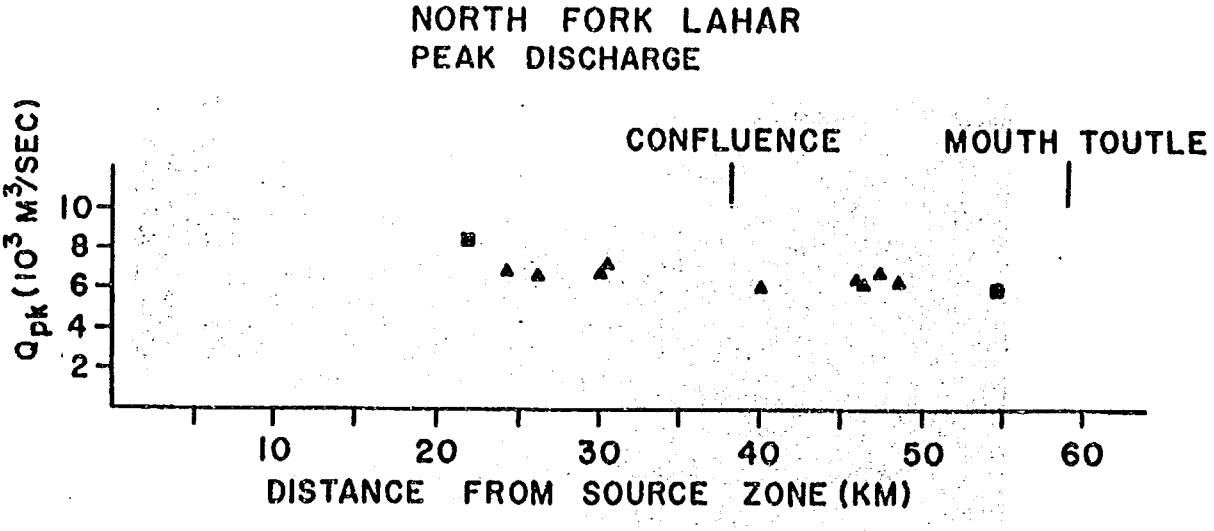


Figure 7: Average velocities and peak discharges for the North Fork lahar calculated from measurements made at locations plotted in Figure 1.

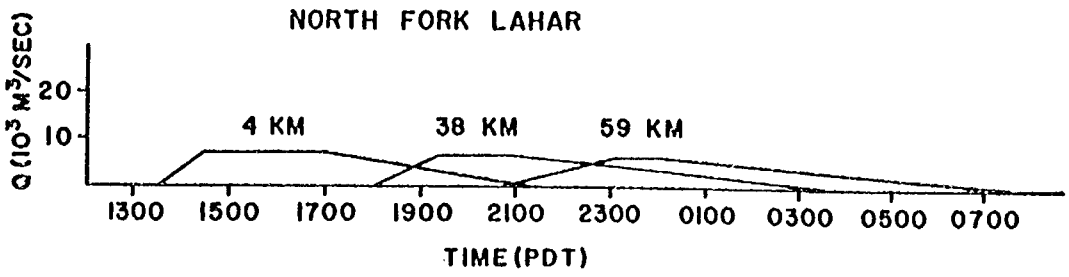


Figure 8: Hydrographs constructed for the North Fork lahar at locations plotted in Figure 1.

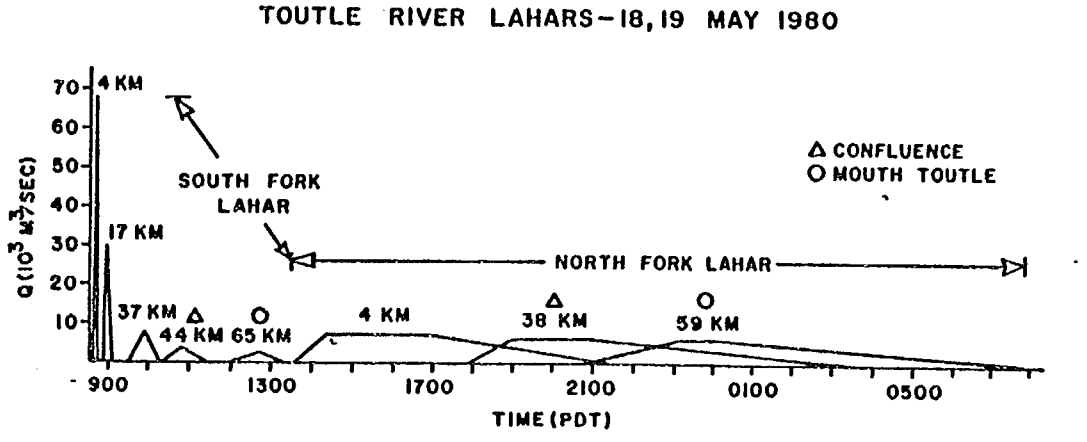
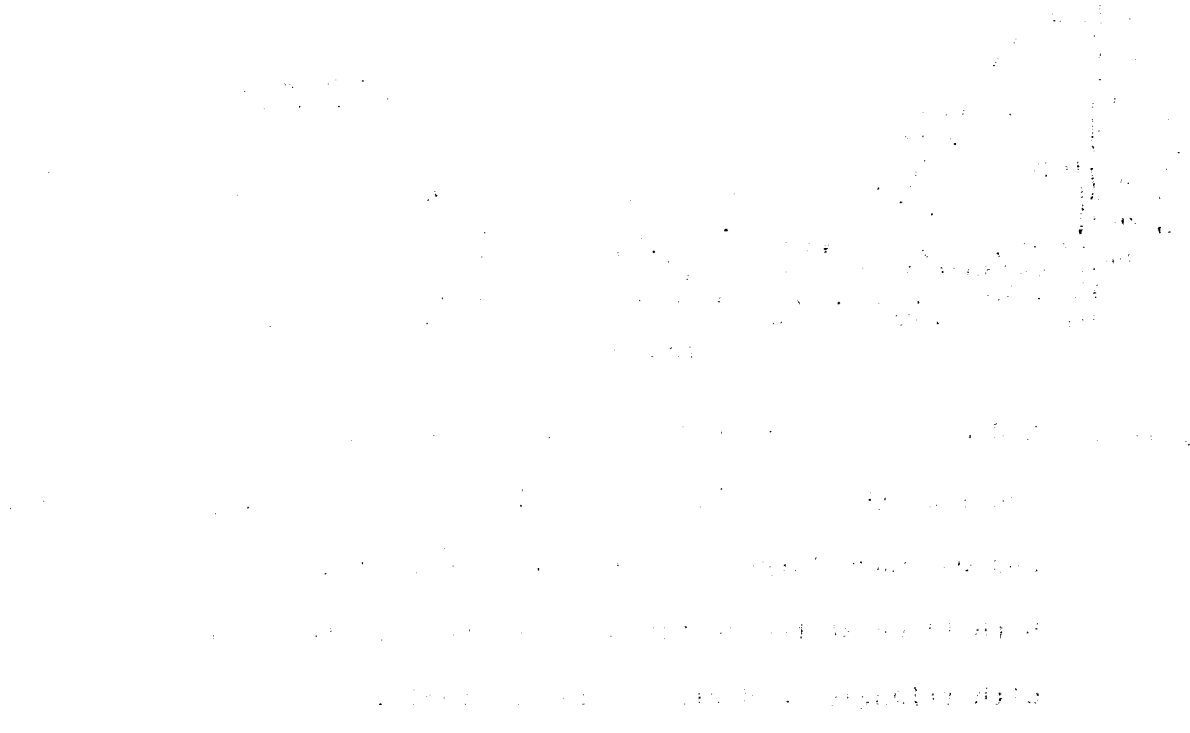


Figure 9: Hydrographs for both lahars plotted together. The North Fork lahar began after the South Fork lahar reached the Cowlitz River, and was much larger than the South Fork lahar. Hydrographs for both flows at the confluence and mouth of the Toutle are marked with triangles and circles respectively.



SEDIMENT YIELD FROM HILLSIDE SLOPE OF ACTIVE VOLCANOES

By
Etsuro SHIMOKAWA
Faculty of Agriculture, Kagoshima University
1-21-24 Korimoto, Kagoshima-shi, 890 Japan
and
Yoshinobu TANIGUCHI
Faculty of Agriculture, Miyazaki University
3-210 Funatsuka, Miyazaki-shi, 890 Japan

ABSTRACT

Volcanic Mt. Sakurajima was taken as an example to examine the process of sediment to be yielded on hillside slope of active volcanoes.

Mt. Sakurajima which is composite stratovolcano is one of the most active volcanoes in Japan, located at north of Kagoshima bay, southern Kyushu, Japan. The method of examination consists of field investigation, soil tests, and the interpretation of aerial photographs. The authors put emphasis particularly on the field investigation to clear the form, mechanism and cause of slope failure and erosion on the hillside slope including torrents.

Under the long period of lively valcanic activity, continuous deposits of volcanic ash fall makes the slope surface unstable and makes the permeability of the surface soil layer extremely worse. As the results of these, various types of slope failures and erosions have occurred and a great amount of sediment been produced. The destruction of vegetation have proceeded also tremendously under this activity.

INTRODUCTION

Volcanic mountains are widely distributed throughout Japan. Among them are Mt. Usu, Mt. Asama, Mt. Mihara, Mt. Aso, and Mt. Sakurajima. And all of these are very much active.

Mt. Sakurajima is one of the most active volcanoes and erupts continuously even today. Along with this volcanic activity, volcanic ashes fall and gases emit. These ashes and gases do great damage not only to the agricultural and fishery products, and the health of the residents of Sakurajima but also to the neighborhood region. The mud flows from the hillside slope and torrents threaten the life and fortune of residents.

Mt. Sakurajima is the stratovolcano of both lava flows and volcanic clastic materials. These volcanic deposits have a tendency to be easily eroded. In addition to this, the heavy volcanic ash fall deposits produced by the recent continuous activities make the permeability of the surface soil layer worse, and consequently the surface runoff large. Because of these, the erosion of the mountain itself is remarkably proceeded and a great amount of abnormal sediment have been yielded in the hillside slopes and torrents.

The purpose of this research work is to study the sediment yield process from the hillside slopes including the torrents of active volcanoes.

The authors performed this research work in Mt. Sakurajima. However, the result of this research work is very much related to the study of sediment yield from the hillside slope of active volcanoes such as Mt.Usu and Mt. Aso.

AN OUTLOOK OF VOLCANIC MT. SAKURAJIMA

Mt. Sakurajima is located at the northern part of Kagoshima bay, southern Kyushu, Japan(Figure 1) and its circumference is approximately 52 km, and the area is approximately 80 km^2. It is a penisula and almost round in shape. There are three peaks of that mountain, Kita-dake(1117 m) the highest, Naka-dake(1059 m), and Minami-dake(1011 m). The angle of the mountain slope above 400 to 500 m from sea level is 20 to 30 degrees, which is very steep. Otherwise, the mountain slope is gentle under 400 to 500 m above sea level, which angle 3 to 10 degrees.

Sakurajima volcano is a composite stratovolcano, which is a post-caldera cone of Aira caldera, in the period of Quaternary. The structure rock is pynezene andesite. And the bed is composed by andesite, welded tuff, and the pyroclastic deposits of Aira caldera. The outer layer is covered by old and new volcanic products as shown in a geological map of figure 2[1,2].

According to the histrical records of this volcano, the oldest eruption was in the year of 708. The eruption of Bunmei(1471-1476), Anei (1779), and Taisho(1914) eras were counted as the large scale of activity that produced a great amount of pumice and lava. The lava produced by the big eruption in Taisho era buried the strait between Osumi penisula and Sakurajima island, and turned the island into a penisula. The most production by the eruption of Showa era(1946) was lava but not much of the other products[1,2]. The present vocanic activity is eruptions with ashes and gases from Minami-dake crater and has lasted for about 25 years since autumn in 1955. Figure 3 shows frequencies of the eruption and smoke emission from 1955 to 1980[3]. The vegetation on the hillside slope has been damaged by the ash, gas, and fire of the volcanic activity[4].

ACTURAL CONDITIONS OF SEDIMENT YIELD IN MT. SAKURAJIMA

A lot of sediment has been yielded every year in Mt. Sakurajima. Figure 4 shows the location of the typical watersheds in Mt. Sakurajima. Table 1 shows the sediment yield volume and specific sediment yield volume at each basin[5]. Accompanied with the volcanic activity, the sediment yield volume has been extremely increased since 1974. As one form of sediment yield, mud flow will be taken up. Table 2 shows the frequencies of mud flow[6] that has occurred every year, and that has been observed at the lower part of streams. Around the typhoon and rainy season, many mud flows have occurred every year to transport a great amount of sediment for the downstream. Research studies concerning the occurrence and mechanism of mud flow has been proceeded at the Ministry of Construction, Forestry Agency, Universities and so on. Through these studies, we begin to understand the specificity of the mud flow of Mt. Sakurajima that it can be produced even though the rainfall was only less than 4 mm for ten minutes rainfall intensity[7], and the critical rainfall intensity for occurrence of mud flow will be lower along with the increase of smoke emission[8]. This specificity can fit the mud flow occurred at Mt. Usu[9].

The slope failures and erosions range over the area from the middle stream to upper stream. According to Haruyama[10], the area of slope failure and erosion, which was interpreted by the aerial photographs in 1974, was extended to 2293 ha, which is 68 per cent of the entire research area of watersheds and 29 per cent of the whole area of Mt. Sakurajima.

SLOPE FAILURE AND EROSION OF VOLCANIC FALL DEPOSITS ON THE HILLSIDE SLOPE OF KITA-DAKE AT MT. SAKURAJIMA[11]

The slope failure and erosion widely occurred not only on the slope

of active Minami-dake that presently erupts and emits smoke, but also on the slope of Kita-dake, which is not active and is covered with vegetation at the comparatively high area above sea level. Based on the field investigation of the slope failure and erosion in the area of the hillside slope of Kita-dake, the process of sediment yield from the slopes is examined.

1 Investigated area and method

The investigated area is the northern part of Mt. Sakurajima, the slope of Kita-dake(Figure 4). The river basins of Hase, Fukatani, Nishi-michi, Matsuura, Amida, Fukaya and Kurokami are included in the field of the study. The mountain slope is widely and thickly covered with old and new volcanic deposits.

The method of examination consists of field investigation, tests of soil samples collected from volcanic ash fall and pumice fall deposits, and the interpretation of aerial photographs. The field investigation is to examine the form and mechanism of the slope failure and erosion, the shape and scale of eroded valley, the deposit form of ash and pumice, and the distribution of vegetation. The investigation of the distribution and the deposit form of volcanic ash fall was done through the visual observation of soil profile. The form and distribution of pumice fall were examined through the observation of the profile of the eroded valley. The middle and upper river basin, which is 200 to 900 m height above sea level, was chosen as the main investigated area.

The soil tests is to find out the geotechnical properties of volcanic ash fall deposits. The tests consist of the following items: permeability, unit weight, water content, specific gravity, and particle size distribution. The permeability test was performed by a constant head

permeameter with undisturbed sample collected in the cylindrical sample (height:60 mm, diameter:55 mm).

The interpretation of aerial photographs is to ascertain the progression of erosion and the destruction of vegetation on the mountain slope. The five pairs of photos taken by the Ministry of Construction in 1947, 1966, 1974, 1978 and 1980 were used for the interpretation.

2 Progression of the erosion and destruction of vegetation on the hillside slope

Figure 5, 6, 7 and 8 shows distribution of erosion and vegetation that was read from the aerial photographs taken in 1947, 1966, 1974 and 1980, respectively. The vegetation was roughly divided into two parts, one of which is the grass mainly composed of miscanthus, and the other part is the broad leaved tree forest partially with Japanese black pine. The broad leaved tree forest is shrub at the hillside slope of over about 600 m above sea level. According to Figure 5, the scale and eroded valley and the distribution density are still small. The sediment at Kurakami fan is not yet observed. The top of the mountain and slope are mostly covered with forest and grass. The forest including shrub zone is distributed as high as 900 m above sea level.

In 1966 after 19 years, as shown in Figure 6, the scale of eroded valley and its distribution density are partially expanded. Because of this expansion, the sediment at Kurokami fan is observed. At the north east upper stream region of Kurokami river in Minami-dake, the retreat of vegetation is probably caused by the lively volcanic activity since autumn in 1955 which is shown in Figure 3.

The volcanic activity which was quiet from 1964 to 1971 became active again in 1972. As shown in Figure 7, the erosion of the hillside slope in

1974 is proceeded. The sediment in Kurokami fan is also continuously increasing. The vegetation such as broad leaved tree, Japanese black pine and miscanthus is retreating toward the lower region of the mountain.

The lively volcanic activity has lasted since 1972 untill today. Under the circumstances, the erosion and destruction of vegetation on the hillside slope have extremely increased in 1980, as shown in Figure 8. The distribution density of the eroded valley is extremely high in the regions without vegetation in the upper stream of the Kurokami river. The quantity of sediment in Kurokami fan has increased remarkably. The destruction of vegetation has increased in both quality and quantity.

Figure 9 shows a result of quantitative analysis about the progression of erosion, based on the distribution maps above. A density of erosional valley in this graph is a number of that per unit area, which was calculated for each river basin. This figure leads to the following: the density of erosional valley is closely related to accumulated frequencies of smoke emission, and strongly influenced by the existence and frequency of vegetation. Concerning the vegetation of the entire Mt. Sakurajima, Tagawa[4,12] drew the detailed vegetation maps(1962,1972), based on the field investigations and interpretation of aerial photographs.

3 Forms and mechanisms of the slope failure and erosion

Various forms of slope failure and erosion have occurred in the hillside slope. The slope failure and erosion are primarily divided into four forms, topsoil slide including topsoil fall, surface, rill and gully erosions, valley head erosion and erosion of torrent. Figure 10 shows the basic forms of these.

The topsoil slide is a collapse of shallow topsoil such as volcanic ash fall deposits. There are types of the topsoil slide such as, typical

topsoil slide at the hillside slope(type a), topsoil slide on the slope that the pumice fall or volcanic ash fall irregularly piled(type b), topsoil slide at the torrent side slope(type c), and topsoil slide at the head of the valley along with the retreat of valley(type d). Type c and d are mainly caused by the unstable foot of the slope as a result of proceeded erosion of the valley side and head. This form of slope failure occurs at the discontinued part of the deposits such as a border between volcanic ash fall deposit and Taisho pumice fall deposit, or the one between Taisho pumice fall deposit and Anei pumice fall deposit. Inclination of the slide surface is more than 30 degrees. The thickness of the deposit of volcanic ash fall at the hillside slope near Minami-dake crater is over 50 cm, and created a condition for easy slope failure. According to the result of the shear test of disturbed samples[13], angle of shearing resistance of void ratio being suited to natural deposit state is 30 to 32 degrees, and is in accord with minimum slope inclination upon the slope surface of topsoil slide. A greater part of this type occur on the hillside slope with vegetation.

The surface erosion is splash and wash out of the volcanic ash fall and pumice fall deposits by both raindrops and surafce runoff. The type occurs frequently on the hillside slope without vegetation and eroded slopes. The rill erosion is a type of debris yield accompanied with formation of very small streams(rill) by running water(type e). The rill is about 10-100 cm in depth and width. The rill become gradually larger in scale under the action of running water and develops into the gully (type f). The gully is about 1-10 m in depth and width.

There are two types of valley head erosions; one type of which vertical surface slope of the valley is gentle(type g), and another type

of which vertical surface slope of the valley is steep(type d). In the case of type g, at first, through the process of depression of the surface volcanic ash fall deposit, the feeble pumice fall deposits to be easily eroded exposed and erosion will be proceeded. In the case of type d, topsoil slide occurs because the slope is steep, and valley head retreats to the upper stream.

There are various types of torrent erosion as well, type h, type i, type j, type k and type l. Type h is a small scale erosion of torrent, which occurs near the head of the valley. Loose pumice fall deposits are eroded by raindrops or surface runoff, and the torrent is gradually expanded. Type i is a type of erosion to be eroded or expanded vertically and horizontally by effect of running water and mud flow. Stream side slope becomes unstable because of the foot being eroded, and is sometimes broken like a piece of block. Type j is an erosion of torrent at the large scale valley(40-60 m in depth). The slope failure and erosion of the stream side slopes are caused by percolation of rainwater and surface runoff. These types of erosion are formed to maintain the stable slope of the stream side depending upon the depth of the valley. The torrent grows to type j from type h through type i. Although the torrents are under the same condition, where the slope of pumice fall and volcanic ash fall deposits are steep, the slope failure of type k can be observed.

Type l is the stream bed erosion by running water and mud flow. The welded pumice layer has comparatively strong resistance against erosion, and formed stream bed. However, under the continuous action of running water and mud flow, the erosion is proceeded. As soon as this layer is eroded, non-welded pumice layer will be washed out and the lower welded pumice layer will make the stream bed stable. Thus, the water fall will

be formed. Because of the continuation of erosion, this water fall will retreat to the upper stream. As mentioned above, the torrent has widely ans deeply expanded.

Usu volcano had a big eruption in August, 1977. The hillside slope was covered with a great amount of pumice fall and volcanic ash fall produced by the eruption. As the result, various types of slope failure and erosion such as topsoil slide, surface erosion, rill erosion, and gully erosion originated from the volcanic fall products have occurred on the hillside slope of Mt. Usu[9,14,15,16].

4 Distribution and geotechnical properties of volcanic ash fall deposits

Volcanic ash fall deposits by the volcanic activity after the eruption in Taisho era, covered the entire part of the hillside slope on Mt. Sakurajima. According to the observation of soil profile, the total deposit thickness is extended to 20-80 cm as well. From the deposit state such as tone, density, hardness and mixture state of humus, the volcanic ash fall deposits can be divided into three layers, upper, middle, and lower. Judging from the age of planted trees(Japanese black pine) in the place of soil profile, and the position of fallen leaves included in volcanic ash fall deposits, it can be considered that the upper layer (black volcanic ash (1)) is deposits for 9 years from 1972 to the present time. Thickness of the layer is 10-40 cm as well. As the middle layer (blackish brown volcanic ash (2)) contains a lot of humus, it may be deposits in the time of calm volcanic activity in 1964 to 1971. The lower layer(black volcanic ash (3)) may be deposits by the volcanic activity before 1964 including Showa eruption. Thus, transition of volcanic activity have much influence over the deposit state of volcanic ash fall.

Figure 11 is plots of the total deposit thickness and the thickness of the upper layer against the distance from an investigated point of soil profile to Minami-dake crater. In this figure, some values of accumulated deposit thickness from 1970 to 1975 by Kamo et al[17] were quoted and plotted. In either case, the thickness of volcanic ash fall deposit decrease against the increased distance from the Minami-dake crater as the graph of exponential function. The similar retionship holds for short term deposit thickness of the volcanic ash fall[18]. By applying this relationship, the deposit volume of volcanic ash fall on the hillside slope can be laughly calculated. The total volume after Taisho eruption amounts to 21,840,000 m^3, as shown in Table 3. Already, some of this volume was eroded.

Figure 12 shows a geologic column of the volcanic ash fall and Taisho pumice fall deposit, and the geotechnical properties such as coefficient of permeability, water content, void ratio and so on. The geotechnical properties of volcanic ash fall deposit show the difference between the upper layer and the middle and lower layers. There is a large difference between, especially, coefficient of permeability, density, and void ratio. The permeability of the upper layer is small compared with that of the middle and lower layers. As the result, the surface runoff increases, and the erosion of the hillside slope and torrents has proceeded. Figure 13 is a plot of permeability-coefficient against void ratio. In the upper layer of volcanic ash fall deposits, the permeability-coefficient at Japanese black pine forest land shows more or less high value than that at broad leaved tree and miscanthus land. According to the result of permeability experiment in field by Takeshita[19], for the case of steep slope, infiltration capacity at Japanese black pine

forest land is higher than that at other kinds of vegetation lands.

5 Distribution of pumice fall deposits on the hillside slope

The volcano hillside is covered with various kinds of volcanic products, which are pumice fall, volcanic ash fall and lava flow. Among these, pumice fall deposits are piled so thick and loose that erosion is very much proceeded. According to the field survey, the most part of pumice fall deposits are considered to be the one in Anei and Bunmei era, and include several layers of welded pumice, which is as thick as several meters to several tens meters. The Taisho pumice fall deposit is thin and only about 50 to 100 cm thick. Soil is formed on the surface of Taisho and Anei pumice fall deposit.

In oredr to guess future sediment to be yielded, it is important to estimate the deposit volume of this volcanic products in the hillside slope.

Fukuyama et al[1,2] say that volcanic pumice and ash precede to fall before outflow of lava at the time of the big eruption in Taisho era. Therefore, Taisho pumice and volcanic ash did not pile over Taisho lava flow deposit, in same way, it is clear that this fact is applicable in the cases of the deposits in Anei and Bunmei eras. Based on this fact, it can be assumed that the older the lava flow deposit is, the thicker the pumice fall deposits on it is. And, to calculate the volume of deposits, it is necessary to consider a difference of deposit form between pumice fall and lava flow. In other words, pumice fall deposit and volcanic ash fall deposit pile widely over the volcano hillside slope including steep slope. The lava flow, however, does not pile thick over the steep slope, because of faster speed of outflow, but spreads over the gentle slope zone

which is the end of the steep slope. Figure 14 shows the schematical deposit forms of pumice fall and lava flow on the hillside slope. Furthermore, for the estimation of the volume, the depths of the eroded valleys must be obtained quantitatively. Figure 15 shows the relationship between the depth of eroded valley and the catchment area. As a whole, no fixed tendency will be observed between the two. However, if the watersheds are divided into the following three, Matsuura main river, Kurokami main river and other rivers, the fixed relation can be observed in each watershed. In other words, the depth of eroded valley increases along with the catchment area.

Based on the above mentioned conditions, the deposit volume of pumice fall was estimated, as shown in Figure 16 and Table 4. The total volume in Kurokami and Matsuura river basin amounts to 63,227,000 m^3 and 25,360,000 m^3, respectively. These volumes are extremely large.

CONCLUSION

Based on the field investigation, soil tests, and interpretation of the aerial photographs, the authors researched the process of sediment yield on the hillside slope of the active volcano. The results of the works are summarized in Table 5.

1) As is clear from the interpretation result of aerial photographs, the volcanic activity, and the progression of erosion and destruction of vegetation on the hillside slope are closely related. At present time, under the continuation of volcanic activity, the erosion on the hillside slope and the destruction of vegetation are extremely proceeded.

2) The slope failure and erosion on the hillside slope and torrents consist of four forms; topsoil slide including topsoil fall, surface,

rill and gully erosion, valley head erosion and erosion of torrent.

3) Under the continuation of volcanic activity, the volcanic ash fall deposit is as thick as 20 to 80 cm and is very unstable. The thickness of the deposit decreases with the distance from Minami-dake crater along with the exponential function. It can be recognized that there is a large difference of the coefficient of permeability of the volcanic ash fall deposit between the time when the volcano is active and not active. In the upper layer of volcanic ash fall deposit, the coefficient of permeability at Japanese black pine forest land is little higher than the one at the broad leaved tree forest and miscanthus lands. A cause of slope failure and erosion may be the decrease of coefficient of permeability(the increase of surface runoff) through continuous volcanic ash fall.

4) The erosion of pumice fall deposits in the hillside slope has been remarkably proceeded. In order to guess future sediment yield, the deposit volume was estimated by considering the deposit order to the lava flow at the time of big eruption, deposit form, and the depths of valleys.

REFERENCES

1) Fukuyama, H.: Geology of Sakurajima volcano, southern Kyushu. Jour. Geol. Soc. Japan, 84, 309-316(1978)(in Japanese with English summary)
2) Fukuyama, H and Ono, K.: Geological map of Sakurajima volcano. Geol. Survey Japan, 1981(in Japanese with English summary)
3) Datas of Kagoshima local meteorological observatory(in Japanese)
4) Tagawa, H.: Vegetation of Sakurajima and its relation to soil erosion. Report of conference on scientific studies in Sakurajima area, 128-142 (1980)(in Japanese)
5) Ministry of Construction: Report of a research work on sediment yield in Sakurajima, 1980(in Japanese)
6) Toshida, M., Yamauchi, O., Hetsugi, S. and Koga, S.: Observation of mud flow in Sakurajima. Jour. Erosion Control Eng. Soc. Japan, 33, 26-29 (1980)(in Japanese)
7) Tawara, M.: Mud flow of Sakurajima and its research. Jour. Erosion Control Eng. Soc. Japan, 28, 26-31(1976)(in Japanese)

8) Tsubaki, T., Hirano, M., Ashida, K. and Sawada, T.: On the mud flow of Sakurajima. Report on slope failure and mud flow disasters in Kagoshima Pref. caused by a heavy rain in June 1976, 111-117(1977) (in Japanese)
9) Suekane, A.: On the occurrence of mud-flows in Ichino-sawa, Mt. Usu, 1977. Geographical Review Japan, 52, 302-310(1979)(in Japanese with English summary)
10) Haruyama, M. and Taniguchi, T.: Topography, geology and vegetation, and evaluation of noxious sediment yields in Sakurajima volcano area. Report of conference on scientific studies in Sakurajima area, 207-250(1980)(in Japanese)
11) Shimokawa, E. and Arimura, M.: Slope failure and erosion of volcanic products in Kita-dake hillside slope of Sakurajima. Proc. Annual Meeting Erosion Control Eng. Soc. Japan, 74-75(1982)(in Japanese)
12) Tagawa, H.: A study of the volcanic vegetation in Sakurajima, South-west Japan. 1. Dynamics of vegetation. Mem. Fac. Sci., Kyushu Univ., Ser. E(Biol), 3, 3/4, 165-228(1964)
13) Haruyama, M., Shimokawa, E. and Inoue, T.: Geotechnical properties of the volcanic ash and sand in Sakurajima volcano. Bull. Kagoshima Univ. Forests, 5, 65-92(1977)(in Japanese with English summary)
14) Higashi, S. et al: Agricultural damages caused by the 1977 eruption of Usu volcano. Investigation of volcanic disasters caused by the 1977 Usu eruption, Ministry of Education, 82-123(1978)(in Japanese with English summary)
15) Higashi, S. et al: Studies on the geomorphic changes of hillside slope and channel-bed, and on the effects of Sabo-works. Investigation of Usu volcano mud flow disasters on Octover 24, 1978, Ministry of Education, 21-40(1979)(in Japanese with English summary)
16) Ikeya, H. and Yozawaya, S,: On sediment yield in Nishiyama river basin, Mt. Usu. Jour. Erosion Control Eng. Soc. Japan, 22-27(1979)(in Japanese)
17) Kamo, K., Egashira, Y., Ishihara, K. and Kawaharada, R.: On deposit of volcanic ash fall in Sakurajima. Report on slope failure and mud flow disasters in Kagoshima Pref. caused by a heavy rain in June 1976, 77-86(1977)(in Japanese)
18) Hikida, M., Hirano, M. and Hadano, K.: Investigations on the disasters caused by volcanic ashes of Sakurajima. Studies report Kagoshima Technical College, 15, 73-90(1980)(in Japanese with English summary)
19) Takeshita, K.: Infiltration capacity of soil and erosion accompanied with volcanic ash fall of Sakurajima volcano. Proc. 92nd annual meeting Japan Forest Soc., p.132(1982)(in Japanese)

Table 1 Sediment yield in each watershed of Sakurajima

Watershed	Catchment area (Km^2)	Sediment yield volume ($X10^3m^3$)			Specific sediment yield volume ($X10^3m^3/Km^2/Year$)		
		1	2	3	1	2	3
Nojiri	2.99	521	1384	1126	18	125	188
Harumatsu	2.09		138	84		18	20
Mochiki	1.61		190	222		33	69
No.1 Furusato	0.86		84	42		26	24
No.2 Furusato	1.40		27	62		5	12
Arimura	3.65		216	513		16	70
Kurokami	6.88	2972	922	1894	44	36	138

1: Mar. 1961-Feb. 1971, 2:Feb.1971-Oct. 1974,
3: Oct. 1974-Sept. 1976

Table 2 Annual occurrence-frequencies of mud flow in each watershed

Watershed	Year							
	1973	1974	1975	1976	1977	1978	1979	1980
Nojiri	12	16	20	24	22	24	15	21
Harumatsu			3	6	4	2	4	4
Mochiki			4	6	10	14	13	10
No.1 Furusato			4	5	6	5	8	7
No.2 Furusato			3	5	10	4	7	4
Arimura			4	8	11	4	6	5
Kurokami			2	6	11	10	11	9

April-March(1973-1979), April-July(1980)

Table 3 Deposits volume of volcanic ash in the hillside slope after Taisho eruption in 1914

Depth of ash, cm	80	70	60	50	40	30	20	10	Total
Area, Km^2	0.925	1.800	2.850	3.350	8.325	15.175	39.775	6.175	
Volume of ash, $X10^3 m^3$	740	1,260	1,710	1,675	3,330	4,552.5	7,955	617.5	21,840

About 40 per cent of total volume have deposited in the erosional areas.

Table 4 Deposits volume of pumice fall in the hillside slope

	Depth of pumice, m	60	50	40	30	20	10	5	2	Total
R. Matsuura	Area, km^2		0.063	0.15	0.49	0.44	1.53	2.43	1.53	
	Volume, $X10^3 m^3$		3,150	6,000	14,820	8,760	15,310	12,125	3,062	63,227
R. Kurokami	Area, km^2	0.050	0.094	0.075	0.081	0.22	0.69	0.14	0.13	
	Volume, $X10^3 m^3$	3,000	4,700	3,000	2,430	4,380	6,880	720	250	25,360

Table 5 Sediment yield on the hillside slope and torrent of active volcanoes such as Mt. Sakurajima

Form	Location	Angle of slope	Collapsed materials	Vegetation	Scale	Mechanism	Cause
Topsoil slide or Topsoil fall	Hillside slope, Headward of valley	Over 25-30 deg.	Ash, Pumice, Volcanic clastic materials	With vegetation	5-30m in width 10-50m in length 0.5-5m in depth	Increase of topsoil weight itself by infiltration of rain water, Reduction of shearing resistance by topsoil saturation, Occurrence of intermediate flow and development of excessive pore water pressure in topsoil layer, Piping, Surface runoff, Slope failure caused by removal of slope foot	Accumulated deposits of volcanic ash caused by volcanic activity, Reduction of permeability in topsoil, Increase of surface runoff, Destruction of vegetation, Change of permeability in the direction of depth, Change of topography caused by diastrophism(Mt. Usu)
Surface erosion	Hillside slope	Unrelated to slope angle		Without vegetation or with little vegetation	Under 10 cm in depth	Splash and wash out of soil particles by rain drops and surface runoff	Accumulated deposits of volcanic ash caused by volcanic activity, Reduction of permeability in topsoil, Increase of surface runoff, Destruction of vegetation, Erodible properties of volcanic ash and pumice fall layers
Rill erosion	〃	〃	〃	〃	0.1-1m in width 0.1-1m in depth	Formation of small streams by surface runoff	〃
Gully erosion	〃	Under 25-30 deg.	〃	With vegetation	1-10m in width 1-10m in depth	Formation of large streams by running water and mud flow	〃
Topsoil slide or Topsoil fall	Torrent side slope	Over 30 deg.	Ash, Pumice, Volcanic clastic materials	Without vegetation or with little vegetation	5-30m in width 10-50m in length 0.5-5.0m in depth	Increase of topsoil weight itself by infiltration of rain water, Reduction of shearing resistance of topsoil saturation, Occurrence of intermediate flow and pressure in topsoil layer, Piping, Slope failure caused by removal of slope foot	Accumulated deposits of volcanic ash caused by volcanic activity, Reduction of permeability in topsoil, Increase of surface runoff, Destruction of vegetation, Change of permeability in the direction of depth, Occurrence of mud flow
Surface erosion	〃	〃	〃	〃	Under 10cm in depth	Splash and wash out of soil particles by rain drops and surface runoff	Accumulated deposits of volcanic ash caused volcanic activity, Reduction of permeability in topsoil, Increase of surface runoff, Destruction of vegetation, Occurrence of mud flow, Erodible properties of volcanic ash and pumice fall layers
Rill erosion	〃	〃	〃	〃	0.1-1.0m in width 0.1-1.0m in depth	Formation of small streams by surface runoff	〃
Gully erosion	〃	〃	〃	〃	1-10m in width 1-10m in depth	Formation of large streams by running water and mud flow	〃
Erosion of torrent bed	Bed of torrent	10-30 deg. (longitudinal grade of bed)	〃	〃	5-30m in height of waterfall	Failure and erosion of torrent bed caused by running water and mud flow, Formation of waterfall	〃

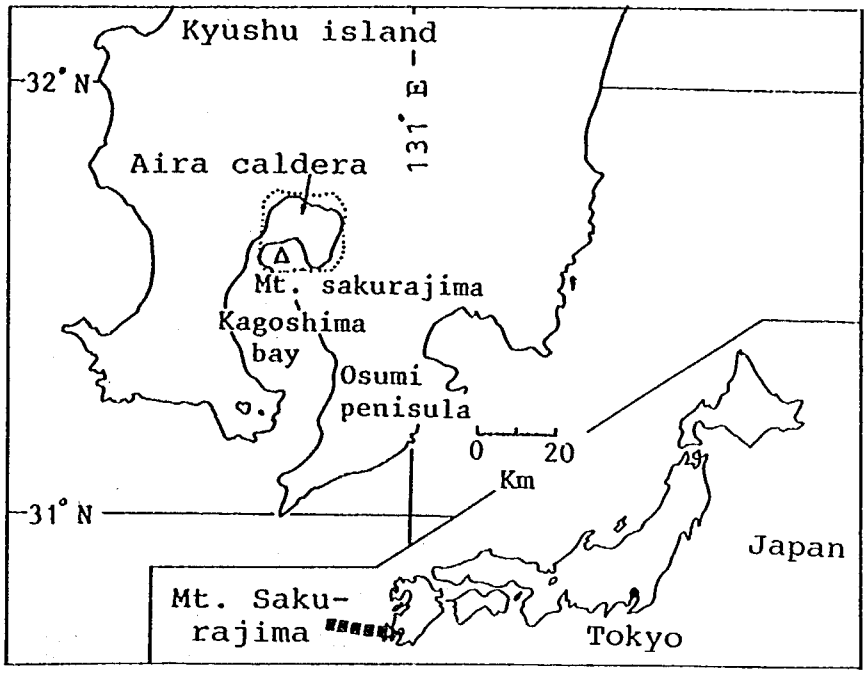


Fig. 1 Location of Mt. Sakurajima volcano.

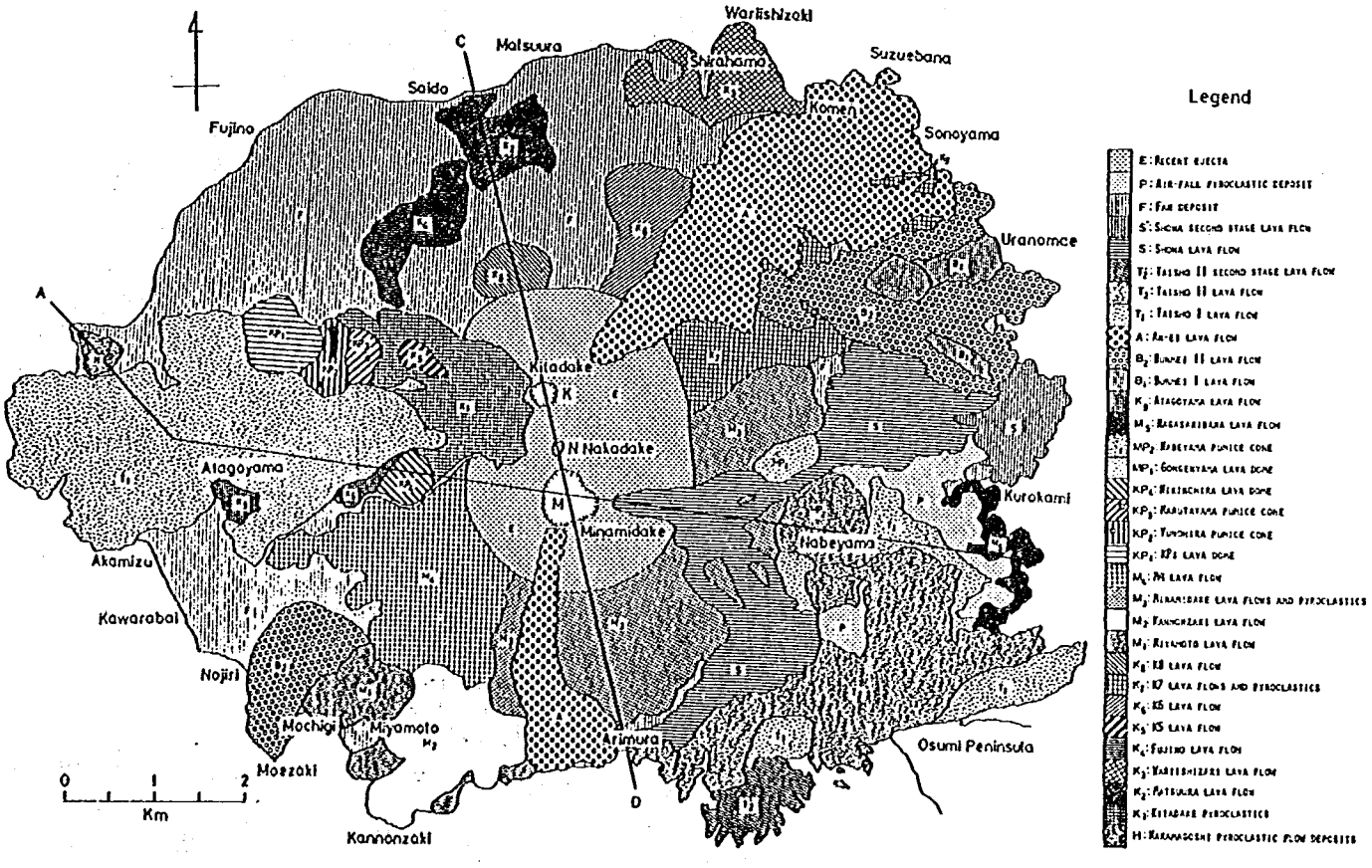


Fig. 2 Geologic map of Sakurajima volcano(After Fukuyama).

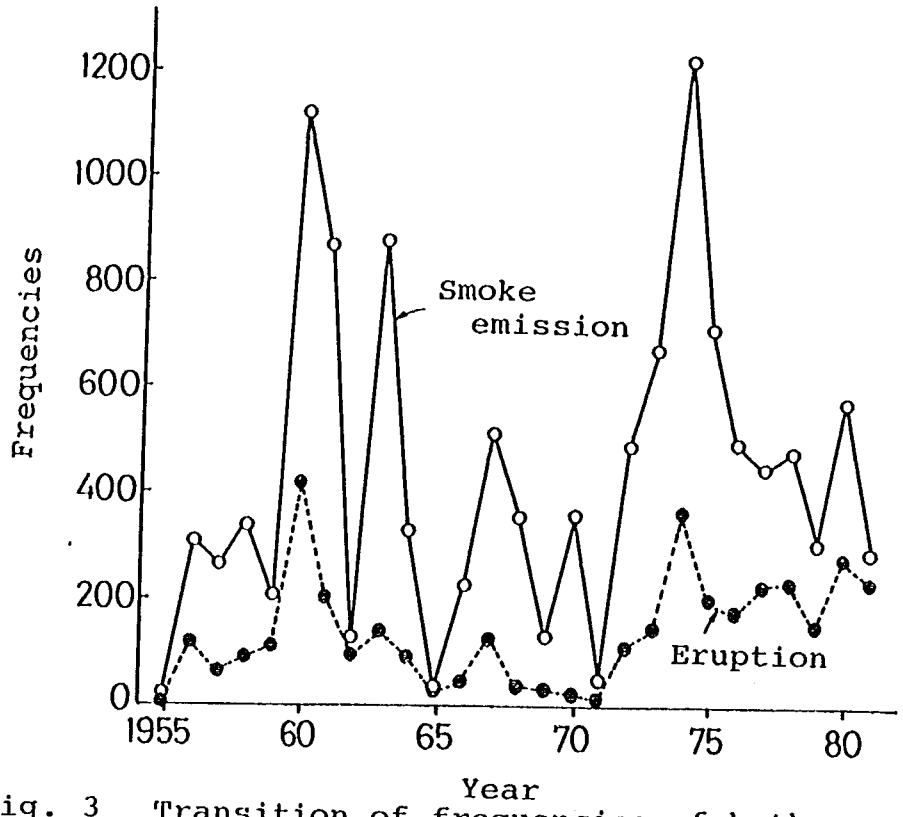


Fig. 3 Transition of frequencies of both eruption and smoke emission.

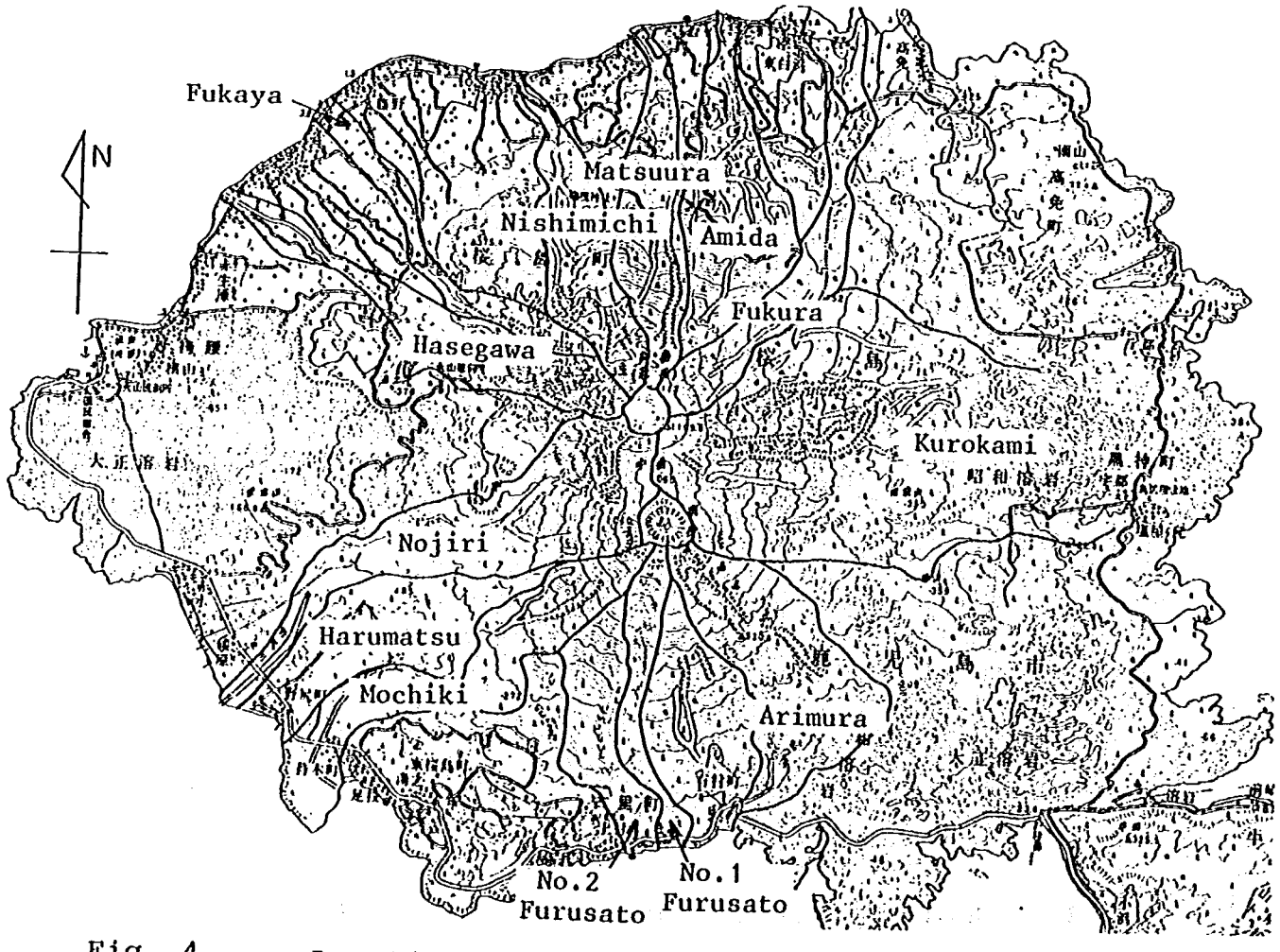


Fig. 4 Location of main watersheds in Sakurajima.

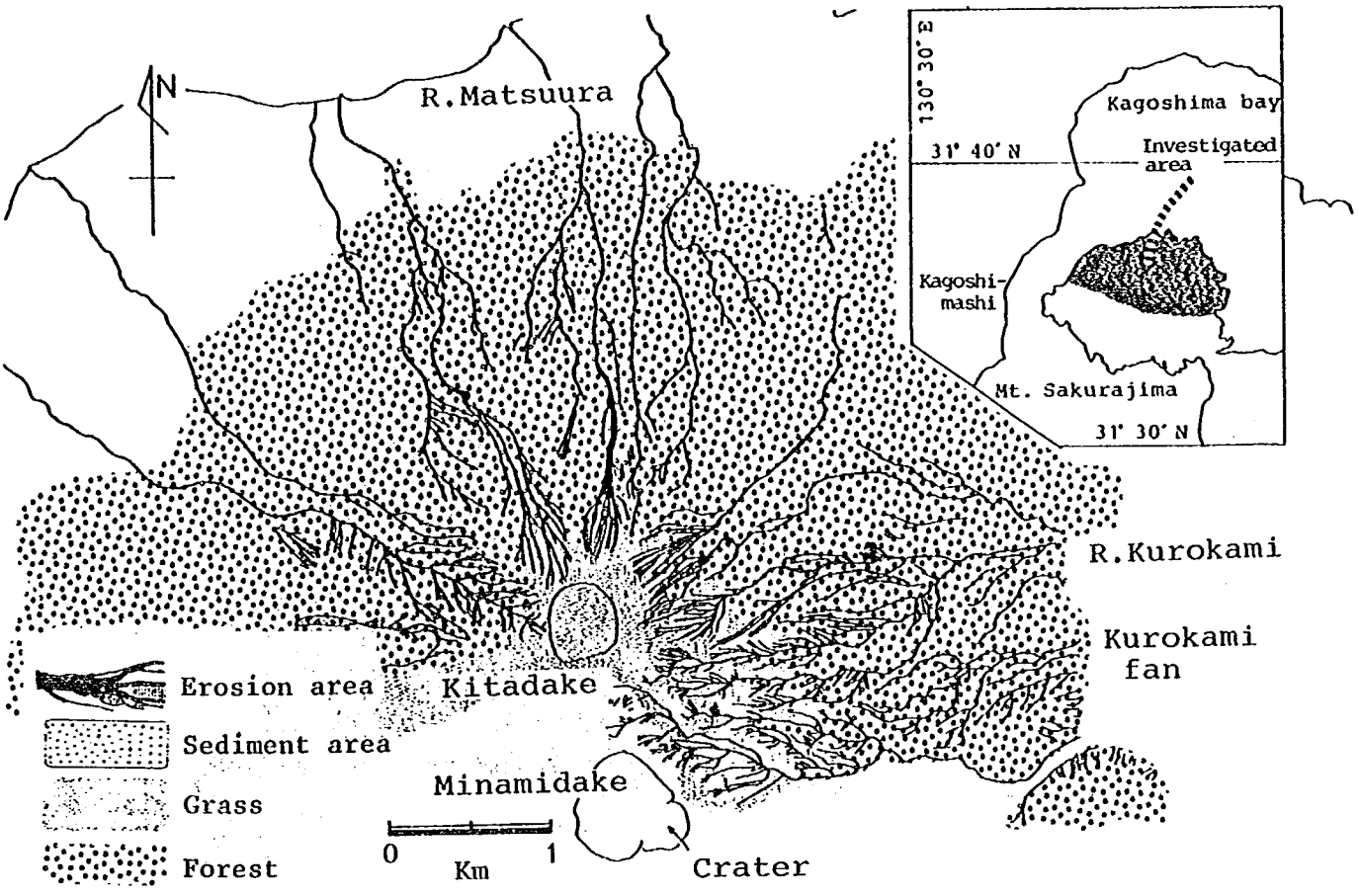


Fig. 5 Distribution of both erosion area and vegetation in Kitadake(north mountain) hillside slope in 1947.

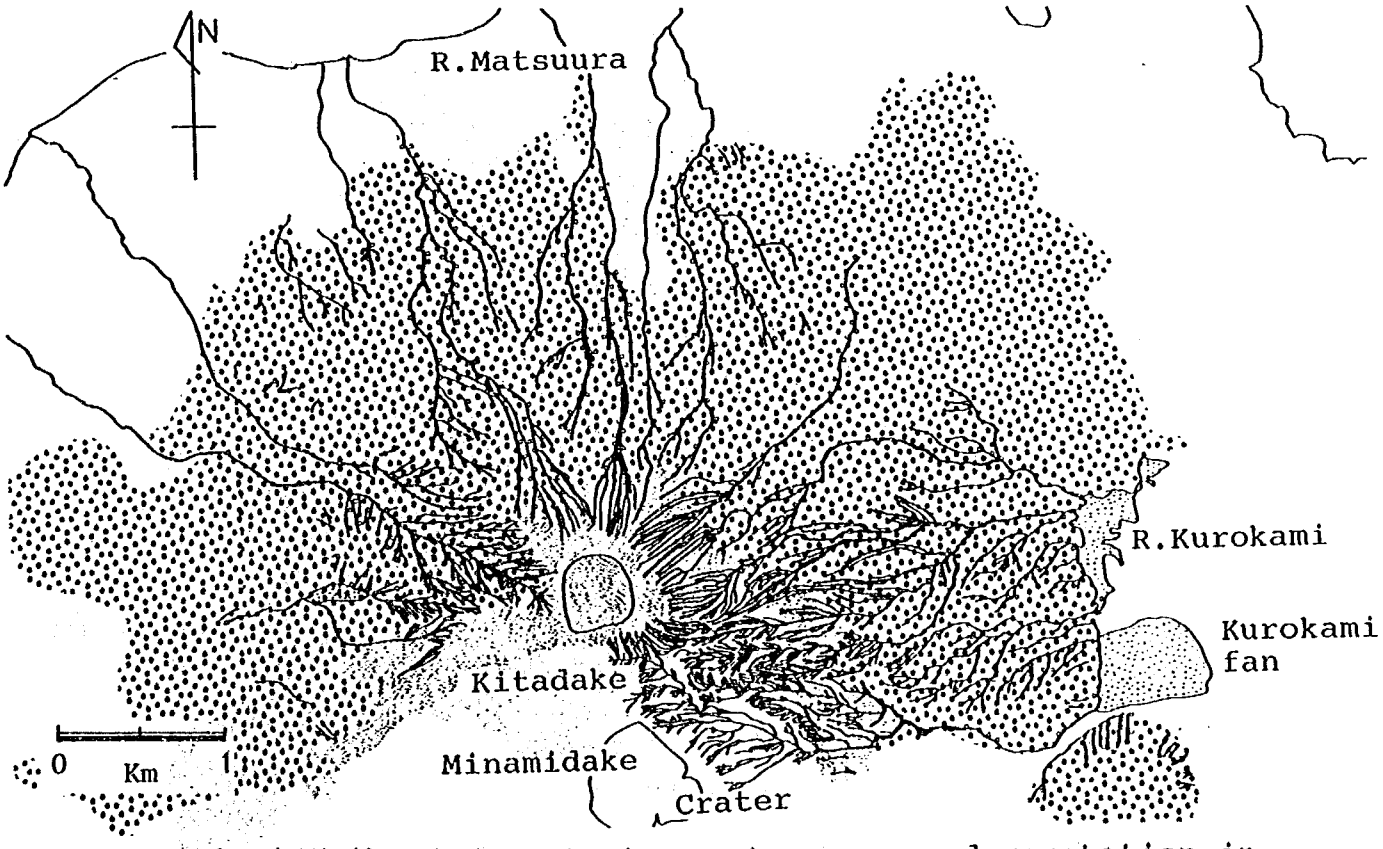


Fig. 6 Distribution of both erosion area and vegetation in the hillside slope in 1966.

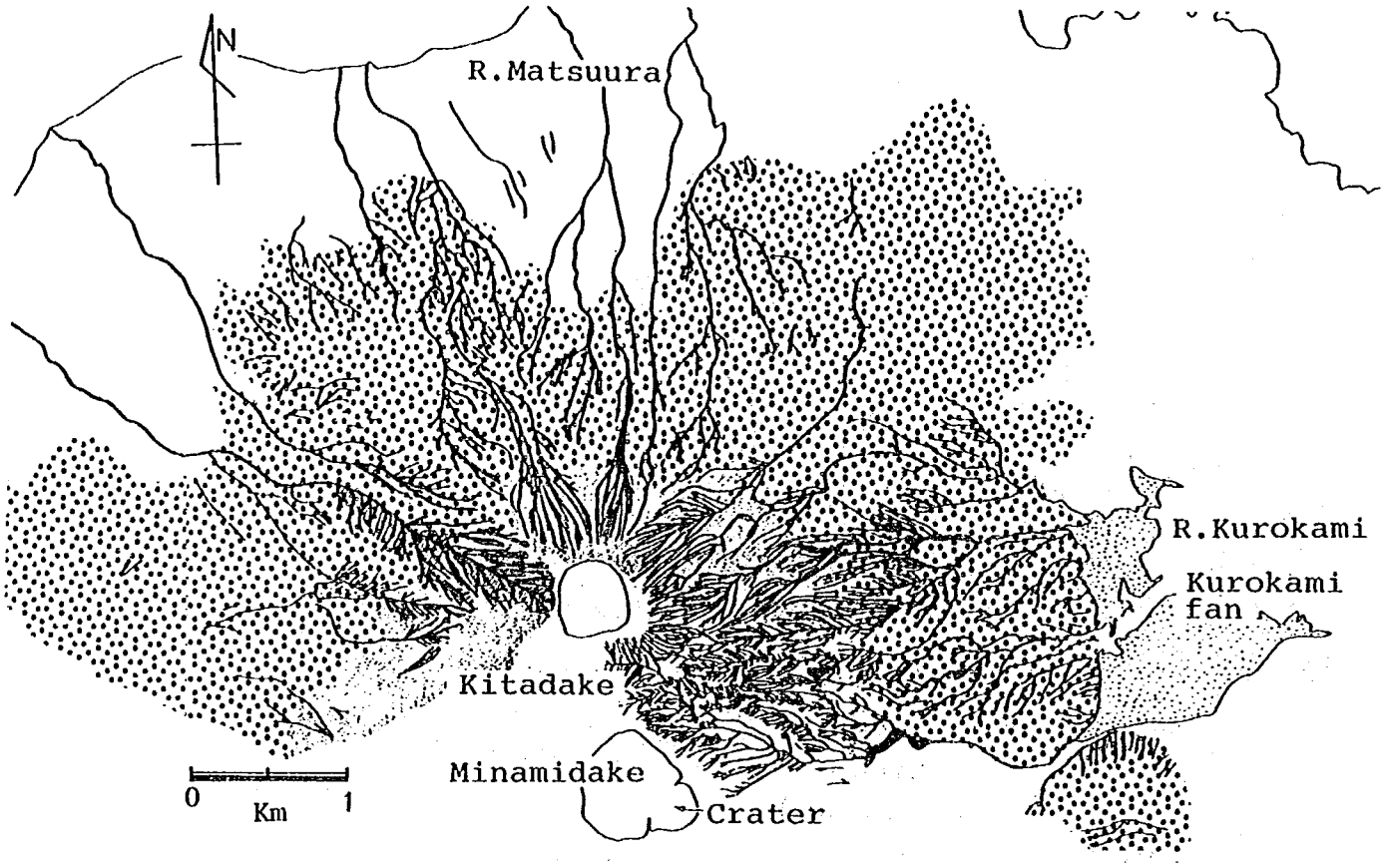


Fig. 7 Distribution of both erosion area and vegetation in the hillside slope in 1974.

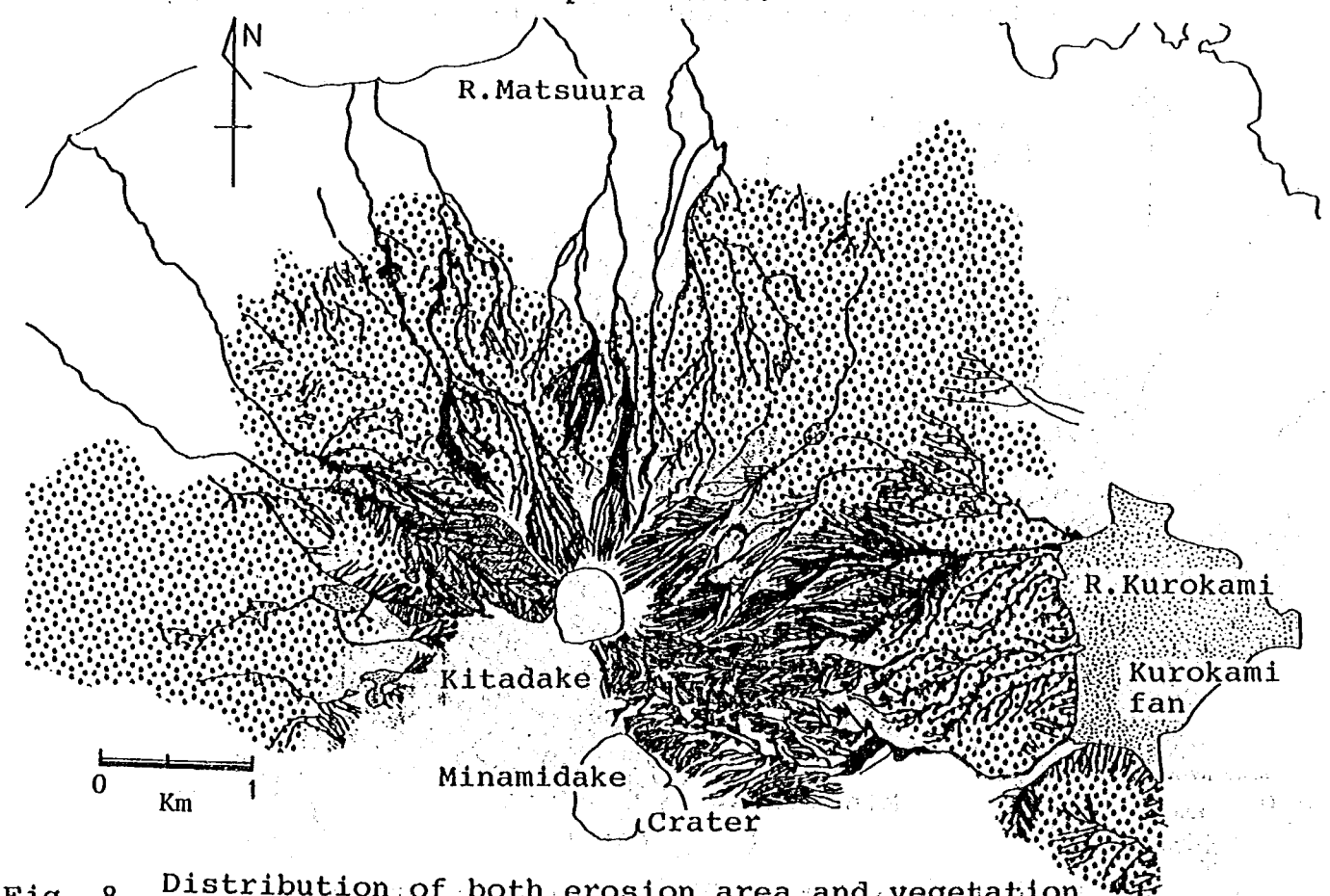


Fig. 8 Distribution of both erosion area and vegetation in the hillside slope in 1980.

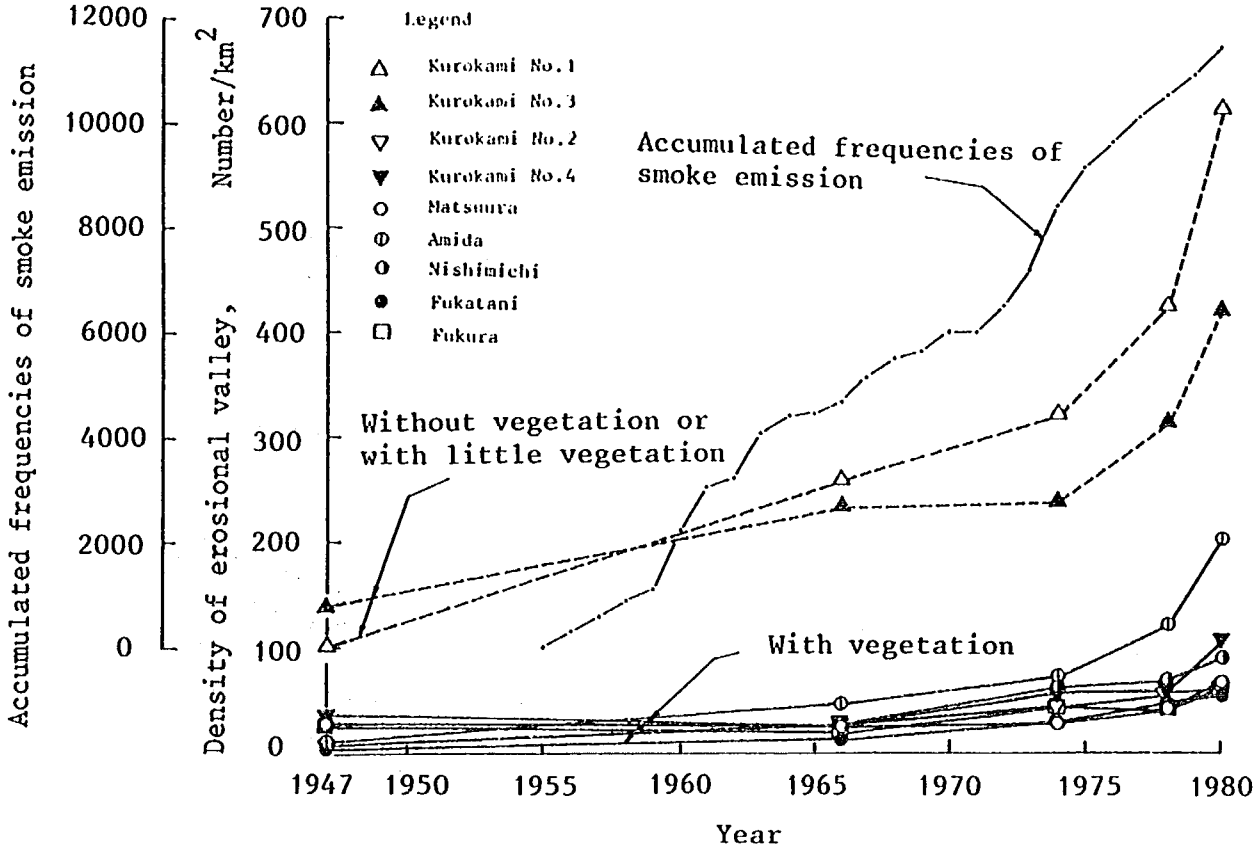


Fig. 9 Relationship between progression of erosion in the hillside slope and volcanic activity in Mt. Sakurajima.

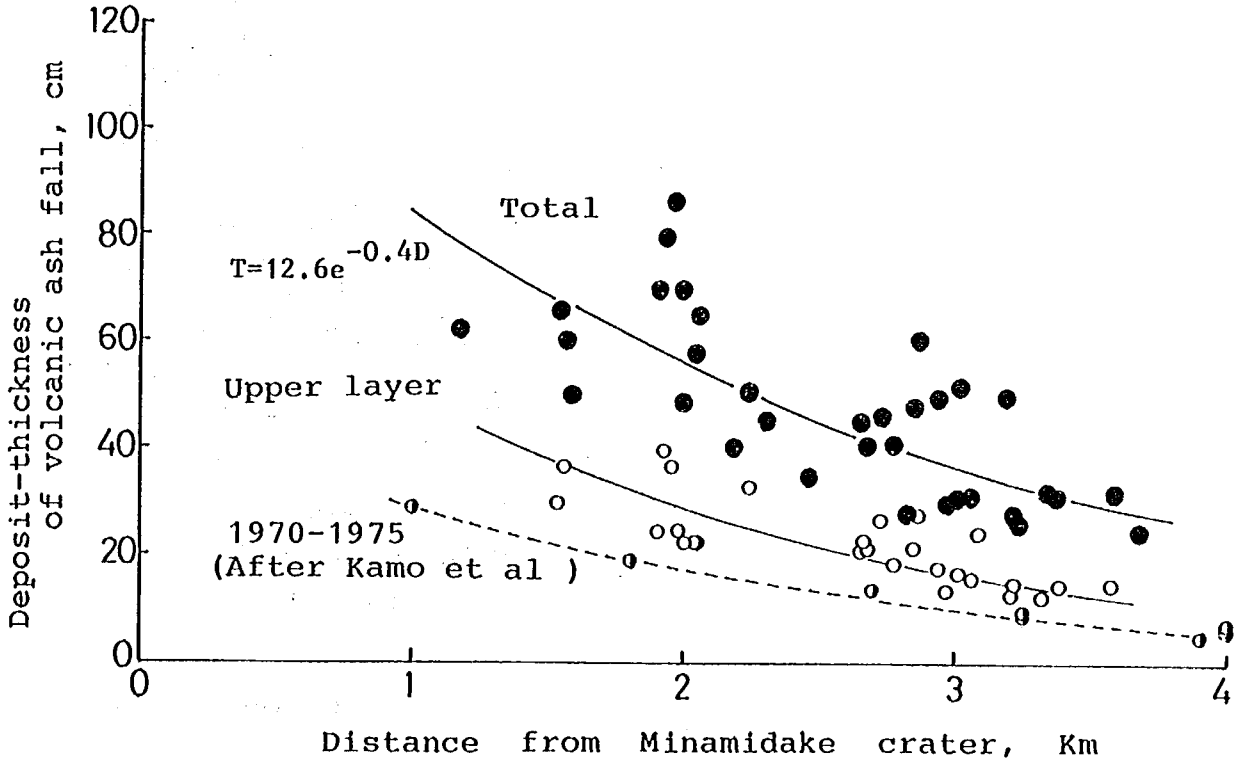


Fig. 11 Distribution of volcanic ash fall deposit.

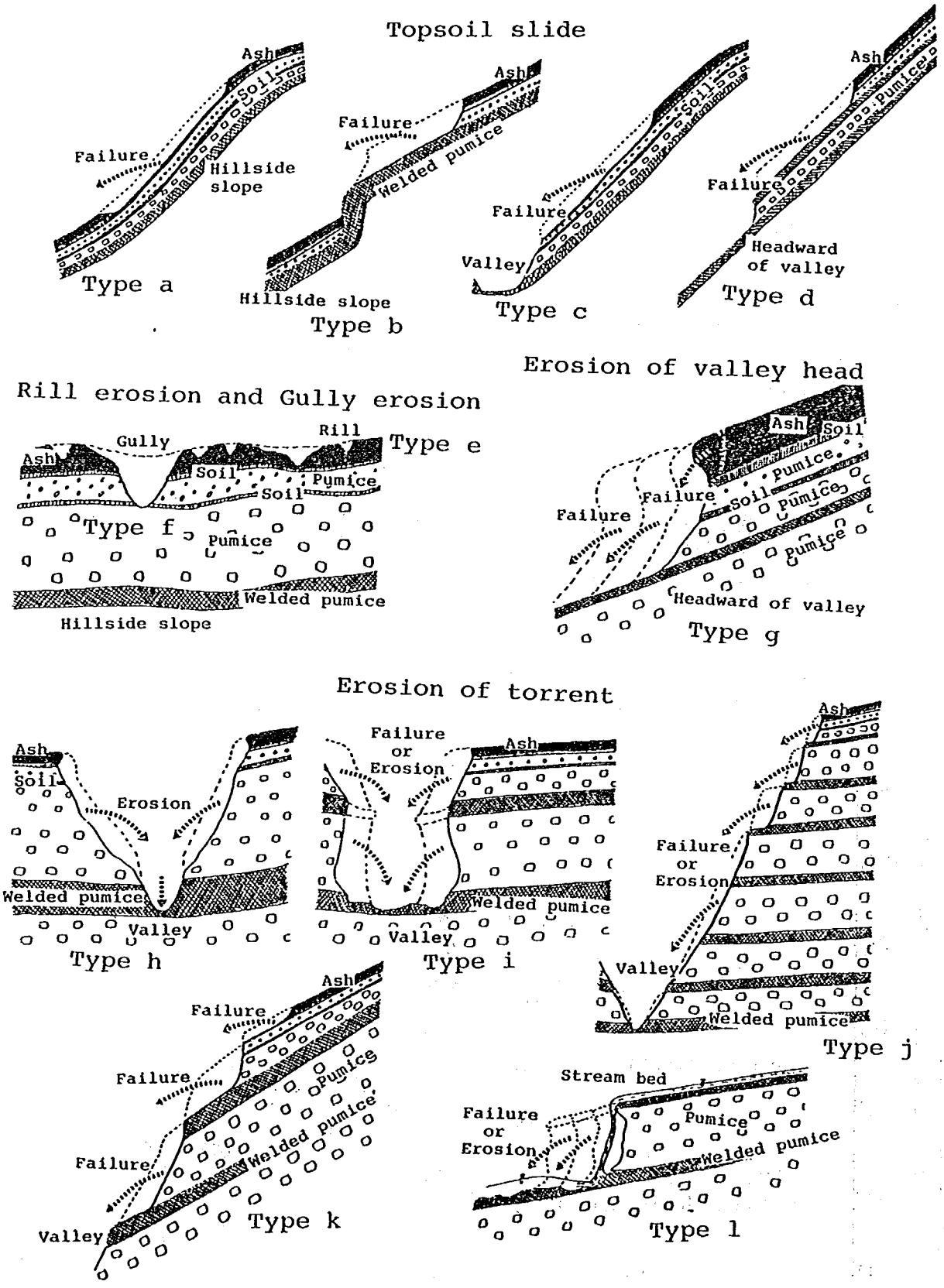


Fig. 10 Basic forms of slope-failure and erosion in the hillside slope and torrent.

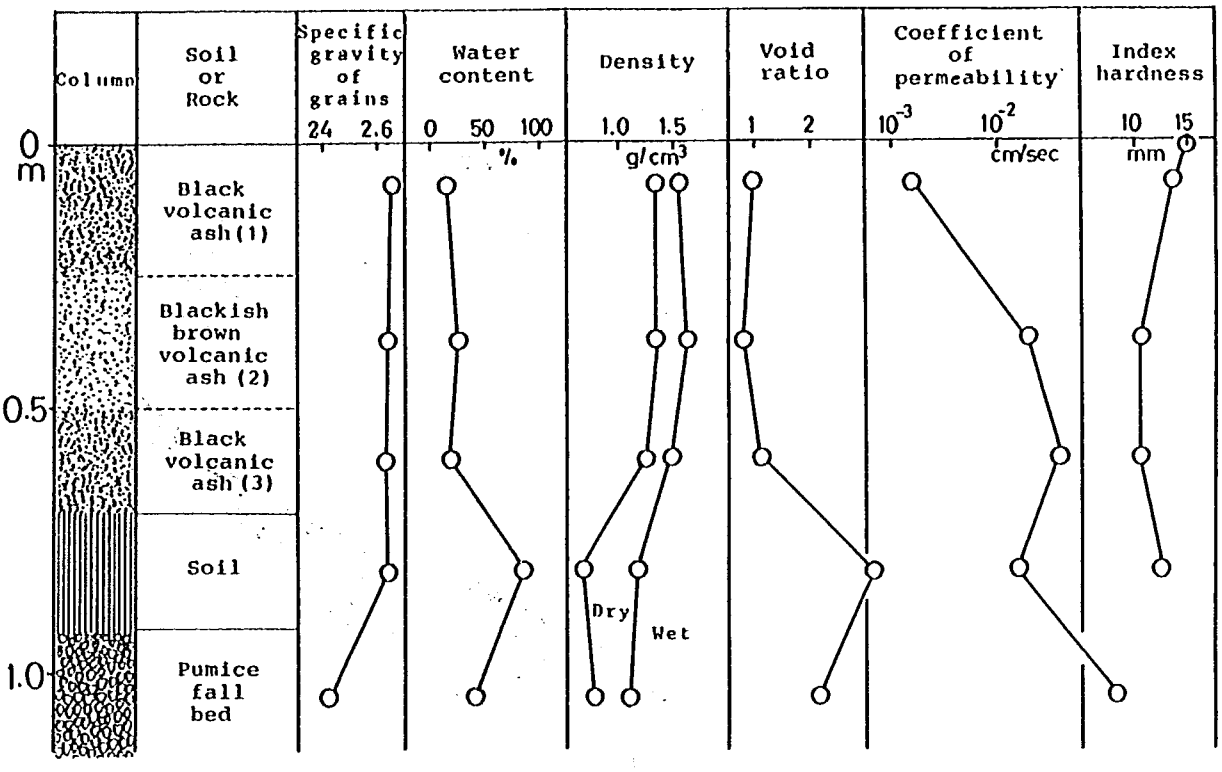


Fig. 12 A example of geologic columnar section and geotechnical properties of both volcanic ash fall and Taisho pumice fall deposits.

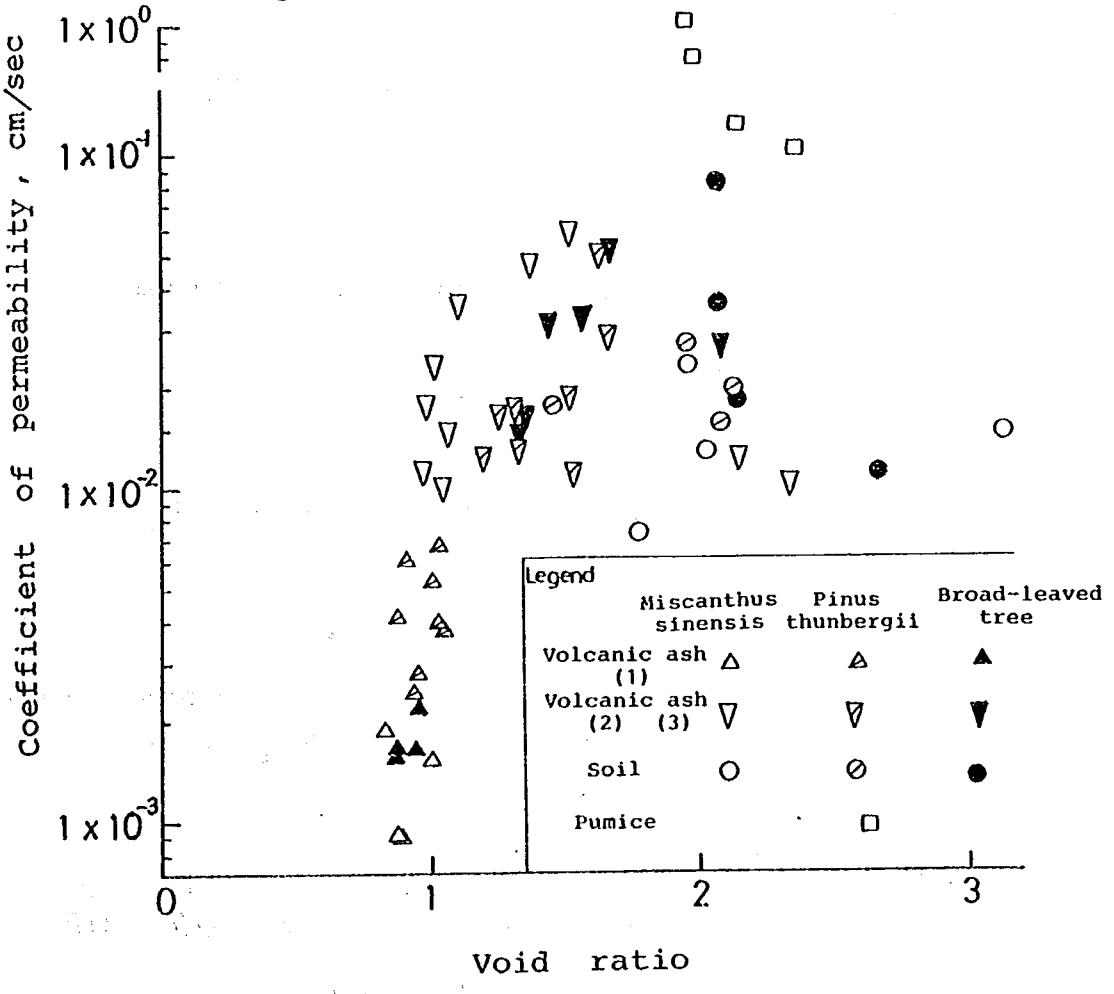


Fig. 13 Relationship between coefficient of permeability and void ratio.

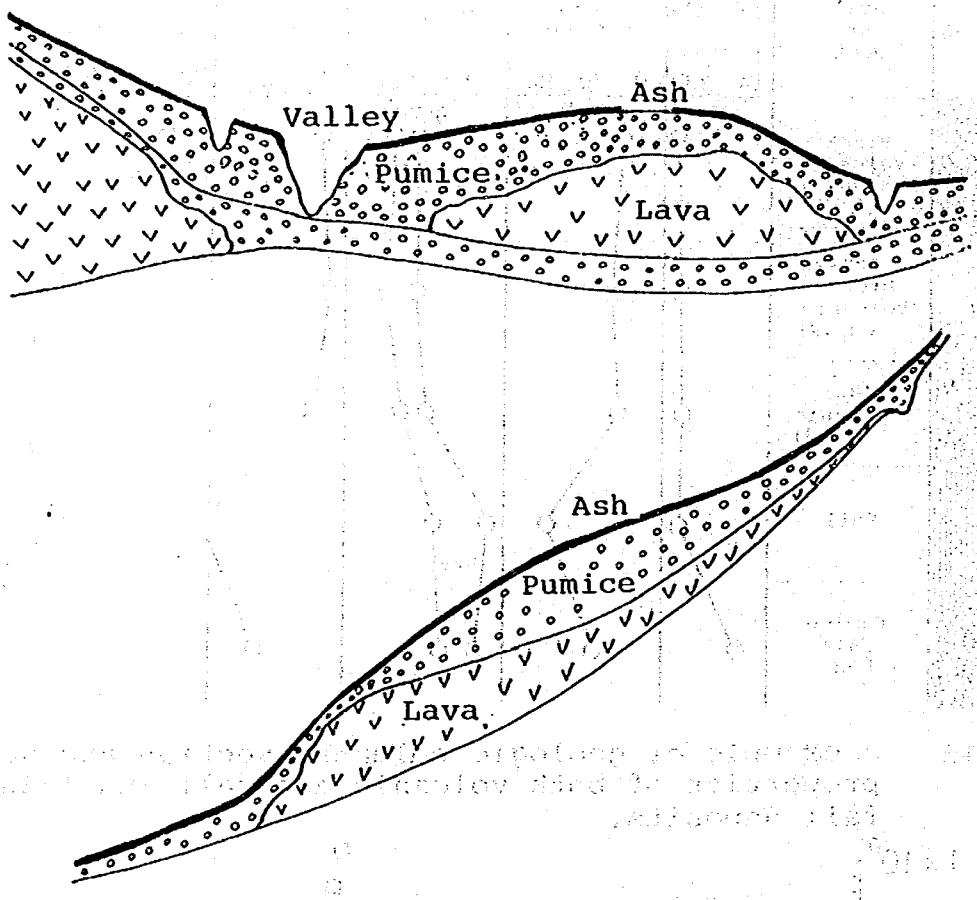


Fig. 14 Deposit forms of both lava flow and pumice fall.

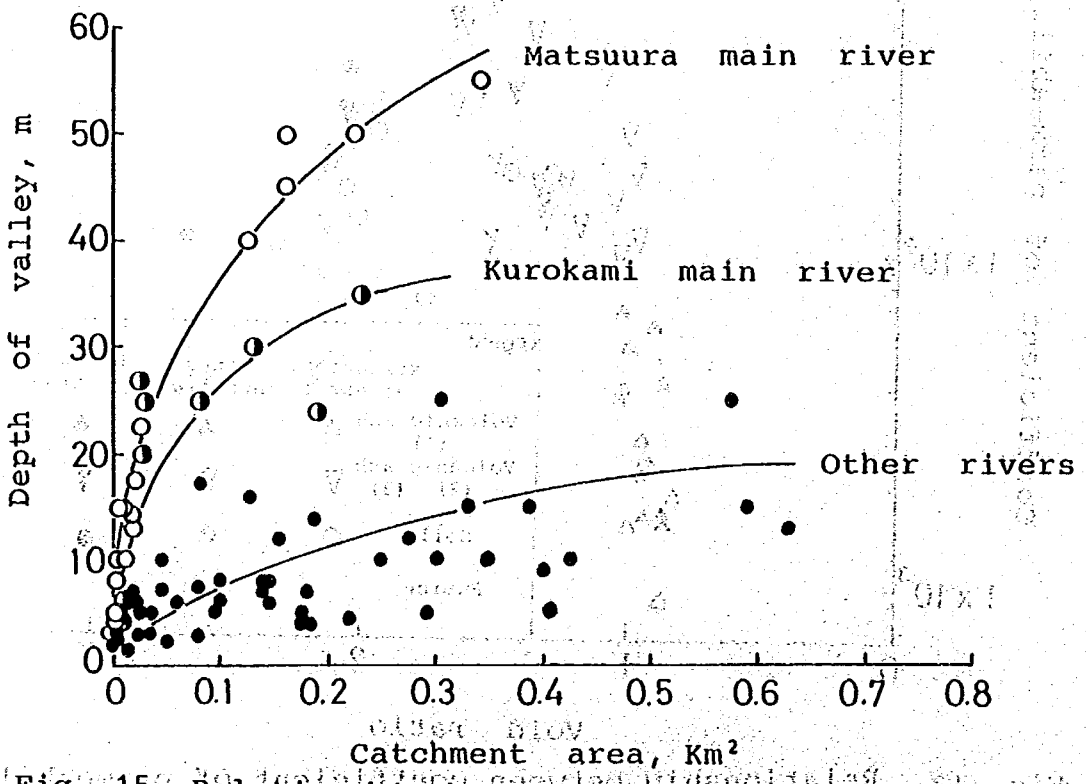


Fig. 15 Relationship between depth of valley and catchment area.

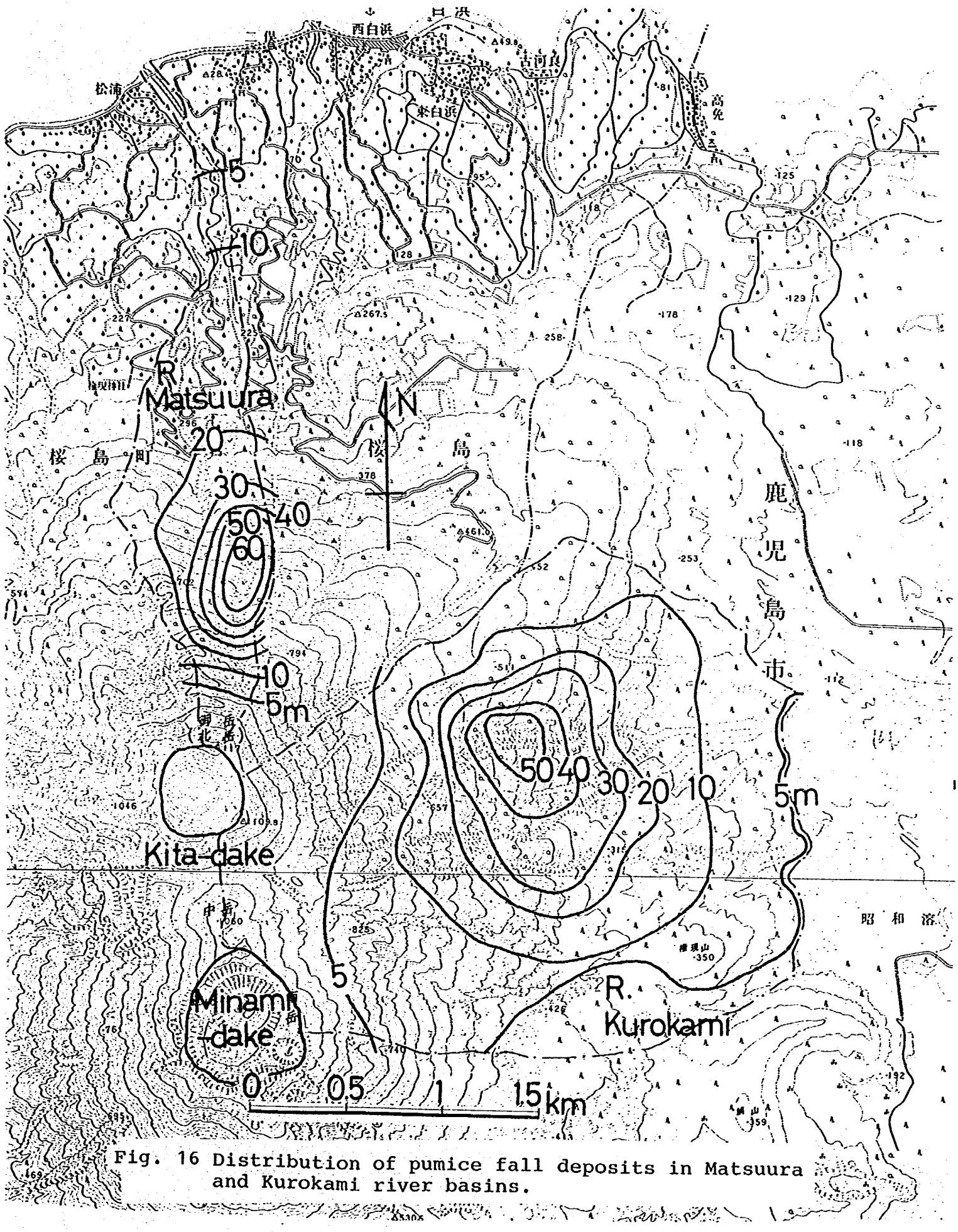


Fig. 16 Distribution of pumice fall deposits in Matsuura and Kurokami river basins.



EROSION OF TEPHRA FROM HILLSLOPES NEAR MT. ST. HELENS AND OTHER VOLCANOES[1/]

F.J. SWANSON
USDA FOREST SERVICE
FORESTRY SCIENCES LABORATORY
3200 Jefferson Way
Corvallis, Oregon 97331

B. COLLINS
T. DUNNE
DEPARTMENT OF GEOLOGICAL SCIENCES
UNIVERSITY OF WASHINGTON
Seattle, Washington 98195

B.P. WICHERSKI
DEPARTMENT OF GEOLOGY
OREGON STATE UNIVERSITY
Corvallis, Oregon 97331

1/ This work was supported in part by Weyerhaeuser Co., Washington State Department of Fisheries, the Gifford Pinchot National Forest and by cooperative agreements PNW 80-179, PNW 80-286, and PNW 81-306 between the USDA Forest Service, Pacific Northwest Forest and Range Experiment Station, Oregon State University, and University of Washington.

ABSTRACT

Rates of erosion from hillslopes affected by the 1980 eruptions of Mt. St. Helens vary in relation to hillslope gradient, thickness and surface texture of deposits, and conditions of vegetation and organic debris. Rill erosion has been greater than sheet and debris slide erosion in the first 2 years after the eruption. Erosion of tephra and underlying soil over this period has been greater in the zone of downed vegetation than in areas where vegetation was killed but not downed and where airfall tephra accumulated but vegetation was not killed. Rates of rill erosion were higher in areas clearcut before the eruption than in downed forest.

The rate of rill erosion appears to have peaked and declined during the first rainy season because of changes in hillslope hydrology and erodability of the ground surface. Living vegetation had little effect on this decrease in erosion rate. This pattern of an early peak in rill erosion, followed by a rapid decline, has been observed after eruptions of several other volcanoes.

Management activities such as salvage logging, scarification, and grass seeding appear to have had minor effect in reducing surface erosion of hillslopes in the first 2 years after the eruption primarily because the most rapid erosion took place before these practices were carried out. However, salvage logging and contour scarification have reduced erosion by increasing infiltration.

The frequency of debris slides in the eastside of the blast zone has increased dramatically in areas of downed forest vegetation. Toppling of groups of trees on very steep slopes during the blast triggered some slides and subsequent slides have occurred in response to lost rooting strength caused by uprooting of trees during the blast and by decomposition of roots in the ground.

INTRODUCTION

Volcanic eruptions alter the erosional regime of surrounding areas by distributing great quantities of readily eroded material over the

landscape, changing hillslope hydrology, and reducing or eliminating vegetative cover. The increased erosion associated with these events reduces water quality, damages fisheries resources, and aggravates flood hazards. Increased runoff and sediment yield can also initiate and aggravate mudflows that pose extreme hazard to downstream areas (Waldron 1967). Patterns of hillslope erosion may also strongly influence the rate of recovery of terrestrial and aquatic ecosystems.

Volcanic eruptions create a great diversity of new environments for erosion. Each type of volcanic eruptive event results in distinctive topography, deposits of varying thickness and texture, and a range in degree of destruction of vegetation. For these reasons, the dominant processes and rates of subsequent erosion may differ among areas affected by various volcanic events. For example, the flanks of an actively growing cinder cone at the angle of repose may be carved by different processes and at different rates than gently sloping landforms blanketed by a thin layer of tephra. In general, fresh volcanic deposits experience erosion rates many times higher than older deposits of similar origin or other substrates in an area.

Our objectives in this paper are to 1) review the literature published in English on processes and rates of hillslope erosion in areas of very recent volcanism, 2) report observations and results of hillslope erosion studies at Mt. St. Helens, including the effects of efforts to reduce erosion, and 3) speculate on future trends in hillslope erosion in the Mt. St. Helens area. We are particularly interested in changes in erosion rates through time caused by changing physical and biological conditions, because these considerations are important in planning response to erosion hazards. We limit this discussion to the erosion of tephra and soil by water, wind, and gravity over several years. We do not discuss erosion of intrusive rocks, lava flows, domes, and welded ash flows, erosion by volcanic processes, or the dynamic development of crater walls.

PREVIOUS WORK

Numerous non-quantitative studies and photographs document rapid erosion of fresh tephra deposits in a broad range of volcanic settings and

environments extending from the arctic to tropical rain forests. Quantitative studies of tephra erosion from hillslopes, however, are rare. Research in volcanology has centered on eruptive mechanisms and products; subsequent erosion has been studied primarily in terms of the hazards it poses to downstream areas (Waldron 1967) or in relation to ecological recovery (Griggs 1918, Segerstrom 1950, 1960, Eggler 1963). Detailed descriptions and quantitative results are available from studies following eruptive episodes of four volcanoes: Paricutin (Mexico), Irazu (Costa Rica), Vulcan (New Guinea), and Fernandina (Galapagos Islands).

Paricutin

Segerstrom (1950, 1960, 1961, 1966) described erosion and redeposition of basaltic tephra erupted by Paricutin mainly in the 2 years beginning on February 20, 1943, when the volcano first appeared in a cornfield in the State of Michoacan, Mexico. The main cone of Paricutin grew to a height of 360m and its eruptions blanketed the surrounding hills and pine-oak forests with up to 6 m of predominantly sand-sized tephra. Annual precipitation in this temperate climate averaged about 1500 mm and occurred mainly as high intensity storms during the summer rainy season (Eggler 1959). Between July and October 1946 Segerstrom (1950, p. 12) measured rainfall intensities up to 40mm/hr for 1 hour.

Erosion of the cone itself was not significant by 1965 because of the high permeability of surface deposits (Segerstrom 1966). Finer textured deposits further from the vent were eroded rapidly by mass movement, water, and wind. Creep of new deposits on slopes steeper than 0.62 (gradient expressed as tangent of slope angle) was indicated by the lean of dead trees (Segerstrom 1950). Landslides rapidly removed tephra deposits up to 6m in thickness from slopes steeper than about 0.70 (Segerstrom 1950). In some cases landsliding removed the entire mantle of fresh tephra; elsewhere failure planes developed along bedding surfaces within the new deposits. Mass failures also occurred in stream banks more than a few meters high.

Erosion by sheetwash, raindrop splash, and rills was widespread and intensive. The generation of overland flow was greatly increased by development of a surface crust, which Segerstrom (1950) attributed to accumulation of fine particles in the interstices of the tephra. At ten sampling locations where tephra thickness originally ranged from 25 to 165cm, Segerstrom (1950, p. 75) measured tephra thickness at drainage divides to estimate the original thickness of deposits. Based on these measurements, he concluded that sheet and rill erosion had removed 20 to 100 percent (mean = 48 percent) of tephra by September 1946, or about 5.5cm/yr in four years. Rill development was common, but the rates of sheet and rill erosion were not quantified separately.

Widespread erosion and redeposition by wind was indicated by dune forms up to 3m in amplitude and the filling of rill heads during the dry season (Segerstrom 1966).

The rapid rate of tephra erosion in 1943-1944 declined dramatically over the next 20 years (Segerstrom 1961, 1966) as the most easily eroded deposits were removed. By 1965, revegetation was vigorous on the widespread areas where erosion of tephra exposed pre-eruption soil. In areas where plants were not killed by the eruption the formation of a layer of organic litter caused erosion rates to decline even more rapidly than where plants were killed (Segerstrom 1966).

Irazu

Irazu Volcano (elevation 3,432m) in central Costa Rica, erupted silt- and sand-sized, basaltic-andesite tephra between March 1963 and March 1965. Up to 2m of tephra fell in the summit area and thinner deposits accumulated on the flanks of the volcano and downwind to the west. The tephra eruptions killed much of the dense shrub vegetation and sparse tree-cover on the upper part of the volcano. This area received between 950 and 2000mm of annual precipitation (based on a 22-yr. record at Sanatorio Duran, 2,337 m in elevation) mainly during a summer rainy season, characterized by brief, local, high intensity rainstorms (Waldron 1967).

The tephra surface developed a relatively impermeable surface crust which Waldron (1967) argued was cemented by precipitation of salts. Copious overland flow then resulted in extensive sheet, rill, and gully erosion. Waldron (1967) estimated that during the 1964 rainy season alone one-third to one-half of all tephra deposits averaging 15cm in thickness were removed from the upper Rio Reventado basin (Waldron 1967).

Waldron (1967) observed few active mass movements until the end of the 1964 rainy season when mudflows down the Rio Reventado channel eroded toes of dormant slumps and earthflows, reactivating mass movement features which individually covered 40+ha. The reactivated earthflows moved up to 2 to 4m/wk and delivered large quantities of older, altered lahar deposits to stream channels where the older deposits were incorporated in mudflows moving downstream into the City of Cartago.

By the end of the 1964 rainy season the volume of runoff and frequency of mudflows had decreased. These hydrologic changes resulted from exposure of more permeable substrates by erosion of tephra, recovery of natural vegetation, and application of intensive watershed rehabilitation measures. The effectiveness of erosion control measures, including terracing, contour trenching, and revegetation with introduced grasses, was not systematically evaluated.

Vulcan

The volcano Vulcan (New Guinea) grew to a height of 156m in only four days beginning on May 29, 1937. This cone of andesitic scoria had smooth upper slopes with a gradient of 0.58 soon after the eruption. However, the 2240mm of annual precipitation, some of it coming in torrential downpours, rapidly carved deep gullies heading 10 to 30m below the crater rim (Ollier and Brown 1971). In 1968 Ollier and Brown (1971) surveyed gully cross-sections along six transects each 95m in length across the slope. The transects were all located 10 to 150m below the crater rim. The volume of gullies represented an average erosion rate of 1.7cm/yr when averaged over the 31-year period. Based on field observations in 1941 and 1968, Ollier and Brown argue that most

of this erosion occurred during the first 5 years after the eruption. Assuming a 5-year period of gully formation, the volume of gullies represents an erosion rate of 10.5cm/yr. Ollier and Brown (1971) noted the existence of stone-capped pedestals as equivocal evidence for sheet erosion of 10 to 20cm of tephra from the upper slopes during the 31 year period.

The field observations made in 1941 and 1968 indicated that gully incision had stopped by 1941. Interpretation of aerial photographs (Ollier and Brown 1971) indicated that revegetation of the upper slopes of the cone did not occur until 1944. This apparent delay between cessation of gully cutting and revegetation suggests the importance of physical rather than biological factors in reducing erosion.

Fernandina

Fernandina volcano in the Galapagos Islands erupted explosively in 1968, depositing up to 8 m of tephra in the shrubby vegetation of its flanks. Although no measurements have been made, precipitation was low in general in this area. Rates of tephra erosion were not measured either, but Hendrix (1981) noted that gullies that had formed by 1971 appeared unchanged on successive visits made in 1973 and 1977. Vegetation was too sparse to have been a significant factor in suppressing erosion, suggesting that physical factors caused a reduction in erosion rate.

EROSION OF HILLSLOPES NEAR MT. ST. HELENS

Conditions Before and During the 1980 Eruptions

Rates and patterns of hillslope erosion near Mt. St. Helens before the May 1980 eruptions can be inferred from results of sediment budget studies in other steep, forested landscapes of the Pacific Northwest (Dietrich and Dunne 1978, Reid 1981, Swanson et al. 1982). These studies indicate that small landslides, soil creep, surface erosion, and root throws are the dominant processes transporting soil from hillslopes to channels. Surface erosion of litter-covered forest soil is dominated by freeze-thaw, wetting-drying, and splash processes. Sheetwash and rill erosion are extremely rare except on compacted and disturbed sites,

such as road cuts and skid roads. Despite steep slopes, the low rainfall intensities characteristic of the region and the high infiltration rates of forest soils result in moderate erosion rates under conditions of natural and managed forest vegetation. Based on a review of suspended sediment yield from Pacific Northwest rivers by Karlin (1980) and erosion studies in smaller basins in the region (Dietrich and Dunne 1978, Larson and Sidle 1980, Reid 1981, Swanson et al. 1982) we estimate that sediment yield from lands around Mt. St. Helens prior to the 1980 eruptions was approximately 100 to 200t/km^2-yr.

Before the 1980 eruptions dense forests, composed predominantly of Douglas-fir (Pseudotsuga menziesii), western hemlock (Tsuga heterophylla), and true firs (Abies spp.), covered the mountainous landscape within 30km of the volcano. Natural forests ranged in age from the young stands that post-date wildfires earlier this century to old-growth stands in which some individual trees exceeded 2 m in diameter and 600 yrs. in age. Extensive timber harvest by clearcutting between about 1940 and 1980 produced a mosaic of young conifer stands of differing ages and an extensive road network.

The 1980 eruptions of Mt. St. Helens dramatically changed the surrounding landscape. The volcanic events of 1980, particularly those on May 18, resulted in six distinctive types of deposits and associated vegetation (debris avalanche, downed vegetation, and standing dead vegetation in the blast zone, mudflow, pyroclastic flow, and airfall tephra on live vegetation).[1/] The deposits differ in texture,

[1/] We use terminology for volcanic events, deposits, and zones of impact defined on Plate 1 of Lipman and Mullineaux (1981), except that we use "downed vegetation" as synonymous with the "no-tree" plus "tree down" zones in Plate 1.

thickness, and topography, and the extent to which their emplacement destroyed existing vegetation (Fig. 1).

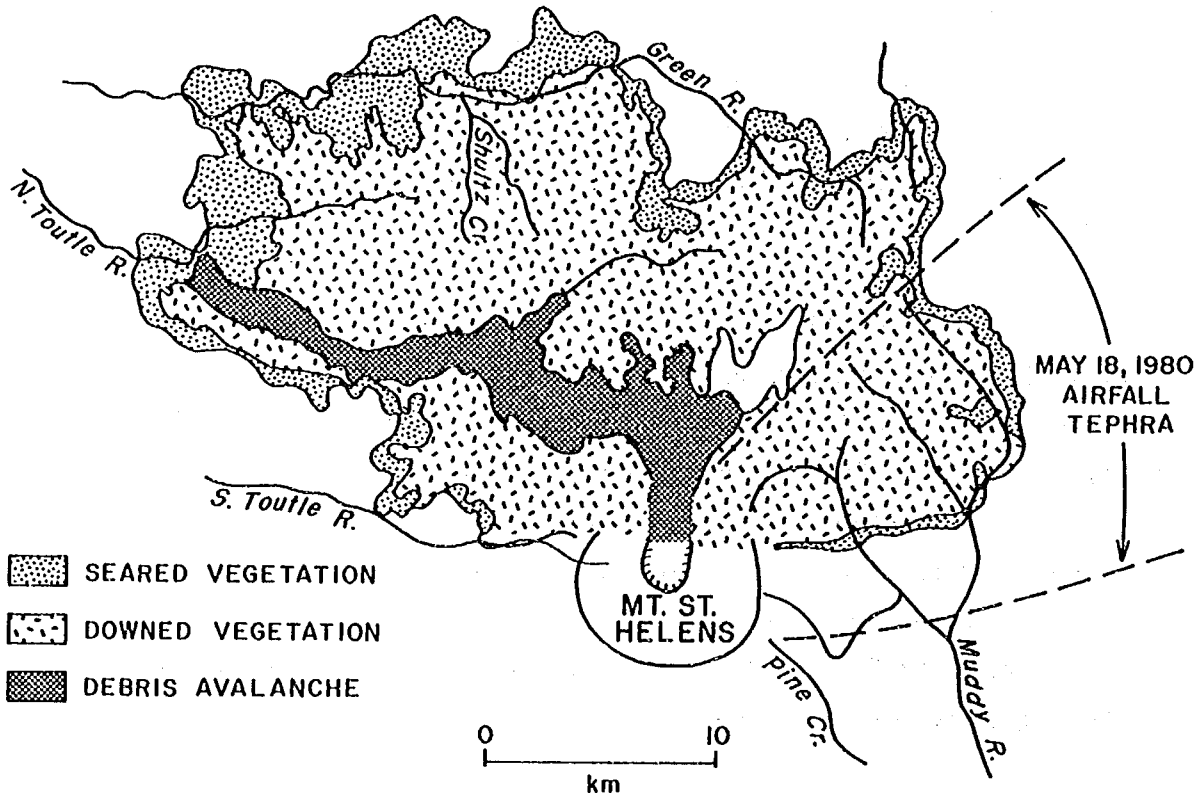


Fig. 1. Map showing areas proximal to Mt. St. Helens affected by the 1980 eruptions.

The major debris avalanche associated with the cataclysmic eruption on May 18 spread a mixture of material ranging from clay-size to huge blocks in a deposit 10 to 195 m thick over 60 km^2 of the N. Fork Toutle River Valley (Voight et al. 1981). As the debris avalanche moved down the Toutle Valley, a directed volcanic blast stripped vegetation from most hillslopes within 12km north of the mountain and leveled all vegetation as far as 28 km from the mountain in a 180° arc to the north (Hoblitt et al 1981, Moore and Sisson 1981, Waitt 1981). In the 370 km^2 area of downed vegetation silt- to gravel-sized lithic fragments and organic matter blanketed the pre-existing landscape with tephra layers ranging from 8 cm to over 1m in thickness. Ringing the zone of toppled vegetation is a 110 km^2 band of seared but standing

vegetation where the silty to sandy deposits of the lateral blast thin from about 8 to 2 cm.

Eruptions on May 18-19, May 25, June 12, and July 22 cumulatively deposited from less than 1 cm to about 25 cm of airfall tephra in most quadrants near the mountain (Waitt and Dzurisin 1981, Waitt et al 1981) (Fig. 1). Tephra deposits greater than 5cm thickness fell on about 1000km^2. The size distributions within these airfall tephra units varies greatly from one ash-fall plume to another and with position within an individual plume. The airfall deposits were thin enough that resulting plant mortality was mainly restricted to understory vegetation.

In this paper we discuss temporal and spatial distribution of erosion processes on hillslopes affected by the directed blast in the zones of downed and seared vegetation and on hillslopes affected only by airfall tephra where tree cover was not destroyed. Our field measurements have been concentrated on hillslopes in the zone of downed vegetation because erosion rates are greater in this area are greater than in the other two zones. Furthermore, we want to evaluate the effects of erosion-control measures and extensive salvage logging of downed trees that have been conducted in this area.

Erosion of Tephra in the Zone of Downed Vegetation

There is broad geographic variation in the patterns and rates of hillslope erosion in the zone of downed vegetation. Most of the blast zone north and northwest of the mountain is characterized by long, moderately steep slopes covered with blast deposits with a silty surface layer (Fig. 2). These lands were mainly in private and State ownership and a large proportion of the forest land had been clearcut in the four decades before the eruption. Federal lands concentrated to the north and northeast of the mountain have steeper, more irregular slope profiles, a less extensive patchwork of clearcuts, and more natural forest openings in areas of bedrock exposure and alpine ecosystems. Deposits (5-15 cm thick) of gravel-sized airfall pumice, a 1-2 cm-silty surface layer, both from the May 18 eruption, and a scattering of lithic

dacite gravel from the July 22 eruption mantle the blast deposits northeast of the mountain.

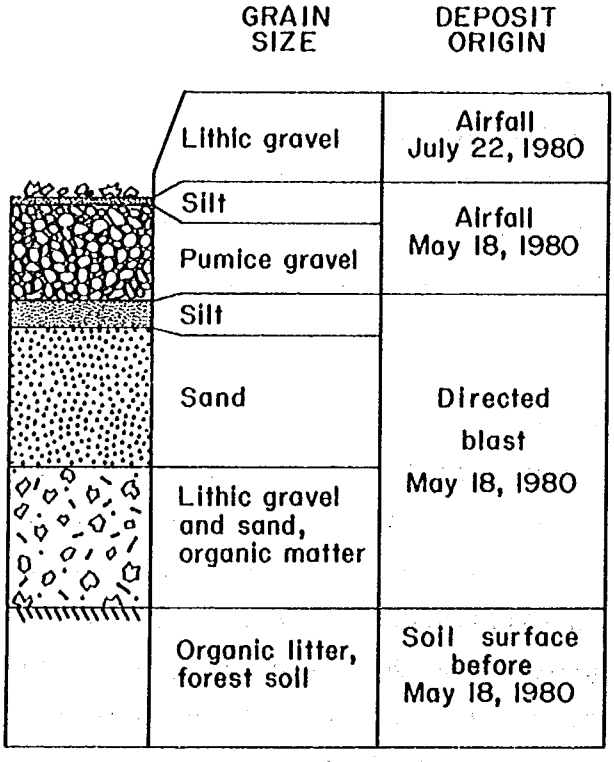


Fig. 2. Generalized stratigraphy of 1980 deposits in the blast zone. Blast deposits accumulated throughout the blast zone and May 18, and July 22, 1980, airfall tephra was deposited northeast of the volcano (Fig. 1).

Studies of hillslope erosion in the blast zone have centered on two contrasting areas. Collins, Dunne, and their colleages at the University of Washington have worked north and northwest of the volcano in areas without the coarse pumice deposits. Swanson, Wicherski, and others of the U.S. Forest Service and Oregon State University studied the area northeast of the volcano blanketed by coarse pumice airfall on May 18, 1980.

Mass movement, sheet, and rill erosion processes have eroded the tephra deposits. During the first 2 years after the 1980 eruptions, sheet and rill erosion have dominanted.

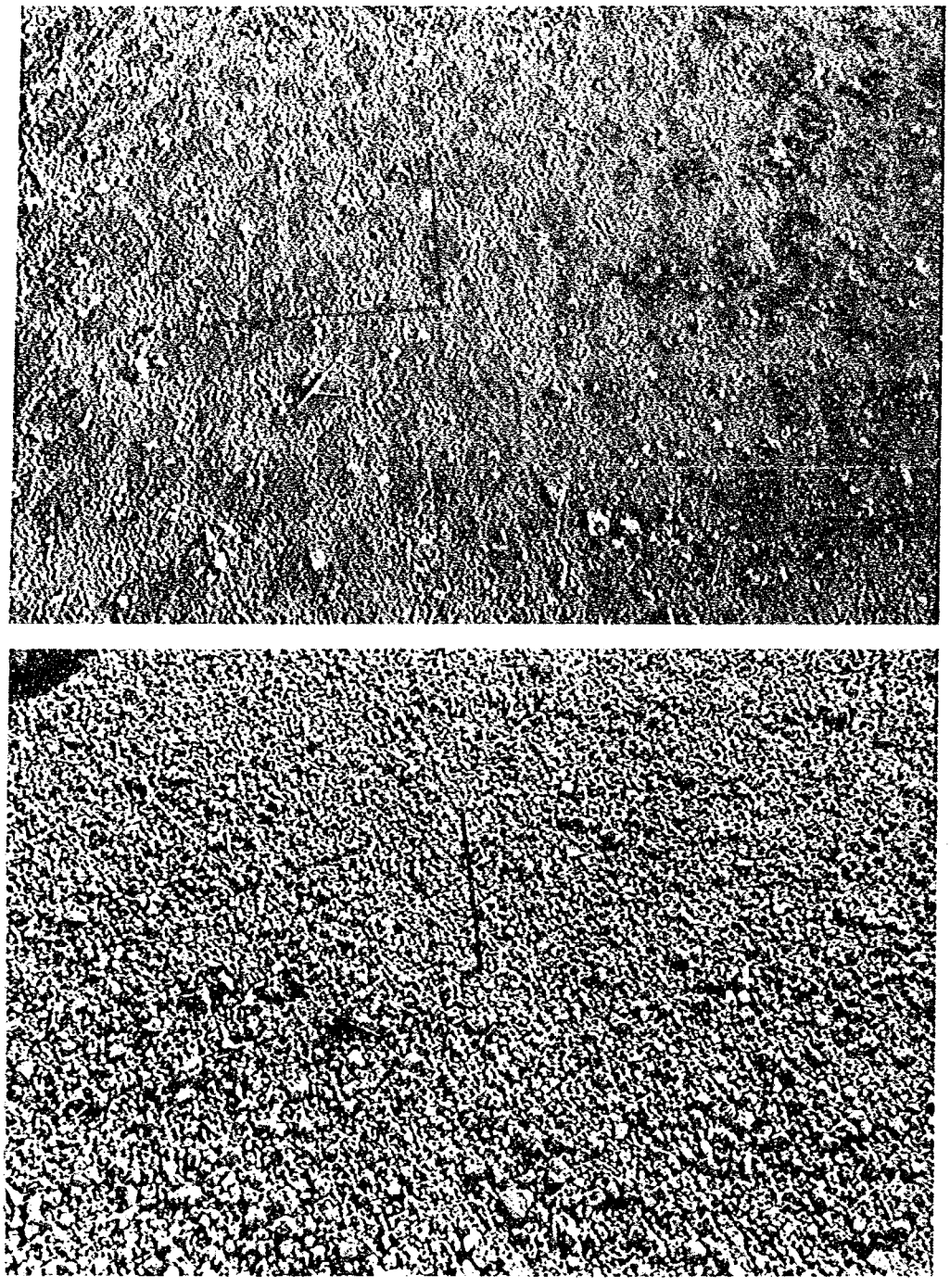
Surface Texture and Hydrology

Rates of processes eroding tephra were strongly influenced by the hydrology of surface deposits. A feature common to the proximal airfall tephra was formation of a hard, relatively impermeable surface crust similar to that described at Paricutin and Irazu. Crusting of the surface 1 to 3cm of silty material occurred on drying in late May and June 1980 and strongly affected the surface hydrology. The crust contained abundant vesicles up to several millimeters in diameter. No one, to our knowledge, is conducting a systematic study of crust formation at Mt. St. Helens.

The infiltration rates have varied through time and with the difference in texture of surface deposits. Herkelrath and Leavesley (1981) measured infiltration rates of 1 to 4mm/hr in August 1980 on undisturbed deposits with a silty surface layer. This rate increased to 7 to 9mm/hr by the following August (G. Leavesley, pers. comm.), because (1) sheet erosion removed the fine-grained surface material, exposing sandier deposits with higher infiltration rates, (2) freeze-thaw action mixed the fines and coarser deposits and (3) rill erosion exposed some of the underlying pre-eruption soil.

Infiltration rates of about 13 mm/hr were measured in summer 1981 (Wicherski, unpubl. data) on a hillslope in the Clearwater Creek basin northeast of the volcano where coarse pumice deposits cover the surface. Unfortunately no infiltration rates were measured in summer 1980 in the area of coarse pumice deposits, but dramatic changes in surface texture over the 1980-1981 wet season (Fig. 3) argue that the infiltration rate increased. An increased surface roughness resulted from removal of finer particles by sheet erosion and lifting of coarse particles to the surface by cycles of ice formation and melting (B. Wicherski, unpub. data). We infer that this rough surface had lower velocities of surface flow and higher infiltration rates than the smoother surface present in summer and early fall 1980.

Undisturbed forest soils in the Cascade Range typically have infiltration capacities in excess of 100 mm/hr (R. D. Harr, personnal



a

b

Fig. 3. Change in surface texture of deposits between September 1980(a) and January 13, 1981(b) in area of coarse pumice airfall tephra 8km ENE of mountain. Erosion pin of 1 cm diameter in center of each photograph.

communication, 1982). Rainfall intensities are typically in the same range as measured values of infiltration capacity of the 1980 tephra conditions, so storms in fall 1980 frequently generated overland flow. The observed modest increases in infiltration capacity could result in substantially reduced frequency of overland flow.

Rates of Sheet and Rill Erosion in the Zone of Downed Vegetation

Sheet and rill erosion were measured using erosion pins (steel rods 60 to 90cm long) driven into the ground at regular 2 to 5 m spacings along 50 to 200 m long transects crossing the slope at several positions downslope from the drainage divide (Collins et al. 1982). The distance between the top of each pin and the ground surface was measured at the time of installation and successive surveys, giving a measure of erosion or deposition in the intervening period. We noted which erosion pins we located in rills and interrill areas.

Any change in the bulk density of tephra caused by expansion or compaction would produce spurious estimates of sheet erosion. Undisturbed tephra samples taken at the time of each measurement of erosion pins at sites north and northwest of the volcano revealed no measureable changes in bulk density during the study (Collins et al. 1982). Bulk density samples were not taken on hillslopes northeast of the volcano because of difficulty in sampling the coarse pumice layer.

Rates of rill erosion were determined by measuring the cross-sectional area of all channels intersected by each transect. Separate measurements were made of the portion of each channel cut in fresh tephra and into underlying pre-eruption soil. Total erosion for each sampled hillslope was calculated as the sum of sheet erosion and rill erosion. Sampled hillslopes represented a range in slope gradient, length, and surface texture and included sites with downed forest vegetation and areas clearcut before the eruption.

Sheet erosion removed tephra from sites with coarse pumice surface deposits at rates varying from about 2 to 10 mm/yr between May 1980 and May 1981. An average of about 4mm (n = 8) of net sheet erosion occurred

on slopes with an average gradient of 0.50 in this area. Hillslopes with the same gradient but with silty surface deposits averaged about 16 mm of sheet erosion (Fig. 8 in Collins et al. 1982) Where the coarse pumice surface was present, there was no significant difference in rates of sheet erosion between plots set up in downed forest (n = 4) and in adjacent areas clearcut before the eruption (n = 4). Where the silty surface was present, sheet erosion at the two sites in downed trees was about 30% lower than on hillslopes clearcut before the 1980 eruption (Collins et al. 1982).

Rates of rill erosion at most study sites within the area of downed vegetation were in the range of 5 to $40 \times 10^3 m^3/km^2$-yr (5-40 mm/yr) for the first year after the May 1980 eruptions. These rates were strongly influenced by a variety of factors, including hillslope gradient, texture and thickness of deposits, and quantity and spatial arrangement of large woody debris (Collins et al. 1982). Measurements on hillslopes north and northwest of the volcano during the May 1980-May 1981 period showed higher rates of rill erosion on steeper slopes (Collins et al. 1982) . Hillslope gradient had the strongest effect on rill erosion at sites of highest for erosion -- where a minimum amount of woody debris covered the surface, deposits were thick, and the surface deposits were fine textured.

On slopes clearcut before the eruption and with tephra exceeding 15 cm in thickness, rill erosion of deposits with a silty surface layer was about 60 percent higher than on sites where the coarse pumice airfall was present (Figure 4). Some of the variability in these data may be explained by variation in deposit thickness. Collins et al. (1982) point out that thinner deposits limit erosion of tephra because rills commonly incise rapidly to the buried soil surface where further cutting is impeded by roots and woody litter.

Working in the area of silty surface deposits north and northwest of the volcano, Collins et al. (1982) observed rill erosion rates through May 1981 substantially higher in pre-1980 clearcuts than on hillslopes with large downed trees at sites with tephra thicknesses between 15 and 30 cm (Figure 5).

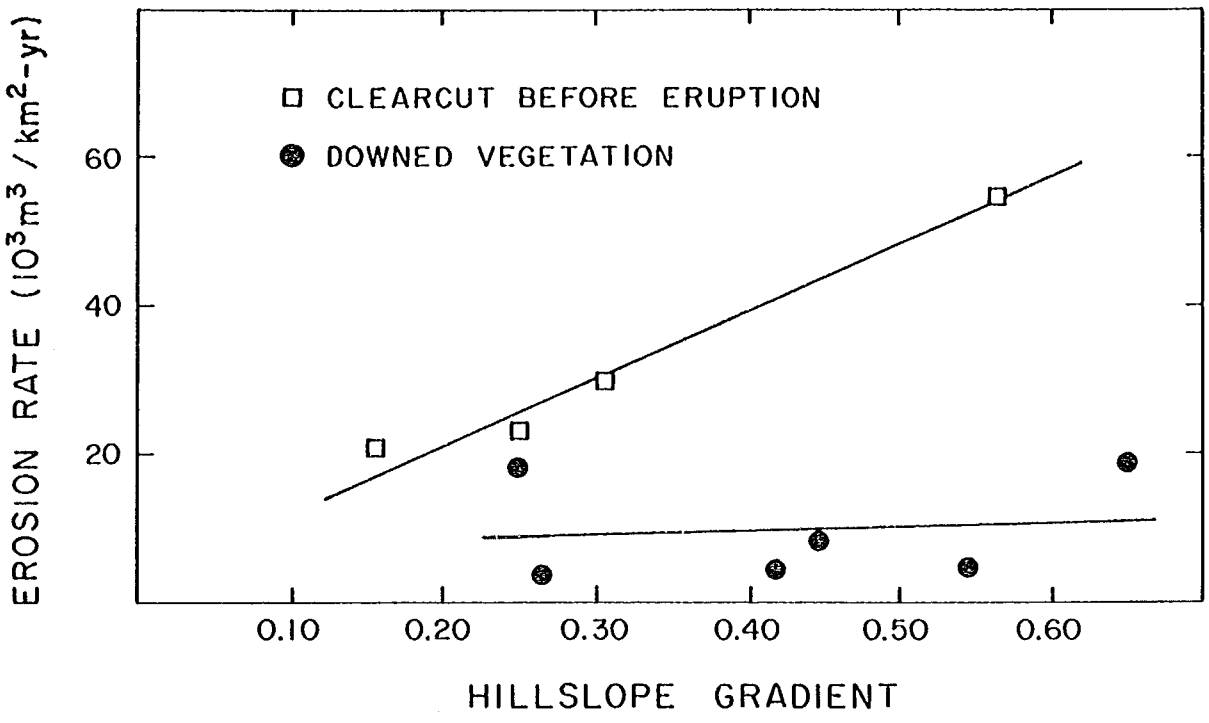


Fig. 4. Rate of rill erosion for May 18, 1980 - May 1981 vs. hillslope gradient for areas of silty surface and coarse pumice deposit at sites clearcut before the eruption with tephra greater than 15cm thick.

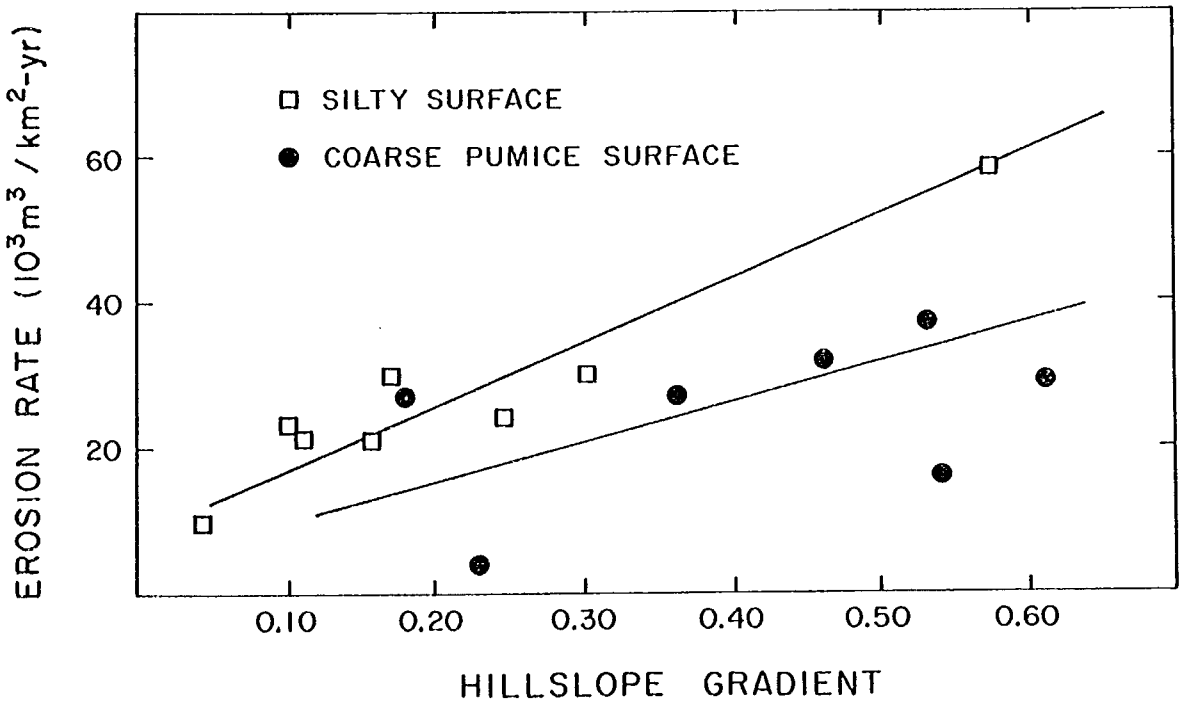


Fig. 5. Rate of rill erosion for May 1980 - May 1981 vs. hillslope gradient for sites in downed forest and areas clearcut before the eruption. All sites had silty surface and tephra deposits 15-30 cm thick.

Swanson and Wicherski (unpub. data) measured rill erosion on eight sets of paired plots located in the coarse pumice area northeast of the volcano. Each set consisted of adjacent plots in downed forest and pre-1980 clearcut. In each case, rill erosion through summer 1981 was lower on the plot with downed trees. The differences, however, varied from 10 to 800 percent and these differences had no relation to hillslope gradient.

Temporal Trends in Sheet and Rill Erosion

Rates of sheet and rill erosion have declined dramatically in the first 2 years after May 18, 1980. North and northwest of the volcano rill erosion in the second wet season was 5 percent of rill erosion in the first wet season and sheet erosion was 40 percent of that in the first wet season (Collins unpub. data). Overall surface erosion decreased 85 percent in May 1981-May 1982 compared with the previous year.

A plot of rill erosion divided by total precipitation versus time for seven sampling periods during the two years since the May 1980 eruption, reveals a clear decrease in rate of erosion by January 1981 on sites north and northwest of the volcano (Figure 6). This relationship describes relative erosion; that is, a given amount of rainfall in January 1981 caused much less erosion than during earlier periods. Absolute rates of erosion are still correlated positively with periods of precipitation sufficiently intense to generate overland flow. Sheet erosion exhibits a less dramatic decline (Figure 6).

Rapid rill development followed by a period of little change in erosional landforms is recorded in a sequence of photographs from a study site in the blast zone northeast of the volcano (Figs. 7 and 8). Here rill development was largely complete by January 13, 1981, and the volume and position of rills was modified little over the next 1.5 years.

The observed decline in erosion is consistent with observations by Herkelrath and Leavesley (1981) and Leavesley (pers. comm.) that infiltration rate increased between summer 1980 and summer 1981.

Furthermore, the surface became more resistant to erosion early in this period, as erosion exposed more permeable and less erodable underlying tephra and buried soil.

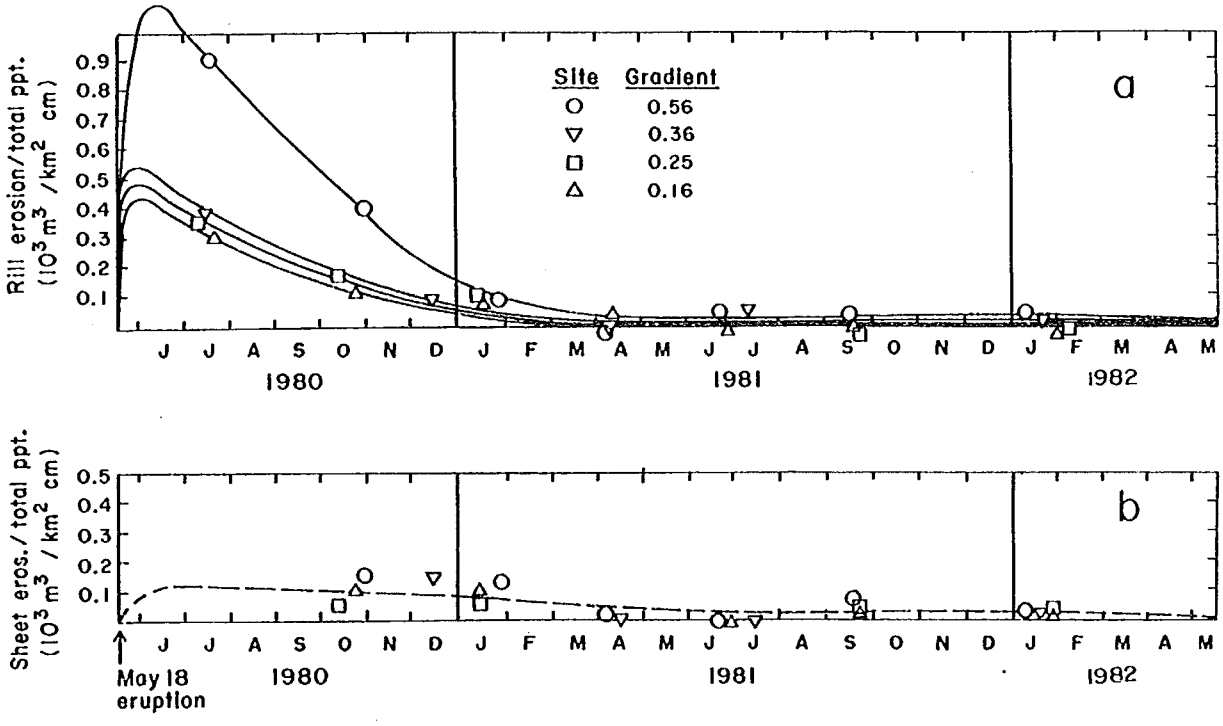


Fig. 6. Change in rates rill (a) and sheet (b) erosion per unit of total rainfall, on sites north and northwest of the volcano for seven period of measurement over two years beginning in May 1980. All sites were clearcut about 10 years before the 1980 eruptions.

Effects of Management Activities on Sheet and Rill Erosion

Various management activities have altered tephra deposits since the 1980 eruptions. Large areas were seeded with a mixture of grasses and legumes in the fall of 1980. Gently sloping hillsides were scarified in 1981, and downed trees have been removed from much of the western half of the blast zone since the fall of 1980. The seeding project had the primary goal of slowing sheet and rill erosion. The primary objective of scarification was the exposure of the soil layer beneath the 1980 tephra to facilitate planting of commercial tree species; the control of erosion was a secondary objective. Removal of downed trees had the purposes of salvaging timber value and returning forest land to tree

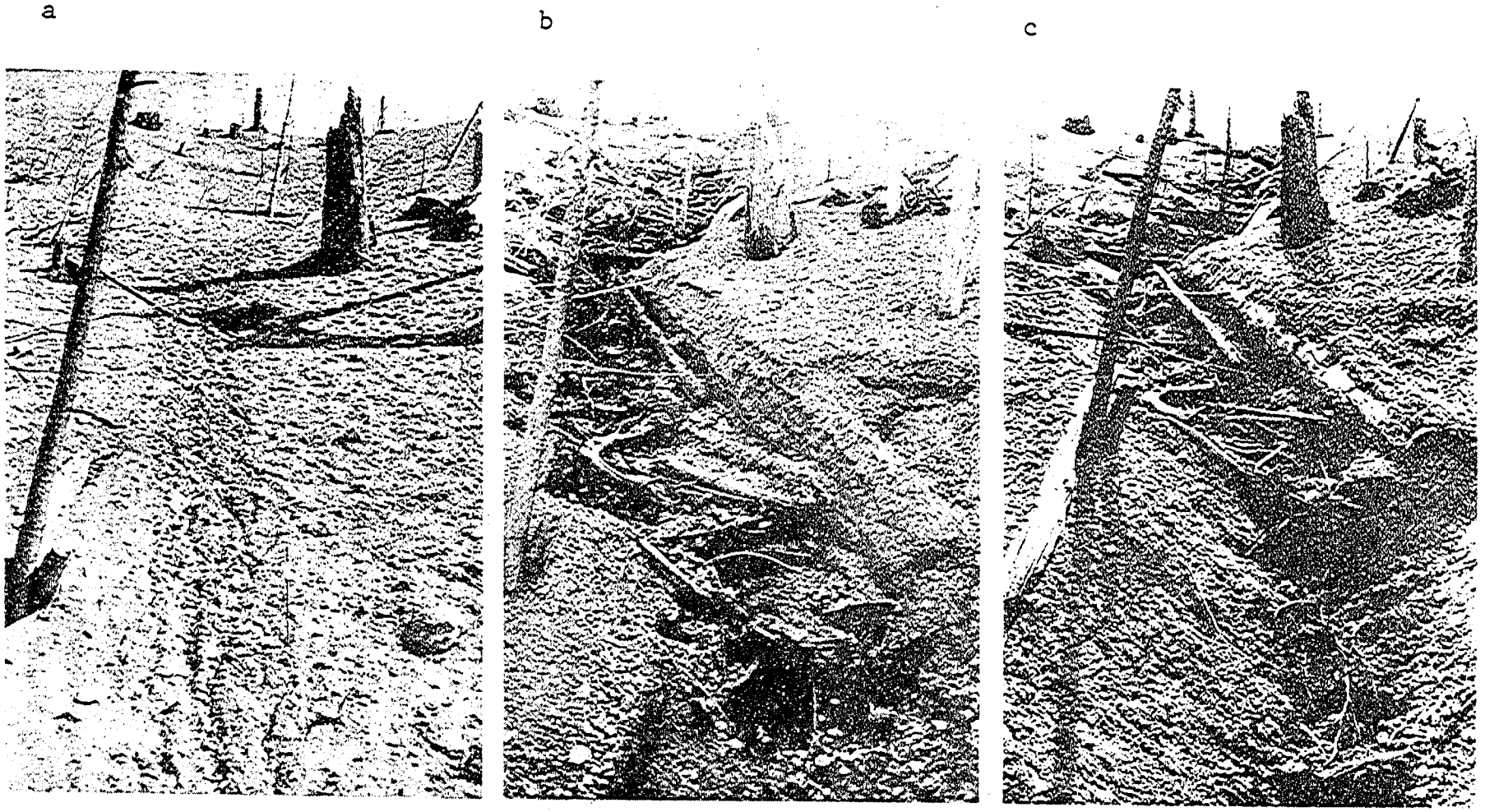


Fig. 7. Gully cut during the September 1980(a) to January 13, 1981(b) period and showing little change by June 1982(c). Downcutting stopped upon reaching woody debris on pre-eruption ground surface. Photo location is 8 km ENE of volcano where tephra thickness is 50 cm.



Fig. 8. Erosion over the same time period and at the same site shown in Figure 7.

production. Some logging programs were designed to minimize subsequent surface erosion. Although erosion control was not the primary purpose of all of these activities, we evaluate their effectiveness as erosion control measures in the following discussion.

Grass Seeding--Mixtures of grass and legume seed were applied with fertilizer to about 8260 ha of the blast zone in September and October 1980. Stroh and Oyler (1981) and Klock (1982) evaluated the cover of native and introduced species in May, June, and July 1981. Plant cover averaged about 70 percent (n=12) in one site favorable to grass establishment (thin tephra, steep slope, silty surface deposits, and elevation below 850 m) (Klock 1982), but in most sampled areas plant cover was less than 15 percent. Klock (1982) observed highest cover on slopes steeper than 0.50 where erosion had been most effective in removing the new tephra and exposing the relatively nutrient-rich pre-1980 soil surface.

Unfortunately no direct measurements have been made of the control of erosion by plants of various types and cover densities. However, most of the vegetation sampled in these evaluations was not present until Spring 1981 and in many areas of the blast zone plant cover was insignificant (Collins et al. 1982, McKee, et al. in press) during the May 1980-January 1981 period when sheet and rill erosion were most rapid.

Scarifying - - Private and state forest land managers scarified about 730 ha of forest land in 1981. Scarifying was confined to hillslopes north and northwest of Mt. St. Helens with gradients generally less than 0.30 and tephra thickness generally between 10 and 40cm. Scarifying was done with a tractor moving parallel to the land contours and pushing either a straight or a V-shaped blade designed for this purpose. The objective was to move tephra aside with minimum disturbance to the underlying soil, thereby facilitating reforestation efforts.

Scarification had three effects on erosion. Exposure of soil in the blade path and the mixing of coarse and fine tephra in the plowed berms at the side of the track increased infiltration. The infiltration rate

measured on one treated area in the Shultz Creek catchment was between 10 and 28mm/hr compared to a rate of 2 to 11mm/hr measured on adjacent, undisturbed tephra in spring 1981 (Fiksdal 1981). Trenching resulted in an irregular topography including numerous undrained depressions where water and sediment could collect, thus reducing runoff and net transport of sediment from hillslopes. Where tephra deposits are thick and revegetation is slow, scarification has promoted vegetative recovery. However, isolated instances of vehicle movement up and down slope lead to formation of discontinuous gullies.

Preliminary analysis of erosion pin measurements indicates that surface erosion from scarified areas between August-October 1981, when treatment occurred, and March 1982 was no more than erosion from adjacent, unscarified areas (Collins et al. unpub. data). Field observations indicate there has been very little sediment transport from scarified sites.

Salvage logging - - Timber knocked down by the May 1980 blast has generally been logged by tractor systems on slopes gentler than 0.30 and by cable yarding methods on steeper slopes. Salvage logging has mixed the more impermeable surface tephra with the underlying coarser tephra and soil, thereby increasing infiltration rates. Fiskdal (1981) measured an infiltration rate of 28mm/hr in a salvaged area with silty surface deposits where undisturbed tephra had rates of 2 to 11 mm/hr. Working in both areas with and without coarse pumice, Wicherski (unpub. data) observed a doubling of infiltration rate as a result of mixing of tephra deposits with a shovel. Actual salvage logging has the additional effect of creating microdepressions that can interrupt the flow of water downslope.

Collins et. al. (unpub. data) measured erosion from cable-yarded sites north of the mountain where tephra thickness is between 15 and 30cm. On each of three hillslopes, surface erosion subsequent to removal of downed trees was less than from hillslopes with comparable gradients and tephra thickness where downed trees were not removed. No measurements were made in areas where standing killed trees were removed. The generally thin tephra layer and abundant woody debris in the zone of the

standing, killed trees suggests, however, that removal of trees probably did not accelerate erosion in these areas.

Mass Erosion in the Blast Zone

The blast from Mt. St. Helens directly triggered mass movement of tephra and underlying soil and set the stage for increased mass movement in the future. Studies at other volcanoes suggest that three types of mass erosion processes might be promoted by the effects of volcanic eruptions: 1) shallow, rapid mass movements (debris slides, avalanches and flows of Varnes (1978)), 2) deeper-seated, slow moving (mm to m/yr) slumps and earthflows (Varnes 1978), and 3) creep which occurs at slow rates and without the development of a discrete failure surface.

We know of no direct monitoring of creep of fresh tephra or underlying soil in the blast zone and have observed no indirect indicators of creep such as the tipped tree trunks described at Paricutin (Segerstrom 1950). The sandy and gravelly texture of the tephra suggests that significant rheological creep common in more clayey materials is unlikely. Killing of vegetation and suppression of revegetation by scorching, uprooting of trees, and deposition of tephra, however, may accelerate creep in soil by decreasing root strength and evapotranspiration. The resulting increase in soil moisture levels may accelerate creep of buried soils.

Slumps and earthflows in soil and colluvium cover about 1.4 percent of the 117-km^2 area of the upper Green, Quartz, Smith, Bean, and Clearwater Creeks drainage basins in the zone of downed vegetation (Figure 9). Based on interpretation of freshness of landforms produced by mass movement, activity of these features range from currently active to long dormant, As a result of volcanic events, slumps and earthflows can accelerate, decelerate, reactivate, or remain dormant. The reactivation of large mass movements by erosion of the toe of these features by repeated mudflows, as described by Waldron (1967) at Irazu, has not occurred at Mt. St. Helens. Mt. St. Helens produced major mudflows on May 18 only. These lahars moved down steep channels cut in hard, erosion-resistant bedrock or down channels with moderate to low

slope gradient where little erosion occurred. Northeast of the volcano, channel incision by more typical fluvial processes has not significantly accelerated mass movement, but lateral channel cutting has caused slope failures north and northwest of the mountain. At some locations, channel aggradation associated with the 1980 eruptions may buttress and temporarily stabilize the toe of hillslopes and earthflows.

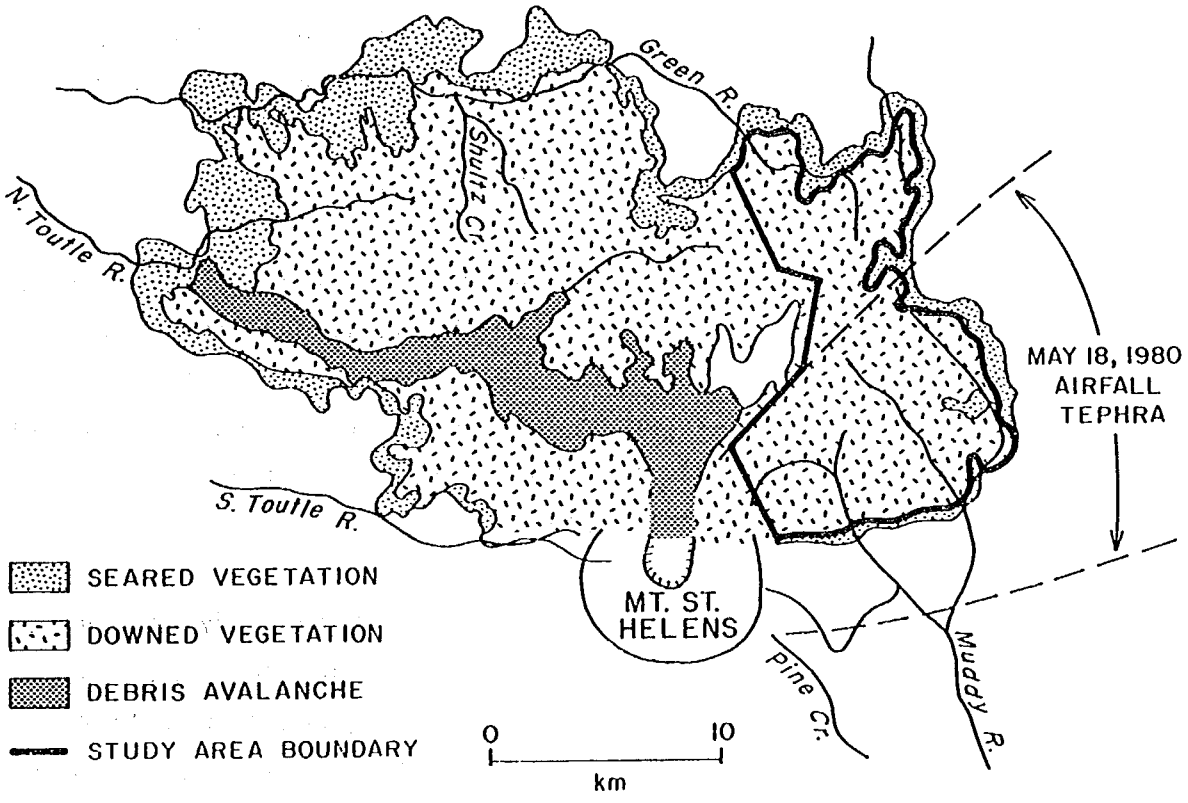


Fig. 9. Location of debris slide inventory.

The loss of live vegetation in the blast zone may lead to accelerated or reactivated earthflow movement as a result of reduced evapotranspiration and increased soil moisture. Studies elsewhere in the region demonstrate that the rate of earthflow movement increases with increased water availability during individual storm events and over the wet season (Swanson et al. 1980). Conditions of reduced evapotranspiration are likely to persist for decades because plant recovery is slowed by the deposits of nutrient-deficient tephra on the ground surface (McKee,

et al. in press). However, the degree to which evapotranspiration affects large, slow-moving mass failures has not been quantified. Some of the reduction in evapotranspiration from a site may be partially compensated for by a reduction in the infiltration rate of the hillslope surface.

Shallow, rapid mass movements, hereafter referred to as debris slides, are common in steep mountain terrain such as the areas surrounding Mt. St. Helens. Numerous researchers have argued that reduced tree root strength following clearcutting results in increased debris sliding. Conditions within the blast zone at Mt. St. Helens present an interesting point of comparison with the case of clearcutting.

We mapped debris slides in areas of downed vegetation and pre-eruption clearcuts in the upper Green, Quartz, Smith, Bean, and Clearwater Creeks drainage basins (Fig. 9). Mapping was based on interpretation of four sets of aerial photographs taken in June-August 1967 (scale = 1:15840), 1979(1:12000), 1980 (1:24000), and 1981 (1:24000). Sites were field checked by aerial reconnaissance only.

Occurrence of slides before 1980 was estimated by identifying events that occurred between 1967 and 1979 (Table 1). The study area is mantled with Holocene tephra deposits generally greater than 30cm thick. Although other sites of debris slide inventories in the Pacific Northwest lack such thick tephra-derived soils, the frequencies of debris slides in clearcuts and road rights-of-way in this study area (Table 1) are very similar to frequencies observed in three studies in the Western Cascades of Oregon (Morrison 1975, Swanson and Dyrness 1975, Marion 1981). The frequency of debris slides in forest areas is about an order of magnitude lower at the Mt. St. Helens site than in the Oregon sites partly because forest cover obscures features examined from aerial photographs only. The Oregon studies included field searches for debris slide scars in forested areas.

Table 1. Number and frequency of debris slides observed in aerial photographs for three time periods in upper Green, Quartz, Smith, Bean, and Clearwater Creek basins where the 1980 eruption downed vegetation.

	Area	1967-1979		1979-1980		1980-1981	
	(km^2)	(a)	(b)	(a)	(b)	(a)	(b)
Forest/downed vegetation	83.2	2	0.002	18	0.28	16	0.19
Clearcut before 1980	30.8	26	0.07	1	0.033	0	0
Road right-of-way	3.7	48	1.08	0	0	3	0.81
	117.7						

a. Number of events

b. Number of events per km^2 per year

Most debris slides identified in June 1980 photographs but absent in 1979 appear to have been triggered by groups of trees blown off steep slopes with shallow soils during the directed blast on May 18. Twenty-three of 24 debris slides identified in the photographs began in areas of downed forest at a frequency of occurrence two orders of magnitude higher than the 1967-1979 rate in live forests (Table 1). Only one event occurred in a clearcut area and no slides occurred along roads, perhaps reflecting the low precipitation intensities during the 1979-1980 wet season before the May 18 eruption which so dramatically altered hillslope hydrology.

During the 1980-1981 wet season, another 16 debris slides originated in downed forest while only three failures took place in areas clearcut or in roads before the eruption. Several factors may have been responsible. Areas previously stabilized by roots may have become more sensitive to failure because of reduced contribution of tree roots to soil strength. Root strength was

lost by decomposition of root of trees whose root systems remained in the ground but were killed during the blast and by removal of roots from the soil where rootwads were ripped from the ground by the blast. To estimate the relative importance of these causes of lost root strength, we sampled 50 to 75 tree stems greater than 10 cm diameter at breast height (DBH) at the heads of debris slide scars. DBH is strongly correlated with root biomass (Santantonio et al. 1977). We use the percent of cumulative DBH of each sample that is accounted for by root-thrown trees as a measure of the proportion of total root strength lost as a result of removal of root systems from the soil. Root systems of trees killed but left standing by the blast lose strength by slow decomposition. At the 4 study sites, 57 to 76 percent of cumulative DBH was root thrown, suggesting that a large component of root strength was lost by removal of roots from the soil during the blast. A confounding factor is that low infiltration rates of new deposits, particularly during early fall storms, increased overland flow at the expense of high groundwater levels that trigger slides.

Another common type of mass movement occurred where fresh tephra deposited on bare slopes steeper than about 0.70 immediately slid to the base of the slope--commonly below bedrock exposures, road cuts, and sides of v-notch channels. These sites cover about 5 percent of the North Fork Toutle and Green River basins in the blast zone (Lehre et al. 1982).

Hillslope Erosion in Zones of Seared Vegetation and Airfall Tephra

Few plots to measure erosion have been established outside the zone of downed vegetation. This is unfortunate because on a global scale airfall tephra is a much more widespread phenomenon than laterally directed blasts. The zone of downed vegetation at Mt. St. Helens, however, presents greater hillslope erosion problems, particularly with respect to forest management and downstream hydrologic hazard, than the zones of seared vegetation and airfall tephra in live forest.

Both reconaissance observations and direct measurements reveal very low rates of erosion of tephra in the zone of seared vegetation (Table 2). Rill and sheet erosion appear to be much lower than in the zone of downed vegetation because a dense mat of needles from killed trees forms a protective layer on the surface of the new tephra in much of the zone of seared vegetation. The needles have been mixed with the surface tephra by raindrop splash and the simultaneous fall of dead needles and tephra from the forest canopy

Table 2. Measured rates of sheet (summer 1980-summer 1981) and rill (May 18, 1980- summer 1981) erosion in areas of seared vegetation and airfall tephra. All plots in airfall tephra are located 22 km east-northeast of the volcano.

Study Site	Sheet Erosion ($10^3 m^3/km^2$)	Rill Erosion ($10^3 m^3/km^2$)	Slope Gradient	Deposit Thickness (cm)	Presence of Coarse Pumice Airfall
Seared Vegetation					
R1		0.5	0.18	18	No
R2		0	0.60	6	No
HV		0.4	0.55	19	Yes
HF	0*	0.5*	0.45	8	No
Airfall Tephra					
1977 Clearcut	3.8	1.9	0.55	10	
1951 Clearcut	5.0	0.2	0.19	10	
Forest	2.0	0	0.73	10	

*May 1980 - February 22, 1981, approximates annual rate (Collins et al. 1982)

in the months following the May 18, 1980, eruption. This mixture forms a rough surface that retards overland flow and surface erosion. Erosion in areas of airfall tephra deposits outside the blast zone has been examined in detail at only one site. In this area, where 10 cm of the May 18 airfall tephra fell, the rate of sheet erosion in a mature forest was about half the rate from plots in two adjacent clearcuts (Table 2). Rates of rill erosion between May 18, 1980, and summer 1981 were neglible on the forest plot on steep slope and in a 1961 clearcut (Table 2). Rill erosion from a steep area clearcut in 1977 was only about five percent of the rate for a site with the same slope gradient and coarse pumice airfall tephra in the zone of downed vegetation.

The rate of erosion of airfall tephra outside the blast zone is a function of deposit thickness, texture, and vegetation cover. Even the thickest airfall units, those of the May 18 eruption deposited northeast of the volcano, are in many areas thinner than the combined thickness of airfall and blast deposits within the blast zone. Consequently rill erosion is restricted by the thinness of readily eroded tephra. Thin deposits also allow the microtopography of downed logs and other features of the pre-eruption ground surface to shape the surface of tephra deposits, thus forming obstructions to flow and sediment transport. Live vegetation outside the blast zone is also important in reducing erosion by intercepting rainfall and supplying litter to the tephra surface. The litter layer under live forest, however, is not as well developed as under the seared forest where practically the entire needle complement fell within the first year after the eruption. Where tephra less than several centimeters thick fell in forested areas, it was quickly incorporated into the forest floor.

Changes in Hillslope Erosion at Mt. St. Helens Over the First Decade

Rates of erosion of hillslopes close to Mt. St. Helens have been dramatic over the first 2 years since the major eruption on May 18, 1980. Great changes in the rates and geographic patterns of erosion processes are likely to occur over the decade of the 1980's due to biological and physical factors that are natural or the result of efforts by man. Here we speculate, assuming no further volcanic

effects, on the possible course of such changes in the zone of downed vegetation where rates have been greatest.

We suspect that natural physical factors will be the dominant control of changes in erosion rates from hillslopes in the first decade after the eruption. Influences of naturally re-established plants and man's intentional or inadvertent effects on hillslope erosion may be of secondary importance. It is important to consider each erosion process separately, because the timing of the importance of physical and biological controls varies among the erosion processes involved.

Rates of sheet and rill erosion have peaked and declined before revegetation was widespread. This finding parallels the observations by Ollier and Brown (1971) at Vulcan and Hendrix (1981) at Fernandina that rill and gully erosion was largely completed in the first few years after tephra deposition and in advance of significant revegetation.

Both residual woody debris and live plants provide some stability for fresh tephra, but where deposits are less than a meter thick, live and dead plant material is more effective in reducing erosion of underlying soil. Natural plant recovery in the blast zone over the first 2 years following the May 18, 1980, eruption has been dominated by residual plants emerging from snow-protected sites and especially by plants sprouting from buried plant parts (McKee et al. in press, Stevens et al., in press). Recovery from roots and rhizomes is most prevalent where new deposits are less than 30cm thick, particularly where erosion has exposed soil. Under these conditions plants protect the underlying soil from surface erosion much more effectively than the new tephra, as Segerstrom observed at Paricutin. Revegetation from natural seeding after the eruption has been spotty, in part because seed is blown over the relatively smooth surface to catch in localized depressions. In addition, establishment is difficult because of extremes in temperature and moisture conditions of tephra and because of its poor nutrient status. Establishment of enough native vegetation to significantly suppress erosion of new deposits may occur in 3 to 5 years after the 1980 eruption on favorable sites and not for decades where windblown sand and other environmental factors severly limit seed catch,

germination, and plant growth. Wind swept surfaces of the pyroclastic flow deposit erupted in 1912 in the vicinity of Mt. Katmai, Alaska, are still sparsely vegetated (J. Means, pers. comm.).

Woody litter at the surface of the old soil and roots within it retard downcutting of rills and gullies below the base of the 1980 tephra deposits (Fig. 7). Although woody debris on the surface and within fresh tephra retards erosion of tephra to some extent, the continuous mat of organic matter in the upper part of the underlying soil is a more effective barrier to deeper incision of small channels. Establishment of vegetaton in rill floors, reduction of runoff from adjacent slopes, and raveling of rill and gully walls appear to be leading to filling in of rills and gullies.

Occurrence of debris slides may peak several years after the vegetation was toppled and killed. Studies of declining root strength and incidence of debris slides as a function of time since clearcut logging (summarized in Swanston and Swanson 1976) indicate that debris slides are concentrated several years after clearcutting when there has been sufficient time for loss of strength by root decomposition and before new plants have supplied a full complement of root strength. The cover of fresh tephra will suppress revegetation, causing more pronounced and prolonged loss of root strength than in the case of clearcutting. However, the important immediate loss of root strength caused by uprooting of trees during the blast has lead to substantially increased frequency of debris slides in the first few years after the 1980 eruptions. Debris slide erosion may peak and then decline after the most unstable sites have failed, but before revegetation and its contribution to root strength are significant, even in ares where trees have been planted.

Predicting rates of erosion by slumps and earthflow activity in the blast zone is far more speculative. Reduced evapotranspiration because of loss of plant cover may result in higher groundwater levels and accelerated or reactivated deep-seated mass movement, but this has never been quantified.

Comparison Among Volcanic Areas

The four volcanoes where rates of sheet, rill, and gully erosion of tephra have been determined for the first few years after an eruption all exhibit average surface lowering rates between about 25 and 100 mm/yr (Table 3). Erosion in the blast zone and area of coarse airfall tephra at Mt. St. Helens is the lowest of the four areas in terms of rate of removal and percent of new deposits removed. This may reflect lower precipitation intensities and thinner and coarser textured deposits at Mt. St. Helens. The pattern of a rapid decline in erosion rate within the first 2 to 5 years post-eruption is common to Mt. St. Helens, Vulcan, Irazu, and Fernandina; Segerstrom (1961) describes a more gradual decline at Paricutin.

Table 3. Summary of erosion rates at Paricutin (Segerstrom 1950), Irazu (Waldron 1967), Vulcan (Ollier and Brown 1971), and Mt. St. Helens (this paper).

Volcano	Deposit Type	Processes	Erosion Rate (mm/yr)	Deposit Removed (percent)	Period of Record (yrs)
Paricutin (Mexico)	Airfall	Sheet, Rill	55	48	4
Irazu (Costa Rica)	Airfall	Sheet, Rill	50-80	30-50	1
Vulcan (New Guinea)	Cindercone	Rill, Gully	105	--	5
Mt. St. Helens (USA)	Blast Airfall	Sheet, Rill	25	8	2

SUMMARY

Rates of erosion of fresh tephra from hillslopes are extremely variable. Steep slopes, thick deposits, fine textured deposits, and lack of vegetation and organic debris favor high rates of sheet and rill erosion. Sheet and rill erosion rates in the zone of downed vegetation at Mt. St. Helens averaged about 25 x $10^3 m^3/km^2$-yr (25 mm/yr) in the first year after the May 18, 1980, eruption. Rates were substantially lower in the area of airfall tephra and in the zone of seared vegetation. In the zone of downed vegetation rill and sheet erosion rates decreased markedly after 1980 as a result of formation of a more permeable, less erodable surface.

The directed blast appears to have immediately triggered debris slides from steep slopes with very shallow soils. Debris slides in the first wet season after the main eruption occurred mainly in areas of downed forest vegetation. Loss of root strength by uprooting of trees during the blast appears to be an important cause of increased frequency of debris slides in these previously forested areas. Between May 18, 1980 and July 1981 slides from roads and areas clearcut before the eruption occurred at a much lower rate east and northeast of the mountain than over the 1967-1979 pre-eruption period.

Slumps and earthflow landforms cover about 1.4 percent of the drainages in the zone of downed vegetation east and northeast of the mountain. Altered hillslope hydrology, particularly reduced evapotranspiration, and elevation of stream beds may cause acceleration or deceleration of these features. No signs of accelerated creep have been observed.

Revegetation in most areas of the zone of downed vegetation did not stabilize tephra in the first year after the eruption. Removal of readily eroded material, formation of a stable surface layer of coarse particles, exposure of woody material at the soil surface and increased infiltration due to exposure of coarser tephra and the underlying soil caused a dramatic decline in surface erosion before revegetation was significant.

Salvage logging and scarification of hillslopes have generally reduced surface erosion rates.

The general pattern of a high initial rate of sheet and rill erosion followed by a rapid decline observed at Mt. St. Helens has been described for areas affected by eruptions of several other volcanoes.

LITERATURE CITED

Collins, B., T. Dunne, and A. K. Lehre. 1982. Sediment influx to the Toutle River from erosion of tephra, May 1980 - May 1981. In: Proc., Conf. Mt. St. Helens: Effects of Water Resources, Washington State Univ. Press, Pullman, Wash., p. 82-97.

Dietrich, W. E., and T. Dunne. 1978. Sediment budget for a small catchment in mountainous terrain. Zeit. fur Geomorph. Suppl. Bd. 29, 191-206.

Eggler, W. A. 1959. Manner of invasion of volcanic deposits by plants with further evidence from Paricutin and Jorullo. Ecological Monographs 29:267-284.

Eggler, W. A. 1963. Plant life of Paricutin Volcano, Mexico, eight years after activity ceased. The American Midland Naturalist 69(1):38-68.

Fiksdal, A. J. 1981. Infiltration rates of undisturbed and disturbed Mt. St. Helens ash. Abs. for Ann. Mtg., Assoc. Eng. Geol., Portland, Oreg., Sept. 27 - Oct. 2, 1981, p. 34.

Griggs, R. F. 1918. The recovery of vegetation at Kodiak. Ohio J. Sci. 19(1):1-57.

Hendrix, L. B. 1981. Post-eruption succession on Isla Fernandina, Galapagos. Madrono 28(4):242-254.

Herkelrath, W. N., and G. H. Leavesley. 1981. Physical properties of volcanic ash from Mt. St. Helens - relationship to rain infiltration experiments. abs. Agronomy Abs., p. 141.

Hoblitt, R. P., C. D. Miller, and J. W. Vallance. 1981. Origin and stratigraphy of the deposit produced by the May 18 directed blast. U.S. Geol. Surv. Prof. Paper 1250. p. 401-419.

Karlin, R., 1980. Sediment sources and clay mineral distributions off the Oregon Coast. Jour. Sed. Pet. 50(2):543-560.

Klock, G. O. 1982. Stabilizing ash-covered timberlands with erosion control seeding and fertilization. In: Proc. Conf., Mt. St. Helens: Effects on Water Resources, Washington State Univ. Press, Pullman, Wash.

Larson, K. R., and R. C. Sidle. 1980. Erosion and sedimentation data catalog of the Pacific Northwest. U.S.D.A. Forest Service, Pacific Northwest Region. Portland, Or. 64 p.

Lehre, A. K., B. Collins, and T. Dunne. 1982. Preliminary post-eruption sediment budget for the North Fork Toutle River drainage, June 1980 - May 1981. In: Proc. Mt. St. Helens: Effects on Water Resources, Washington State Univ. Press, Pullman, Wash. p. 215-234.

Lipman, P. W., and D. R. Mullineaux. 1981. The 1980 eruptions of Mt. St. Helens, Washington. U.S. Geol. Surv., Prof. Paper 1250. 844 p.

Marion, D. A. 1981. Landslide occurrence in the Blue River drainage, Oregon. M. S. thesis, Oregon State Univ., Corvallis, Oregon. 114 p.

McKee, A., J. E. Means, W. H. Moir, and J. F. Franklin, in press. First-year recovery of upland and riparian vegetation in the devastated area around Mt. St. helens. In: The biological effect of the Mt. St. Helens eruption, D. E. Bilderback (ed.), Amer. Assoc. Adv. Sci.

Moore, J. G. and T. W. Sisson. 1981. Deposits and effects of the May 18 pyroclastic surge. U.S. Geol. Surv. Prof. Paper 1250. p. 421-438.

Morrison, P. H. 1975. Ecological and geomorphological consequences of mass movements in the Alder Creek watershed and implications for forest land management. B. A. thesis, Univ. of Oregon, Eugene, Oregon. 102 p.

Ollier, C. D., and M. J. F. Brown. 1971. Erosion of a young volcano in New Guinea. Zeit. for Geomorph. N. F. B and 15(1):12-28.

Reid, L. M. 1981. Sediment production from gravel-surfaced forest roads, Clearwater basin, Washington. Final Report. FRI-UW-8108. Fisheries Research Inst., Univ. Washington, Seattle. 247 p.

Santantonio, D., R. K. Hermann, and W. S. Overton. 1977. Root biomass studies in forest ecosystems. Pedobiologia 17:1-31.

Segerstrom, K. 1950. Erosion studies at Paricutin, State of Michoacan, Mexico. U.S. Geol. Surv. Bull. 965-A. 165 p.

Segerstrom, K. 1960. Erosion and related phenomena at Paricutin in 1957. U.S. Geol. Surv. Bull. 1104-A. p. 1-18.

Segerstrom, K. 1961. Deceleration of erosion at Paricutin, Mexico. U.S. Geol. Surv. Prof. Paper 424-D. p. D225-D227.

Segerstrom, K. 1966. Paricutin, 1965 - Aftermath of Eruption. U.S. Geol. Surv. Prof. Paper 550-C. p. C93-C101.

Stevens, R. G., R. R. Gilchrist, and J. K. Winjum. In press. Revegetation of recent clearcuts during summer and fall 1980 in the western portion of the Mt. St. Helens devastation zone. In: The biological effect of the Mt. St. Helens eruption. D. E. Bilderback (ed.). Am. Assoc. Adv. Sci.

Stroh, J. R. and J. A. Oyler. 1981. SCS seeding evaluation on Mt. St. Helens. USDA Soil Conservation Service. Spokane, Wash., 15 p.

Swanson, F. J., and C. T. Dyrness. 1975. Impact of clearcutting and road construction on soil erosion by landslides in the western Cascade Range, Oregon. Geology 1(3):393-396.

Swanson, F. J., R. L. Fredriksen, and F. M. McCorison. 1982. Material transfer in a western Oregon forest ecosystem. In: Analysis of coniferous forest ecosystems in the western United States. R. L. Edmonds (ed.), Hutchinson and Ross, Inc., Stroudsburg, Pa. p. 233-266.

Swanson, F. J., R. D. Harr, and R. L. Fredriksen. 1980. Geomorphology and hydrology in the H.J. Andrews Experimental Forest, western Cascades. In: Geologic field trips in western Oregon and southwestern Washington, Ore. State Dept. Geol. and Min. Ind., Bull. 101, p. 217-232.

Swanston, D. N., and F. J. Swanson. 1976. Timber harvesting, mass erosion, and steepland forest geomorphology in the Pacific Northwest. In: Geomorphology and engineering, D. R. Coates (ed.). Dowden, Hutchinson, and Ross; Stroudsburg, Pa., p. 199-221.

Varnes, D. J. 1978. Slope movement types and processes. In: Landslides analysis and control. R. L. Schuster and R. J. Krizek (eds.) Spec. Rep. 176, Transportation Res. Brd., Nat. Acad. Sci., Washington, D.C., p. 11-33.

Voight, B., H. Glicken, R. J. Janda, and P. M. Douglass. 1981. Catastrophic rockslide avalanche of May 18. U.S. Geol. Surv. Prof. Paper 1250, p. 347-377.

Waitt, R. B. 1981. Devastating pyroclastic density flow and attendant airfall of May 18 - stratigraphy and sedimentology of deposits. U.S. Geol. Surv. Prof. Paper 1250. p. 439-450.

Waitt, R. B. and D. Dzurisin. 1981. Proximal airfall deposits from the May 18 eruption - stratigraphy and field sedimentology. U.S. Geol. Surv. Prof. Paper 1250. p. 601-616.

Waitt, R. B., V. L. Hansen, A. M. Sarna - Wojcicki, and S. H. Wood. 1981. Proximal airfall deposits of eruptions between May 24 and August 7, 1980 - Stratigraphy and field sedimentology. U.S. Geol. Surv. Prof. Paper 1250. p. 617-628.

Waldron, H. H. 1967. Debris flow and erosion control problems caused by the ash eruptions of Irazu Volcano, Costa Rica. U.S. Geol. Surv. Bull. 1241-I. 38 p.

Erosion control works in Nikko volcanic area

YOSHINORI TSUKAMOTO
Department of Forestry, Tokyo University of Agriculture and Technology

KOOZOO KOMORI
Nikko Sabo(erosion control) Works Office, Ministry of Construction

MASAO KAWABATA
Erosion Control Section, Maebashi Regional Forest Office, Forest agency, Ministry of Agriculture,Forestry and Fishery

ABSTRUCT

Volcanos in Nikko area are composed of mountains of different ages. Mt. Nantai is the youngest, while Mt.Nyoho-Akanagi, from which Inari torrent originates, belongs to an old era. The former discharges debris from the gullies on the hillslopes, and the latter discharges its sediments through a torrent. Nikko area is proud of the longest history of erosion control practices. The writers tried to show two examples of erosion control practices in Nikko area as being a representative of an inactive volcanic area. As for Mt. Nantai, erosion control works have been practiced by fixing the gully cliffs, stabilizing the talus slopes with hillside works and the gully beds by stepwise check dams. In the case of Inari torrent, high sabo dams on the middle reach and channel works on the lower reach are the two major erosion control works.

INTRODUCTION

Basically, three vulnerable regions in Japan,such as the geologically fractured zones along large faults, volcanic areas and deeply weathered granite areas,are important and well known from the viewpoint of sediment yield and disaster by debrisflow. Among them, volcanic areas are the most important becauseof their high potentials of debris discharge as well as their wide distribution throughout the country. Erosion control works have long been carried out in many volcanic areas. Recently, tourism has accerelated developments in these volcanic areas as resort areas, hotels etc are being built. The activity of tourism has brought about an increase in susceptibility to disaster, and hence acts potentially as an agent of disaster from a social aspect. Because of their inherent dangers, the importance of volcanic areas have increased remarkably in Japan during the past decade.

In this paper, the writers present two examples of erosion control works in Nikko volcanic area which has several features such as holding the longest history of erosion control practices in Japan harbouring the famous national park and having the historic Nikko city and Toshogu shrine in it.

CLASSIFICATION OF VOLCANOES

The writers classify the volcanoes which actively produce sediments into two types, gully and torrent types, from the viewpoint of debris producing patterns. Each is further sub-divided into two groupes.

I : Gully type

This type appears mostly at the initial stage of volcanic erosion. A typical gully of this type can be seen on the hillslope of a coniede

type volcano. In most cases, ten to twenty large gullies develop on the hillslope around a volcano, where the original volcano slope still remains widely. The gully shapes are simillar, when it is expressed by the term of (width/length) of a gully. The gully beds, usually covered with the mixed materials from large rock blocks to pyroclustic rocks, seldom have surface water. The gully discharges much sediment periodically mostly in the form of debris flow. The recurrence period of discharge varies widely. Some gullies discharge very frequently, once in one or two years, while others have a wider frequency.

I-A: Active gully. This gully has a short recurrence period of sediment discharge. An example of this type is the gully which is now developing on the new slope covered with the deposits of recent eruption. All slopes and cliffs in the gully contribute actively to debris production. Mt. Yake is a wellknown example of this type, the slopes of which are covered by volcaniclastic detritus in Taisho eruption(1959). Another example is the gully on an active volcano which supplies frequently its debris as falling ash, as is the case with Mt.Sakurajima. A gully of this type develops a fan very rapidly on the footslope by frequent discharge of sediment.

I-B: Dormant gully. This has a longer recurrence period. Debris production in this gully is rather inactive and it takes a fairly long period of time to accumulate debris enough to discharge or to cause new landslides on the slope. This gully discharges sediment once in several decades or so. Many parts of the slopes and cliffs in this gully are covered with vegetation. Therefore, the gully seems to be very stable superficially. Only at the time of an extraordinary storm with large

recurrence period do stored debris in the gully become movable. The fan at the gully foot is rehabilitated and sometimes utilized. The sudden, unpredictable attack by debris flow makes the disaster serious. Mt. Yotei would be regarded as an example of this type. Mt. Nantai seems to locate nearly in the middle between I-A and I-B.

II : Torrent type

This type appears in the latter stage of volcanic development. A valley is united with the crater or the caldera of a volcano. A steep torrent runs out of the crater. The debris produced in the crater or in the head region of the torrent is discharged periodically. The amount of sediment discharged by a storm is far greater than that of the gully type. A torrent type of gully can also be divided into two groupes, according to the difference in amount of debris production in the head regions.

II-A: Debris production by rockfalls and debris slides. The surrounding steep cliffs of the crater recede mainly by rockfalls or by debrisslides. as the surface weathering advances. These rocky materials accumulate in the source area of a torrent. A heavy storm transports periodically the accumulated sediment down through the torrent as a debrisflow. Inari torrent would be an example of this type. A torrent of II-A type has always the liability to change to II-B type.

II-B: Debris production by a single huge slump slides. In volcanic areas, most rocks on the cliffs of a crater or a caldera are rotted by volcanic activity and subsequent weathering. This weakens the stablity of the slope and causes sometimes a huge slumpslide. Once this happens, the tremendous amount of debris runs down the torrent.

Furthermore, the slided mass, much of which remains in the head region, is discharged frequently and devastates the torrent for many years. The debris production of this type brings about the most serious disaster in the lower reach. The huge landslide at the head of Joganji torrent in 1858 and Urakawa torrent in 1911 are typical examples.

In addition to the above, landslides associated directly with volcanic activity itself do occur, though very rarely, such as Mt.Bandai in Fukushima and Mt. Mayuyama in Simabara. These slides are tremendously huge in scale just like Mt. Saint Helens .

GENERAL DESCRIPTION OF EROSION CONTROL WORKS IN A VOLCANIC AREA

A devastated sediment discharging basin is divided into three areas for the convenience of explanation. Erosion control works in volcanic areas now under practice in Japan have a close association with this zoning of a basin. This zoning is applicable to any basins, even to a small gully, of which the whole area is regarded as a debris producing area.

Debris producing area(Upper basin): This is the uppermost source area of a basin which contributes to the production of debris mainly by rockfall, debrisslides and slumpslides. Erosion control works in this area are: a) Stabilizing the unstable weathered materials on the slope at the origin by coating the surface or by hillside works, b) Stabilizing the debris deposits at the head of a torrent by stepwise check dams.

Sediment transporting area (Middle reach): The middle reach of a torrent contributes mainly to the transportation of the sediments. The topographical steepness in an upper basin impedes the practice of erosion control works in many devastated basins. This increases the importance

of a middle reach in checking sediment discharge. The main erosion control work is the construction of high sabo dams or middle-sized sabo dams to control sediment discharge quantitatively and qualitatively. "Qualitatively" as use in this context means the ability of a sabo dam to sort gravels, retaining the larger gravels and instead washing the smaller ones down, and to change the transporting form of sediments from debris flow(massive transport) to tractive load(individual transport).

Sediment depositing area (Lower reach): This is the downstream reach and the surrounding areas where degradation of a torrent gradient causes a decrease in the tractive force of storm water and induces the deposit of sediments, which form special topographical features such as small steep fans, lower flood terraces and the creation of channel fluctuations. Erosion control works are: a) Banking or constructing levees to stabilize the channel course and as a means of checking the fluctuation of flood water, b) The construction of drop works and ground sills to create a stable flood flow without deposition and without scouring on the channel bed.

OUTLINE OF NIKKO AREA

Nikko area consists of a number of volcanoes. In this paper, the writers will deal mainly with a limited area of Nikko, the southeast slopes of Mt. Nantai and the eastern part of Mt.Nyoho and Mt.Akanagi which are the head region of Inari torrent(Fig. 1). A cross sectional profile of the above named volcanoes is shown in Fig 2. Among the tree, Mt.Nantai is the youngest and Mt.Nyoho-Akanagi is the oldest as shown in Fig.3. Gullies on the southeast slopes of Mt.Nantai are

shown in Fig. 4. The basin of Inari torrent is shown in Fig. 5.

PRACTICE OF EROSION CONTROL WORKS IN THE GULLIES OF MT.NANTAI

According to the previous classification, Mt.Nantai belongs to I-B type. Mt.Nantai has nearly 12 devastated gullies, which discharge debris periodically as debris flow when rainfall exceeds a certain limit. Some of these gullies distribute on the southeast and southern sections, where Chuzenji town and important hotels and roads are located.

History of debris flow from the gullies[1)]

Until recent years, little information about debris yield on Mt. Nantai was available. This comes from the fact that there was nothing except several shrines.

1683: A huge landslide occurred in Oonagi gully as a result of an earthquake(in May). It is said that the present shape of Oonagi gully was formed by this slide. In July, a heavy storm attacked this area and caused a number of landslides and debris flow.

.....

.....Unknown.

.....

1902: Kannon gully was formed newly by a huge landslide and debris flow during a typhoon storm.

1949: A new gully appeared on the eastern slopes of Mt.Nantai

1966: A debris flow occurred in Furunagi gully.

1974: A debris flow took place in Maenagi gully.

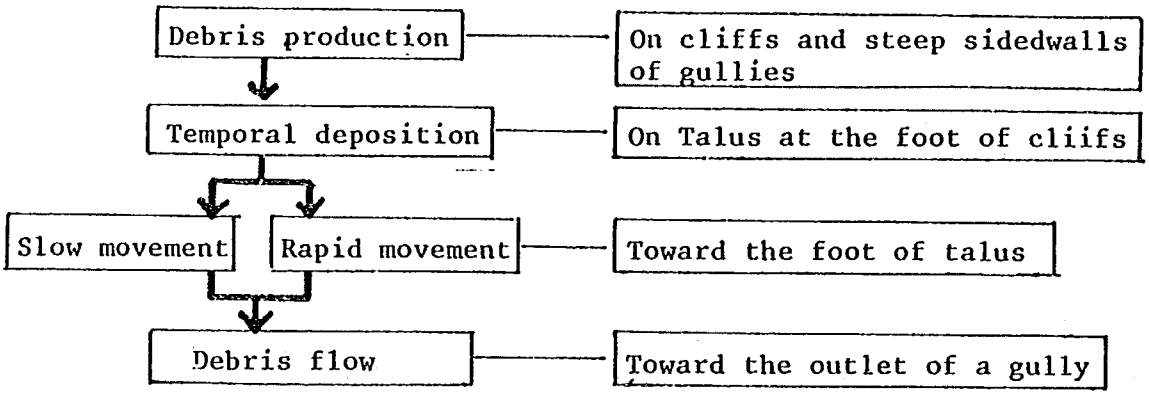
Judging from the frequency of debris flow occurrence since reliable information was available, most gullies seem to discharge debris frequently, once in ten or several decades years.

Geological and erosional characteristics of the gullies

A cross sectional profil of several gullies on Mt.Nantai is depicted schematically to show the geological features(Fig. 6). Most of the

steep sidedwalls of the gullies are composed of alternate deposits of lavas and pyroclastic rocks.

A pattern of process of debris production and debris movement in the gullies is shown in the chart below.



i) Debris production on the cliffs

Three types of cliffs and associated patters of debris production are described as shown in Fig. 7. Among them, Btype is the worst in the light of debris yield. The volcanic breccia of B type is susceptible to erosion by alternate repetition of freezing and melting in cold seasons. The receding of this layer brings about the breaking down of the above lava layer.

ii) Debris movement on talus deposits

When large lava blocks fall down on a talus, they roll down on the talus slope, whereas small blocks, such as volcanic breccia or scoria , stop near the dropped points and move down slowly on the slope. Thus, a talus slope is composed of larger blocks on the lower slope and finer materials on the upper slope. The inclination of talus slopes is 35° - 38° , an angle of repose.

iii) Debris movement out of the gullies

Basing on actual examples, a schematical description is presented on several patterns of debris movement in Fig. 8.

iv) Debris budget in the gullies

A detailed investigation on debris budget was carried out mainly by using aerophotos and partly by field measurement. The aerophotos were taken in Oct. 1957 and Nov. 1966. During these periods, six storms above 300 mm in total amount attacked the area, but the typhoon storm in Sept. 1966 brought about the most remarkable debris movement in the gullies. Debris budgets in the gullies are given in Table 1. The three gullies, Oohiranagi, Shiranagi and Konagi, caused the most striking debris yield. The total debris washed out of the five gullies by the storm amounted to 550,000 m^3, a part of which deposited in the downstream reach, Fukazawa. Consequently, 420.000 m^3 of debris discharged down into Daiya river.

Erosion control works in the gullies

It was 1960 that erosion control works started on the southeast slopes of Mt.Nantai under the direct control of the Forest Agency. Two years later, Tochigi prefecture began similar works on other parts of Mt. Nantai. The Ministry of Construction took care of the foot part of the several gullies which are a part of Daiya river. Countermeasures now under practice are explained by following the above chart.

i) Fixation of cliffs

Almost all debris produced in the gullies were yielded initially on cliffs and steep sidedwalls of the gullies. During the past decade, experiments and practices have been conducted to protect the cliffs against weathering and rockfall at their base. In addition to the

benefit of checking the source of debris, the fixation of cliffs is also needed to protect the erosion control works on talus and torrents against the damage caused by the impact of falling large rock blocks. The fixation of cliff surfaces is carried out in the following procedures for the cliffs, A, B and C in Fig. 7.

a) Smoothing the cliff surfaces which are afterwards covered with iron nets. B type: Jutted lava layers are cut off. A and C type: Jutted and convex parts are smoothed to make a straight slope.

b) Coating and injection by mortar. B type: Mortar is injected into volcanic brrecia layers(grouting) and the whole iron-netted cliff surfaces are coated by mortar(coating depth: 10 cm). A and C type: Smoothed and iron-net covered surfaces are coated by mortar(coating depth: 10 cm). The mortars used in the above practices are mixed with several chemical substances according to the slope's features.

c) Setting of small channels. Small channel works are set up to protect the talus slopes against the concentrated storm water from upper paved cliffs.

Until now, the following statistics can be stated for the treated cliffs.

Area of coated cliffs	34,100 m^2
Area remained uncoated	56,000 m^2

ii) Fixzation of talus slopes

The fixzation of talus slopes is carried out as follows.

a) Construction of soil retaining walls. Retaining walls made of concrete or iron nets are first set up on the slopes at a given interval about 30 m apart, to check debris movement.

b) The cutting of small channels to collect surface water.

c) Terracing for planting.

d) Sodding and planting of trees. Sodding is commonly conducted by placing " vegetation bags" which contain soil, fertilizer and grass seeds. Trees of various species have been tested and Larix leptolepis finally remained as the best.

e) Retaining nets for falling rocks. Where rock blocks fall frequently from the upper cliffs, rock-retaining iron nets are set up.

iii) Stabilization of debris in gully beds.

Gully beds are generally composed of large rock blocks containing smaller volcanic breccia, scoria and others. The channels have usually no surface water. Surface water appears on the gully beds only during a heavy storm. When it exceeds a given limit, the water suspends first light scoria and next other gravels. Finally, large rock blocks begin to move and develop into debris flow.

Stepwise check dams have beeen constructed to stabilize gully beds. First, a large check dam is built on a hard lava layer, and then smaller dams are built stepwisely towards the upper channel with 10 % planning gradient of sediment deposit. The construction of stepwise dams started at places where it has been necessary to construct them and where lava layers appear. The present status of construction of check dams is given in Table 2.

PRACTICE OF EROSION CONTROL WORKS IN INARI TORRENT

Erosion control works in Inari torrent first began in 1899 by Tochigi prefectural office. Afterwards, it transfered to Ministry of Construction in 1918. Inari torrent is one of the famous but devastated

torrent and holds the longest history of erosion control works in Japan. The main vulnerable object in the downstream area is Nikko city.

History of disasters by debrisflow and flood

The following outlines the three major causes of flood and debris disaster in Inari torrent and along Daiya river which is mainly derived from the sediment yield of Inari torrent.

a) The debris coming out of Inari basin deposits at the confluence point and the blockage of Daiya river occrrs. Subsequently, flooding takes place along Daiya river.

b) Debrisflow attacks the living quarters near the outlet of the torrent.

c) The sediment emerging from Inari basin deposits in Daiya river and raises the channel bed gradually. Consequently, the channel tends to fluctuate, bringing about flooding. In the old days, the main channel of Daiya river assumed a different course from what it is now. The present terrace on which Nikko and Imaichi city are located resulted from the flooding and deposition of sediments by Daiya river. An outline of the history of disasters is as follows[2].

827: A huge flood and debrisflow forced to remove the shrine.

1532-1554: A huge flood, but the specific year is unknown

1662: The most disasterous debrisflow in Inari torrent. More than 300 people died and nearly 300 houses were washed away by debrisflow due to the huge landslide at the source area of Inari torrent.

1683: Many landslides by an earthquake and flood in Daiya river.

1684, 1685, 1699, 1704,1713, 1721, 1723 and 1858: Flood in Daiya river and in Inari torrent, by which many bridges were washed away and several persons died

1902: Debrisflow in Inari torrent and flood in Daiya river. Many(but unknown number) of people died, more than 200 missing and nearly 800 houses were destoroyed or washed away in Nikko and Imaichi district.

1906: 1907, 1910 and 1914: Flood in Daiya river.

1918: Debrisflow in Inari torrent.

1947 and 1949: Flood in Daiya river.

1966: Flood in Daiya river and in Inari torrent. 9 persons died, one missing and 500 houses were damaged or washed away.

Planning and practice of erosion control works

The writers explaine the outline of the practices and the investigation of erosion control works in this torrent, by using the above zoning system of the torrent basin.

(1) Debris producing area

Erosion control works have not yet been practiced at all in this area, because of the steepness of the slope and the torrent. The estimation of debris production during a given period and the prediction in the future have been conducted mainly with the aid of aerophotos and partly by field measurements.

i) Debris production in the past

The debris amount produced in each subbasin was estimated through the measurement of the area of new landslides and the expanded area of old landslides with aerophotos taken at a constant interval. The result of estimation is shown in Table 3.

ii) Debris production at a storm of 100 years recurrence period.

Quantification type II (Hayashi's discrimination problem) was employed. The whole Inari basin is divided into approximately 5000 elements with a mesh of 50X50 m. Geological, topographical and vegetational factors were read on the aerophotos. Storm factors were also take into consideration. Debris production (V) is given as

$$V = v1 + v2$$

where v1 is the amount of debris produced by new landslides and v2 is the amount similarly produced by the expansion of the old landslides.

v1 & v2 = f (storm, slope, geology, vegetation)

Storm factors were expressed with a 24 hr intensity and a frequency of storms above a given level. Slope characteristics are expressed as to direction, altitude, relief, distance from the ridge and the shape of longitudinal slope profiles in a mesh. Geology is described by the name of rocks found in existence. Vegetation is represented by the names of mainly occupied trees, shrubs, grasses etc.

Debris production predicted by this method is given as follows at a storm of 100 years recurrence period.

	Debris Producing area	Other subbaisns	Total
New landslides	917,434 m^3	554,096 m^3	1,461,530 m^3
Expansion of the old landslides	227,438	22,992	250,430
Total	1,144,872	567,088	1,711,930

According to the estimation by Ooishi[3] with the volume of terraces formed by the debris deposition in 1662, total amount of debris yield in that event was regarded as approximately 2,000,000 m^3. The predicted amount of 1,145,000 m^3 seems to be a reasonable value, if the accumulation of debris in the head region befor a heavy storm is taken into consideration.

(2) Sediment transporting area

To control the sediment coming out of the upper basin, this reach, which lies above the sediment depositing area, is of great importance. As mentioned above, high sabo dams or stepwise middle-sized sabo dams are generally constructed.

i) Effect of a sabo dam

The effect of a sabo dam on the control of sediment discharge is

classified as in the following, accompanying the figures of Hinata sabo dam, the largest sabo dam in Japan.

Item	Effect of sabo dam	Hinata dam
Dimension of the dam	*Width	176 m
	*Height	46 m
	*Lenght of permanent deposit(L)	950 m
	*Lenght of temporal deposit(ΔL)	200 m
Quantitative effect	*Retention of deposits of the former channel beds(BS)	339,000 m^3
	*Permanent deposit(S)	1,280,000 m^3
	*Temporal deposit(ΔS)	260,000 m^3
	(Total deposit)	(1,879,000 m^3)
Qualitative effect	*Change in the transportation form from massive to individual transportation	
	(*Sorting out transported materials from the upper reach.)	

ii) Arrangement of sabo dams

Nearly thirty dams are spread im this middle reach as in Fig.11. The total amounts of permanent and temporal deposits on these dams, including Hinata dam, are as follows.

Permanent deposit(ΣS)	1,760,000 m^3
Temporal deposit(ΣΔS)	356,000 m^3
Total	2,116,000 m^3

iii) Investigation of the effect of sabo dams on the change in sediment transportation forms.

The observation system using video camera sets was set up in the upper reach of the torrent. At three points, nine video cameras were installed to observe the sediment flow condition. Three cameras were installed at the wing of a sabo dam as a unit to watch the different deposition points at the upper end of sediment deposits, the middle

range and on the sillway, respectively. The purpose of the observation is as follows.

a) The mechanism of deposition of mudflow on the sabo dams constructed stepwisely. A practical purpose is to clearify the length and area of a deposit fan necessary for killing mudflow.

b) Behaviour of sediment flow and process of deposition~a secondary movement of sediment on a deposit fan of a sabo dam.

Six storms have been recorded since 1975, but only two are available for analysis.

(3) Sediment depositing area

The sediment deposition area of Inari torrent is made up of huge supplies of sediment coming repeatedly from the upper basin by mudflow. During low recurrence storms, the channel beds in this reach are rather eroded and lowered. Therefore, the deposition, scoring and resulting in variations in the channel bed have always been repeated many times in this area.

i) Topography of the sediment depositing area[3)]

This area is composed of three terraces as in Fig.10, the higher terrace (specific height: 20-30 m), the middle terrace(8-10 m) and the lower terrace(3-5 m). Judging from the key layers of special volcanic ash, the higher terrace was made several thosands years ago and the middle terrace was formed about a hundred to a thousand years ago. The lower terrace is considered to have been made by huge mudflow in 1662. The above facts suggest that a new terrace is formed with several thousands years interval in Inari torrent by huge mudflow. The present torrent channel runs on the latest terrace varying its course and scoring its beds. A recent investigation on this reach clearified that most of the channel surfaces are composed of debrisflow deposits. This implies that even a secondary movement of deposits gives rise to debrisflow.

ii) Channel works

To change an unstable and fluctuating channel to a fixed one, check dams and ground sills(drop works) have been constructed stepwisely since 1918. Recently, as the sabo works have advanced in the middle reach, accomplishing the planned highest sediment control level, the banking, levee making and revetment works in the downstream reach got started. The present status of channel works is as follows and is shown in Fig. 11.

Length of the revetment works planned	4290 m
Length already practiced	3862 m
Ground sills(drop works) practiced	28(H=4-6 m)

iii) Planning of a channel work

The following is a procedure of determining the form and dimensions of a new channel in Inari torrent.

a) Plane form of a channel..... A straight channel course is always employed to let the sediment flow smoothly. But, this straight channel strengthens flood water energy and quickens flood speed.

b) Width of a channel.....The following three are taken into consideration. 1. The previous channel width. A reliable engineers' decision is most important for the determination of a new width and other figures, though a channel width in the lower reach of a devastated torrent varies but is undeterminable. 2. Regime theory equation, for example, $W = aQ^{1/2}$. 3. Examples of other torrents where channel works have already been practiced and examined their reasonability.

c) Gradient of a channel.....The procedure is as follows. 1. The gradient of the previous channel is first taken into consideration. A preliminary gradient is presumed and drop works are set. 2. Examining the

validity of the gradient and the width by applying theoretical equations of sediment transport to a new channel. The gradients thus determined become smaller by setting the drop works. This degradation of gradients compensates the increase of the energy of flood water by strengthening and smoothening a channel. The new gradient(Ip) is 1/25.0 - 1/20.0 . The previous gradient(Ig) was 1/18.0 - 1/12.8. Then. Ip/Ig is 0.64-0.72.

iv) Survey of depositing and scoring in a new channel.

The survey of a channel bed is carried out to evaluate the effect on the new sabo works, when any remarkable changes take place after a storm. The survey is especially important in the lower channel reaches.

CONCLUSION

i) From the viewpoint of sediment discharges, volcanoes in Japan can be classified into four types, such as I-A: active gully type, I-B: dormant gully type, II-A: torrent type with debris production by rockfalls and debris slides, II-B: torrent type with debris production by a single huge slumpslide

ii) As representatives of erosion control works in Nikko area, both Mt. Nantai(I-B type) and Inari torrent(II-A type) are illustrated. As for Mt. Nantai, the process of debris production and the movement of debris was followed, and the erosion control practices were examined. In the case of Inari torrent, the zoning of a torrent basin into three areas is proposed for erosion control planning, and erosion control practices are explained with actural examples.

ACKNOWLEDGEMENT

The writers wish their gratitude to Mr.M. Ooishi, principal investigater

of the disaster research center, Mr. Y. Suzuki, associate professor of the Utsunomiya university and the menbers of Nikko Sabo Work Office for their valuable suggestions and assistance.

REFERENCES

1) Maebashi Regional Forest Office: Outline of erosion control works, 1980.

2) Nikko Sabo Work Office: Planning of the channel work of Daiya river, 1978.

3) Yano Y. et al: Sabo pocket book, Sankaido Publishing Co. Ltd, 1970

Table 1 An example of debris budget of gullies on the southeaster slope of Mt. Nantai during the period from Oct. 1957 to Nov. 1966

Name	Length of gully	Budget
Oohiranagi	1.55 km	- 195,000 m^3
Shiranagi	1.72	- 243,000
Nakanagi	0.79	+ 20,000
Konagi	3.71	- 184,000
Oonagi	2.63	+ 57,000
Fukazawa	1.56	+ 127,000
Total	11.96	- 418,000

Table 2 The present status of erosion control works by using solid materials.

Name of gully	Area of the gully (ha)	Check dam		Soil retaining wall	
		Number	Volume (m^3)	Number	Volume (m^3)
Maenagi	40.	32	7,182.	27	3,481.
Oohiranagi	32.	12	3,821.	15	2,335.
Shiranagi	40.	2	1,350.	16	4,684.
Nakanagi	17.	4	386.	-	-
Konagi	76.	35	13,916.	9	1,249.
Oonagi	72.	46 (13)	27,245. (14,077)	-	-
Fukazawa		3 (3)	24,366. (24,366)	-	-
Total	280.	134	78,314.	67	11,750.

Figures are of Forest agency. ( ) is of Ministry of Construction.

Table 3 Debris production in the upper basin of Inari torrent

Period	New landslides (m^3)	Expansion of old landslides (m^3)	Total (m^3)
Oct. 1957 - Aug. 1962	291,000	221,000	512,000
Aug. 1962 - Sept. 1966	174,000	261,000	435,000
Aug. 1962 - Nov. 1966	197,000	266,000	463,000
Aug. 1962 - Oct. 1970	98,000	150,000	248,000
Oct. 1970 - Sept. 1976	34,000	41,000	75,000
Sept. 1976 - Oct. 1980	36,000	80,000	116,000
Oct. 1980 - Nov. 1981	36,000	123,000	159,000

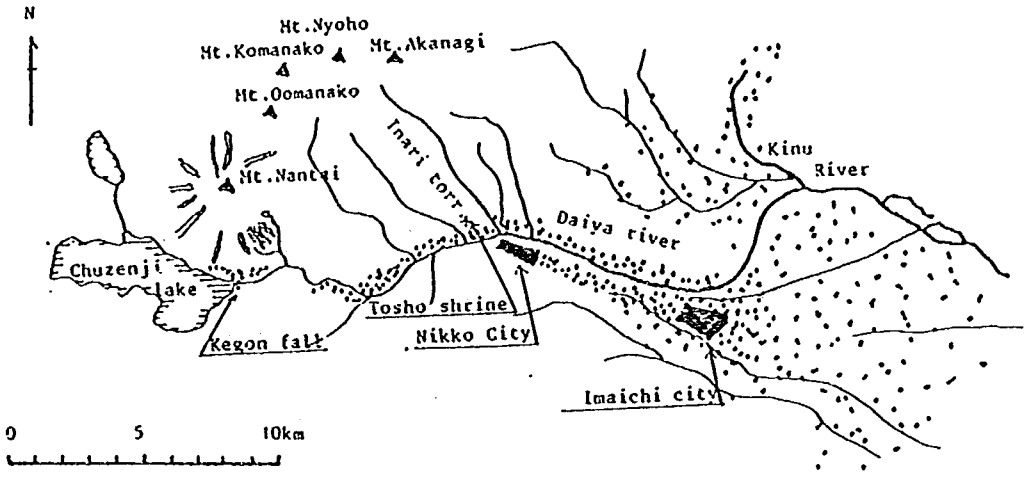


Fig.1 A map of Nikko district and Daiya river

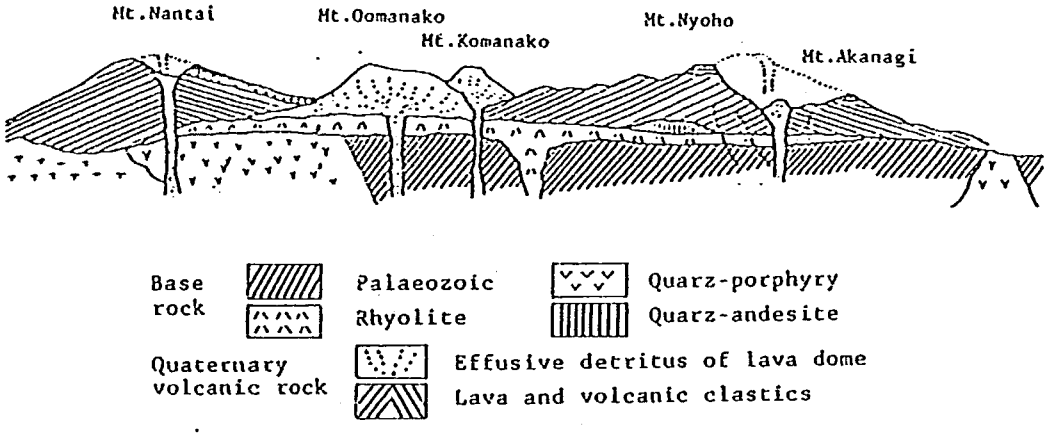


Fig.2 A profile of Nikko volcanoes

Name \ Age	Alluvium 0	11,000	Diluvium	1,800,000 year
Mt. Nantai	←----------→		←------→	
Mt. Oomanako Mt. Komanako			←------→	
Mt. Nyoho Mt. Akanagi			←-------→	

Fig.3 Ages of the three volcanoes

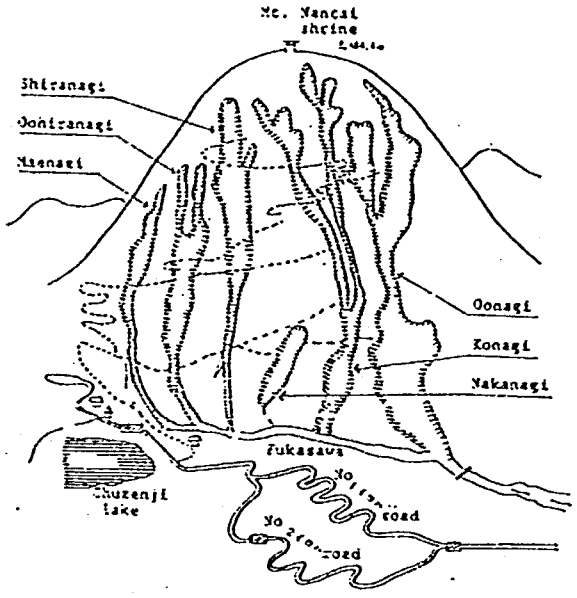


Fig.4 Gullies on the southeastern slopes of Mt.Nantai

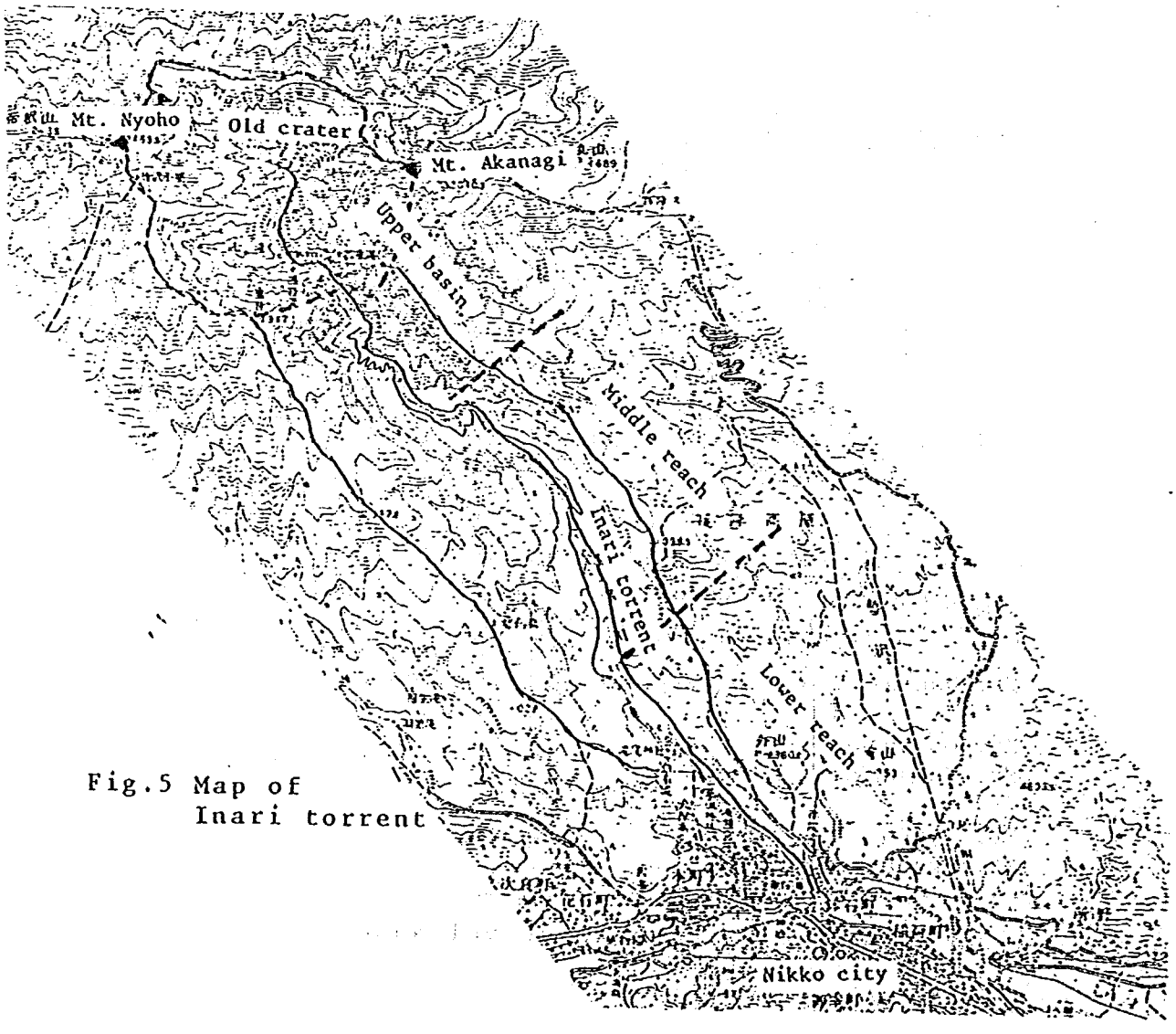


Fig.5 Map of Inari torrent

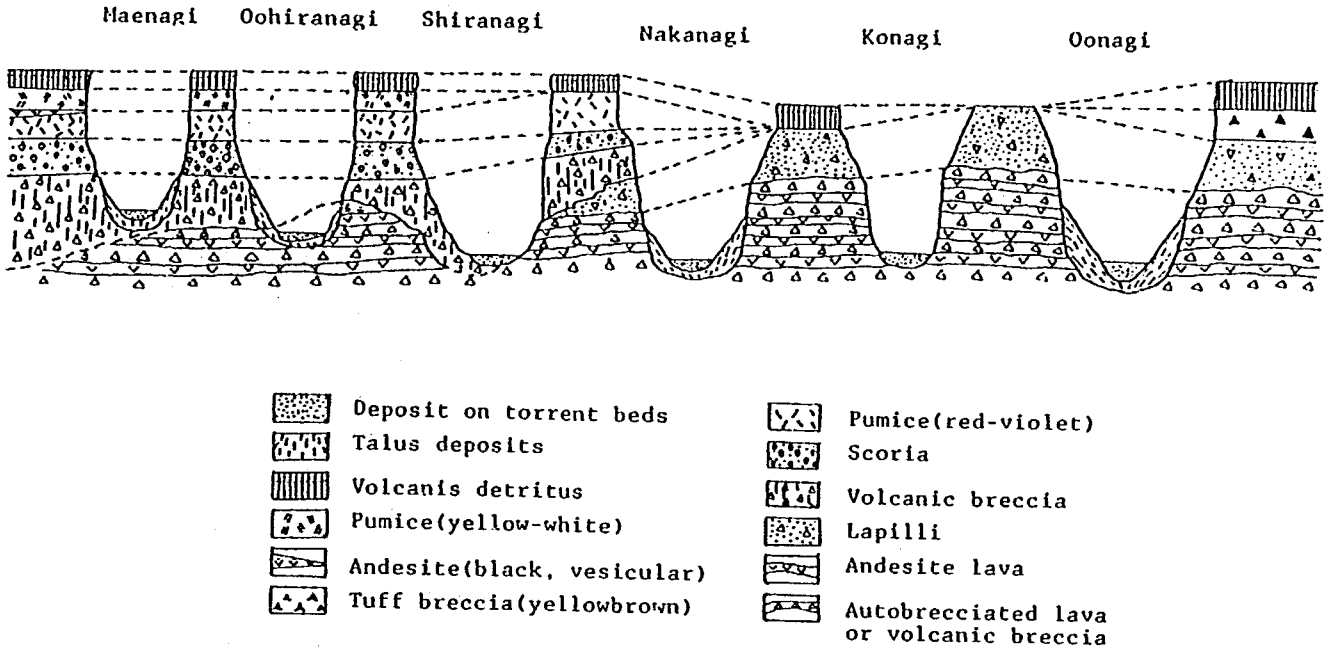


Fig.6 A geological profile of gullies of Mt. Nantai

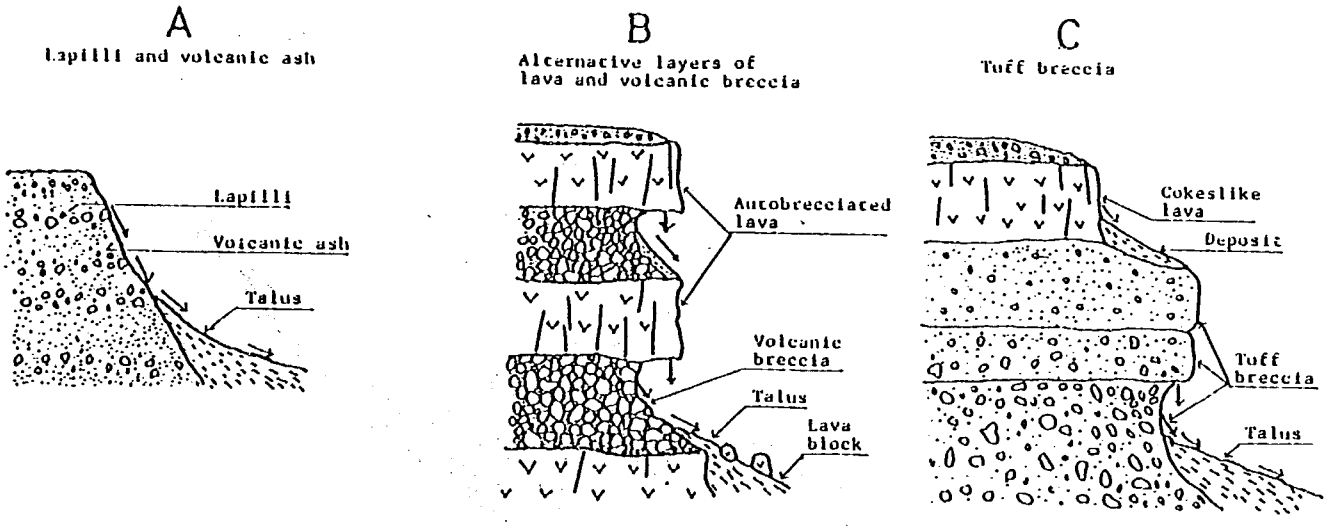


Fig.7 Three types of cliffs and their debris producing patterns in gullies of Mt.Nantai.

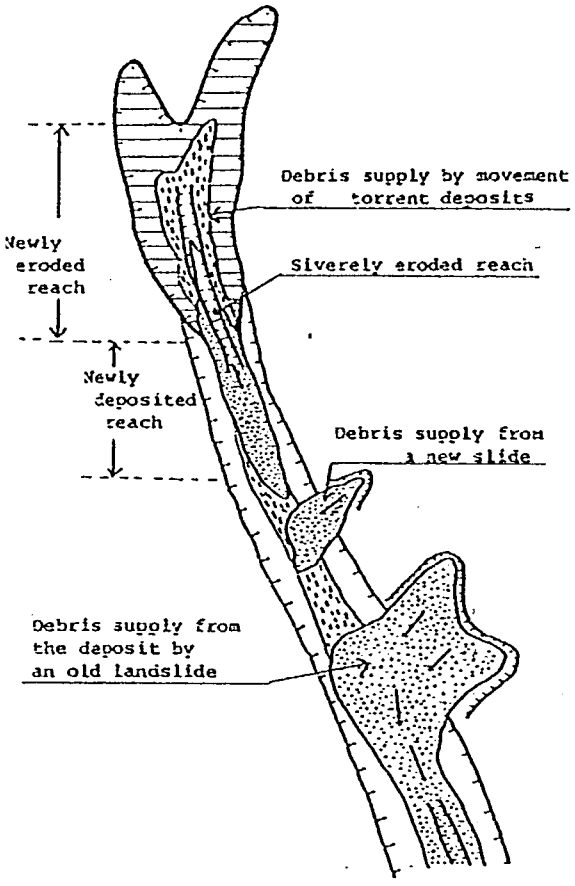


Fig.8 A schematical description of the sources of debris discharge in a gully

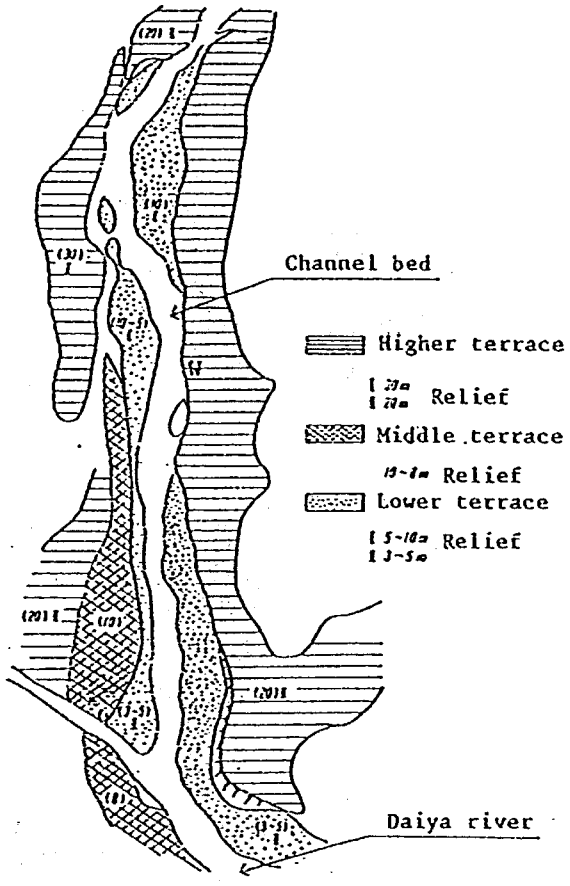


Fig.10 A map of the lower reach of Inari torrent. (After Ooishi[3])

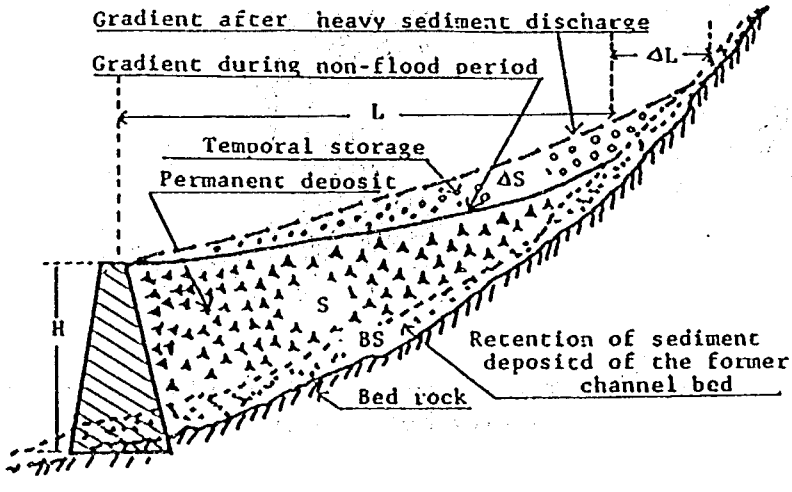
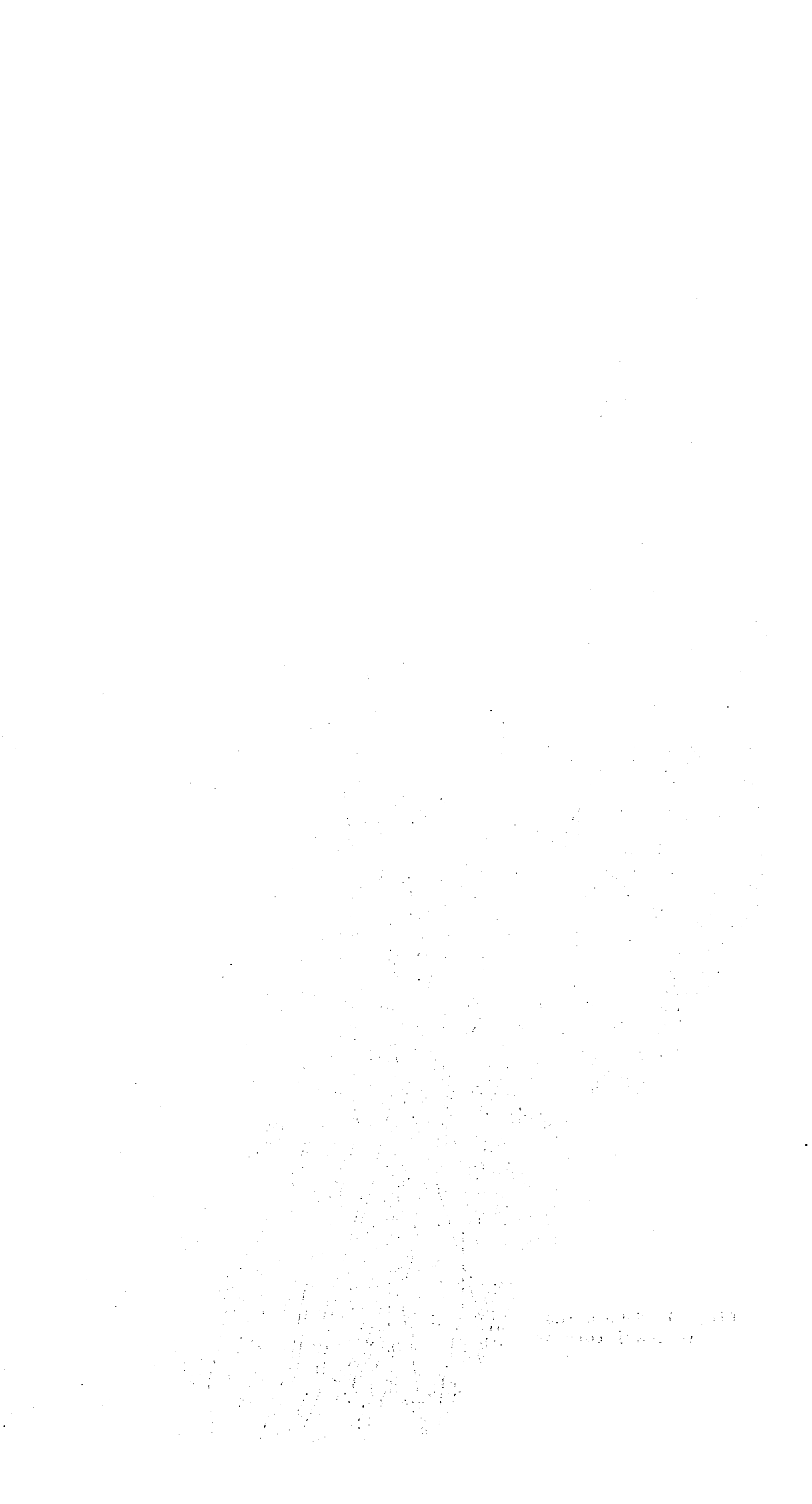


Fig.9 Effect of a sabo dam on sediment storage



Fig. 11 Sabo works in Inari torrent



ENGINEERING RESPONSE TO FLOOD HAZARDS CREATED BY THE ERUPTION OF MOUNT ST. HELENS

Steven L. Stockton

Chief, Soils Engineering Section, Portland District,
U.S. Army Corps of Engineers, P.O. Box 2946, Portland, Oregon 97208

ABSTRACT

The 18 May 1980 eruption of Mount St. Helens significantly altered the configuration of the Toutle and Cowlitz River system. A massive debris avalanche deposited more than three billion cubic yards of material in the upper reaches of the North Fork Toutle River Valley.

The loose, unconsolidated material comprising the debris avalanche created a significant source of sediment. If this material were allowed to move unhindered into the lower reaches of the Toutle/Cowlitz River system, it would diminish the flood carrying capacity of the Cowlitz River to such an extent that flood protection to communities along the Cowlitz River would be reduced to unacceptably low levels. Deposition of this material also blocked tributary drainages thereby creating basins that, if allowed to fill and breach uncontrollably, would cause significant flooding downstream.

To counter these flood threats posed by the eruption of Mount St. Helens, the Portland District, U.S. Army Corps of Engineers implemented a variety of measures. This paper describes efforts to stabilize sediments on the Toutle River system and efforts to provide controlled outlets for newly formed lakes.

INTRODUCTION

The 18 May 1980 eruption of Mount St. Helens significantly altered the landscape of the Toutle-Cowlitz Valley. The explosion and simultaneous landslide released hot gases, pumice, ash and mudflows which devastated more than 150 square miles of forested and lake-covered land north and northwest of the mountain. Much of the material displaced by the eruption blew out or slid in a north-northwesterly direction, primarily into the North Fork and also into the South Fork of the Toutle River. Debris from huge mudflows swept down the Toutle River and into the Cowlitz River.

Approximately 3 billion cubic yards of material was deposited in the upper 14 miles of the North Fork Toutle River, with an additional 58 million cubic yards deposited of material in the upper reaches of the South Fork Toutle River. Mudflows carried more than 50 million cubic yards into the 21 miles of the Cowlitz River from the mouth of the Toutle downstream and deposited an additional 45 million cubic yards in the Columbia River, upstream and downstream of the mouth of the Cowlitz River.

The landslide deposit in the North Fork Toutle River Valley had raised the valley floor several hundred feet. This material blocked tributary drainages and created numerous potential impoundment areas. If allowed to fill and breach uncontrollably, major flooding would occur downstream along the Toutle and Cowlitz Rivers.

The Corps of Engineers initiated a variety of measures to reduce the threat of flooding along the Cowlitz River and to accelerate the recovery of the Cowlitz-Toutle River Basin. The following measures were implemented:

- Reopening of the 40 ft x 600 ft Columbia River Navigation Channel;

- Reestablishment of a 50,000 cfs flood control channel in the Cowlitz River between river mile 0 and 21.5;

- Construction of two debris retaining structures; one each on the North and South Fork Toutle River;

- Construction of sediment stabilization basins downstream of the two retaining structures;

- Raising and/or extending levee systems to protect population centers in Longview, Kelso, Lexington and Castle Rock;

- Emplacement of revetment at selected locations along the Cowlitz River to prevent bank erosion and protect land adjacent to the river;

- A contract with Tacoma City Light was established for use of 600,000 acre-feet of flood control storage in Mossyrock reservoir for flood control storage during the winter of 1980-1981;

- Numerous smaller projects aimed at restoring navigation and flood control works impaired by the eruption.

This paper will address two of the actions taken in the aftermath of the 18 May 1980 eruption of Mount St. Helens. Part one will address the design, construction and performance of sediment stabilization projects on the Toutle River. Part two will discuss engineering aspects of providing outlets for new impoundments created by the North Fork Toutle River debris avalanche.

PART I

DESIGN, CONSTRUCTION AND PERFORMANCE OF SEDIMENT STABILIZATION PROJECTS ON THE TOUTLE RIVER

OBJECTIVE OF WORK

The objective of work on the Cowlitz and Toutle Rivers is to reduce the flood threat on the Cowlitz River; to prevent damage to downstream bridges crossing the Cowlitz and Toutle River; and to reduce sediment reaching the Columbia River Shipping Channel. These objectives can be achieved by stabilizing or removing sediment in the Toutle River before it reaches the Cowlitz River or by removing material from the Cowlitz and Columbia River after it has deposited in these locations. Initial efforts to restore the Cowlitz River flood control channel and Columbia River navigation channel required excavation of 56 million cubic yards from the Cowlitz and 15 million cubic yards from the Columbia. Excavation of this magnitude filled much of the area available for spoil disposal adjacent to the Cowlitz and Columbia Rivers. Since it became more expensive to transport excavated sediments to increasingly distant spoil disposal areas, it was an economic consideration that required sediment stabilization efforts to move upstream into the Toutle River system where area for spoil disposal was more available. Additionally, it soon became apparant that it was considerably less expensive to stabilize material in place, whether it be on the hillside, in the river channel, or in the debris avalanche, than to excavate, load, haul and place material in a spoil area. Although economic considerations were not the sole factor, they did play a major part in the selection of measures implemented.

SEDIMENTATION

Efforts to predict sediment volumes and depositional patterns in the Cowlitz River were initiated shortly after the May 1980 eruption and continue today. Initial estimates (Dunne and Leopold, 1981), indicated that between 22 and 37 million cubic yards of sand would be deposited in the Cowlitz River during the winter of 1980-1981. They also noted that the majority of this deposition would occur during high flow periods, and therefore, is directly dependent upon the weather.

Recent Corps sedimentation studies, based upon two years of data and computer modeling, indicate that 20-25 million cubic yards of sand will be deposited in the Cowlitz River during the winter of 1981-1982 assuming "normal" hydrologic conditions. Continuing studies will be aimed at monitoring of the system, expanding the hydrological analysis required to assess the potential of flooding, assessment of the continuing sediment yield from the avalanche area, and formulating the transport capabilities of the Cowlitz River.

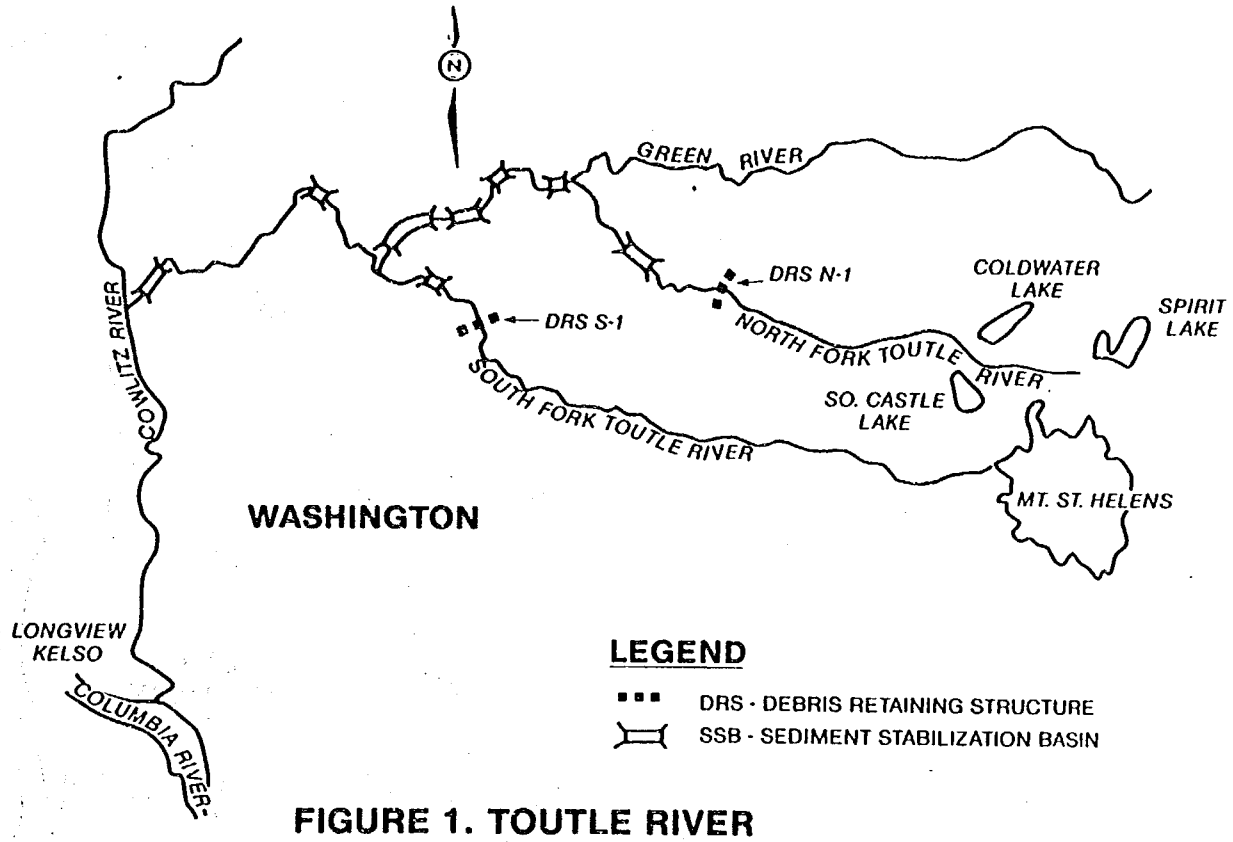


FIGURE 1. TOUTLE RIVER SEDIMENT STABILIZATION SITES

DEBRIS RETAINING STRUCTURES

Basis for Design

Debris retaining structures are essentially small rockfill dams that retain sediment and floating debris in impoundment areas behind the structures. Due to the small dead storage capacity of the projects, material trapped behind the structures must be continually removed and spoiled under an operation and maintenance contract. The basic design concept behind the structure is simple. As sediment laden water ponds in the small pool behind the structure, stream velocities decrease, and heavier sediment particles drop out. Water and suspended fine grained sediment particles then flow through the open graded, permeable rockfill embankment. Flows in excess of embankment infiltration capacity are passed over a spillway.

Embankment Design

Site Selection

Primary factors affecting debris retaining structure site selection include nearness to major sediment sources, availability of disposal areas, availability of real estate, and availability of construction materials.

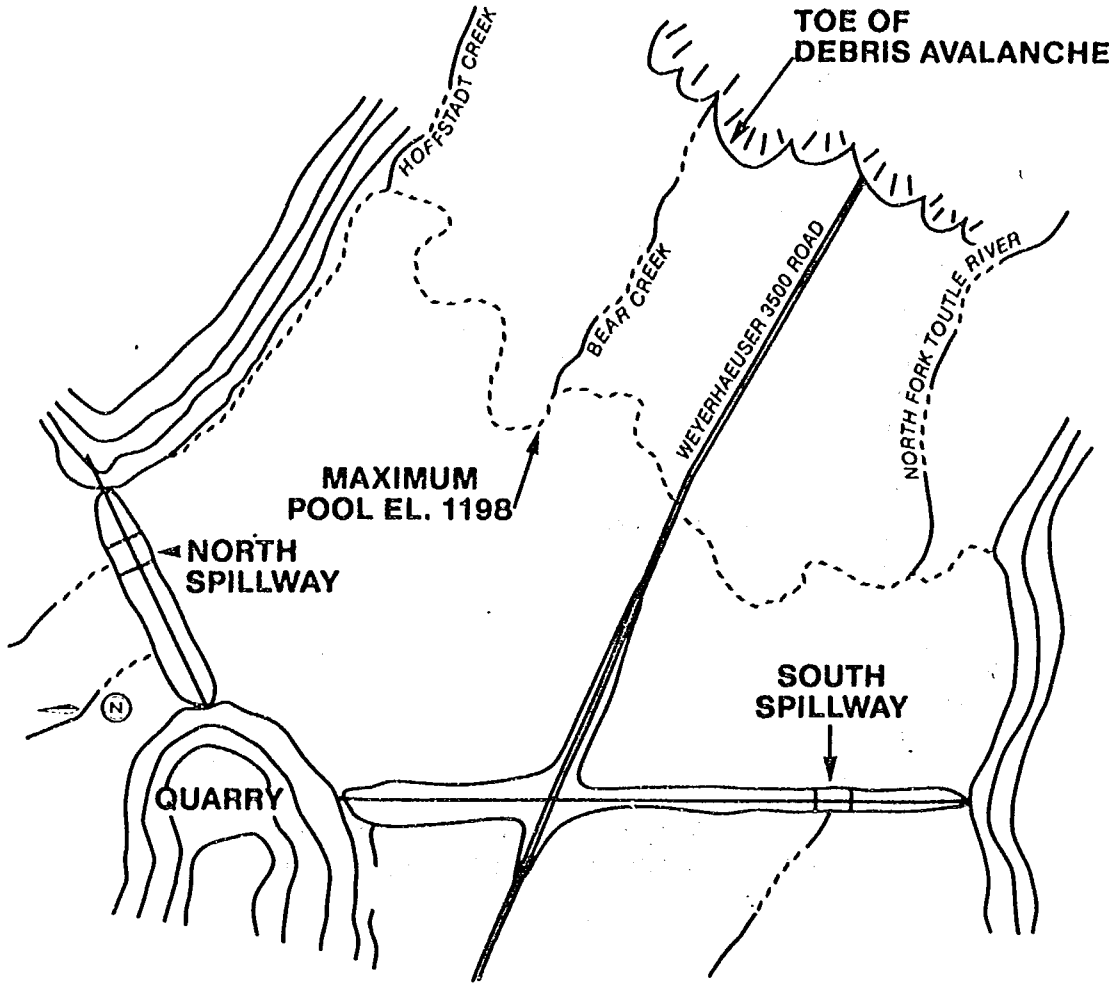


FIGURE 2. NORTH FORK TOUTLE RIVER DEBRIS RETAINING STRUCTURE SITE PLAN

By locating structures as close to sediment sources as possible, downstream reaches of the river are able to stabilize more quickly. A site plan of DRS N-1 on the North Fork Toutle River is shown in Figure 2.

Embankment Sizing

Embankment height is directly related to impoundment capacity requirements. Since sediment transport data was not available when the embankment was designed, the decision was made to keep the overall height of the embankment low, and to make the embankment relatively long in order to achieve an appreciable amount of storage capacity. It was recognized that there would not be enough capacity to trap all of the material being transported downstream, so provisions were made to have this material continuously removed to nearby disposal areas.

The North Fork DRS is in excess of 6000 feet long with an average height of 30 feet. This results in a rated storage capacity, at spillway crest, of 6 million cubic yards (MCY). The DRS on the South Fork is considerably smaller with a length of 600 feet, a height of 20 feet and a rated storage capacity, at spillway crest, of 0.7 MCY.

Two other factors that favored a low embankment were; (1) due to the many uncertainties involved with future volcanic eruptions and the limited explorations data available, it was desireable to keep the volume of water impounded as low a possible to minimize releases if the DSR were to fail, and; (2) the time available for construction of the structure limited, to some degree, the total volume of embankment material that could be placed. Design of the debris retaining structures began less than one week after the 18 May 1980 eruption. Design was completed in June 1980 and the construction contract was awarded on 8 July 1980.

Rockfill Embankment

Rockfill material was specified to be sound, angular quarried rock containing less than 10% by weight of material smaller than 4 inches. Maximum size of rockfill allowed was 2 feet in diameter. Rockfill embankment was placed in lifts 2 feet thick and compacted by 3 passes of a 10 ton vibratory roller. As water flows through the embankment, a toe trench at the toe of the embankment catches seepage and directs it to an outlet channel. Class II riprap at the toe of the embankment stabilizes the toe against high velocity flows in the toe trench. A typical embankment section is shown in Figure 3. Downstream slopes of the embankment were designed relatively flat at 1V on 4H in an effort to compensate for unknown foundation conditions and to reduce the rate at which downcutting would occur through the embankment, should the embankment be overtopped.

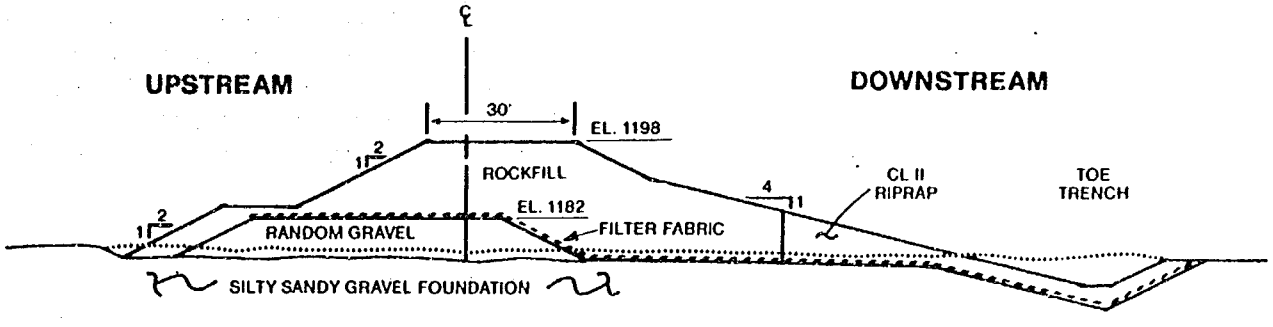
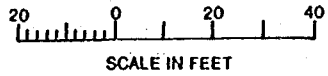


FIGURE 3. DEBRIS RETAINING STRUCTURE EMBANKMENT SECTION



Random Gravel Core

Material used in the random gravel zone of the embankment consisted of well graded gravels having a maximum size of 8 inches. Material was compacted in 12 inch lifts with 2 passes of a vibratory roller. The function

of the random gravel core is to force water to pond at a fixed elevation. Water ponding above this elevation will then be forced to flow through the embankment. Utilization of a random gravel core allowed the interior of the embankment to be constructed with a relatively inexpensive material soon after foundation preparation was complete. This allowed time to strip and develop the quarry for production of rockfill which would follow.

Filter Design

At the time the embankment was designed, foundation conditions were unknown since much of the embankment foundation area was covered with remnants of the May 18th mudflow. Access into the area with exploratory equipment was limited due to the unstable nature of the mudflow deposit. Approximately one dozen backhoe pits were dug in those areas accessible to equipment. The foundation was comprised primarily of cemented gravels, alluvial sands and gravels, and finer grained silty, sandy material from previous lahars. The function of the filter fabric was to separate the coarse embankment materials from the potentially fine grained foundation materials. Material was specified to be woven polypropylene having an equivalent opening size (EOS) no finer than a U.S. Standard sieve No. 100 and no coarser than the U.S. Standard seive No. 70. The filter fabric selected by the Contractor to meet this specification was Mirafi 140X. Filter fabric was placed with its long axis normal to the dam axis in order to gain some additional strength to reduce spreading of the embankment over a potentially weak foundation layer. Two sheets of filter fabric 10 feet wide were sewn together in the factory to form a sheet 20 feet wide. Overlap between sheets was 18 inches for each strip. Securing pins with washers were inserted through both strips of overlap fabric at 3-foot intervals to prevent displacement of the filter fabric during embankment placement operations. One foot of bedding material was placed over the filter fabric prior to placing rockfill. The purpose of the bedding is to form a cushion between the rockfill and the relatively fragile filter fabric. Some difficulty was encountered when the cleated crawler tracks of the dozers placing the bedding passed over oversized material in the bedding, forcing larger rocks through the filter fabric. During bedding placement on the embankment slopes, problems were encountered with the dozer slipping on the slope. The slipping action of the tracks would displace the bedding material and tear the filter fabric.

Spillway Design

The spillway was designed as a temporary structure with a 5 year life. Gabions were used to construct the spillway since a source for other suitable spillway materials was not readily available. Four inches of shotcrete was placed over the gabions for erosion resistance and as protection against floating debris snagging the wire baskets. The downstream vertical face of the gabions were not shotcreted in order to promote drainage and prevent hydrostatic pressure from building up behind the structure. A typical section through the gabion spillway is shown in Figure 4. Due to the limited size of the impoundment area at DRS N-1, the reservoir filled with sediment and debris before the operation and maintenance contractor could excavate accumulated debris. As the south impoundment area at DRS N-1 filled to capacity, the riverbed became elevated and a ponding area no longer

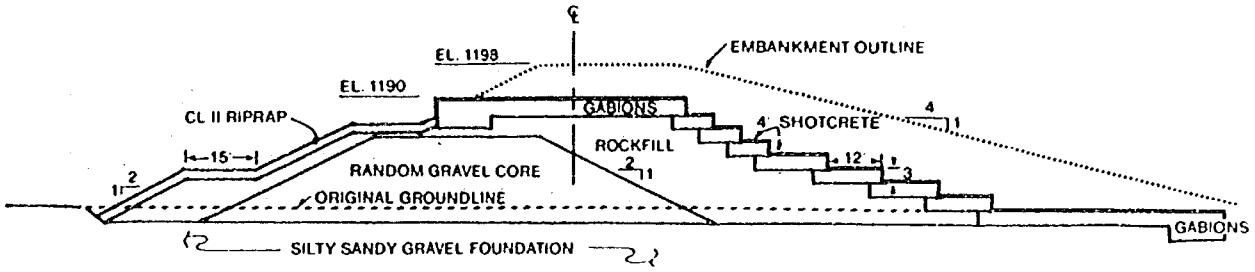


FIGURE 4. DEBRIS RETAINING STRUCTURE GABION SPILLWAY SECTION

existed. Shotcrete covering the gabion spillway was eroded due to the abrasive effects of sediment and due to the impact of cobbles, boulders and large logs rolling down the stairstepped spillway. The south spillway at DRS N-1 failed on Christmas Day 1980.

A new spillway design was formulated in January and February 1981. A Roller Compacted Concrete (RCC) design was adapted to gain more impact resistance. A typical RCC spillway section is shown in Figure 5. Six-inch by six-inch welded wire fabric mats were used as reinforcing in the roller compacted concrete slab. Some problems were experienced during placement of these mats. When several mats were placed in an overlapping position and roller compacted concrete was placed over them, there was a tendency for the edges of the mats to tip up. A sheet pile cutoff was used upstream and downstream of the spillway slab to prevent scour at the upstream end and undermining of the slab at the downstream end. Three inch diameter drain holes were drilled in a 10-foot by 10-foot grid pattern to relieve uplift pressure beneath the slab.

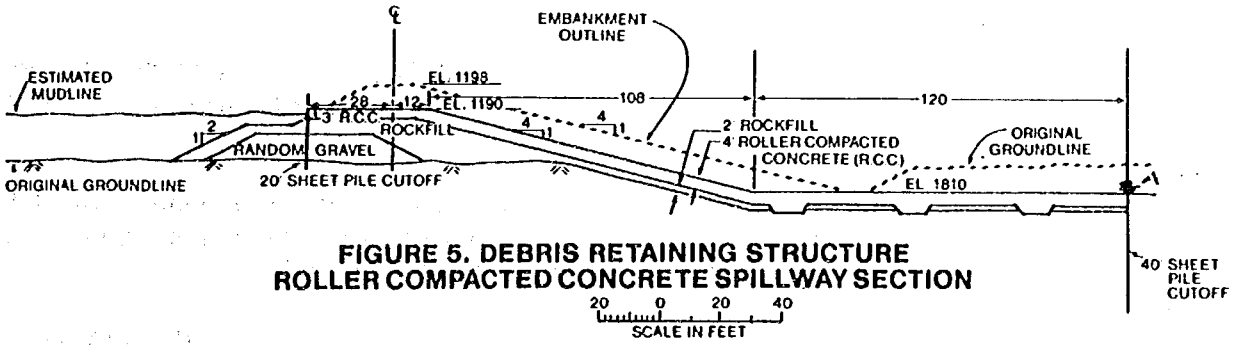


FIGURE 5. DEBRIS RETAINING STRUCTURE ROLLER COMPACTED CONCRETE SPILLWAY SECTION

PERFORMANCE OF STRUCTURES

The volume of sediment delivered to the structures greatly exceeded their limited capability to retain material. Consequently, much of the sediment available for trapping was passed over the spillways once the impoundment areas initially became filled. Figure 6 depicts North Fork Toutle sediment transport volumes for the period July 1980 through March 1981.

	VOLUME ERODED (MCY)			
	Gravel/Boulders	Sand	Silt/Clay	Total
Debris Avalanche	22	25	8	55
North Fork Mudflow	1	2	1	4
Hillslope	1	7	2	10
Total	24	34	11	69
	VOLUME DEPOSITED (MCY)			
Debris Avalanche	3-5	3-7	1	7-13
DRS N-1	3	6	2	11
Channel Excavation	0.3	0.8	0.1	1
Bed Storage	0.1-0.5	1-3	0	1-3
Total	6-8	11-17	3	20-28
Net Output To Mainstem Toutle	16-18	17-23	8	41-49

FIGURE 6. NORTH FORK TOUTLE RIVER SEDIMENT TRANSPORT VOLUMES, JULY 1980 - MARCH 1981. (U.S. Army Corps of Engineers, 1981)

Based on experience gained from operation and maintenance of debris retaining structures N-1 and S-1 for a period of two years, the following observations have been made and conclusions reached:

- Provisions must be made for hydraulic structures, in particular spillways, to withstand the effects of passing large volumes of debris. Once impoundment areas fill, material from the debris avalanche passes directly over the spillways. This material included highly abrasive sand as well as gravel, cobble and boulder sized rock fragments up to several feet in

diameter. Floating logs and tree stumps were also very destructive due to their large mass and resultant high impact loads imposed on the structures;

- Adequate allowances for freeboard must be made due to the large volumes of sediment being transported. Spillway crest elevation must be well below the embankment crest due to the steep gradient of the sediments as they are deposited. At DRS N-1 sediment was deposited with an upstream gradient of 1.5 percent and an average gradient parallel to the embankment of 1 percent. The result of this phenomenon was that, due to the deposition of sediment, the river bed at the toe of this artificially created alluvial fan actually built to an elevation higher than the embankment crest even though from strictly a hyraulic standpoint, spillway size and freeboard allowances were several times those required;

- The open graded rockfill embankment worked well in passing water and fine grained sediments as long as debris accumulation could be kept directly off the upstream face. Once the embankment became covered with coarser grained sediments, impounded water was passed over the spillways.

SEDIMENT STABILIZATION BASINS

Basis of Design

Sediment stabilization basins (SSB's) are basically large sumps excavated in the river channel. SSB's were constructed at naturally occurring deposition sites where the river gradient flattens. The capability of the basins to trap sediment further enhances this natural process since widening of the channel creates an even flatter gradient. As material is trapped, it is continually excavated under an operation and maintenance contract and placed in nearby disposal fills. Locations of sediment stabilization basins are shown in Figure 1. Sectional view of a typical sediment stabilization basin is shown below.

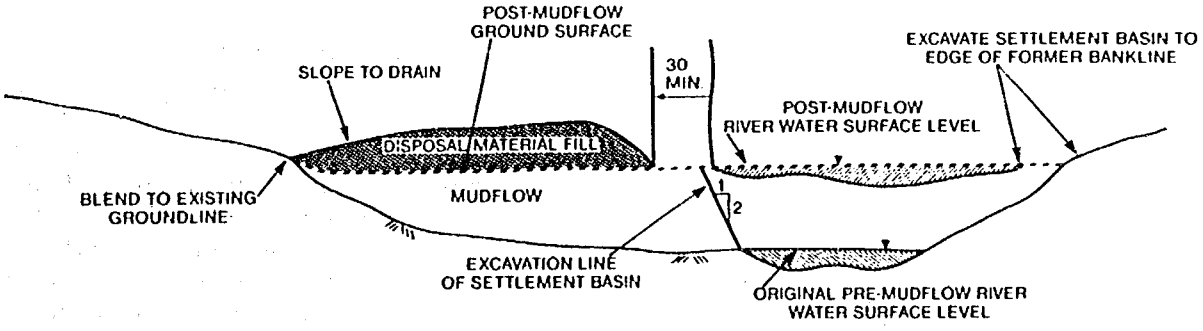


FIGURE 7. SEDIMENT STABILIZATION BASIN SECTION
(NOT TO SCALE)

Performance

Over 8 million cubic yards of material have been removed from sediment stabilization basins. Problems have been experienced when sediment volumes are excessive and the basins fill too quickly causing the river to meander and attack some of the disposal piles located close to the river. In order to alleviate this problem new sediments stabilization basin work will utilize revetment in order to channelize the river and eliminate meandering.

FUTURE SEDIMENT STABILIZATION WORK

Relatively costly excavation of material from sediment stabilization basins and debris retaining structures has forced designers to look for less expensive alternatives to stabilize sediment. Two of the most promising alternatives found to date are channel constrictions and a large debris retaining structure that would not require continual excavation of trapped sediment.

Channel Constrictions

When the south spillway at debris retaining structure N-1 failed, a large opening was left in the embankment. This opening was approximately 25-30 feet deep and 200 feet wide. Even with this relatively opening large in the embankment, the structure still trapped large quantities of sediment during subsequent storm events. Based upon this observation, work was initiated to investigate alternative means by which the river channel could be constricted to promote the deposition of sediment.

Basis for Design

Conventional sediment traps force water to pond at a set elevation by using a vertical restraint, in most cases this restraint is the spillway crest. Alternate designs were formulated that attempted to create horizontal river constrictions. Thus a ponding area would form behind these structures during high flow periods, when the largest volume of sediment is being transported. During low flow periods water would flow unconfined in its natural river channel.

Two embankment designs were considered. One design utilizes earth and rockfill embankments with an erosion resistant opening located in the center of the embankment through which the river must flow. The other design utilizes H-pile groups that act similar to pile dikes. During low flow periods the river is allowed to flow through the opening between the piles, during high flow periods water is forced to pond upstream. As the water ponds, sediment is deposited. An additional consideration is that fish passage would be underhindered by these channel constrictions since water would flow through them during low flow periods. Two of these structures could be sited approximately one half mile apart in order to evaluate the effects of backwater on the deposition of sediment at the upstream structure. Cross sections of the river channel would be taken periodicaly to monitor the effectiveness of these structures. If test structures function well they could be used at other suitable locations if appropriate.

Large Debris Retaining Structure

Basis for Design

Preliminary cost estimates indicate it would be much more economical to stabilize sediments by trapping them behind a debris retaining structure and leaving them in place rather than the current mode of operation where material is trapped, excavated, loaded, and transported to a disposal site. However, for this measure to be feasible the debris retaining structure would need to be large enough to trap anticipated volumes of material. Analysis of storage volume vs. embankment height curves for several likely damsites revealed that a structure would need to be several hundred feet high to trap all future material expected from the debris avalanche.

One of the most important criteria used in selecting possible sites for a structure of this nature is its nearness to the debris avalanche. By constructing a debris dam close to the debris avalanche, the effects of sediment transport could be localized. Additionally, a site close to the debris avalanche would allow downstream reaches of the river to stabilize more quickly.

Sizing of Embankment

The size of the embankment is dependent upon storage requirements (how much impoundment area is needed to contain the sediment expected to be trasported downstream). Sediment yields are dependent upon hydrologic conditions as well as the rate of stabilization of the upper watershed. An extremely gross prediction of the total quantity of sediment which could be transported down the Toutle River from the debris avalanche is 1 billion cubic yards. It is assumed that most of these sediments would be transported downstream over a period of 10-25 years. It is further assumed that of this total quantity 400 million cubic yards will be of sand sizes and that 400 million cubic yards will be of silt sizes. The remaining 200 million cubic yards would be in the gravel, cobble and boulder size range. Ideally, the proposed dam would trap sand and coarser sizes while allowing most of the silt sizes to pass through the system. Trapping silt at the dam would be counterproductive since, if allowed to freely pass through the system, most of the fine grained materials would eventually be transported to the Columbia River and Pacific Ocean and would thus not impact the Cowlitz-Toutle system. Local topography will dictate the size of the impoundment area which will in turn determine the flow velocities and detention times for the system. If the predicted sediment deposition pattern for any given dam height was not desirable, then appropriate adjustments to the embankment height would be made. Also influencing embankment height are freeboard requirements. Ample freeboard would be provided to protect against the effects of small mudflows or lakes breaching upstream of the dam. Thirty to fifty feet of freeboard from spillway crest to embankment crest is proposed.

Embankment Design

The primary factor in determining embankment design is the availability of construction materials. Since there are plentiful quantities of sands, gravels, cobbles and boulders available in the debris avalanche, these would be likely embankment construction materials. Rock removed from spillway or regulating outlet excavation would also be available. Depending on the results of foundation explorations there would probably be no technical limitations in the construction and operation of a dam in the 200-300 foot range. Proposed embankment cross sections would incorporate as much material from the debris avalanche as possible. Embankment sections would have upstream slope protection zones composed primarily of cobbles and boulders processed from alluvial materials or riprap processed from required spillway excavation. The remainder of the upstream shell of the dam would be composed of granular, relatively free draining material. This could be either rockfill or processed gravels. Since the prime purpose of this dam would not be to hold water but rather to control sediment transport downstream, an impervious core would not be required; therefore, the core zone of the embankment could be constructed of riverrun materials which are primarily silty sandy gravels. The most important feature of the embankment would be the downstream filter zone and the downstream filter blanket underneath the downstream shell of the dam. This would act as a chimney drain and would possibly need to be constructed with one or two stage filters in order to provide adequate drainage downstream and prevent the phreatic level within the downstream shell from rising. The downstream shell of the embankment outside of the filter zones and drainage zones would be of random materials. Riverrun gravels which are plentiful near the proposed damsites could be utilized in the downstream shell. Some slope protection of the downstream shell would be required for control of erosion.

Outlet Works

Preliminary analyses indicate that outlet works should consist of a regulating outlet with intake tower and/or an emergency type ungated spillway. An outlet works scheme consisting solely of an ungated spillway was considered but was rejected because it would not provide sufficient control over:

a. The volume of water impounded in the reservoir; and
b. The deposition of sands instead of silt in the reservoir.

A reservoir regulation system relying only on a spillway would have control over flows out of the reservoir but not the degree of control that would be provided by an outlet works, which includes a regulating outlet (R.O.) and spillway. If an R.O. were to be used it would need to be designed to allow for large infills of sediment. Variable elevation openings in the R.O. intake tower would allow sediment to be taken from upper levels when lower levels became plugged with sediment and debris. Releases through the R.O. could be controlled to aid in passing silts throught the system. The spillway could be cut in either abutment or constructed of roller compacted concrete through the embankment.

Project Scheduling

Construction of a large debris retaining structure in several stages appears to be the most practical approach to project scheduling for the following reasons:

a. The quantity of sediment which will be transported downstream over a given period of time is not known with great accuracy. A sediment volume versus time curve would need to be developed using sediment transport data. Elevations and length of time between phases would be adjusted as dictated by infill rates into the impoundment area observed. This procedure could save considerable construction monies if it were determined that additional embankment construction phases were not necessary because infill was too small to warrant such construction.

b. Construction of a large debris retaining structure in one or two construction seasons appears to be a very difficult task due to the large quantities which would have to be placed in a relatively confined area during a short time frame.

c. Infill which occurred behind the dam during a two or three phase construction sequence could be excavated and used in the next phase of construction providing a convenient borrow source. The benefits of constructing a dam in several stages appear to outweigh the benefits of building a dam in one construction season. However, one benefit of the one construction season alternative is that constructing the entire embankment at one time would provide significant additional protection against potential catastrophic events which might occur upstream, such as sudden releases from breaking lakes and new mudflows. Any large dam designed would have to take into consideration:

1. Future volcanic risks;
2. Earthquake hazards; and,
3. Potential for mudflows or lakes breaking upstream.

However, by utilizing conservative design procedures and limiting the amount of water impounded behind the debris dam, it would be possible to design a safe, economical structure.

PART II

DESIGN OF OUTLET CHANNELS FOR NORTH FORK TOUTLE RIVER LAHAR LAKES

Background

The debris avalanche filling the North Forth Toutle River Valley formed a barrier to drainage from tributary streams. The most notable drainages blocked were those of Spirit Lake, South Castle Creek, North and South Coldwater Creek, Jackson Creek and numerous smaller drainages. If these impoundments were left untouched, the individual debris dams would eventually fail due to overtopping, piping or liquifaction. Progressive downstream slope failures and erosion would lower the ultimate elevation that overtopping would occur. As overflowing water rapidly downcut through the loose, unconsolidated, cohesionless materials comprising the debris avalanche, a large surge of water would be released.

It was evident immediately following the 18 May 1980 eruption that the impoundment at Spirit Lake posed a potential hazard of unknown magnitude. Preliminary work was performed within days following the eruption to determine the stability of the debris dam retaining Spirit Lake. Methods used to evaluate this potential hazard are presented in a paper by Youd, Wilson and Schuster entitled, Stability of Blockage in North Fork Toutle River, 1980. Failure potential of the blockage was examined for failure by liquifaction, piping and overtopping. This report concluded that the blockage was stable against failure due to piping or seepage through the embankment or slope instability either from earthquake or gravitational forces. Additionally, it was concluded that with Spirit Lake at an elevation of 3,400 feet immediately following the eruption, the lake had 135 feet of freeboard and was not in imminent danger of overtopping, primarily due to the small drainage area (14.2 square miles) directing flows into the lake. After a cursory look at the other large impoundments, it was apparent there was adequate freeboard to allow studying them more closely prior to taking any action. Time vs. filling curves were developed for these lakes. These curves were generated utilizing relatively conservative assumptions to ensure that there would be sufficient time to perform any preventative work should it be required. Development of filling curves consequently assumed average annual precipitation and low infiltration rates due to the devastated, ash covered watershed. Evaporation and seepage losses were assumed to be negligible. Projected and actual filling curves for South Castle, Coldwater and Spirit Lakes are shown in Figure 8.

Evaluation of filling curves indicated that immediate action was not necessary for the major lakes but some of the smaller lakes were filling quite rapidly. The failure of a small debris dam retaining approximately 250 acre-feet of water near Elk Rock, in August 1980, made it clear that if lakes of much larger volume were to fail, the results could be disasterous. The failure of the Elk Rock impoundment is documented in work by Jennings, Schneider and Smith, 1980.

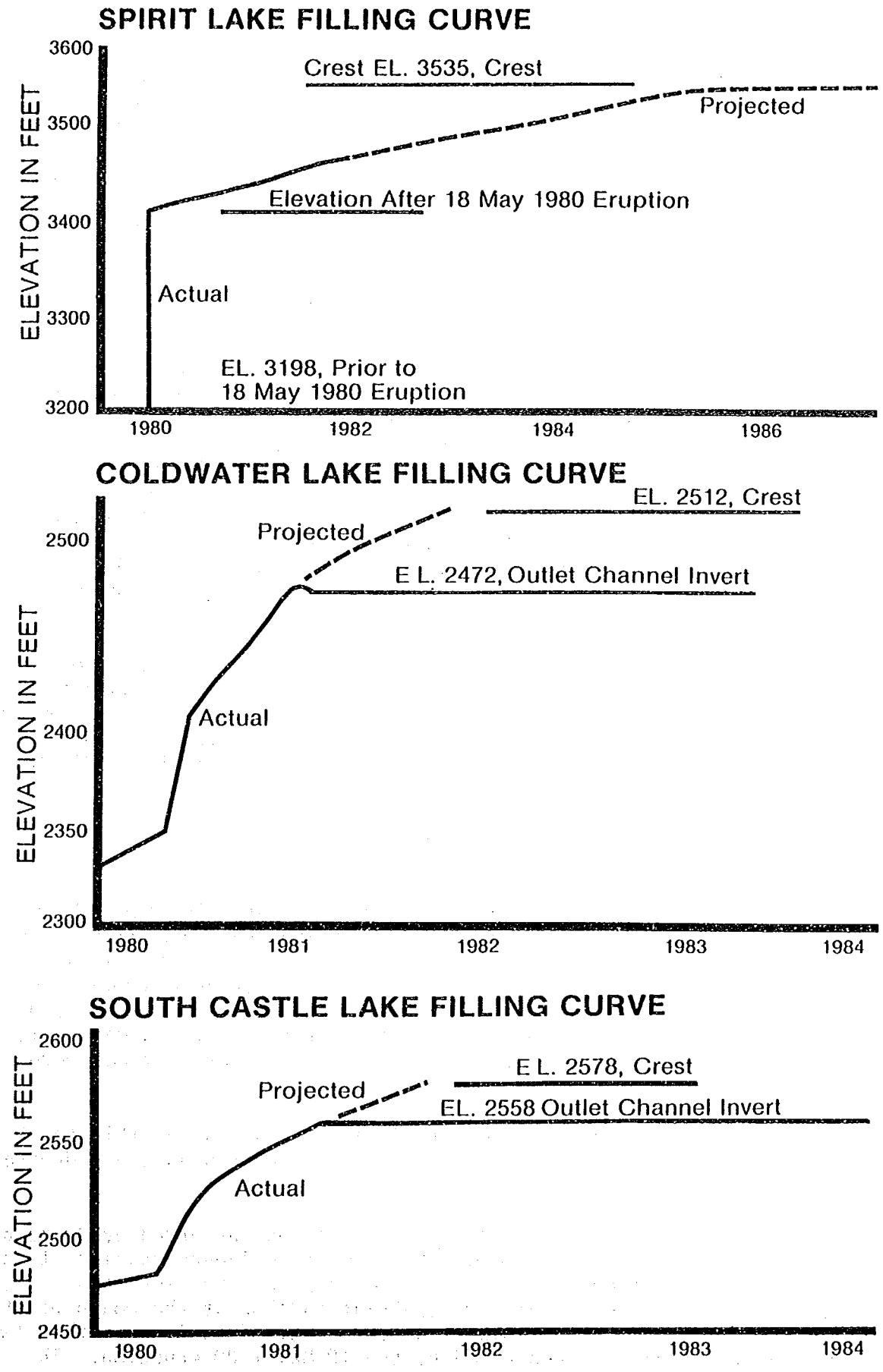


FIGURE 8. FILLING CURVES FOR NORTH FORK TOUTLE RIVER LAHAR LAKES

The failure of this smaller lake near Elk Rock made it clear that work would be necessary to reduce the potential hazard posed by two other small lakes that were rapidly approaching capacity. The intent in breaching these lakes was not to provide a permanent stabilized outlet channel, but to reduce the potential volume of water stored behind them. An outlet was established at Jackson Lake in September 1980 by utilizing a backhoe and D-7 tractor. A 20 foot wide channel with an invert forty feet lower than the embankment crest was excavated at this location. Maximum volume of water stored by the lake, if allowed to fill, would have been approximately three thousand acre-feet. By excavating the outlet channel, this potential volume was reduced to about 870 acre-feet.

Shortly after Jackson Lake was breached, work began to breach another small lake approximately 1/2 mile downstream on the south side of the valley. This unnamed lake contained approximately 20 acre-feet of water. The breaching of this lake was remarkable in that a relatively minor amount of water (40 cfs) rapidly eroded a gaping chasm as it downcut into unconsolidated sediments. Within a period of two hours a notch approximately 300 feet wide and 70 feet deep had been eroded in the oversteepened south bank of the Toutle River. Although a relatively minor event in itself, observation of the accelerated erosion process reemphasized the limited ability of loose, unconsolidated, cohesionless soils stay in place when subjected to high velocity flows.

Based upon these observations and preliminary hazard assessments, studies began to determine the most prudent course of action with regard to the larger lakes due to the large volume of water impounded in each. Maximum potential volume of water impounded at overtopping would be; South Castle - 25,120 acre-feet, Coldwater - 105,000 acre-feet, and Spirit - 522,000 acre-feet.

COLDWATER LAKE

Design studies to provide an outlet channel for Coldwater Lake began in 1980 since the projected filling curves indicated the lake would overtop during the winter of 1982-1983. If any action was to be taken to preclude overtopping it would need to be taken during the spring and summer of 1981 when access to the site could be attained. Winter access was very difficult since hillside erosion of the thick ash deposits quickly plugged culverts which resulted in water ponding, overtopping and eventually destroyed virtually all roadfills.

Five alternatives were investigated during studies to mitigate the hazard posed by Coldwater Lake. Principal features of each plan are addressed below.

1. No Action - Based upon dam break analyses performed by Dunne and Leopold, 1980, as well as independent Corps of Engineers studies, this was not an acceptable alternative. Dunne and Leopold determined that if allowed to overtop, peak discharge of the resultant mudflow at the mouth of the Toutle River would be approximately 500,000 cfs. This is more than twice the discharge of the mudflow generated by the 18 May 1980 eruption. The

consequences of this occurrence could be catastrophic due to the suddenness with which it could occur and the resultant loss of life and property.

2. Drain Lake - This alternative would have required lowering the lake through unwatering and then excavating a deep, channel to intercept the North Fork Toutle River. Although this alternative would have been the most conservative action and would have reestablished the drainage, it was deemed unacceptable due to the large costs involved in dewatering and excavation. Total estimated cost of this alternative was 50 million dollars.

3. High Channel Through Debris Avalanche - This alternative consisted of a relatively high channel through the debris avalanche. This alternative was rejected since it was impossible to get channel velocities low enough to prevent scouring and headcutting without extensive use of channel revetment.

4. Outlet Structure - Cursory investigation of this alternative showed it to be prohibatively expensive to install tunnels, siphons or other structures of the size necessary to pass required flows. These structures would also be prone to clogging, breakage and require continual maintenance.

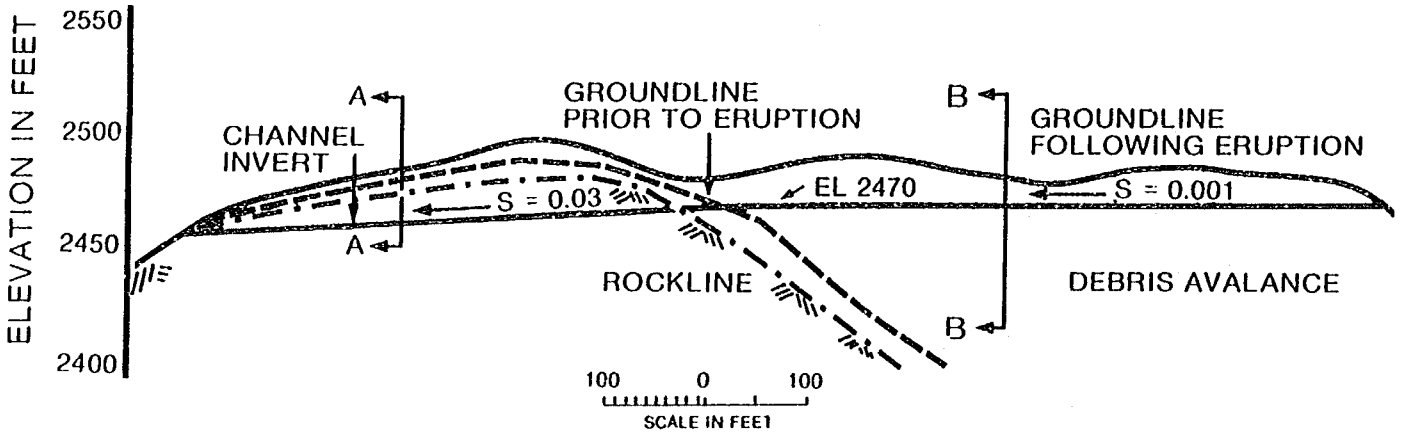
5. Channel Through Rock Ridge - This was the preferred alternative. By excavating a channel across the rock ridge to the west of Coldwater into the Maratta Creek drainage, the problem of headcutting in the outlet channel could be avoided. The cost of this proposal was moderate, $2.22 million, and offered an adequate margin of safety. Specific details of the selected alternative are addressed in the paragraphs below.

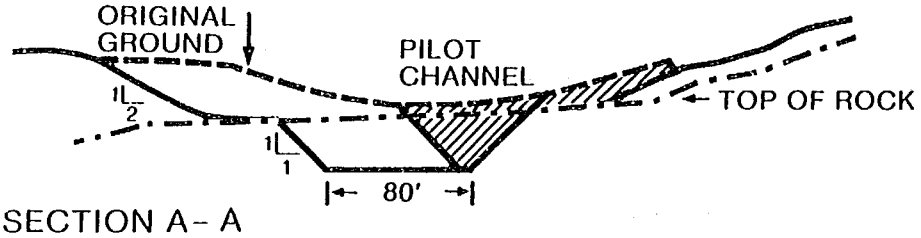
Basis for Outlet Channel Design

After selecting the alternative with the best balance between cost and safety, it was necessary to verify that there was, in fact, adequate rock in the ridge we chose to cut across with the channel alignment.

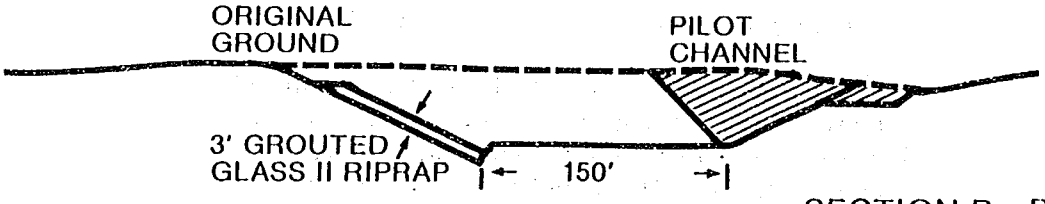
Explorations consisted of 9 core drill borings and several geophysical survey lines in the vicinity of the outlet channel alignment. An additional 8 holes were drilled on the debris avalanche ridge to assess material properties and distribution. Standard penetration tests were conducted in this material to quantitatively determine density of inplace materials. Standard penetration tests indicated that material was relatively loose within 20-30 feet of the surface (< 20 blows/ft) and became denser with depth (40-80 blows/ft). Results may have been skewed somewhat due to the presense of cobble and boulder sized rock fragments in the debris avalanche deposit. Explorations along the channel alignment revealed there was rock of sufficient quality to serve as a spillway for the outlet channel. Profile and sectional views of the outlet channel are shown in Figure 9.

Excavated material from the outlet channel was used to raise and improve the existing debris dam retaining Coldwater Lake. The crest was widened to a minimum of 200 feet at elevation 2520, and 1000 feet at elevation 2500. This provides in excess of 50 feet of freeboard which compensates somewhat for unknowns within the debris dam.





SECTION A - A
NTS



SECTION B - B
NTS

FIGURE 9. COLDWATER LAKE EXIT CHANNEL PROFILE AND SECTIONS

The channel was designed hydraulically to pass the probable maximum flood. Minimum channel width is 80 feet to prevent log jams and resultant blockages from forming in the channel. The surface of the lake was cleared of floating debris to further reduce the risk of log jams.

A pilot channel (see Figure 9) was completed on 6 July 1981 to stabilize lake levels at elevation 2472. The remainder of the channel work was completed in September 1981.

SOUTH CASTLE LAKE

An outlet channel was provided for South Castle Lake in much the same fashion as for Coldwater Lake except there was no rock ridge to cut an outlet channel through.

Alternatives considered included:

1. No Action - This alternative was rejected because it was certain that the mudflow plug would fail and release the water impounded in South Castle Canyon in a manner that would produce limited flooding in the Toutle and Cowlitz basins. Additionally, a large volume of sediment would be released into the Toutle and Cowlitz Rivers.

2. Drain Lake - This alternative would prevent the potential damages of the widespread flood event described above. Work for this alternative would consist of lowering the water surface in the lake by pumping or siphoning to elevation 2468. A deep exit channel would then be excavated connecting a much smaller South Castle Lake to Castle Creek of the North Fork Toutle drainage system. Channel gradients would be low enough to prevent headcutting and subsequent breaching of the lake. Construction cost of this alternative was estimated at $15 million (3.1 mcy of excavation plus dewatering).

3. Exit Channel with Structural Measures to Prevent Headcutting at Elevation 2555 - This plan was considered the only viable alternative to resolve the problem of headcutting through the exit channel and subsequent failure of the mudflow plug currently impounding South Castle Lake. A reinforced channel through the mudflow plug on the east side would control the outflow from the lake. Flows would enter Castle Creek at this point and proceed down Castle Creek's established channel to the North Fork Toutle River. Structural measures to reinforce the exit channel would include riprapping both sides and placing a rock groin on the east side of the exit channel outlet to help divert Castle Creek away from the outlet and prevent erosion and increased gradient at that point. South Castle Lake would also serve as a sediment trap for the 3.2-square-mile drainage area, completely eliminating future excavation costs for this material. Total cost of this alternative was $573,000.

Basis for Design

The outlet channel was designed to pass the probable maximum flood. Since headcutting in the outlet channel could not be prevented, the objective

of the design was to control the rate of erosion. A very flat channel gradient (0.005) was used. Additionally, the left side of the channel (toward the mudflow) was heavily revetted to prevent lateral widening of the breach. Additionally, the channel cannot widen to the right since original ground rises abruptly in this direction. By laterally restraining the breach in this manner, headcutting is confined to the vertical direction and with the thalweg of Castle Creek the same as the outlet channel, the two channels should aggrade or degrade at roughly equal rates.

The South Castle Lake exit channel was completed during the summer and fall of 1981. While presently in good condition, there is still concern that significant changes in channel configuration in the drainages in front of the debris dams retaining Coldwater and South Castle Lakes could reduce the stability of the impoundments. Monitoring of these lakes should be continued in the future until the drainages on the debris avalanche have stabilized.

SPIRIT LAKE

Studies are currently underway to determine the need for a controlled outlet from Spirit Lake. If this assumed need is valid, possible solutions include construction of an outlet channel similar to those at Coldwater and South Castle Lakes or construction of a diversion tunnel into the North Fork Toutle River or into drainages west of the mountain.

Preliminary studies are expected to be completed in January 1983.

CONCLUSION

Some of the temporary measures taken to control sedimentation within the Toutle/Cowlitz/Columbia River system have met with limited success. What began as an emergency response to control short-term flooding must now be viewed as a long term project. The three cubic kilometers of material deposited in the North Fork Toutle River Valley will eventually be eroded from the debris avalanche. Current projections indicate that under normal hydrologic conditions, 20-25 million cubic yards of sandload will be delivered to the Cowlitz River during the next year. If no action is taken to stabilize sediment sources within the Toutle River Valley or remove infill from the Cowlitz River, within a period of five years, it is estimated that the condition of the Cowlitz River will approach those immediately following the May 1980 eruption.

During the next year, hydrological analyses of the potential sedimentation problem will continue to be refined as additional data becomes available. Concurrent with the hydrological studies and sediment transport modeling work that is being conducted, engineering studies will be made to determine the most effective and environmentally acceptable ways to stabilize sediment.

Additional work is necessary to insure that existing measures taken to provide controlled outlets for lakes near the debris avalanche are maintained in good operating condition. Monitoring programs need to be continued until such time the North Fork Toutle River has stabilized.

Plans to stabilize Spirit Lake, if required, need to be implemented at the earliest time in order to stabilize the lake at a level that will give an adequate degree of freeboard and resultant safety.

REFERENCES CITED

Crandell, D.R. and Mullineaux, D.R., 1978, Potential Hazards from Future Eruptions of Mount St. Helens Volcano, Washington: U.S. Geological Survey Bulletin 1383-C.

Dunne, T. and Leopold, L.B., 1981, Flood and Sedimentation Hazards in the Toutle and Cowlitz River System as a Result of the Mount St. Helens eruption: Federal Emergency Management Agency, Region X.

Jennings, M.E., Schneider, V.R. and Smith, P.E., 1980, Computer Assessments of Potential Flood Hazards from Breaching of Two Debris Dams, Toutle River and Cowlitz River Systems.

U.S. Army Corps of Engineers, Portland District, July 1981, Long Term Program for Cowlitz and Toutle River Basins; Portland, Oregon.

Youd, T.L., Wilson, R.C. and Schuster, R.L., Stability of Blockage in North Fork Toutle River, 1980.

Countermeasures for Debris-flow Disasters in Volcanic Areas

NOBUO ANYOJI*, YASUO TOMOMATSU**, and HIROSHI SUZUKI*

ABSTRUCT

Countermeasures for debris-flow disasters in volcanic areas are important problem for national land conservation in widely cultivated land of Japan.

The objective phenomena on countermeasures for debris-flow disasters are not direct movements from destructive eruption but secondary movements from erosive materials on volcanic mountain side, in this paper.

The classification of mass-movements areas suggests us to take measures with their charactristics of each motion. The mountain side is classified into four sections, 1) Resources of sediment yield area, b) Sediment transporting area, c) Flooding area, d) Downstream area.

Sediment budgets are made by forecasting of sediment motions and estimation of their volumes in each classified section. They should make erosion control countermeasures.

Authors present the process and method of sediment control measures to prevent debris-flow disasters in volcanic areas. And we think that establishment of sediment control measures is important and urgent.

* Sabo Technical Center

** Sabo Division, Sabo Department, River Bureau, Ministry of Construction, Japan

INTRODUCTION

Japan is one of the countries where have plenty volcanos in the world, and many mountain sides have been developed for cultivation and habitation, because she is densly populated in mountainous national land. Particularly, volcanic mountain side has gentle slopes and then people have cultivated there for long time. The volcano, when it has been dormant, is not so disastrous, but when it has been active, it is more dangerous than any other ordinary mountains. Volcanic loose sediments are easy to move and movements occur frequently to grow up larger in scale.

We have to make countermeasures on those volcanic areas to protect plowed land, habitants and constructions from debris-flow disasters. But we cannot make them against destructive volcanic actions. We only make them against the secondary sediment movements.

Authors have been making Sabo (erosion control) plans, and suggested their works by understanding of comparison among erosion, motion and sedimentation, and by estimation of their volumes, in some volcanic areas in Japan, Philippines and Indonesia.

This paper shows the process for making countermeasures for debris-flow disasters and examples of facilties at some practical places.

ACKNOWLEDGEMENT

We would like to thank several committees that had made some pertinent suggestions to Sabo Planning in volcanic areas. Dr. Saburo Higashi and Dr. Aritsune Takei were chairmen of some committees. And a lot of researchers and engineers of Sabo engeneering or relative fields had given us beneficial advices. We thank them, too.

DISASTROUS SITES

There are many disastrous sites of volcanic debris-flow. They are shown in Fig. -1. They are region where debris-flow disasters have occured directly caused by volcanic action, and are dangerous areas of debris-flow.

Now, authors will mention several principal mountain sites as follows;

1) Mt. Tokachidake (Hokkaido): In May, 1926, the mountain had explosed. Then the mountain slope near the crater had been destructed (about 2 million cubic meters volume), and mudflow had run down the slope rapidly. It had been occured by sudden snow melting due to hot ejecta, and it run down toward Kami-Furano Village, where was about 20 km far from the crater, for about 40 minutes, with 144 dead (Fig. -2). Because the mountain has been acting for about thirty or fourty years cycle, we expect there should be dangerous area of volcanic mudflow.[2)]
2) Mt. Usu (Hokkaido): The mountain has erupted many times and disasters have been occured at the same time. We attend to the mountain desolated by 1977's ejecta and many erosion control facilities have been constructed in this area since the mountain had been acting (Fig. -3).[3)]
3) Mt. Sakurajima (Kyushu): This is one of the most active volcanos in Japan. Torrents around the mountain have been frequently discharging massive ash, pumices and boulders into the Kinko-wan Bay every rain fall. Sometimes Lava-flows run over villages and habitants at the time of explosion. The mountain have been being desolated by frequent ash fall, surface erosion and sediment discharging (Fig. -4).
4) Others: There are hundreds volcanos in Japan. They are almost dangerous areas of debris-flow disasters. Some of them are Mt. Iwaki, Mt. Komagatake, Mt. Myoko, Mt. Nantai, Mt. Asama, Mt. Yake, Mt. Fuji, Mt. Tateyama, Mt. Hakusan, Mt. Daisen (all in Honshu), Mt. Aso and so on. They are active, extinct or dormant.
5) South East Asia: There are the most active volcanos in the circum-Pacific volcanic zone in South East Asia that are Philippines and Indonesia. Some of them are Mt. Mayon (Philippines), Mt. Merapi, Mt. Kelud (Indonesia) and so on. Especially, Mt. Merapi was investigated and have made countermeasures on debris-flow disasters by the government of Indonesia and Japanese consultation and cooperation.[6)]

PROCESS FOR MAKING DEBRIS-FLOW DISASTERS COUNTERMEASURES

Object

Authors classified volcanic disasters;

a) Explosionally mobilized sediment by eruption (ex. volcanic mudflow, pyroclastic flow, Nueé Ardente etc.)

b) Secondary movement of volcanic materials (ex. mudflow, debrisflow, etc.)

a) is so massive and destructive that it is impossible to prevent artificially. Another b) is comparablly easier to control sediment moving than a), and it has an ability of arrest motions and control sediment to make Sabo (erosion control) plan. So, the disastrous motion described in b) is the objective phenomena for making debris-flow disasters countermeasures in this paper.

Scale of objective movements

The motion of sediment should be presumpted but their volume should be embarrassingly to estimate. For making sediment control facilities, it is necessary to estimate the volumes of sediment motions.

In ordinary Japanese Sabo Plan, the plan scale is usually set up as the probability of sediment motion that is analyzed by statistical method. But in volcanic areas, the motion and scale of sediment are so accidental that it is difficult to forecast. Then we often use the scale as the maximum volume that had been occured in disasters last time we are able to know. The plan scale is established by investigations of basinary sediment in some practical methods.

Classification of basin by charactristics of mass-movement

The movements should be classified as geomorphological area in the basin, as follow.

a) Resources of sediment yield area: This area spreads widely around the mountain side. Particularly steep hillside slope and torrents are main resources of sendiment yield. Scars of landslides, rill and gullies are spreadly distributed and torrents are devastated in unstable sediment.

b) Sediment transporting area: Principally in gullies or torrents, sediment run through as mass-movement or bed-load transport.

c) Flooding area: The first flooding area in the basin is often alluvial fans where mass-movement, for example debrisflow, decreases the energy rapidly, then sediment gradually deposits on the fan surface. And debris cone, with boulders, cobbles and fine grained matrixes, is formed there. Lately, because developement of alluvial fans are progressingly increasing, the dangerous indication of debris-flow disasters augments rapidly.

d) Downstream area: Flood flows down including fine grained soil in the channel where ordinary water infiltlates under the surface. Sometimes there are indistinct channel forms in cultivated areas.

COUNTERMEASURES FOR SEDIMENT CONTROL

Measures in classified areas

Above mentioned four areas have defferent mechanism of motion to each other. Then after forecasting of sediment motional quality and quantity, countermeasures for sediment control would be made.

a) Resources of sediment yield area: It is necessary for making measures to suppose the volumes of sediment yield in the plan scale. They are estimation of erosive volumes on slopes and scouring volumes in channel beds.

b) Sediment transporting area: It is necessary to estimate scouring volumes in gullies, torrents beds and banks. Quantity of discharge and valley capacity of sediment transport are necessary to be culculated, too.

c) Flooding area: In this area, flooding flow direction, sediment depositting range and their volumes should be supposed.

d) Downstream area: Peak flow rate and sediment concentration of flood should be made sure of, and determination of channel capcity at the planned scale time should be, too. (Fig. -7).

Calculation of sediment budget

We have defined that sediment budget is in-and-out sediment yield and discharge in each torrential section after estimaing of their volumes. The planner makes its flowchart in case of

before the constructions of facilities, present time and after the plan.

At first, we divide the basin to some sections considering sediment motions charactristics. Next we estimate sediment volumes, which are yield, deposit and discharge, in each section.

The relation of them are shown as follow (Fig. -8);

$$V_{out} = (V_{in} + V_y) - V_d \tag{1}$$

where, V_{out} : sediment discharge volume to downward section

V_{in} : sediment discharge volume from upper section

V_y : sediment yield volume in the section

V_d : sediment depositional volume in the section, not to discharge

Sediment yield volume is an addition of erosive, collapsing and moval volumes in the whole unstable sediments of slopes and torrents. Practical surveyed factors, for example which are depth, width and volume of sediment yield, suggest to the calculation. Table-2 shows the slope erosed volume by rill erosion in erupted devastational site of Mt. Usu, Hokkaido.[1] The plan volume of sediment yield have been made to refer them.

Torrential movements volumes are estimated by investigation of river bed forms, which are talus, terrace, alluvial cone and fan, and their scale is suposed by the informations from past sediment movements.

It is difficult to forecast slope collapes site and volume, but we should be able to estimate them by aerophoto-readings and statistical analysis.

There are two ways to calculate sediment discharge volume. One is estimating deposit volume (V_d), and subtracting (V_d) from (V_{in} + V_y). Another is calculation of hydraulical sediment discharge volumes by some experimental formulas.

Hydraurical sediment discharge volume is often calculated by Brown's formula in volcanic areas.

$$\frac{q_B}{U_*^d} = 10\left\{\frac{U_*^2}{(\sigma/\rho - 1)\, gd}\right\}^2 \tag{2}$$

where, q_B : sediment transport ratio per unit width of flow

U_* : friction velocity

d : grain diameter (m)

σ : density of grain

ρ : density of water

g : gravitational acceleraation (9.8 m/sec^2)

This formula is roughly conformable to practical sediment discharge volume observed at Nojiri River, Mt. Sakurajima,[5] where high muddy concentrated flows often run through after rain fall.

It is essential to estimate sediment volumes of each factors in the sediment budget calculation. Particularly, estimation of sediment discharge volumes is the most important and perplexing to suppose, because it runs down toward the preserve areas to be disastrous and its motion has not been recognized in details to us.

Then, the sediment motion is supposed to refer practical flood data, which are observed flow concentration and hydrological factors.

Table-3 shows the mudflow volume concentration observed at several points along Sohbetsu-Onsen River, Mt. Usu, Hokkaido in 1979.[3] Cd, that means volume concentration of mud in the mudflow, indicates from 0.181 to 0.534 in the table.

The hydraulical theory of them may be concerned as follow discription.

Authors consider about flow rate in the mudflow to add not only running water from upper stream, but also pore water from bed layers at the time of the mudflow starts to move.

The law of conservation energy of running water and stable sediment before and after making fluid is shown in equations (3) and (4),[7] where fluidizing layer depth of bed is "D", depth of mudflow is "h", and pore water saturation is "s".

water : $q \equiv Uh(1 - C_d) = q_0 + UD(1 - C_*)\, s$ (3)

sediment : $q_s \equiv UhC_d = U\, D\, C_*$ (4)

where, U : velocity of mudflow

C_d : volume concentration of mud in the muflow

C_* : volume concentration of sediment on the bed

q_0 : water ratio per unit width of flow

q_s : sediment transport ratio per unit width of flow

Total ratio per unit of flow (q_T), added water and sediment, is led from equations (3) and (4).

$$q_T = \frac{C_*}{C_* - \{S + (1-S)\, C_*\}\, C_d} \cdot q_0 \tag{5}$$

When the motion starts, authors make assumption that the pore of layers is fillful with water, then $S \fallingdotseq 1$, equation (5) is transfered as equation (6);

$$q_T = \frac{C_*}{C_* - C_d} \cdot q_0 \tag{6}$$

The relation between C_d and q_T/q_0, in the case of parameter C_* = 0.5, 0.6, 0.7, is shown in Fig. -9.

Authors consider the maximum mudflow concentration might be about 30% by the results of observed data and hydraulical examination.

An example of sediment budget flowchart is shown in Fig. -10, planned in Showa River, Mt. Usu, Hokkaido.[3)]

COUNTERMEASURES WORKS

Countermeasures by facilities costruction

The planner investigates applicability of works to control sediment after making the sediment budget flowchart.

Our often planning and constructing countermeasures works are shown as follow;

a) Resources of sediment yield and sediment transporting areas: There, we often make hillside works to prevent slope erosion and denudation. They are often fence works of wood, braided twigs or metal plates, and sometimes packed soil sacks set on the slopes with step cutting, usually attending planting works. They are effective for surface erosion but ineffective for collapse, slide and slump on slopes. It is difficult to prevent whole motions on talus or scars of landslides, then we often make the foot fixing works to keep their feet scoured. In torrents, continuous arranged check dams (step dams) are very effective to prevent downward and lateral erosions.

b) Flooding area: On alluvial fans, we plan the check dams to control irregular lateral changing of debrisflow course at the fan apex, a series of cross dikes (cross consolidation dams) to prevent fan surface erosion and to make boulders and cobbles separate from debrisflow to deposit them on the surface, and training levee to protect overflowing besides the fan. Further a large scaled sand pocket downstream of the fan is effective to trap smaller cobbles, that are transported on flood, in larger sediment discharge. However, it is necessary to maintain that is periodical artificial sediment excavation from the pocket or transfer of the pocket site.

c) Downstream area: We usually make the plan of open channel works and have constructed them there, in where we should make flood run through safely, not to overflow.

Disasters forecasting, warning and evacuation systems

It is important to make countermeasures not only by technological facilities but also by sociological systems.

The social countermeasures systems indicate some important forecasting informations. They are disastrous informations of volcanic activity and meteological prospect. Another hands, settlement of warning and evacuation systems, and also transfer of habitants and residences from the dangerous area, are very important to prevent debrisflow disasters.

EXAMPLES OF FACILITIES

Some examples of practically constructed facilities are shown in some pictures, which were taken at the site of Mt. Usu, Hokkaido, from 1977 to 1982.

The facilities for mudflows were made of steel frameworks packed with boulders, concrete or steel sheet piles, because ground fluctuation had been continuing by volcanic action. And there, an aerial seeding works by helicopter attended by hillside works have been gotten great success to prevent surface erosions by Forestry Conservancy Works. In torrents, a plenty of check dams were constructed by Sabo Works or Forestry Conservancy Works. And on fans along the shore of Tohya Lake, which is Tertiary caldera lake, open channel works were made to prevent overflowing of flood and make flood run down safely.

CONCLUSION

Authors have made some countermeasures for debrisflow disasters in volcanic areas, and we discribed how to make them in this paper. The conclusion of our insistence is mentioned as follows.

1) Many disastrous volcanic sites are distributed in Japan, Philippines and Indonesia, that are included in circum-Pacific volcanic zone. In some area of Philippines and Indonesia, Japanese Sabo engineering has been applied for prevention and control of debrisflow disasters.
2) Mass-movements in volcanic areas should be divided in two phenomena, one is destructive large scale movement with eruption, another is secondary movement of volcanic erosive materials. The objective phenomena which would be able to make countermeasures are secondary movement in this paper.
3) The movements should be classified as geomorphological areas to understand their characteristics of motions. Resources of sediment yield area is mountain slopes, torrents beds and banks. Sediment transporting area is gullies and torrents. Flooding area is usually alluvial fans and downstream area continues them.
4) Countermeasures of sediment control should be made by understanding of characteristics of motions in each classified areas. To make measures, it is necessary to suppose and estimate each motional scale and sediment volumes. Then, calculation of sediment budget would be made to plan the countermeasure works.
5) There are some methods to suppose factors of sediment budget. Practically investigated data suggest to suppose the volumes of sediment yield, deposit and discharge. And hydraulical analysises support the planned volumes of them.
6) Countermeasures works for sediment control are made by above mentioned methods to protect preserve areas from debris-flow disasters.
7) At last in this paper, authors introduced some practical sediment control facilities made around the mountain side of Mt. Usu, Hokkaido.
8) Countermeasures for debris-flow disasters in volcanic areas have been grown by Japanese investigations and practices. Sabo engineering has not been enough to control disasters, but it has taken many examples in active, extinct or dormant volcanos, and Japanese Sabo engineering is useful to another countries erosion control measures applying our experiences.

REFERENCES

1) Anyoji, N., 1979, Study on Sediment Discharge in Mountain Basins (Japanese description), Thesis for a Master of Agriculture, Hokkaido Univ.

2) Engineering Office of Asahigawa and Sabo Technical Center, 1980, Report on Sabo Control Plan in Frano River (Jap.)

3) Engineering Office of Muroran and S.T.C., 1980, Report on Geomorphological Survey in Sobetsu-Onsen River, Mt. Usu (Jap.)

4) Higashi, S., 1982, Series of Cross Dikes Works Method—Theory of Prevention for Debris Disasters (Jap.), Hokkaido Univ. Press

5) Ikeya, H., and Uehara, S., 1978, Experimental Report on Hydraulical Model in Nojiri River Channel Works, Mt. Sakurajima, Report of the Public Works Research Institute, Ministry of Construction, Japan, No. 1442

6) Mt. Merapi Project, 1980, Volcanic Debris Control in the Mt. Merapi Area, Ministry of Public Works, Indonesia

7) Takahashi, T., 1977, A Mechanism of Occurrence of Mud-Debris Flow and Their Characteristics in Motion (Jap.), Disaster Prevention Research Institute of Kyoto Univ., No. 20B-2

8) Takei, A. and others, 1980, Landslide, Collapse and Debrisflow—Their Forecasting and Countermeasures (Jap.), Kajima Press Co.

Table-1 Classification volcano in motion

AREA	MATERIAL	MOTION
a)Resources of sediment yield	tephra pumice lava-fragment	erosion excavation slide collapse
b)Sediment transport	boulders cobbles fine grained + water	debris flow mud flow
c)Flooding		
d)Downstream	fine grained + water	flood

Table-2 Process of slope erosed volume by rill [1)]

surveyed date	mean depth (cm)	mean width (cm)	numbers of rills (/ m²)	estimated volume of the basin (m³)	(m³/km²)
Sep.16,'77	4.0	5.0	5	6000	(10000)
Oct.17,'77	5.0	6.0	4	7000	(12000)
Jul.4,'78	4.0	7.0	4	6000	(11000)
Oct.5,'78	20.0	13.0	2	29000	(52000)
Nov.2,'78	20.0	15.0	2	34000	(60000)

Basin area: 0.565 km²

Table-3 Volume concentration of mud in mud flow [3)]

picked up site	Wb	Wd	Mc	Mp	Cd
1.30m upper from the slit dam	1308	487	821	63	0.181
2.In the pocket of slit dam	3192	2441	781	24	0.534
3.20m down from the slit dam	1712	872	840	49	0.278
4.Main stream(1)	2488	1590	898	36	0.397
5.Main stream(2)	2058	1260	798	39	0.370
6.Discharge point to No.1 dam	1685	854	831	49	0.274

where; Wb:weight of a backet of mudflow(g)
Wd:dried weight of mud(g)
Mc:moisture content(g)
Mp:moisture percentage(%)
Cd:volume concentration of mud
density of grain: 2.69 g/cm³

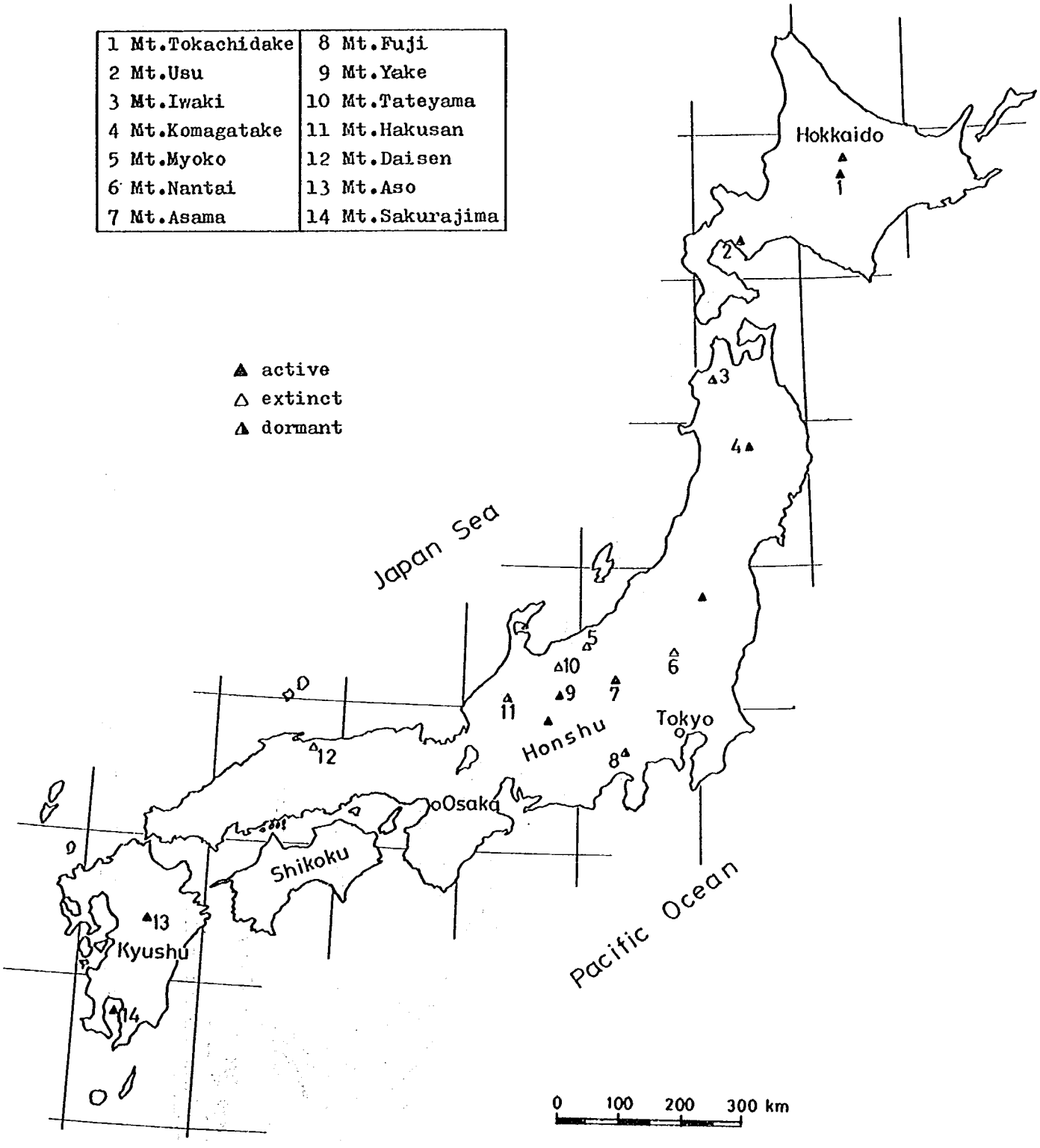


Fig.-1 Distribution of Volcanic Disastrous Sites in Japan

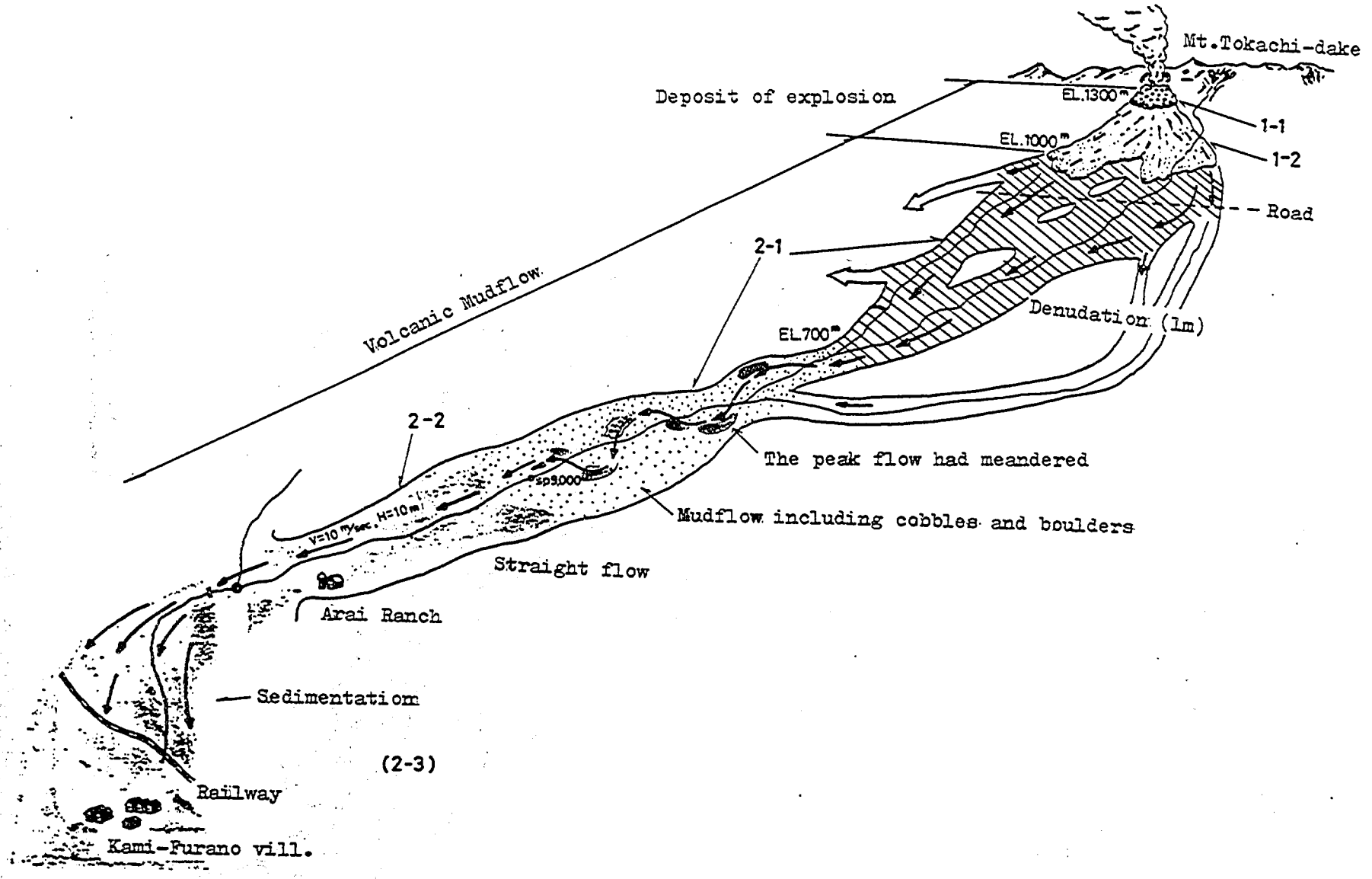


Fig.-2 1926 Volcanic Mudflow at Mt.Tokachidake, Hokkaido

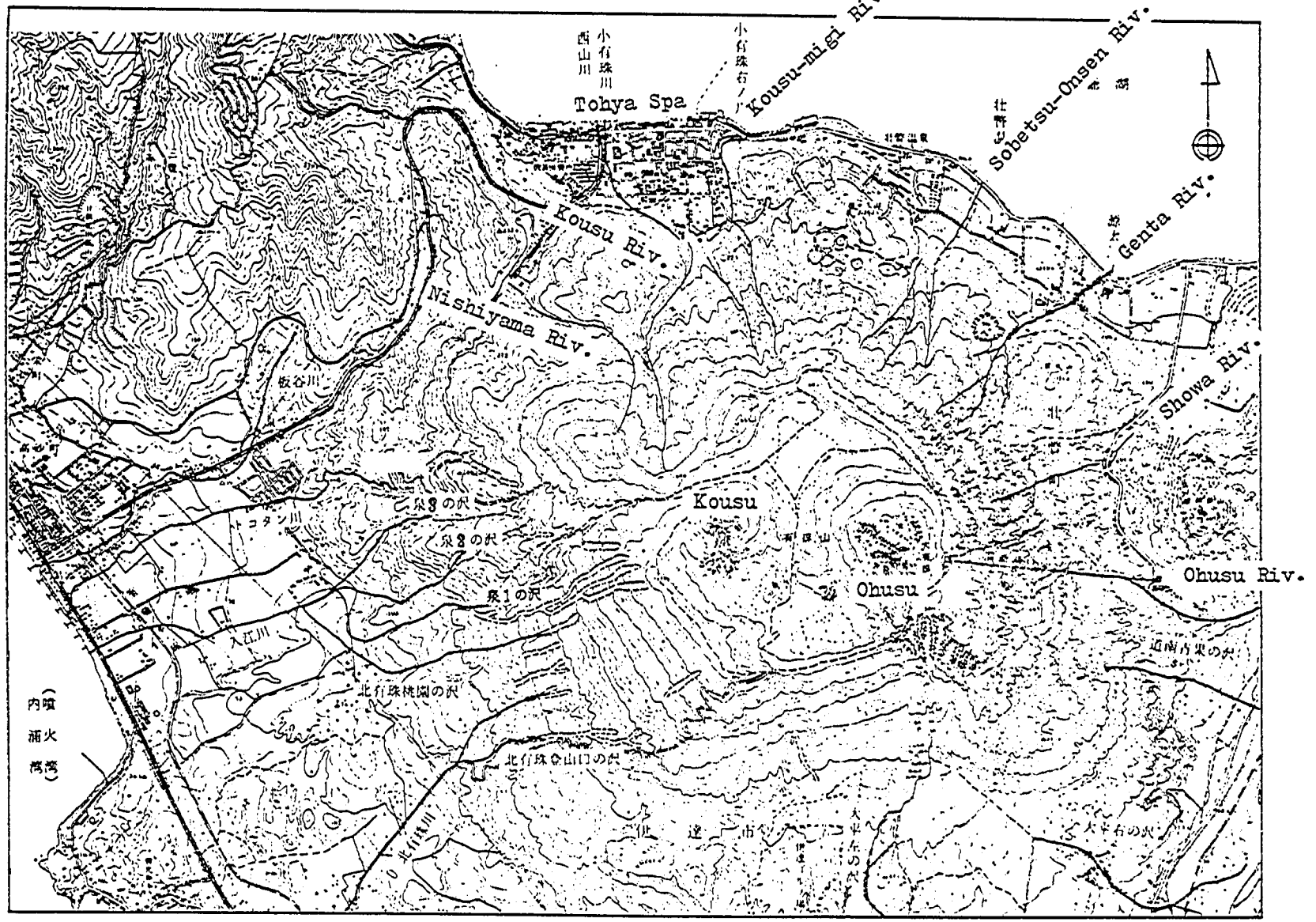
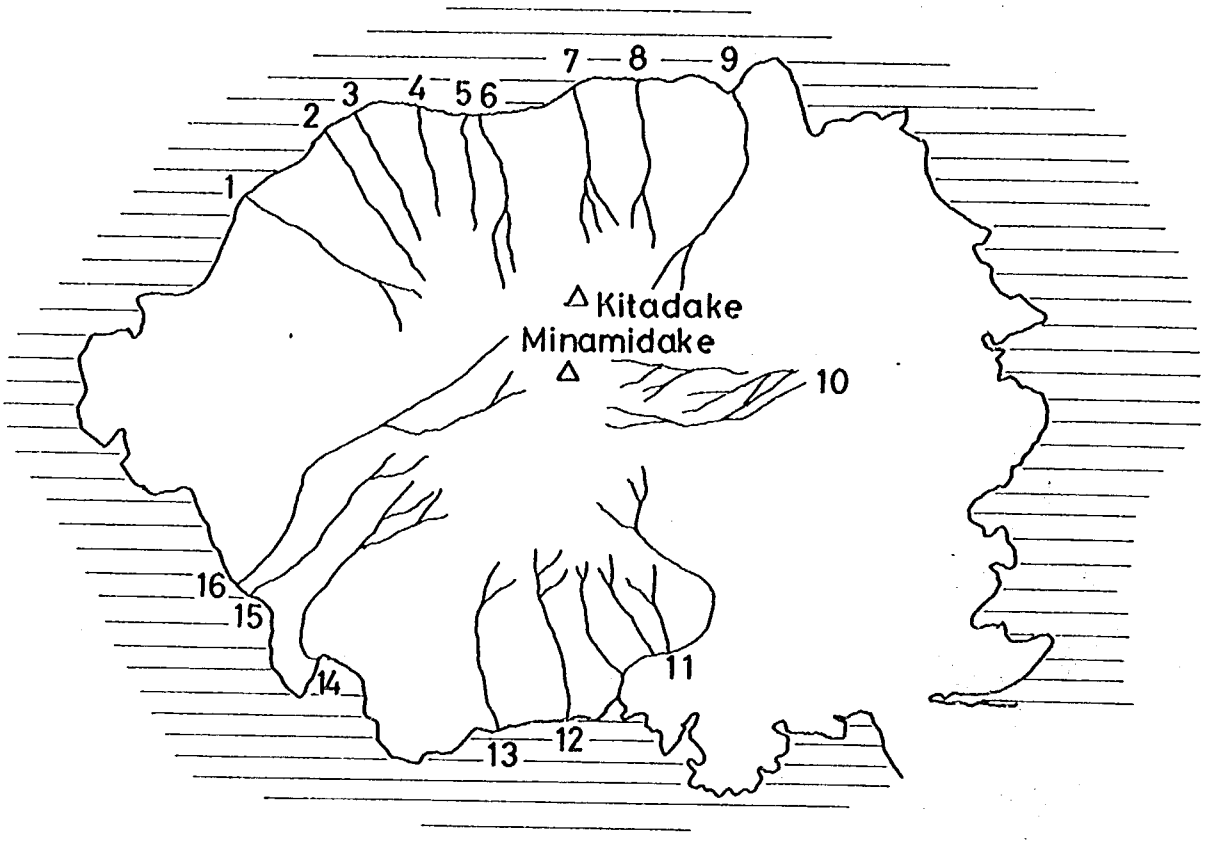


Fig.-3 Location Map of Mt.Usu,Hokkaido



1 Hase Riv.	9 Fukura Riv.
2 Fukatani Riv.	10 Kurokami Riv.
3 Nakatsuno Riv.	11 Arimura Riv.
4 Kanatoko Riv.	12 Furusato Riv. No.2
5 Nishimoto Riv.	13 Furusato Riv. No.1
6 Saido Riv.	14 Mochiki Riv.
7 Matsu-ura Riv.	15 Harumatsu Riv.
8 Amida Riv.	16 Nojiri Riv.

Fig.-4 Debris Disastrous torrents in Mt.Sakurajima

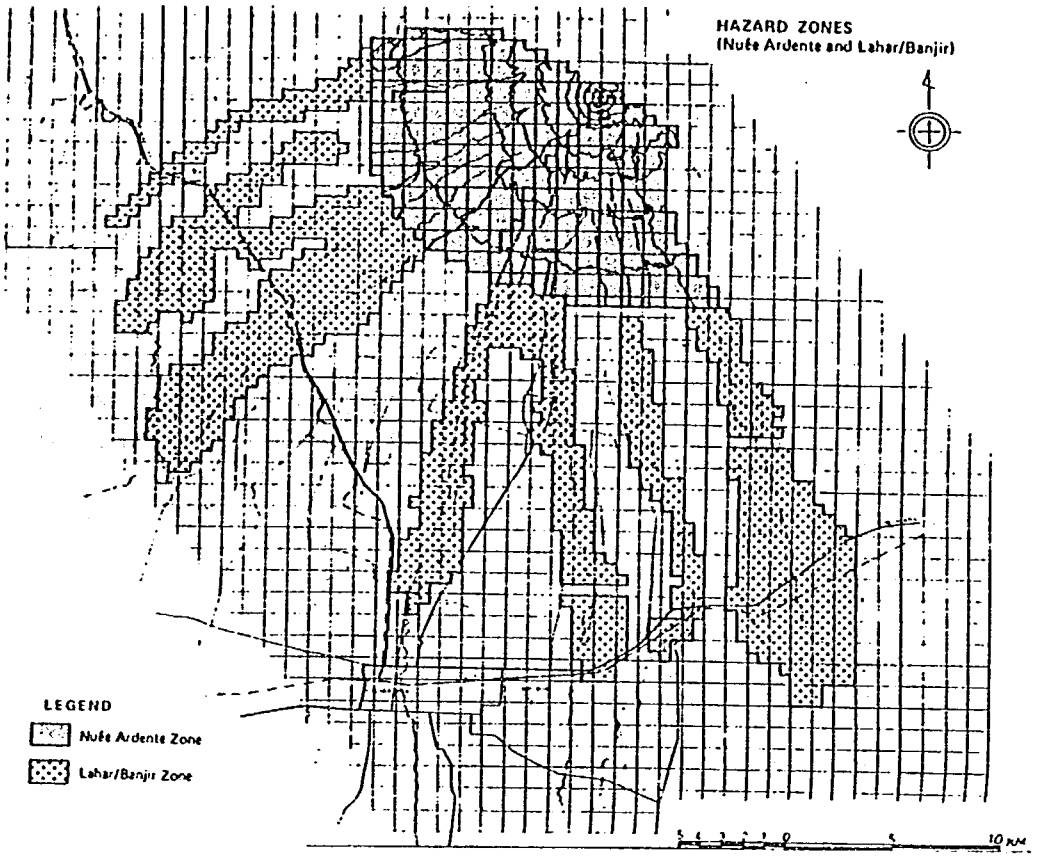


Fig.-5 Hazard map of Mt.Merapi,Indonesia [6]

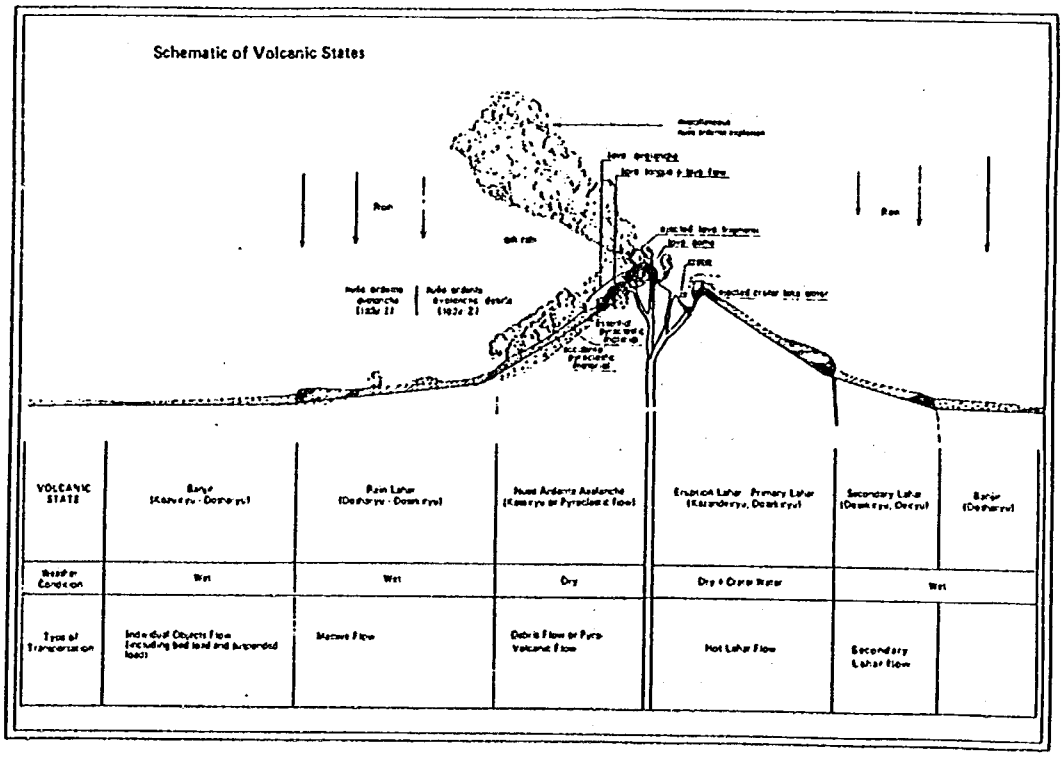


Fig.6 Classification of Motions in Volcanic Area [8]

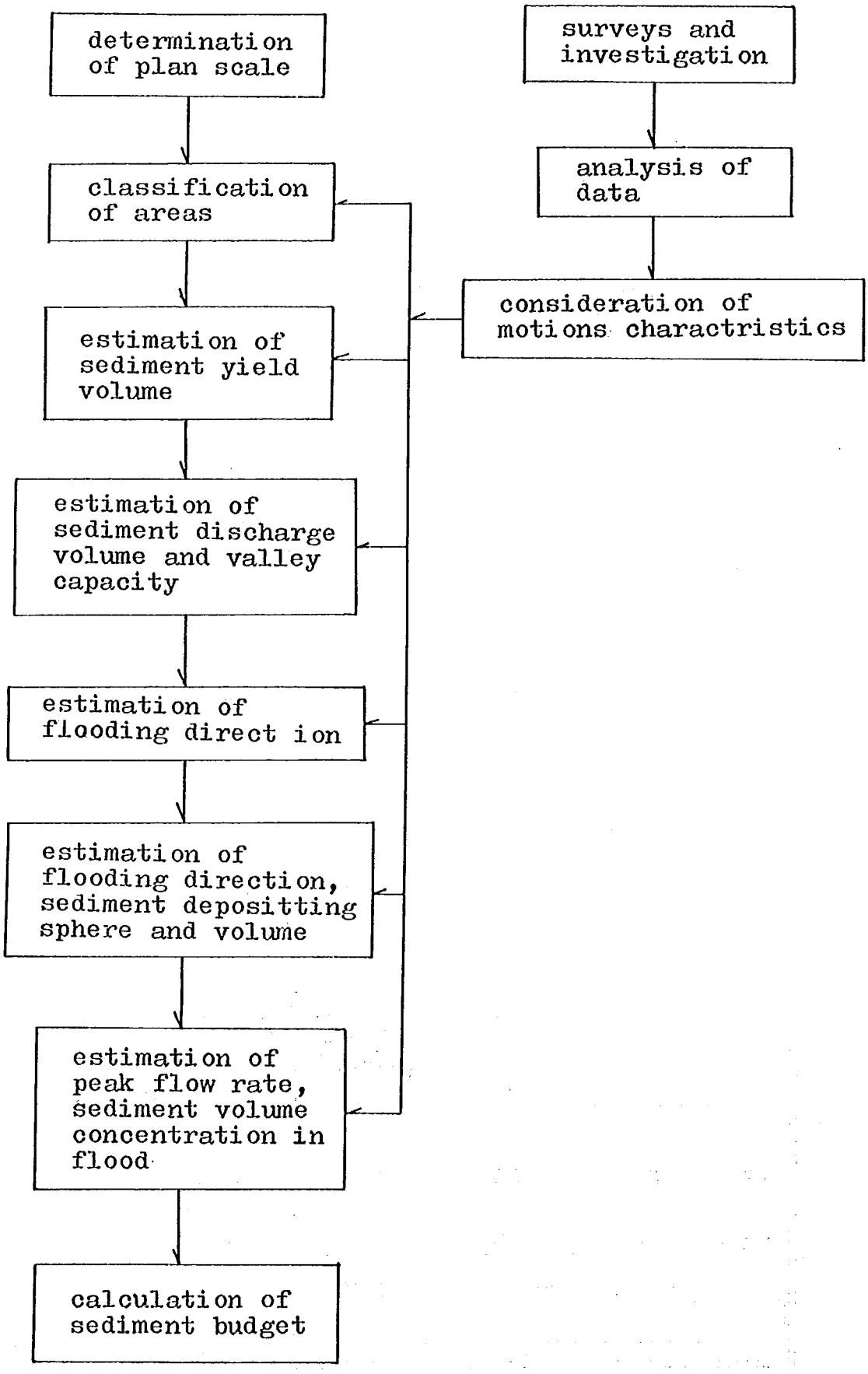
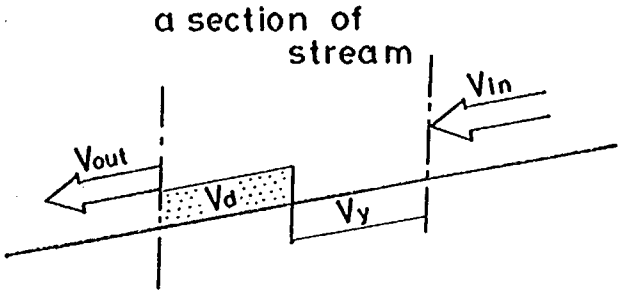


Fig.-7 Flowchart on Process of Coutermeasure



Vout=(Vin + Vy) - Vd

Vout: sediment discharge volume to downward section

Vin : sediment discharge volume from upper section

Vy : sediment yield volume in the section

Vd : sediment depositional volume, not to discharge

Fig.-8 Sediment Budget Definition

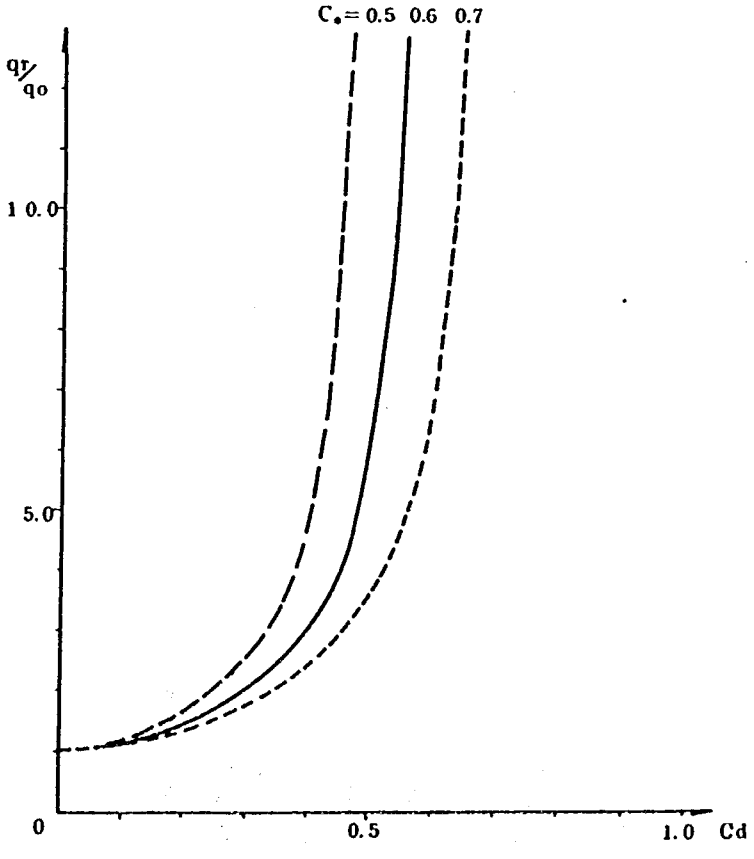


Fig.-9 Relation between Cd and q_T/q_o

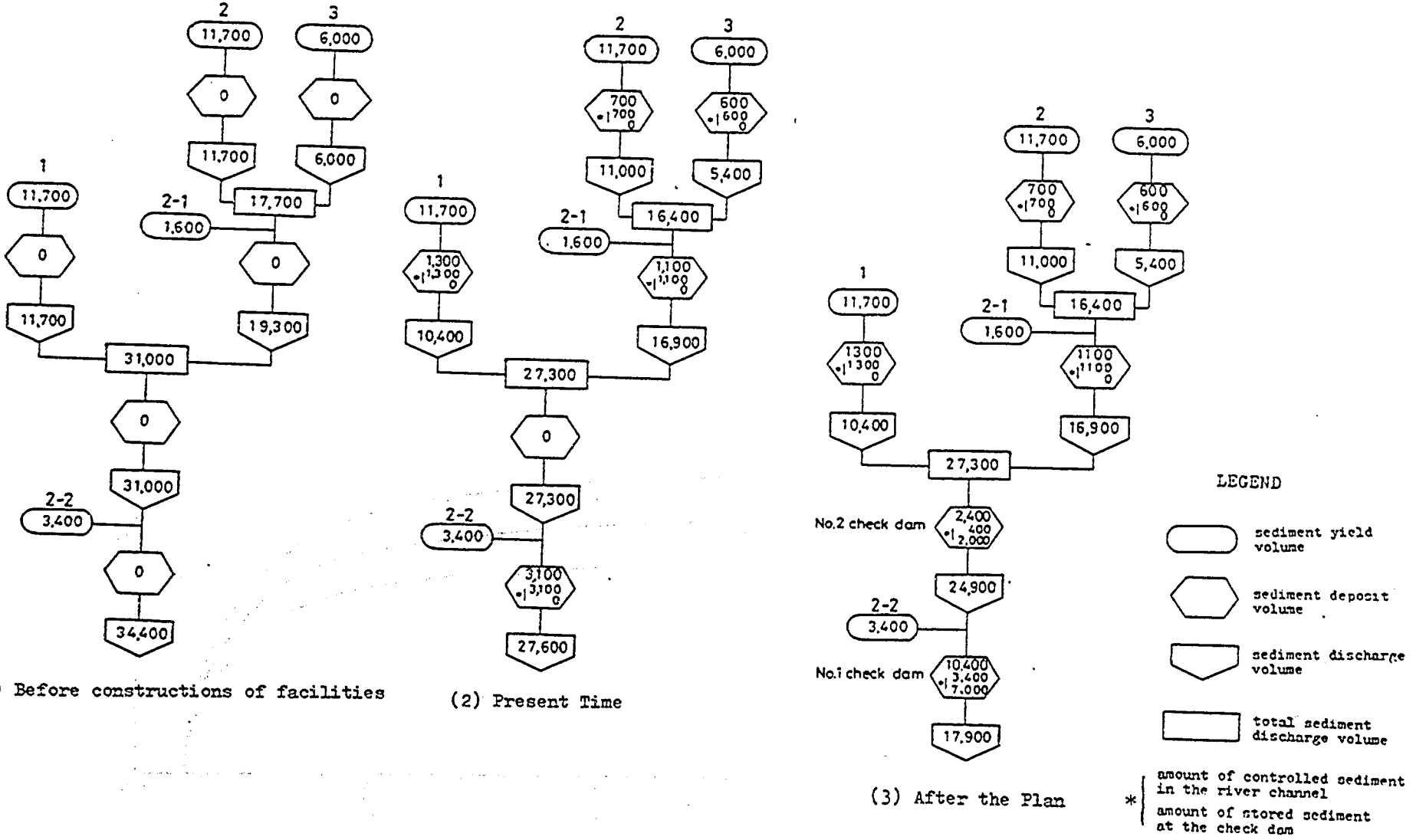


Fig.-10 Sediment Budget Flowchart in Showa Riv.,Mt.Usu [3)]

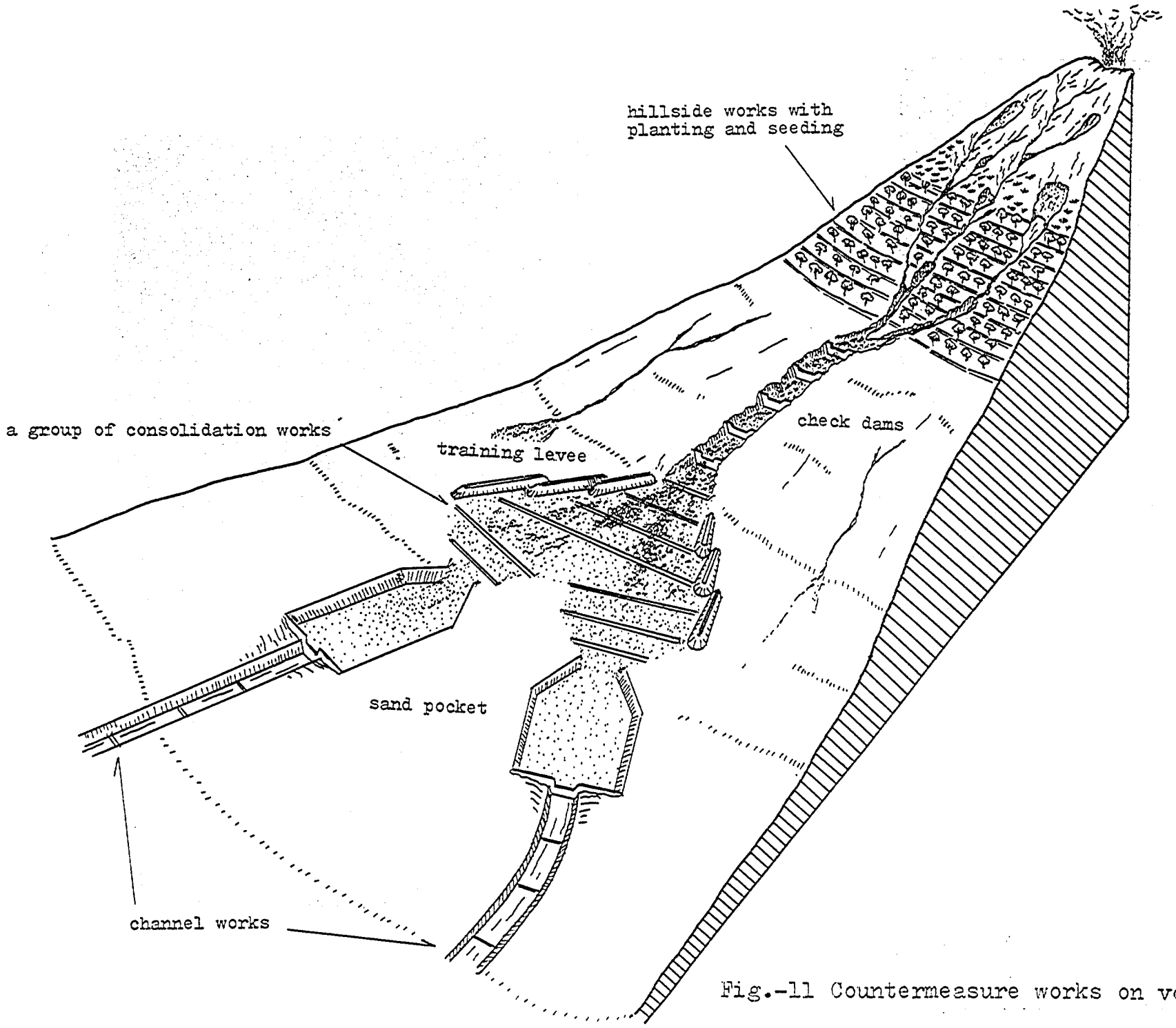


Fig.-11 Countermeasure works on volcano

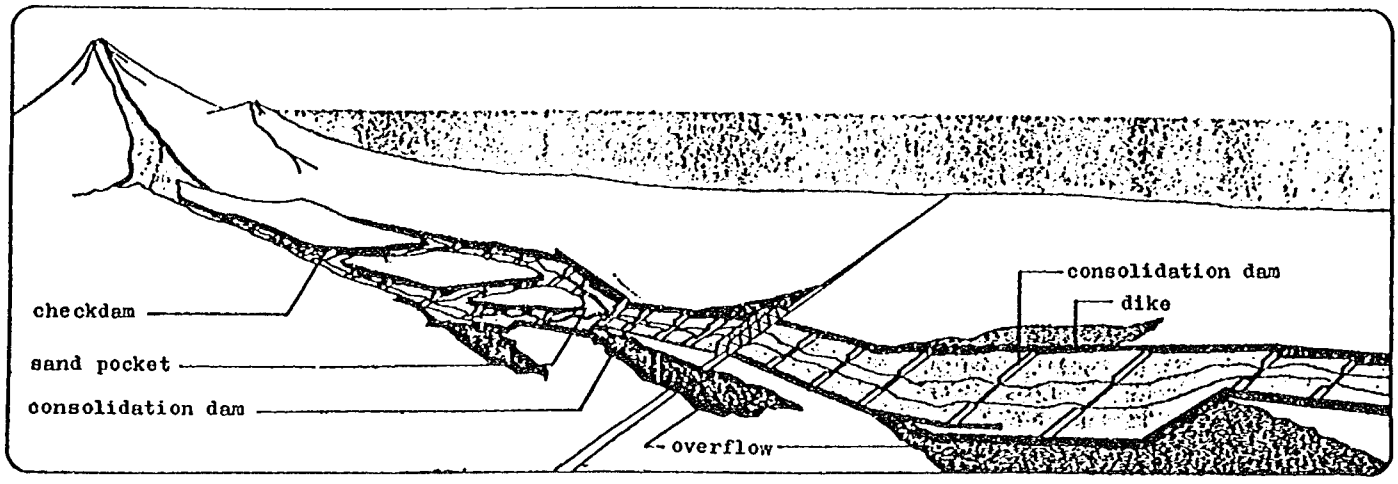


Fig.-12 Countermeasures of Mud Flow in Mt.Merapi [6)]

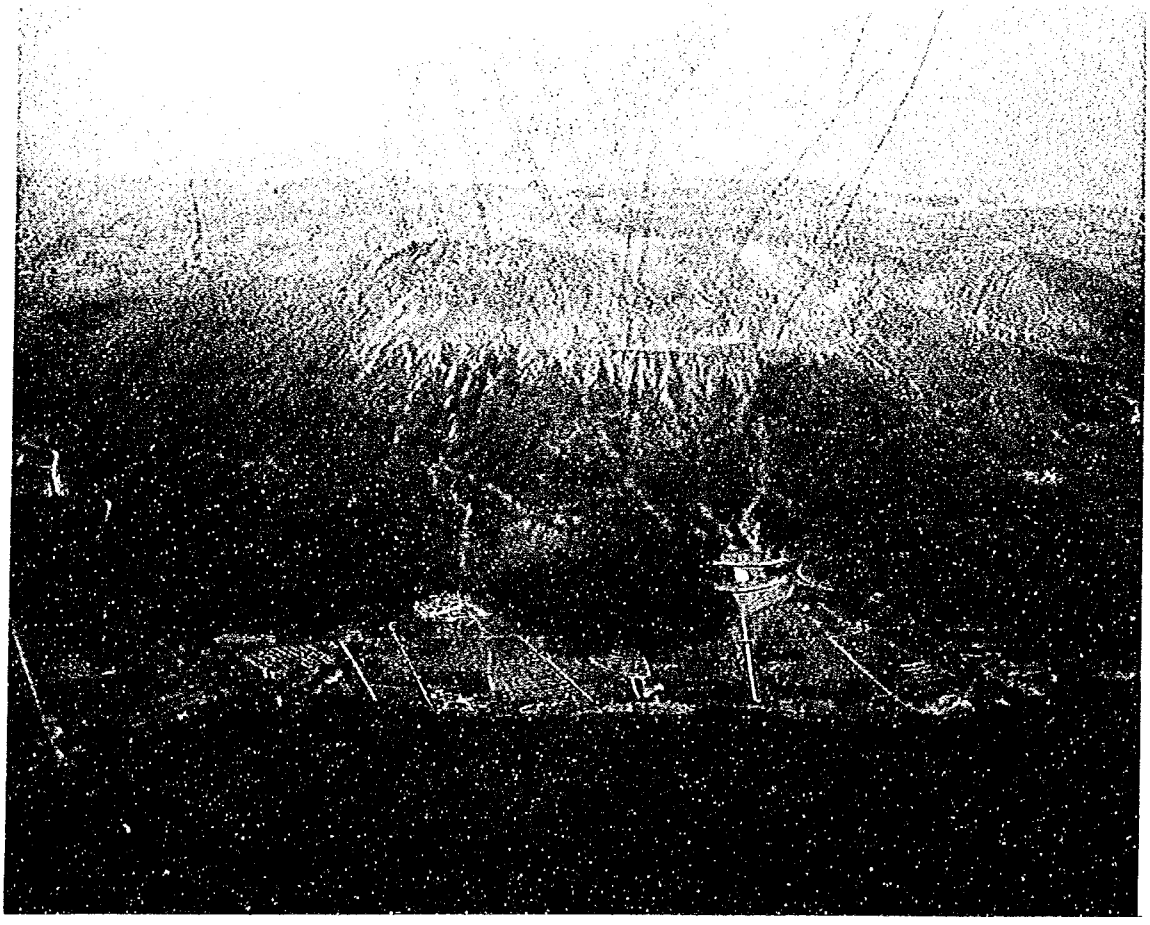


Fig.-13 Countermeasures works in Mt.Usu

ANTICIPATING VOLCANIC HAZARDS AT MOUNT ST. HELENS, WASHINGTON

C.G. Newhall

U.S. Geological Survey,

David A. Johnston Cascades Volcano Observatory

Vancouver, WA 98661 U.S.A.

Abstract

Geologic mapping and stratigraphic studies of volcanic deposits, reviews of the literature describing historical eruptions, and volcano monitoring are all essential for a comprehensive analysis of volcanic hazards. The contribution of each factor depends on the timeframe being considered, on the state of activity of the volcano, and on present knowledge about the volcano. Preliminary forecasts of hazardous activity are commonly empirical, based simply on the recognition of patterns in the data; subsequent forecasts are commonly based on both pattern recognition and inferences about the volcanic processes that cause the observed patterns.

The long-term volcanic-hazards assessment for St. Helens by D.R. Crandell and D.R. Mullineaux identified areas that could be affected in a "worst probable" eruption. After eruptive activity resumed in 1980, their map was revised to take into account the new morphology of the volcano. Additional bulletins and briefings have described hazards and risks expected within short- and intermediate-term timeframes (hours to days and weeks to months, respectively). Intermediate- and long-term risks have also been quantified, though with large uncertainties; short-term hazards and risks still remain to be quantified, using either monitoring data alone or a combination of monitoring data, stratigraphic information, and information from other volcanoes. Quantitative risk estimates have helped public officials to determine acceptable risks, mitigate losses from continuing eruptions, and maximize land use between eruptions.

Introduction

Volcanic-hazards assessments are forecasts of what hazardous volcanic events may occur, when or how frequently they will occur, and where they will occur (including areas likely to be affected). Most volcanic-hazards assessments are probabilistic in the broad sense of the word, in that they give quantitative or qualitative estimates of the likelihood of volcanic events; fully deterministic volcanic-hazards assessments are rare. Probabilities may be explicitly stated, or they may be implied by the inclusion of likely events and the exclusion of unlikely events in a hazards assessment. This paper describes the techniques and nature of volcanic-hazards assessments at Mount St. Helens; it is not a comprehensive discussion of volcanic-hazards assessment, although some of the discussion here is applicable to other active volcanoes.

Hazards at active volcanoes include: eruptive phenomena (pyroclastic flows and surges, air-fall tephra, ballistic fragments, lava flows, and lahars that develop during eruptions), post-eruptive phenomena (rain-induced lahars, increased sedimentation and clogging of streams, increased soil and bank erosion, and other hydrologic hazards), and other special volcano-related hazards (e.g., landslides, rockfalls and locally dangerous concentrations of fumarolic gases). Volcanic risks are the expectable adverse effects of these hazards on people and property. All the above-mentioned hazards pose risks to property; some threaten life as well.

Most of the papers in this symposium describe non-eruptive hazards. One of the aims of the present paper is to stimulate instructive comparisons of the ways by which both eruptive and non-eruptive hazards are assessed, and of how the risks posed by these two kinds of hazards can be mitigated.

Some general aspects of volcanic-hazards assessment

Five general points regarding hazards assessment at Mount St. Helens will help the reader through the remainder of this paper.

1. Hazards assessments may differ according to the timeframe being considered. The timeframe for which a forecast applies must be specified because what is likely in the distant future may not be likely in the near future, and vice versa. Three timeframes may be defined for the study and description of volcanic hazards: long term (years, decades and centuries), intermediate term (weeks to months), and short term (hours to days). Long-term assessments are most useful for land-use and other long-range planning. Short- and intermediate-term assessments are most useful during volcanic crises. Walker (1974) noted that long-term ("general") forecasts tend to be indefinite about both the projected date and type of an eruption, whereas short-term ("specific") forecasts tend to be more specific about both the date and type of an eruption.

2. Hazards assessments require information about the eruptive history and geologic evolution of the specific volcano in question, about the current geologic, geophysical, and geochemical behavior of the volcano, and about historical volcanism at similar volcanoes. Different timeframes require different combinations of such information. Stratigraphic studies and mapping are the principal bases for long-term hazards assessments, whereas monitoring and historical studies are the principal bases for short- and intermediate-term assessments. Information from the geologic record is also considered in short-term forecasts of the likely type of an eruption, however, and monitoring and historical information can change the long-term outlook for a volcano.

3. Some hazards assessments are wholly empirical, whereas others are based partly on patterns in the data and partly on inferences about volcanic processes. Depending on the data and time available, hazards assessments may rely primarily on the recognition of patterns in the data or on a combination of pattern recognition and inferences about the volcanic processes causing those patterns. In general, pattern recognition must be relied on until these processes are well enough understood to be useful in hazards assessments. An understanding of volcanic processes (the "why" of "what, where, when, and why") improves the reliability and timeliness of hazards assessments, and should be discussed in such assessments unless it is too speculative or becomes too confusing to the intended audience.

4. It is sometimes possible and often useful to estimate the quantitative probabilities of volcanic events. Crandell and Mullineaux (1978) noted approximate recurrence frequencies for tephra falls of varying magnitudes, as well as the relative frequencies of various eruptive phenomena (e.g., pyroclastic flows), as represented in the recent geologic history of Mount St. Helens. Newhall (1982) has used the stratigraphic data of Crandell and Mullineaux (1978), along with information about the historical eruptions of Mount St. Helens and similar volcanoes, to estimate semiquantitative, intermediate- and long-term probabilities of hazardous events at Mount St. Helens. The probability of an initial general event--an eruptive period of several decades or longer of relatively frequent eruptions--was calculated from the past frequency of such eruptive periods at Mount St. Helens. The probabilities of increasingly specific events--of individual eruptions,

specific types and magnitudes of eruptions, and specific hazards affecting specific locations around the volcano--were then calculated by multiplying the probability of the initial event by the conditional probabilities of increasingly specific events and locations, i.e. the probabilities of those specific events and locations given that the necessary prior events have occurred. Conditional probabilities were calculated from the absolute and relative frequencies of various types of events, from lengths of flows, from distance vs. thickness curves for airfall tephra, and from topographic considerations. For intermediate-term assessments, Newhall used an interpretation of recent activity at Mount St. Helens to make a subjective estimate of the explosive potential of the next eruption. This subjective estimate relies heavily on geophysical and geochemical monitoring data from the past 2 years and on the most recent episodes of dome growth, and gives less weight to the explosive events of 1980. To date, only intermediate- and long-term probabilities have been estimated. As the number of well-monitored eruptions increases at Mount St. Helens, short-term probabilities may also be estimated. Most of these probability estimates, which are based on patterns in the data, can and should be refined by further studies of volcanic processes. Although it might seem that increasing reliance on interpretations of processes will bring increasing subjectivity to probability estimates, the opposite is probably true. A better understanding of the processes controlling patterns in the data will permit us to know whether or not to use the assumption in empirical probability estimates that future eruption precursors will mimic past eruption precursors.

5. Hazards assessments are an application of what is learned regarding the past and present behavior of a volcano, to the practical needs of people living and working near that volcano. They are forecasts of future volcanic activity, stated clearly enough to be understood by laymen, and in enough detail about the types and areal extent of hazards that the associated risks can be mitigated if desired.

Long-term hazards and risk assessments

For most purposes, long-term volcanic-hazards assessments can be based on the past eruptive history of the specific volcano in question (Crandell and Mullineaux, 1975). Stratigraphic studies and mapping of the deposits of a volcano provide information on the types of activity that have occurred, the relative and absolute frequencies of these various types of activity, and the areas affected by each type of activity. Studies of unconsolidated deposits around a volcano are especially important for hazards assessments, because pyroclastic flows and surges, lahars, and falling tephra (in sharply decreasing order of severity) are the principal hazards beyond the steep slopes of a volcano. Studies of the prehistoric eruptions at Mount St. Helens include those by Verhoogen (1937), Lawrence (1941; 1954), Crandell and others (1975), Hyde (1975), Crandell and Mullineaux (1978), Hoblitt and others (1980), Hopson and Melson (1980), and Mullineaux and Crandell (1981). Crandell and Mullineaux (1978) presented a generalized map of volcanic deposits of the past 4,500 years (a period selected because it is relatively well known and likely to approximate future behavior) and

another map of potential flowage hazards from future eruptions of Mount St. Helens. They also discussed hazards from air-fall tephra in the text of their report.

On the basis of the frequency of eruptions at Mount St. Helens during the past 4,500 years, Crandell and others (1975, p. 441) concluded that another eruption was "likely within the next hundred years, possibly before the end of this century." The long-term forecast of Crandell and Mullineaux (1978) was intended primarily for use by planners, although Crandell and Mullineaux anticipated that it would also be useful during the next eruption of Mount St. Helens. Their forecast described what might be called a worst probable case--areas that might be affected by an eruption as large as the largest known at Mount St. Helens. Such an eruption would be larger than approximately 90 to 99% of all future eruptions of Mount St. Helens. The area subject to flowage hazards in this worst probable case is slightly larger than that affected by eruptions of Mount St. Helens during the past 4,500 years but slightly smaller than that affected by eruptions during the past 40,000 years (Crandell and Mullineaux, 1978). The worst probable case described or exceeded all of the 1980 and subsequent eruptions of Mount St. Helens except for that of May 18, 1980. The forecast adequately described the air-fall tephra, pyroclastic flows and lahars of May 18, but because it was made before the precursory activity of March-May 1980, it did not anticipate the landslide and the magnitude of the lateral blast (Miller and others, 1981).

If a large population is at risk, or if a volcanic hazard might create another more serious hazard (as in the case of nuclear powerplants), planners may wish to consider even larger but less likely

events, e.g., those larger than 99% of all future eruptions at a specific volcano. In contrast to the worst probable case described above, this new case might be called the worst foreseeable, worst conceivable, or, for comparison with terms used in the nuclear industry, the worst credible case. For these special purposes, long-range hazards assessments should consider all activity known to have occurred at the volcano in question, as well as information about the petrologic and structural evolution of that volcano. If one needs to know about all "credible" events, one must consider not only the most recent activity but also the complete evolution of a volcano. Although some volcanic events recur only once every few thousand, few tens of thousands or even few hundreds of thousands of years, even these infrequent events will occasionally become likely in the short term. The entire known history of Mount St. Helens (approximately 40,000 years) is not much longer than or significantly different from the 4,500-year history considered by Crandell and Mullineaux (1978), nor are there any trends in its geologic evolution that would argue against use of this 4,500-year record. The recent history of some other volcanoes, however, differs considerably from their total history (e.g., in the Long Valley caldera-Inyo Domes area of eastern California); there, a longer timespan includes eruptions both more and less hazardous than recent ones.

Special long-range hazards assessments may also need to consider activity known to have occurred at similar volcanoes around the world. If the history of a specific volcano is well known, similar volcanoes can be identified in the International Association of Volcanology and Chemistry of the Earth's Interior's "Catalogue of Active Volcanoes of the

World Including Solfatara Fields," the Volcanological Society of Japan's "List of the World's Active Volcanoes," or the Smithsonian Institution's "Volcanoes of the World." A relevant subset can be selected with some confidence, although it may not expand the range of possible hazards much beyond what is already known. If the history of a specific volcano is not well known, a larger subset will probably be selected, encompassing a larger range of kinds and scales of possible hazards. There is an irony here--that worldwide data can be used most confidently when they are least needed, and vice versa. Even when worldwide data are not demonstrably applicable to a specific volcano, however, careful inspection of those data will almost always lead to a better hazards assessment than can otherwise be made. The geologist's decision about how large a subset to select depends on how critical it is that all future activity be described. In those special cases requiring the use of a worldwide sample, large subsets are usually required.

Our current long-term forecast of the volcanic hazards at Mount St. Helens includes: episodic dome growth, with or without small explosions; a lesser but significant possibility (less than 20%/yr) of renewed explosive activity, similar to that which occurred between May 25 and October 18, 1980; and a still smaller possibility (less than 5%/yr) of a renewal of strong explosive activity resulting in eruptions like the prehistoric "W" eruptions of Mount St. Helens. The "W" sequence included two eruptions that produced more air-fall tephra than did the May 18, 1980, eruption and three eruptions that produced significantly more air-fall tephra than did the May 25-October 18, 1980 explosive eruptions, all within a period of about a century or less. This current long-term

forecast is based on the known eruptive history of Mount St. Helens and on activity that has followed major eruptions of Bezymianny (1956-), Lamington (1951-), Santa Maria (1902-) and other volcanoes with growing domes.

Three interesting problems in the use of volcanic deposits for long-term hazards assessments are illustrated by recent events at Mount St. Helens. One problem is that certain types of eruptive activity tend to destroy their deposits, or modify them so thoroughly that it becomes difficult to decipher the original events. At Mount St. Helens (and at all other volcanoes that are seasonally or permanently snow covered), pyroclastic flows and surges onto snowpack can melt large volumes of snow quickly; some of the factors determining how much of the snowpack will be melted have been discussed by Dunne and Leopold (1981). Although many details of the melting process remain to be learned, it is clear that rapid melting can destroy primary pyroclastic deposits or even prevent formation of a pyroclastic-flow deposit. A small blast (aborted pyroclastic flow?) on March 19, 1982, melted snow in the crater of Mount St. Helens and immediately transformed what little primary deposit that was there into a layer of pumice floating on a very short lived pond. The pond then breached, and some of the newly erupted pumice was carried in a hot, "clear water" flood that evolved into a warm mudflow downslope. The blast also triggered an avalanche of snow, old lithic fragments, and both freshly erupted and older pumice. Much of this avalanche deposit was eroded within minutes by the flood of melt water from the crater, and even that which survived the early flood was greatly modified as warm weather melted the remaining snow. It is doubtful that

either the blast or the avalanche of March 19, 1982 could have been inferred from the geologic record of these events, had there not been observations during and shortly after the eruption. Pyroclastic surges and (or) flows onto the east, south, and west sides of Mount St. Helens during the early stages of the May 18, 1980 eruption caused similar snowmelt but are known only from photographs, from field studies conducted shortly after the eruption, and from derivative lahars. The same general problem arises whenever pyroclastic flows mix with surface water and are converted to hot lahars. Fortunately, the occurrence of these "vanishing" pyroclastic flows can subsequently be inferred by using paleomagnetic techniques described by Aramaki and Akimoto (1957) and Hoblitt and Kellogg (1979).

A second, related problem is that some volcanic deposits are easily eroded or buried by normal slope and channel processes, and thus missed in the geologic record. Thin fine-grained ash deposits on steep slopes are especially susceptible to erosion; at Mount St. Helens, distal deposits of the May 18, 1980, blast are already missing from the steepest slopes. Downed timber will eventually disappear, removed by timber-salvage operations and by gradual decay. Even the massive debris-avalanche deposits in the valley of the North Toutle River may, within a few hundreds or thousands of years, be exposed only in isolated outcrops, where they have been preserved on high ground or between channel-filling lahar and fluvial deposits.

A third problem is that deposits from closely-spaced, small to moderate-size eruptions can be indistinguishable in the geologic record. Each of the six moderate-size explosive eruptions of Mount St. Helens

since May 18, 1980, has produced one or more thin tephra layers, which today appear to be only a single layer. Pumice lapilli from a single eruption lie beside (rather than above) lapilli from the previous eruption, and distinctions between ash layers have been blurred with the passage of time, by wind, rainsplash, frost heaving, bioturbation, and other processes.

Modification during eruptions, erosion or burial after eruptions, and loss of fine distinctions between different deposits all degrade the record of past events. Much more has occurred at Mount St. Helens in the past 2 years than now meets the eye. Estimates of the frequency of various volcanic events, based on the geologic record, are thus minimum estimates and can be as much as several times too low.

Short- and intermediate-term hazards and risk assessments

When a volcanic crisis begins, both the techniques and uses of hazards assessments change; land-use plans are set aside, and questions of immediate health and safety arise. The consequences of errors in these assessments, or of calculated risk-taking even with correct assessments, can be immediate and severe. Like long-term hazards assessments, short- and intermediate-term assessments must anticipate "what," "where," and "when". Studies of eruptive history remain useful for assessing what the hazards will be and where they will occur (i.e., the areas that they will affect). This information can be expressed simply as possibilities or as the relative likelihoods of different hazards at various points around a volcano. Once a volcanic crisis begins, studies of eruptive history rarely add information about "when," but they can still add information about "how frequently" events might recur. Some information on the probable frequency of different events can be obtained by using high-resolution dating techniques (e.g., those based on tree rings, pollen, and paleomagnetic secular variation curves).

In a volcanic crisis, geophysical and geochemical monitoring provides the best information about when a volcano might erupt and supplemental information about what type of eruption might occur. Increased seismicity and ground deformation are common precursors, sometimes accompanied by changes in fumarolic emissions or other geophysical and geochemical parameters. Eruptions may follow, and these, too, can be monitored as possible precursors of further eruptions. At present (July 1982), the following parameters are being monitored at Mount St. Helens:

seismicity, deformation (slope distances, vertical uplift, and tilt and fault movements in the crater, and slope distances and tilt on the whole volcano), gravity and magnetic-field strength at selected stations, composition and flux rates of volcanic gases, petrology of successive eruptive products, and eruptive style.

Monitoring data from Mount St. Helens are used in two ways--to define empirical relations between precursors and ensuing eruptions, and to infer the physical and chemical processes that control eruptive activity. Figure 1 plots patterns of seismicity, changes in the distances between points on the dome and "fixed" reference points several hundred meters away, tilting of the crater floor, and SO_2 emissions. Similar patterns have been observed before most of the recent eruptions. A fortuitous combination of repetitive precursor patterns, a crater-floor geometry that allows detailed deformation studies, and an intensive monitoring effort at Mount St. Helens has allowed quite specific predictions of both the date and type of the most recent eruptions. The week of an eruption has been predicted as much as 3 to 4 weeks in advance, the day as much as 3 to 4 days in advance, and the hour as much as 1 to 2 hours in advance. The likely type of an eruption has been predicted as much as 3 to 4 weeks in advance, though with increasing confidence as the eruption approaches. In a more general case, monitoring indicates the approximate day or week when an eruption will start and may also allow a long-term forecast about the type of an eruption to be made slightly more specific for the short term.

Monitoring can also provide information about the likely type of eruptions over future weeks to months (intermediate term), before the exact timing becomes apparent. At Mount St. Helens, monitoring showed inflation of the cone and a stepwise increase in magmatic-gas emissions from March until June-July 1980, followed by deflation, decreasing seismicity, and decreasing SO_2 and CO_2 fluxes since that time (with CO_2 decreasing faster than SO_2). Temporary increases in these parameters have occurred before eruptions, but there has been little deep seismicity and no edifice-wide inflation since August 1980. These observations argue that the eruptions since May or June 1980 have been from a single magma body that is progressively degassing (Casadevall and others, 1982) and imply that the explosive potential for the foreseeable, intermediate-term future is low relative to the long-term likelihood of explosive activity. As another example of the role of monitoring in intermediate-term hazards forecasts, continuing slow deformation of the crater floor between recent eruptions has indicated each time that the eruptive sequence was not yet over, even before the exact date of the next eruption could be forecast.

Information from the record of historical, worldwide volcanism can contribute to short- and intermediate-term hazards assessments in at least three circumstances: (1) when little is known of possible activity at the volcano in question, (2) when monitoring indicates that current activity is unprecedented at the volcano in question, and (3) when a larger data base is needed for statistical calculations. Each of these cases is discussed below.

(1) The eruptive history of Mount St. Helens was well known before the current eruptions began in late March 1980, and so at the onset of activity the worldwide sample did not offer much additional insight into what might occur. Had there been no prior studies on Mount St. Helens, however, the set of subduction-related volcanoes with andesitic and dacitic products would have provided some information about likely activity.

(2) When the increased seismicity and phreatic eruptions began at Mount St. Helens in March 1980, short-term forecasts were for more of the same unless a magmatic phase began, and intermediate-term forecasts stated that a magmatic phase would probably follow, including eruptions like those which had occurred at Mount St. Helens in the past (known from stratigraphic and historical records). But when it became apparent that the upper north flank of Mount St. Helens was bulging subhorizontally northward at 1.5 to 2.5 m/d, scientists searched the literature for analogs of such rapid deformation. As it turned out, there were no perfect analogs to the events of late March-May 18, 1980; there were partial analogs from Usu (1943-44), Bezymianny (1955-56) and Bandai-san (1888), but unfortunately the similarities to Bezymianny were clouded at the time by the differences (dome growth and vertically-directed magmatic eruptions had occurred at Bezymianny for approximately 5 months before the cataclysmic landslide and blast, whereas magmatic eruptions had not yet begun at Mount St. Helens before May 18, 1980). After the May 18 eruption, information about post-cataclysmic activity at Bezymianny (1956-) and Lamington (1951-) was instructive.

(3) To estimate the probabilities of volcanic events, a large data base is needed. A data base such as that of Simkin and others (1981) can be used to define the recurrence frequency and characteristics of eruptions at similar volcanoes. For short- and intermediate-term forecasts, generalizations about the timing of various events (e.g., onset of precursors, onset of eruptions, first pyroclastic flows, etc.) are also helpful (cf. Decker, 1973; Tomblin, 1982).

Graphical portrayal of volcanic hazards and risks

It can be as difficult to describe and portray volcanic hazards and risks as it is to assess them. Geologic maps and stratigraphic sections are informative to an audience of geologists, but other formats must be devised for lay audiences. One common approach is to describe hazard and risk zones. Hazard zones can be defined as areas that might be affected by various hazards (e.g., by pyroclastic flows or lahars; see fig. 2), or as areas of greater or lesser hazard. These two definitions can also be combined (e.g., by showing areas of high pyroclastic flow hazard or areas with greater than X% probability of a pyroclastic flow). Any hazard map that shows only one zone per hazard or one zone per volcano has an implicit lower probability cutoff, as in the "worst probable" hazard zone of Crandell and Mullineaux (1978) described above; events with probabilities less than the cutoff are not shown.

Volcanic risks can be portrayed in the same ways but will take into account populations or property at risk and (or) the severity of each hazard's effects on people or property. Figure 3 shows an individual's long-term risks of death from eruptions of Mount St. Helens, as they might have been estimated in February 1980. The three volcanic risk-zones closely resemble the three pre-May 18, 1980, flowage-hazard zones of figure 2.

Population-adjusted risk zones will, for the same level of hazard, show higher risks where the population is higher. Because the population around Mount St. Helens is sparse, however, zones of population-adjusted risks have the same shapes as zones of risk to individuals. Property-adjusted risk zones near Mount St. Helens would be modified according to timber stands; farther away from the volcano, where ash-fall

is the chief hazard, property-risk zones would be determined by the likelihood of ash-fall and by the type and amount of property at risk.

Long-term hazard and -risk zones changed drastically on May 18, 1980, when the morphology of the volcano changed. The shapes of current long-term risk zones resemble those of current intermediate-term-risk zones (see fig. 4).

Short- and intermediate-term hazards and risks can also be portrayed in zones, for discussions of public safety and such short-term mitigation measures as evacuations. Figure 4 shows an intermediate-term hazards assessment at Mount St. Helens as of February 1982; like figure 3, figure 4 shows the estimated risks of death from eruptions, although the zones are greatly modified from those of figure 3 (and will continue to be modified as new information becomes available). Zones of equal short-term risk will change even more rapidly--from day to day or even from hour to hour. With advances in computer graphics and communications technology, it is technically feasible to draw and quickly disseminate short-term-hazard zones, but can public officials use rapidly changing assessments? Unless the morphology of the volcano changes again, or a major bulge appears outside the crater proper, or the distribution of surface water changes markedly (e.g., with the seasons), the shapes of successive short-term-hazard zones will remain approximately the same, and only the degree of risk will vary rapidly. Multiple zones can be defined in advance, marked in the field with signs or gates, and then closed or opened within hours if necessary, depending on the short-term forecast. The State of Washington and the U.S. Forest Service have recently adopted this approach and will place even greater reliance on short-term forecasts in the future.

Acceptable risks and mitigation measures

After volcanologists have described potential hazards, land managers, engineers, health professionals, and others can translate these hazards into risks; risks can then be balanced with the benefits of, for example, developments or work or visits near the volcano. Decisions about what projects should be undertaken and about what access will be allowed can theoretically be made by land managers and public officials or by individual citizens. Decisions about access and land use around Mount St. Helens are made by the Governor (and the Department of Emergency Services) of the State of Washington, by the Supervisor of the Gifford Pinchot National Forest, and by the responsible officials of Skamania, Cowlitz and Lewis Counties. To make these decisions, these government officials have referred to probabilistic assessments of the risks to life and property. As of this writing (Sept. 1982), the general public is allowed access to areas in which an individual's risk of death from eruptions is less than about 10^{-3}/yr if no mitigating measures are taken (e.g., radio communications, reduced time of exposure) (Newhall, 1982). Downstream on the flood plains of the Toutle and Cowlitz Rivers, new residential developments are forbidden in what is approximately the 100-year flood plain (probability of flooding, approximately 10^{-2}/yr).

Government decisions about acceptable risks at Mount St. Helens have not been universally popular. Many citizens advocate that individuals be allowed to decide for themselves which risks are acceptable. Individual decisions and self-reliance are a cultural heritage of Americans, but in recent decades Americans seem to have assumed less and less responsibility for their own well-being. Individuals are anxious to have the freedom to take risks and are even eager to take such risks, but are less willing to assume personal responsibility for taking them. Legal precedents involving other natural hazards have held federal, state and local governments responsible for the consequences of some of the risks that its citizens might want to take. Distinctions between a government's responsibility to inform its citizens of natural hazards and its responsibility to safeguard citizens from those hazards are rarely clear and are commonly tested in American courts (Panel on the Public Policy Implications of Earthquake Prediction, 1975; Huffmann and Rosen, 1976). Some of these questions are being tested anew in a current lawsuit against the State of Washington, relating to fatalities near Mount St. Helens on May 18, 1980. As long as natural hazards exist and governments continue to make decisions about acceptable risks, government officials, lawyers, representatives of the news media, and others will continue to debate those decisions. Especially interesting debates will arise when unlikely hazardous events "defy the odds" and occur even though the risks of those events were judged to be acceptably low!

Some risks that are deemed unacceptable can be mitigated to acceptable levels. Volcanic risks to people visiting and working near Mount St. Helens have been mitigated in four ways: (1) by limiting access around the volcano; (2) by monitoring the volcano and predicting its activity; (3) by requiring that those who work near the volcano carry safety equipment, including radios to receive information about volcanic activity; and (4) by a general-education campaign to inform the public of potential hazards and how to cope with them.

In the period from late March to mid-May 1980, limitations on access were clearly the most effective way of mitigating risks of death or injury. Hazards were clearly high, but the chances of useful short-term predictions of hazardous events were low. Since then, intensive monitoring and a carefully coordinated radio and telephone communication system has made it possible to warn of hazardous events at least several hours in advance, allowing people in the area to leave if necessary. Well-publicized predictions at Mount St. Helens have reduced the risks of immediate death or injury by several orders of magnitude. The general-education program takes longer than other mitigative measures but will become increasingly important if or when the land managers allow freer access, on the condition that citizens keep themselves informed of any forecasts of hazardous activity.

Property values around Mount St. Helens before May 18, 1980 were based mainly on timber and recreational opportunities. Timber values were sharply reduced on May 18, but recreational opportunities, though changed, have probably increased. Most areas near the volcano are now included in the Mount St. Helens National Volcanic Monument; dedication of this area to low-density recreational use effectively mitigates most property risks near the volcano. Property risks downstream from Mount St. Helens remain substantial, owing to mudflow and flooding hazards, but these risks are being mitigated by warning systems and by limitations on flood-plain development. Property damage from ash fall at greater distances from Mount St. Helens is being mitigated through various engineering and other measures, such as extra filters for engines, turbines, and cooling systems; and by adjusting schedules of maintenance, cleaning, planting and harvesting, and other work, according to whether explosive activity is forecast in the near future.

Summary

A relatively general long-term eruption forecast for Mount St. Helens (Crandell and Mullineaux, 1978) has been followed by increasingly shorter term and more specific forecasts. Recent eruptions have been forecast with moderately specific notices several weeks in advance, followed by remarkably specific notices a few hours in advance of eruptions. For use as hazards assessments, these forecasts have noted both what is and what is not likely to occur. Volcanic-hazards and -risk assessments at Mount St. Helens are increasingly being stated in probabilistic terms.

Once the hazards and risks have been described, public officials and individuals must decide how much risk is acceptable and which mitigative measures would be the most effective, most economical, and least disruptive in reducing risks to acceptable levels. Volcanologists can offer useful technical information throughout this process, but decisions about risk mitigation require information and judgments about social and economic matters that are generally beyond the volcanologists' expertise and mandated responsibility. Risks at Mount St. Helens have been effectively mitigated by teamwork between scientists who have anticipated nearly all the hazards, and public officials who have taken generally adequate mitigative measures. Considering the tremendous devastation from the eruptions during and since 1980, casualties and avoidable property damage have been slight; at the same time, economic and social disruptions have also been minimized, in part because monitoring and short- to intermediate-term hazards assessments have allowed people to return to work or to visit the Mount St. Helens area with a minimum of risk.

Acknowledgments

Many of the ideas presented here have grown out of discussions with D. W. Peterson and others of the U.S. Geological Survey's Cascades Volcano Observatory, D. R. Mullineaux and others of the U.S. Geological Survey's Volcanic Hazards Project (Denver, Colo.), J. J. Brown and others of the U.S. Forest Service, and H. H. Fowler and others of the Washington Department of Emergency Services.

References cited

Aramaki, S. and Akimoto, S., 1957, Temperature estimation of pyroclastic deposits by natural remanent magnetism: Am. J. Sci., v. 255, pp. 619-627.

Casadevall, T.J., Rose, W.I., Jr., Gerlach, T., Ewert, J., and Wunderman, R., 1982, Gas emissions and the 1981-82 eruptive behavior of Mount St. Helens: Science, in press.

Crandell, D.R. and Mullineaux, D.R., 1975, Technique and rationale of volcanic-hazards appraisals in the Cascade Range, northwestern United States: Environ. Geol., v. 1, pp. 23-32.

Crandell, D.R. and Mullineaux, D.R., 1978, Potential hazards from future eruptions of Mount St. Helens volcano, Washington: U.S. Geol. Surv. Bull. 1383-C, pp. C1-C26.

Crandell, D.R., Mullineaux, D.R., and Rubin, Meyer, 1975, Mount St. Helens volcano; recent and future behavior: Science, v. 187, pp. 438-441.

Decker, R.W., 1973, State-of-the-art in volcano forecasting: Bull. Volcanol., v. 37, pp. 372-393.

Dunne, T. and Leopold, L.B., 1981, Flood and sedimentation hazards in the Toutle and Cowlitz River system as a result of the Mt. St. Helens eruption: Bothell, Washington, Federal Emergency Management Agency, 92 p.

Hoblitt, R.P., Crandell, D.R. and Mullineaux, D.R., 1980, Mount St. Helens eruptive behavior during the past 1,500 years: Geology, v. 8, pp. 555-559.

Hoblitt, R.P. and Kellogg, K.S., 1979, Emplacement temperatures of unsorted and unstratified deposits of volcanic rock debris, as determined by paleomagnetic techniques: Bull. Geol. Soc. Am., v. 90, pp. 633-642.

Hopson, C.A. and Melson, W.G., 1980, Mount St. Helens eruptive cycles since 100 A.D. (abs.): Eos, v. 61, p. 1132-1133.

Huffmann, J. and Rosen, S., 1976, Legal constraints on the planning and development of disaster home warning systems: Portland, Oreg., Lewis and Clark College, Northwestern School of Law Report GAEN 76-22057, 145 pp.

Hyde, J.H., 1975, Upper Pleistocene pyroclastic flow deposits and lahars south of Mount St. Helens volcano, Washington: U.S. Geol. Surv. Bull. 1383-B, pp. B1-B20.

Lawrence, D.B., 1941, The "floating island" lava flow of Mount St. Helens: Mazama, v. 23:12, pp. 56-60.

Lawrence, D.B., 1954, Diagrammatic history of the northeast slope of Mount St. Helens, Washington: Mazama, v. 36:13, pp. 41-44.

Miller, C.D., Mullineaux, D.R. and Crandell, D.R., 1981, Hazards assessments at Mount St. Helens, in Lipman, P.W. and Mullineaux, D.R., eds., The 1980 Eruptions of Mount St. Helens, U.S. Geol. Surv. Prof. Paper 1250, pp. 789-802.

Mullineaux, D.R. and Crandell, D.R., 1981, The eruptive history of Mount St. Helens, in Lipman, P.W. and Mullineaux, D.R., eds., The 1980 Eruptions of Mount St. Helens, U.S. Geol. Surv. Prof. Paper 1250, pp. 3-15.

Newhall, C.G., 1982, A method for estimating intermediate and long-term risks from volcanic activity, with an example from Mount St. Helens: U.S. Geol. Surv. Open-File Report 82-396, 59 p.

Panel on the Public Policy Implications of Earthquake Predictions, 1975, Earthquake Prediction and Public Policy: Washington, U.S. National Academy of Sciences, 142 p.

Simkin, T., Siebert, L, McClelland, L, Bridge, D., Newhall, C. and Latter, J.H., 1981, Volcanoes of the World: Stroudsburg, Penn., Hutchinson Ross Publ. Co., 232 p.

Tomblin, J., 1982, Managing volcanic emergencies: UNDRO News, January 1982, pp. 4-10.

Verhoogen, J., 1937, Mount St. Helens, a recent Cascade volcano: Univ. Calif. Berkeley Dept. Geol. Sci. Bull., v. 24 pp. 263-302.

Walker, G.P.L., 1974, Volcanic hazards and the prediction of volcanic eruptions: Geol. Soc. London Misc. Publ. 3, pp. 23-41.

FIGURE CAPTIONS

Figure 1. Simplified plots of geophysical and geochemical precursors to the March 19, 1982, eruption of Mount St. Helens. Data from S. D. Malone, D. A. Swanson, D. Dzurisin, and T.J. Casadevall (unpubl. data, 1982).

Figure 2. Zones of long-term flowage hazards around Mount St. Helens (from Crandell and Mullineaux, 1978).

Figure 3. Zones of long-term volcanic risk at Mount St. Helens as they might have been estimated in February 1980. Annual risks of death from volcanic activity are approximately as follows: zone I, 10^{-9}-10^{-8}; zone J, 10^{-10}-10^{-9}; zone K, 10^{-11}-10^{-10}; zone L, 10^{-12}-10^{-11}. Zones are labeled with two letters: the first letter indicates risk for a full-time resident, with no provision for warning or evacuation; the second letter indicates risk for a person who works in the area, with provisions for warning and evacuation, and lives elsewhere.

Figure 4. Zones of intermediate-term volcanic risk at Mount St. Helens, as estimated in February 1982. Annual risks from death from volcanic activity are approximately as follows: zone A, 10^{-1}-10^{0}; zone B, 10^{-2}-10^{-1}; zone C, 10^{-3}-10^{-2}; zone D, 10^{-4}-10^{-3}; zone E, 10^{-5}-10^{-4}; zone F, 10^{-6}-10^{-5}; zone G, 10^{-7}-10^{-6}. Zones are labeled with two letters: the first letter indicates risk for a full-time resident, with no provision for warning or evacuation; the second letter indicates risk for a person who works in the area, with provisions for warning and evacuation, and lives elsewhere.

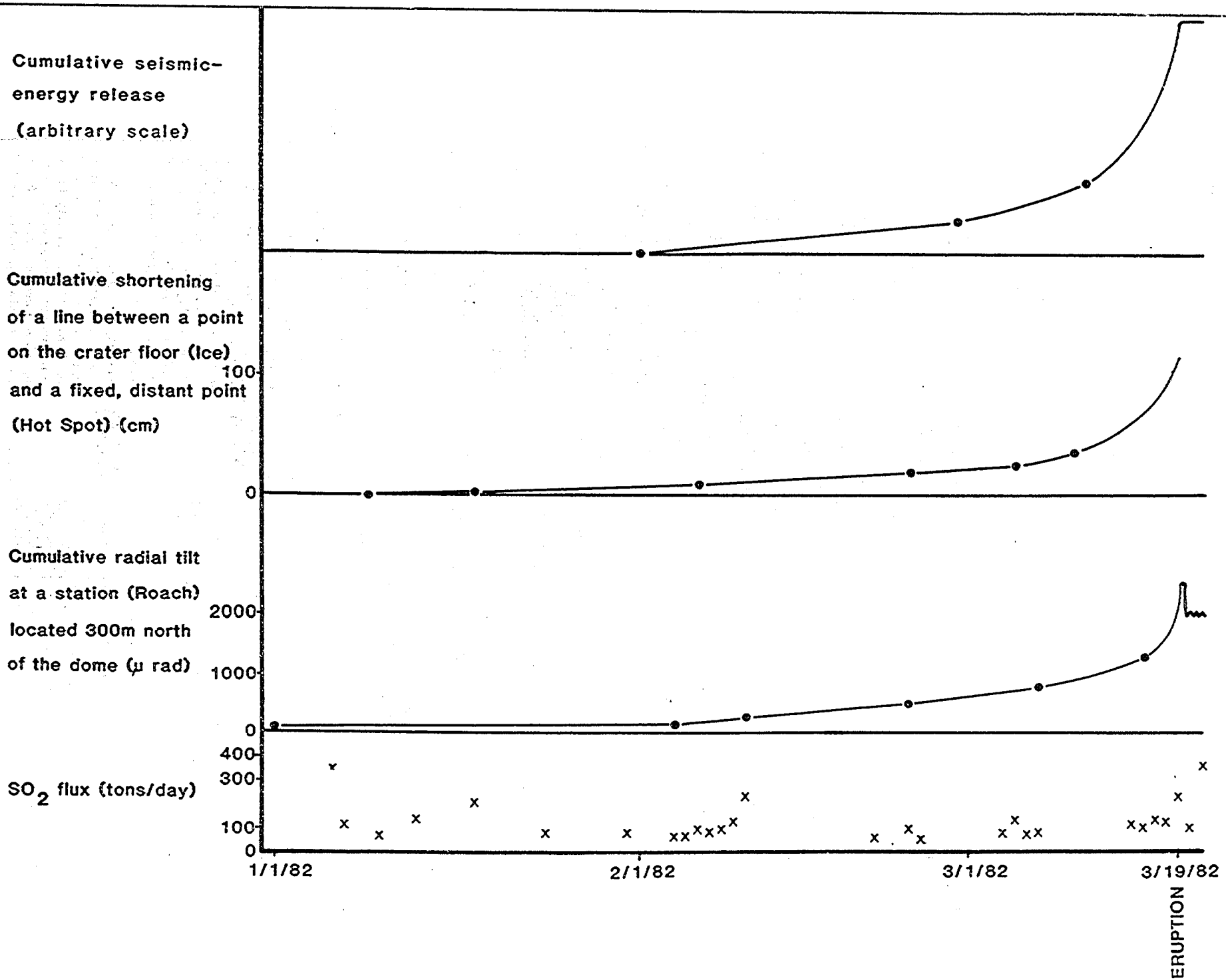

Cumulative seismic-energy release (arbitrary scale)
Cumulative shortening of a line between a point on the crater floor (Ice) and a fixed, distant point (Hot Spot) (cm)
100
0
Cumulative radial tilt at a station (Roach) located 300m north of the dome (μ rad)
2000
1000
0
SO_2 flux (tons/day)
400
300
100
0
1/1/82
2/1/82
3/1/82
3/19/82
ERUPTION

Figure 1

Figure 2

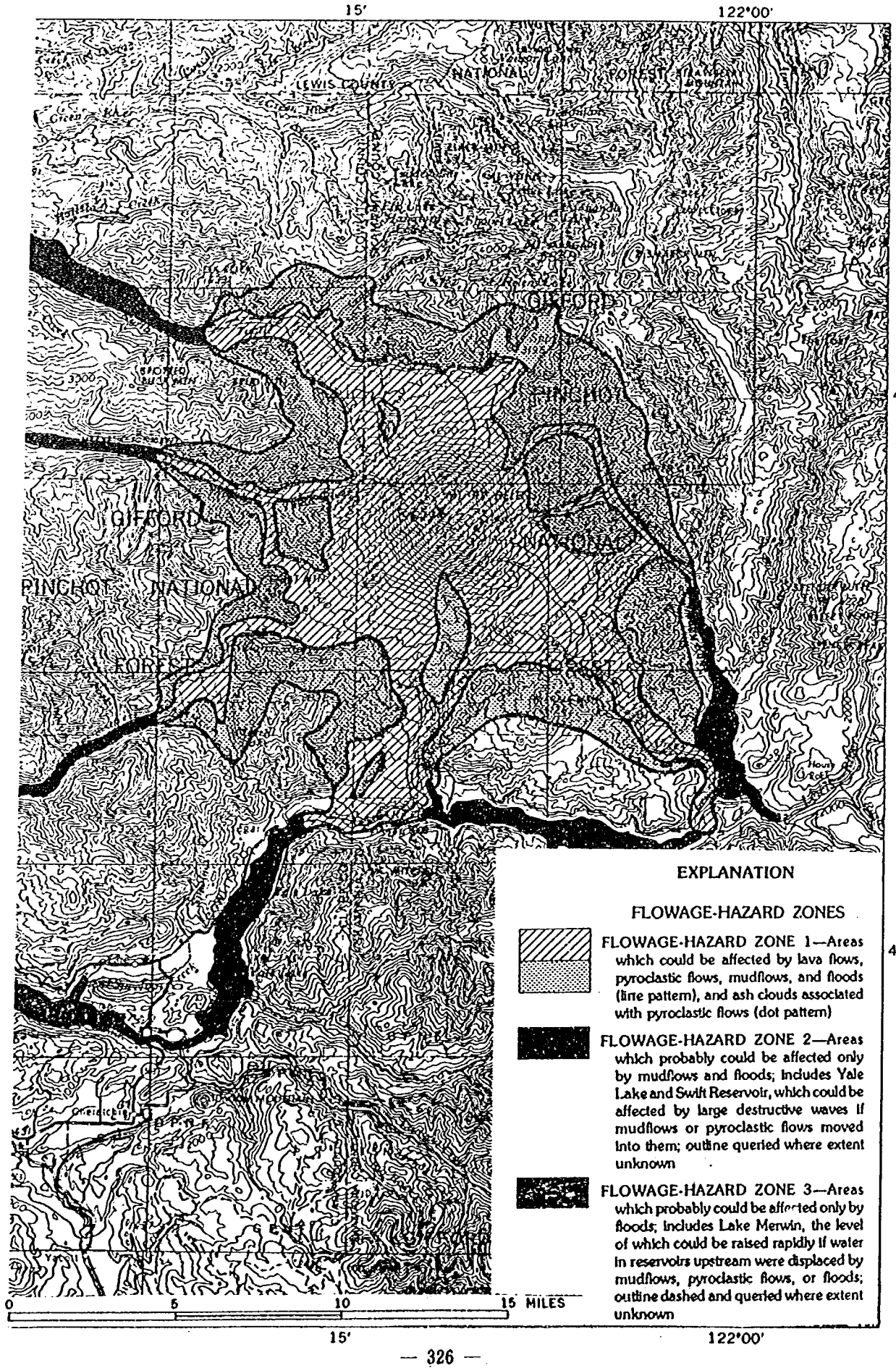

15'
122°00'
46°15'
46°00'
GIFFORD
PINCHOT
NATIONAL
FOREST
LEWIS COUNTY
EXPLANATION
FLOWAGE-HAZARD ZONES
FLOWAGE-HAZARD ZONE 1—Areas which could be affected by lava flows, pyroclastic flows, mudflows, and floods (line pattern), and ash clouds associated with pyroclastic flows (dot pattern)
FLOWAGE-HAZARD ZONE 2—Areas which probably could be affected only by mudflows and floods; includes Yale Lake and Swift Reservoir, which could be affected by large destructive waves if mudflows or pyroclastic flows moved into them; outline queried where extent unknown
FLOWAGE-HAZARD ZONE 3—Areas which probably could be affected only by floods; includes Lake Merwin, the level of which could be raised rapidly if water in reservoirs upstream were displaced by mudflows, pyroclastic flows, or floods; outline dashed and queried where extent unknown
0
5
10
15 MILES

Figure 3

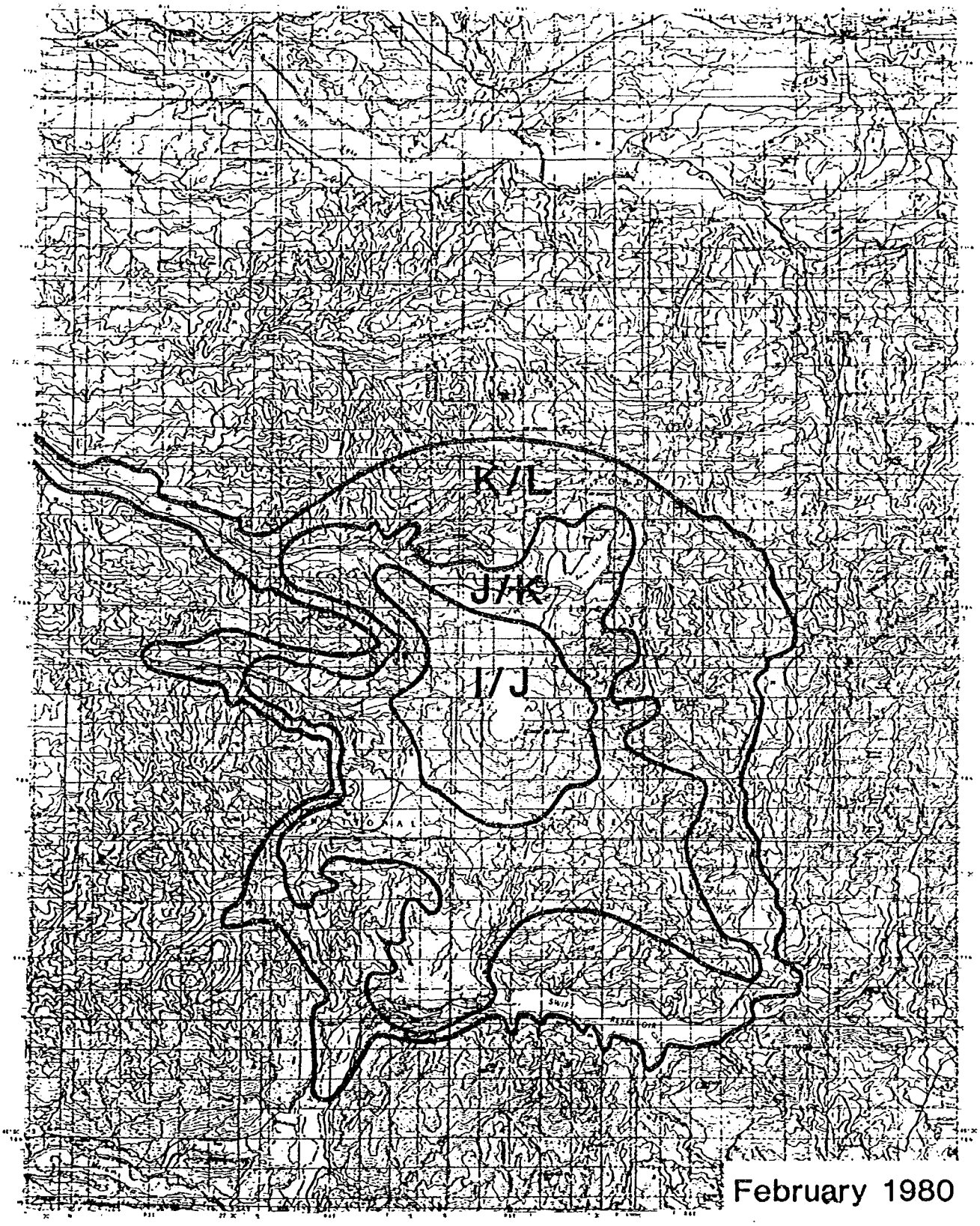
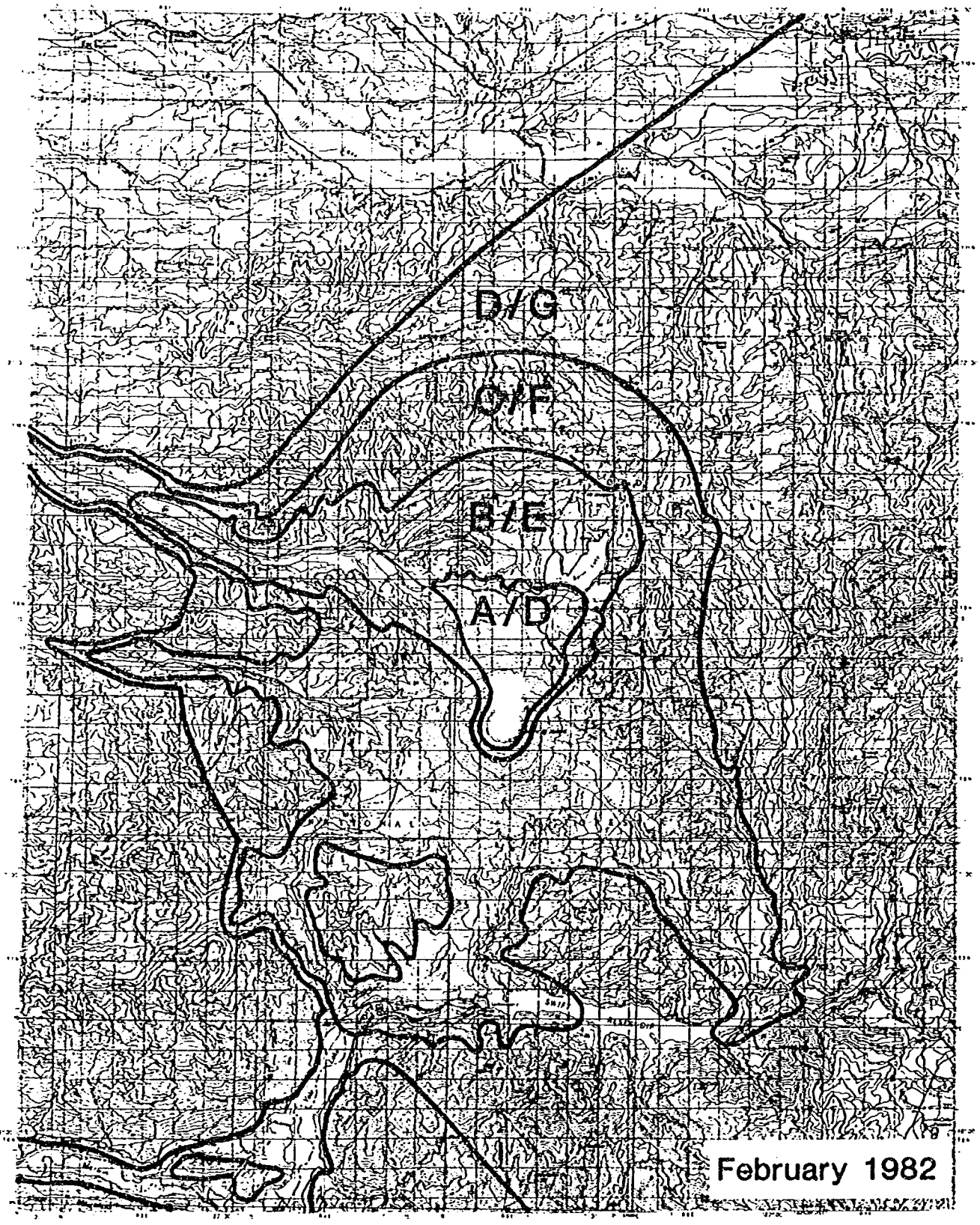

K/L
J/K
I/J
February 1980
MOUNT ST. HELENS AND VICINITY, WASH.-OREG.

Figure 4



MOUNT ST. HELENS AND VICINITY, WASH.-OREG.

Study on Volcanic Disasters and Forecasting of Hazard Areas

Akito Nakasuji*
and
Hiroshi Ikeya**

Preface

Japan is one of the countries in the world which has many volcanoes, having suffered a great number of volcanic disasters in the past. In recent years, there has been a rise in the number of residents in the piedmont of active volcanoes in conjunction with the modern sprawl in living areas, the number of tourists visiting active volcanoes having also increased year by year. Given this situation, there is a high possibility of damage several times that of the old days, once an eruption has started. Therefore, it might be considered as an urgent task to designate hazard areas, impose restrictions on land use, and set a warning and evacuation system.

In this paper we will introduce typical volcanic disasters that have occurred in Japan in the past. In addition, we will report on the results of an investigation into methods of forecasting hazard areas, taking as an example the Usu volcano which erupted recently (1977) and has been the focus of much attention. Further, regarding debris flow disaster which frequently occurs in Japan, we will mention methods of forecasting hazard areas that are being made public as research results at present.

* Geological Survey Department, Kokusai kogyo Co, LTD

** Erosion Control Department, Ministry of Construction, Japan.

I. Overview of Volcanic Disasters in Japan

There exist 830 or so active volcanoes in the world. Of them, about three-fourths are distributed around the Pacific Ocean (including Indonesia). Japanese islands exist 67 active volcanoes. On the average, 10 percent of them (or seven volcanoes) burst into eruption every year. The Japanese archepelago is literally volcanic islands and the population density is quite high. The major eruptions that have been documented are enumerated in Table 1. An attempt will be made to introduce some of the representative ones.

I-1 Disasters by Pyroclastic Flows

A pyroclastic flow is the most dreadful of all volcanic disasters. A typical example is the damage caused by the pyroclastic flows of Mt. Asama which erupted in 1783.

Mt. Asama is situated in the centre of Japan (Fig. 1). It is a conical volcano, the total cubage of which is about 60 km^3 and which is composed to pyroxene andesites. The biggest volcanic eruption on record occurred in 1783. The eruption was a typical one of andesite magma, much evident in Japan, with pumice and ash fall and lava flow being observed at regular intervals. The developments in the eruption are shown in Table 2. In the initial phase, vulcanian explosions took place sporadically over a period of about three months and the eruptions progressively became successive with a rise in intensity. In the last phase, there were pyroclastic flows (known as "Kambara pyroclastic flows") with significant explosions. In a pyroclastic flow, mixtures of hot pumice and volcanic ash flow down with enormous rocks. In the upper part, there was powerful erosion over a length of about 4 km. At a point about 8 km from the crater, the sedimentation of pyroclastic flows began. The flows destroyed and buried Kambara and three other villages and dammed up the Agatsuma River at a point 13 km from the crater. The banks of this river subsequently gave way, giving rise to a big flood and causing greater damage (about 1,200 persons were killed). The temperature of the

pyroclastic flows stood at nearly 1,000°C and their energy was so big as to move rocks, several tens of metres in diameter, at high speed (several tens of metres per second). Immediately after the occurrence of pyroclastic flows, enormous volumes of lava flowed out of the crater, and a series of eruptions ran up to an estimated one billion tons.

Besides the damage produced by the pyroclastic flows of Mt. Asama, the damage caused by the occurrence of nuée ardente, twice, from Mt. Usu in Hokkaido, and the pumice flow several times from Mt. Komagatake in Hokkaido, is well known.

I-2 Major Failures of Mountains with Steam Explosions

For this type, the eruption of Mt. Bandai in 1888 is well known. This eruption was similar to that of Mt. St. Helens.

Mt. Bandai is a typical strato-volcano situated in Northeast Japan. This volcano became active about 30,000 years ago but only two eruptions -- one in 806 and the other in 1888 -- are on record. The developments in the 1888 eruption are enumerated in Table 3, and the topographical changes that took place before and after the eruption, are shown in Fig. 3. One week before an enormous eruption, rumblings and peals of distant thunder were heard in succession as omens of an eruption. Shortly after seven o'clock on July 15, the volcano bursted into eruption with a strong earthquake. With an enormous failure of the mountain (the formation of a U-shaped crater), pylocrastic materials began to flow down at an estimate average speed of 80 km/h. The distribution acreage is estimated at 3.5 km^2 and the total cubage at 1.5 km^3. As a result, three villages were totally immersed and damage was also inflicted on eight other villages, killing 461 persons and afflicting 563 households. One feature of the flows of pylocrastic materials is a dry avalanche. At the ends, the pylocrastic materials mixed with river water, turning into mud flows. The sediments dammed up streams, resulting in the appearance of five big lakes.

Mt. Tokachidake, situated in the centre of Hokkaido, erupted in

1926, resulting in a collapse of the northern half of the central volcanic cone and in the occurrence of debris avalanche. The snow layer melted, and mud flows sped down at a high speed of 60 km/h and hit a village 20 km away, killing 144 inhabitants.

I-3 Other Volcanic Disasters

This has nothing to do directly with volcanic activity, but the secondary mud flows which are generated when there is a localized torrential downpour under unsuitable topographical conditions, such as the sedimentation of volcanic ashes, take place in various parts of Japan every year. The mud flows generated at Mt. Usu in 1978 are well known as they hit a hot spring community at Lake Toya, killing three persons. Mud flows also occur at Sakurajima and Mt. Yakedake several times a year.

The tsunami is also well known for its infliction of huge damage. A tsunami is generated when a volcano bursts into great eruption and its materials send into the sea, and might be described as a kind of indirect volcanic disaster.

II. Forecasting of Hazard Areas at Usu Volcano

II-1 Topographical and Geological Conditions of Usu Volcano

Mt. Usu is one of the most active volcanoes in Japan. Situated in the southwestern part of Hokkaido, it is a young caldera cone located at the southern rim of Toya Caldera which was formed as a result of major eruptions of pyroclastic flows in the late Pleistocene age. The volcanic edifice of Mt. Usu is composed of a somma volcano with parasitic scoria cone and a number of lava domes and cryptodomes. These domes are aligned in two parallel zones, running in the direction of NW-SE through the summit and north flank, probably controlled by the structure of Toya Caldera's southern wall as shown in Fig. 4.

The main volcanic body of Mt. Usu was formed by repeated eruptions of lava flows and a scoria of theoleiitic basalt and mafic andesite in the early Holocene period. After the completion of a strato-volcano, 7,000 or 8,000 years ago, its summit was broken by a violent explosion, accompanied by a debris avalanche which rushed down the southern route into the sea (known as Zenkoji debris avalanche). The destruction of the summit resulted in the formation of a somma, 1.8 km in diameter at an elevation of approximately 500 metres.

In a dormant state that lasted for several thousand years, the nature of the magma became extremely felsic. Then the historic activities during the past three centuries commenced with a strong Plinian eruption of rhyolitic pumice, which was followed by the formation of dacite lava domes and cryptodomes, sometimes occupying nuées ardentes.

II-2 Recorded Activities of Usu Volcano

Seven explosive eruptions in 1663, 1769, 1822, 1853, 1910, 1943∿1945 and 1977∿1978 are on record, as shown in Table 4. During the activities in 1822, nuée ardente flowed down the southern slope and destroyed one village, killing 50 persons and 1,437 horses.

A regular repetition of Mt. Usu's eruptions at an interval of 30 ∿ 50 years in later times attracts our attention in regard to the prediction of an eruption. The duration of the preceding earthquakes was generally short, less than 10 days, except for that of the 1943 ∿ 1945 activity.

II-3 Eruption in 1977 and Mud Flow Disaster

The Usu volcano, which had been dormant for 32 years since the formation of the Showa-Shinzan lava dome, became active with local earthquakes on August 6, 1977. On August 7 at 9^h 12^m, 30 hours after the beginning of the preceding earthquake swarm, a major pumice eruption occurred from the Usu volcano, the eruption cloud reaching a height of 12 km in one hour. Soon, the eastern part of the volcano was blanketed with volcanic ash. Later, three major eruptions took place (Fig. 4), producing four craters in the crater basin. The total cubage of volcanic products ran up to 83 million m^3, as volcanic sediments were piled up to a height of 1 m at the top and 30 ∿ 50 cm at the foot. The fallen volcanic ash destroyed dwellings at the foot (eight houses were completely destroyed and four partially), and damage was broadly inflicted on farm produce right before harvesting, and also forests.

In 1978, there was a repetition of steam explosions of the second phase and the ground surface was blanked with fine volcanic ash, with the result that the infiltration capacity of rainwater was aggravated. The fall of an otherwise insignificant 20 ∿ 30 mm of rain twice resulted in generating a mud flow -- October 16 and 24 -- at the entire area of Mt. Usu's piedmont (Fig. 5). In particular, the mud flow that assaulted a hot spring community at Lake Toya on October 24, was big in dimension, killing three persons and destroying a large number of houses. The damage caused by the eruption was estimated at ¥31,500 million and the mud flows brought about damage to the tune of an estimated ¥10,500 million.

II-4 Area Hazardous to Pyroclastic Flows (nuée ardente)

A pyroclastic flow rushes down at high temperature and speed. Once it has been generated, inhabitants down its course simply do not have time to run away, with the result that a disaster occurs. Fortunately, no major pyroclastic flows have occurred in the last 50 years or so, so that neither hazard areas are designated nor are legal restrictions imposed, thus posing a serious danger. In this context, Indonesia is ahead of Japan. Three different types of areas, the areas off limits at all times and Classes I and II hazard areas, are designated. A warning issue and delivery system, evacuation routes and places of refuge have also been developed.

A nuée ardente has occurred at Mt. Usu three times in recorded history. In each case, the sediments gave rise to the appearance of typical facies which were primarily made up of poor foaming reddish brown pumice so that their distribution could be accurately grasped. What is shown in Fig. 6 was prepared at the suggestion of the authors. This hazard area contains a golf course and some 20 tourist shops and farm houses. As soon as a preceding earthquake has occurred an immediate evacuation order should be issued, and it is necessary for the inhabitants of this area to be aware of a possible danger at all times.

II-5 Area Hazardous to Volcanic Mud Flows

II-5-1 Demarcation by Topographical Analysis

The ground of the piedmont of the volcano is overwhelmingly formed as a result of the erosion, transportation, and sedimentation of volcanic mud flows, etc., though some part is influenced by the fall and sedimentation of volcanic products. Therefore, by classifying the landform of the fan in terms of the land form development history, and sorting and analyzing the factors of relations between the formation of the land form and sediment disasters, it seems possible to some extent to predict an area of subsequent inundation and sedimentation.

On the basis of a land form classification chart (Fig. 7) prepared for a small fan-shaped area of Mt. Usu's piedmont, and a chart of the area exposed to the danger of flood (Fig. 8), which is prepared according to the classification chart, an attempt will be made to elucidate the method of demarcating the area of inundation and sedimentation. As the topographical factors associated with the inundation and sedimentation of volcanic mud flows, the following fine land features are of importance.

(1) Sediment of Tongue Shape

A close check of the aerial photographs taken of the alluvial fan reveals that there exist several surges, vertically in two or three stages and horizontally according to the scale of the alluvial fan. Let us call it a sediment of tongue shape, as it is shaped like a tongue in form. An alluvial fan is formed as a result of the repeated sedimentation of volcanic mud flows and debris flows. In each alluvial fan, an identical debris flow is apt to be generated, depending on the basin characteristics of rear streams, and the flow comes to a stop under similar sedimentation conditions (e.g, slopes). The tongue shape appears to have been formed through a number of debris flow deposits coming together.

(2) Small Valley and Minor Channel (Surface Channel)

In general, a lowland is observed between tongue shapes, and stretches as far as the lower reaches in many cases. This low area is called a minor channel. In many cases, a minor channel appears to have been formed as a result of the surface erosion by the subsequent flows which go down after the main mud flow. Of the small valley, the part where rafting is conspicuous is excavated in the shape of a ditch. This is called a surface channel.

A hazard area is demarcated on the basis of its having a tongue shape and a small valley. Here, it is necessary to take note of the following principle:

In general, the alluvial fan is shaped like a smooth cone. Regular change of flow-down course is generated at the top of an alluvial fan, while the lower part is progressively heaped up with sediment, thus giving rise to the appearance of an alluvial fan. Conseguently, it is a repetition of ① flow down a small valley and ② sedimentation in the small valley (formation of a tongue shape) and new excavation (formation of a small valley). If this phenomenon is taken full note of, it becomes relatively easy to predict a next flow course.

At the foot of a big volcano, broad riparian valleys are developed. In such a case, the method of demarcating hazard areas as used for Mt. Merapi, an active volcano in Indonesia, is useful. Methodologically, it is the same as the aforementioned method. The form and scope of the past floods are grasped in on-the-spot interview, and a potential flood area is hypothesized along with the preparation of a land form classification chart on the basis of aerial photographs. Consequently, a river valley is somewhat different from an alluvial fan, in the sense that narrow parts and meandering points of the river are taken into account.

II-5-2 Demarcating Method with Random Walk Model

W.E. Price (1974) carried out a simulation with a random walk model for the formation of an alluvial fan. Basically, this method is used for the demarcation of a hazard area. In this method, things are grasped in terms of hundreds to thousands of years, so that there is a need to impose a variety of new conditions for volcanic mud flows which are generated every year, or at an interval of several years, as is the case with a volcanic area.

The Random Walk Model is the statistical method in which a mesh is put over an alluvial fan, a variety of conditions are imposed when some fluid passes points of intersection on the mesh, and a simulation is done with an electronic computer in a manner fitted to the actual flow. The fundamental condition of this method is as follows:

The possibility of a fluid moving from one point of intersection to another (transition probability: P_S) is hypothesized as being in proportion to the slant (S) of the given direction.

$$P_S \propto S \quad \cdots\cdots (1)$$

If S = 0 (horizontal), the probability is equal.

Therefore,

$$P_S = 0.25 + a \cdot s \quad \cdots\cdots (2)$$

where, a is the proportional constant of sin α and s is a difference in elevation in the moving direction. In Equation (2), S = 1.0 (vertical), a = 0.75 to make $P_S = 1.0$.

Therefore,

$$P_S = 0.25 + 0.75 \sin \alpha \quad \cdots\cdots (3)$$

where, α is the angle of the moving direction. The force of inertia (straight advance) functions, so that the probability is high for the mud flow to take a same direction from the previous one. Consequently, if the force of inertia (I_n) is multiplied in Equation (3),

$$P_S = (0.25 + 0.75 \sin \alpha) \cdot I_n \quad \cdots\cdots (4)$$

where, $I_n \geq 1.0$.

Incidentally, in the direction of 8, the following equation may be given.

$$P_S = (0.125 + 0.875 \sin \alpha) \cdot I_n \quad \cdots\cdots (5)$$

Next, as a means to compute the probability of the mud flow taking one of the four directions of the mesh from an optional point, a random number is produced and the moving direction is determined on the basis of relations between the random number (U_i) and the transition probability (P_S). The relations may be expressed as follows:

$$R_n = \mathrm{MOD}\ (U_i/(P_{S1} + P_{S2} + P_{S3} + P_{S4})) \quad \cdots\cdots (6)$$

where, MOD is the residual from the brackets. The random walk comes to a stop when the following conditions are imposed.

1) Cases where the mud flow takes a direction other than the given mesh,
2) cases where the designated number of random walks is completed, and
3) cases where the mud flow reaches an obstacle.

The conditions which may be given as initial ones include ① the total cubage of the sediment (the volume of sediment discharge (V)), ② average thickness (H), ③ width between meshes (W) and ④ average width of materials flowed down (A). The walk frequency (n) is determined in the equation of $n = V/H \cdot W \cdot A$.

The Random Walk Model is a probability model in every aspect and essentially is not tied in with an estimate of the sediment volume. For an alluvial fan which is fitted to the actual scope of sedimentation, however, this model is extremely useful for prediction of the place where the probability of sedimentation is high due to the running down of mud flows in the next phase.

Fig. 9 indicates the distribution of mud flows which hit a hot spring community at Lake Toya in October 1978. The distribution is reproduced with a four-direction random walk model in Fig. 10. Once a model with such a good adaptability is produced, it is feasible as a useful yardstick for the demarcation of a hazard area, as a simulation may be made by changing the generated scale, one by one. Fig. 11 shows the flood of the fan of Sobetsu Hot Spring into which mud flows ran down in October, 1978. A simulation is made with and eight-direction random walk models in Figs. 12

The scope of sedimentation is broad, as the simulation has been done on a scale considerably larger than the actual scale of the flow-down, but it might be said that the tendency of sedimentation are comparatively identical.

III. Demarcation of Hazard Area to Debris Flows

Seventy percent of Japan's land is mountainous, and mountainous areas other than those in the volcanic areas are also broadly distributed. There are constantly exposed to residants the danger of dedris flows caused by torrential rains, and it is reported that there are 62,000 such hazardous streams in Japan. It would be almost impossible to cope with that many hazardous streams through check dams and other civil engineering works, in terms of time and cost-effectiveness. For this reason, there is a need to demarcate hazard areas to cope with disasters caused by debris flows, by evacuation and control on land use. Studies in this sector are earnestly conducted by the Public Works Research Institute of the Ministry of Construction and other organizations.

III-1 Demarcation of Hazard Area Based on Actual Disaster

Mr. Ikeya et al. (1977) surveyed many debris flows which occurred on the island of Shodo in Kagawa Prefecture in September 1976 and proposed the following demarcation plan:

(i) The hazard areas are classified into one due to debris flows, and the other due to sediment flows (Fig. 13).

(ii) The exit of a valley or highest point of fan is considered the starting point of a flood, and sedimentation begins when the original incline is less than 15° for debris flows and less than 8° for sediment flows.

(iii) The incline at the sedimentation ceasing point is up to 4° for debris flows and 0° for sediment flows.

(iv) The sedimentation is 3-5 m in thickness for debris flows and 2 ∿ 3 m for sediment flows.

(v) The length (L) of sedimentation of debris flows is expressed in the following equation.

$$\log L = 0.42 \log (\tan \theta \times V_S) + 0.935$$

where, tan θ is the average incline of the flow-down section and V_S is the volume of debris.

(vi) The flow-down width (Bc) of debris flows is computed from the volume of debris (V_S) and the length of sedimentation (L) in the following equation:

$$B_C = 1.5 \sqrt{3V_S/L}$$

or the width is computed from precipitation in the following equation:

$$B_C = 3 Q_p^{1/2}, \quad Q_p = 1/3.6 \cdot f \cdot re \cdot A$$

where, f is the coefficient of runoff, re is the effective precipitation and A is the area of the basin.

(vii) The relations between the flow-down width (B_C) and the dispersion width (L_B) are expressed in the following equation:

$$L_B = (6 \sim 10) B_C$$

The above empirical equations may be put to considerably effective use for small-scale fans.

III-2 Demarcation of Hazard Area with Model Experiment

Ikeya (1982) carried out a model experiment, using as the model the Hora Valley in Gifu Prefecture where debris flows occurred in August 1979 and concluded that it would be possible to demarcate hazard areas.

The model scale was set at 1/70. The values of the discharge, length of time, sediment volume, granularity and other conditions were used according to the fluid rule on a 1/70 scale. For the experiment, nine cases were prepared according to the discharge, sediment volume, length of time and topographical factors. The results may be summarized as follows:

(i) There is a certain critical value to the sediment discharge. When the volume of debris piled up on the bed of a valley is V_{SI} and two-thirds of the total discharge after the occurrence of a debris flow is V_{SII}, V_{SI} may be considered the sediment discharge by the debris flow in the case of $V_{SI} \leq V_{SII}$, and V_{SII} in the case of $V_{SI} > V_{SII}$.

(ii) The hazard area in which a plurality of debris flows are generated by a single rainfall may be demarcated by the sediment length of maximum one and a dispersion width roughly ten times as big as the run-down width.

(iii) Debris flows are entirely different from sediment flows in terms of the impact produced on houses and human lives.

(iv) In case there exists an appropriate flow channel in a fan, the sediment flow is relatively less hazardous and the debris flow is considerably reduced by the first wave of energy.

(v) In a model experiment, it is possible to study the mechanism of the stoppage and sedimentation of debris flows by changing the experiment conditions. This method is also of use in coming to grips with a hazard area by imposing the most dangerous conditions. It is also desirable that experiments be conducted for volcanic mud flows and sediment flows, let alone debris flows.

Conclusion

In the foregoing, an attempt has been made to elucidate on the demarcation of hazard areas, which is under study in Japan primarily on the basis of disasters in the past. The studies do not go beyond the research sector nor are they something which is conducted with legal measures. However, the authors believe that it will become necessary in the near future to make use of the results of these studies.

Acknowledgements

We wish to thank Professor Saburo Higashi at Hokkaido University, related officials of the Debris Disaster Division, Department of Public Works, Hokkaido Government, and Mr. Masaichi Nakayama and Mr. Ryohei Imamura of Kokusai Kogyo K.K. for their kind assistance and guidance in the preparation of this report.

Reference

1) Aramaki, S. (1968), Geology of Asama Volcano. Monograph/14, Association for the Geological Collaboration in Japan

2) Ikeya, H., and Yonezawaya, S. (1977), Study on the Hazard Area of Debris Flow, Civil Engineering Journal, Vol.19, No.12

3) Ikeya, H. (1982), Experimental Study on Debris Flow Hazard Area, Jour. of the Erosion-Control Engineering Society, Vol.34, No.3

4) Imamura, R., and Sugita, M. (1980), Study on the Simuration of Debris Depositing based on a Random Walk Model, Jour. of the E·C·E·S, Vol.32, No.3

5) Katsui, Y., and others. (1978), Preliminary report of the 1977 eruption of Usu Volcano, Jour. Sci., Hokkaido Univ., Ser.4, No.8

6) Nakamura, Y, and Aoki, K. (1980), Mt. Bandai, the Earth Monthly, Vol.2, No.6

7) Nakasuji, A., and others. (1980), Study on Demacation of Hazard Area to Debris Flow, Jour. of the E·C·E·S, Vol.33, No.1

8) Price, W, E. (1974), Simuration of Alluvial Fan Deposition by a Random Walk Model, Water Resource Research, Vol.10, No.2

9) Soya, T., and others. (1981), Geological Map of Usu Volcano, Geological Survey of Japan

Table 1 Main Volcanic Disaster in Japan

Name of Volcano	Age of Eruption	Dead Persons	Main Activity
Komagadake (Hokkaido)	1640	700	Eruption, Failure of Volcanic Body Tidal Wave
Osima Ôshima	1741	1,467	Ditto
Asamayama	1783	1,151	Eruption, Agatuma and Kamahara Pyroclastic Flow, Lava Flow
Unzendake	1792	15,000	Earthquake, Failure of Volcanic Body, Tidal Wave
Usuzan	1822	50	Bunsei Nuée Ardente
Bandaisan	1888	477	Eruption, Failure of Volcanic Body, Debris Flow
Torishima	1902	125	Eruption
Sakurajima	1914	63	Earthquake, Eruption, Lava Flow
Tokachidake	1926	144	Pyroclastic Flow, Mud Flow
Komagadake (Hokkaido)	1926	2	Eruption, Pumice Flow
Myojinsho	1952	31	Submarine Eruption
Asozan	1958	12	Eruption
Usuzan	1977-78	3	Eruption, Mud Flow

Table 2 Progress of The 1783 Eruption of Asamayama (by Aramaki, 1968)

	Situation of Eruption	Volume of Pumice Fall and Ash
May 9	First Eruption (Dormancy during 45 Days)	
June 25	Eruption, Rumbling, Ash Fall (Dormancy during 19 Days)	
July 17	Rumbling, Pumice Fall on The Northern Foot (Dormancy during 7 Days)	0,17 km^3
July 26	Eruption	
July 27- Aug.2	Repeat Eruption and Rumbling. Continue Ash and Pumice Fall.	
Aug. 3	Beginning Violent Eruption from 14:00	
Aug. 4	Occurred Agatuma Pyroclastic Flow (Afternoon ?)	0,1 km^3
Aug. 5	10:00Big Explosion Kamahara Pyroclastic Flow Lava Flow	 0,01-0,001 km^3 0,17 km^3

Table 3 Progress of The 1888 Eruption of Bandaisan (by Nakamura)

	Time	Situation of Eruption
July 8		Rumbling, Thundersound
July 9		Ditto
July 10		Ditto
July 13	15:00-16:00	Rumbling
July 14	8:00	Rumbling
July 15	7:00	Thundersound, Slight earthquake
	7:30	Middle-Strong earthquake
	7:45	First eruption cloud rose up 1,5 km. Eruption continued 15-20 times. Last one erupted on the northern side horizontally. A large quantity of clastics flowed down and destroyed 3 village. Eruption cloud rose up about 5 km and translated eastern side.
	10:00	Main activity was stopped.

Table 4 Record of The Eruption of Usu Volcano (by Katsui)

Age of Eruption	Interval (Year)	Duration of Forerunning Earthquake	Main Activity
1663		3 Days	Pumice and Ash Eruptions, and Formation of Ko-Usu Lava Dome, 5 Persons Death
	- 105 -		
1769		?	Ash Eruption, Nuée Ardente (Named Meiwa)
	- 52 -		
1822		3 Days	Ash Eruption and Nuée Ardente (Named Bunsei) and Formation of Ogariyama Cryptodome 50 Persons Death
	- 30 -		
1853		10 Days	Ash Eruption and Nuée Ardente (Named Tateiwa) and Formation of Ō-Usu Lava Dome
	- 56 -		
1910		6 Days	Steam Explosions, Volcanic Mud Flow and Formation of Meijishinzan Cryptodome 1 Person Death
	- 30 -		
1943-45		6 Months	Steam Explosion and Formation of Showashinzan Lava Dome, 1 Baby Death by Suffocation
	- 32 -		
1977-78		30 hours	Pumice and Ash Eruption, Volcanic Mud Flow and Formation of Usushinzan 3 Persons Death

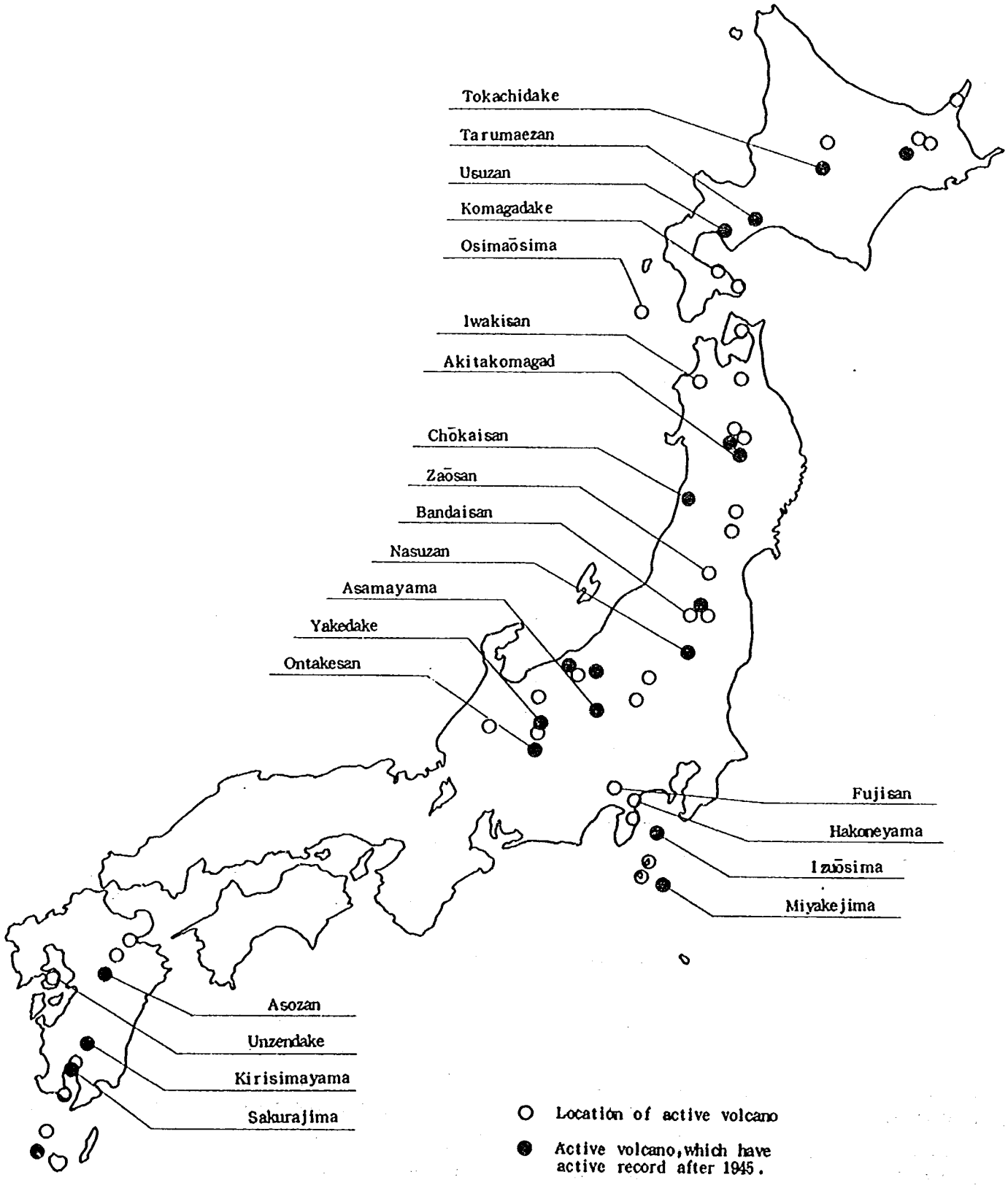
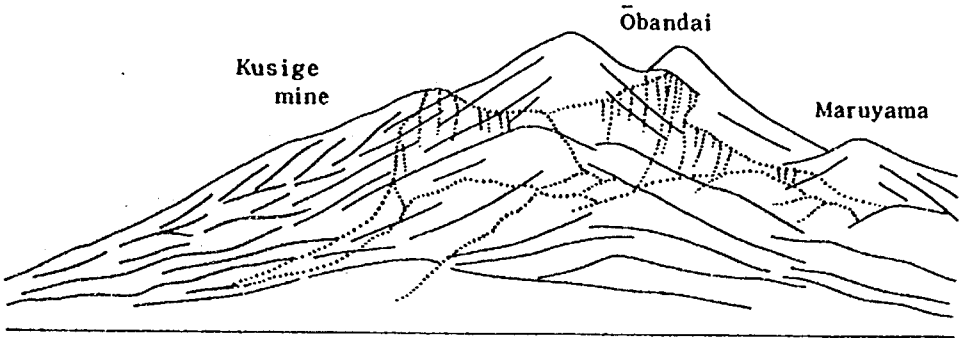


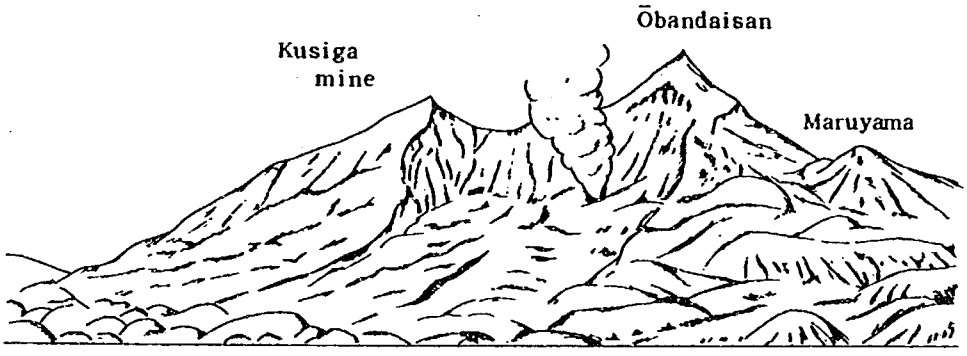
Fig-1 Distribution of Active Volcano in Japan. (by Akira Suwa)

Before Eruption



Interrupted line mean recent slope condition.

After Eruption



Many mudflow hills are distributed on foot slope.

Fig-3 Mt. Bandai of before 1888 eruption and after eruption. (by Sekiya)

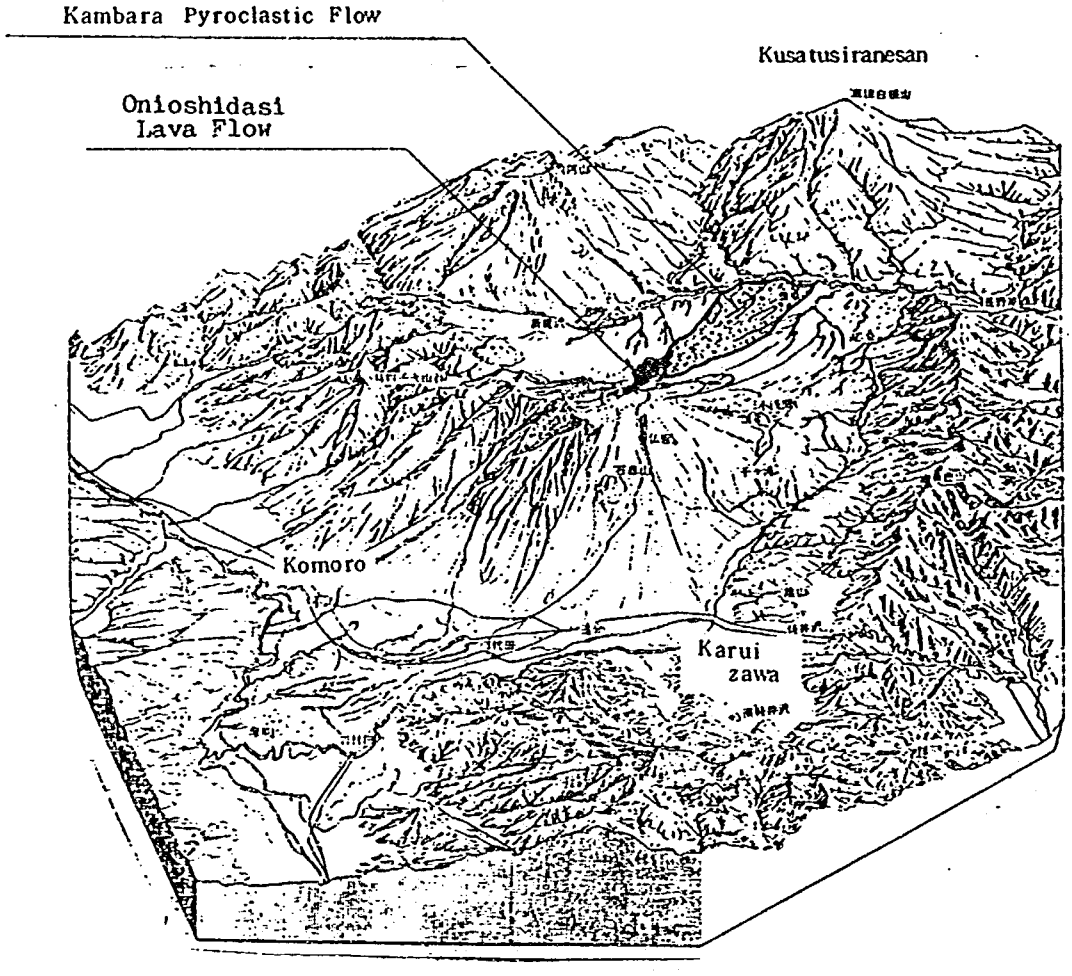


Fig-2 Bird's-eye view of the Asama volcano and it's around district.
(by Aramaki, 1968)

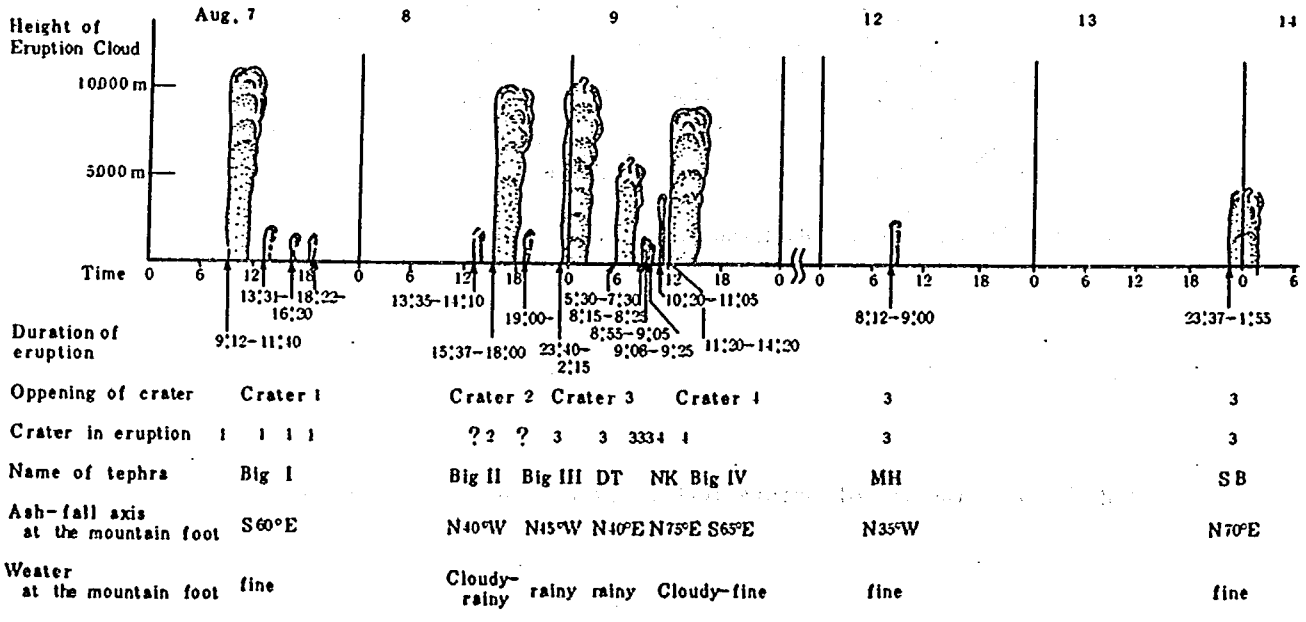
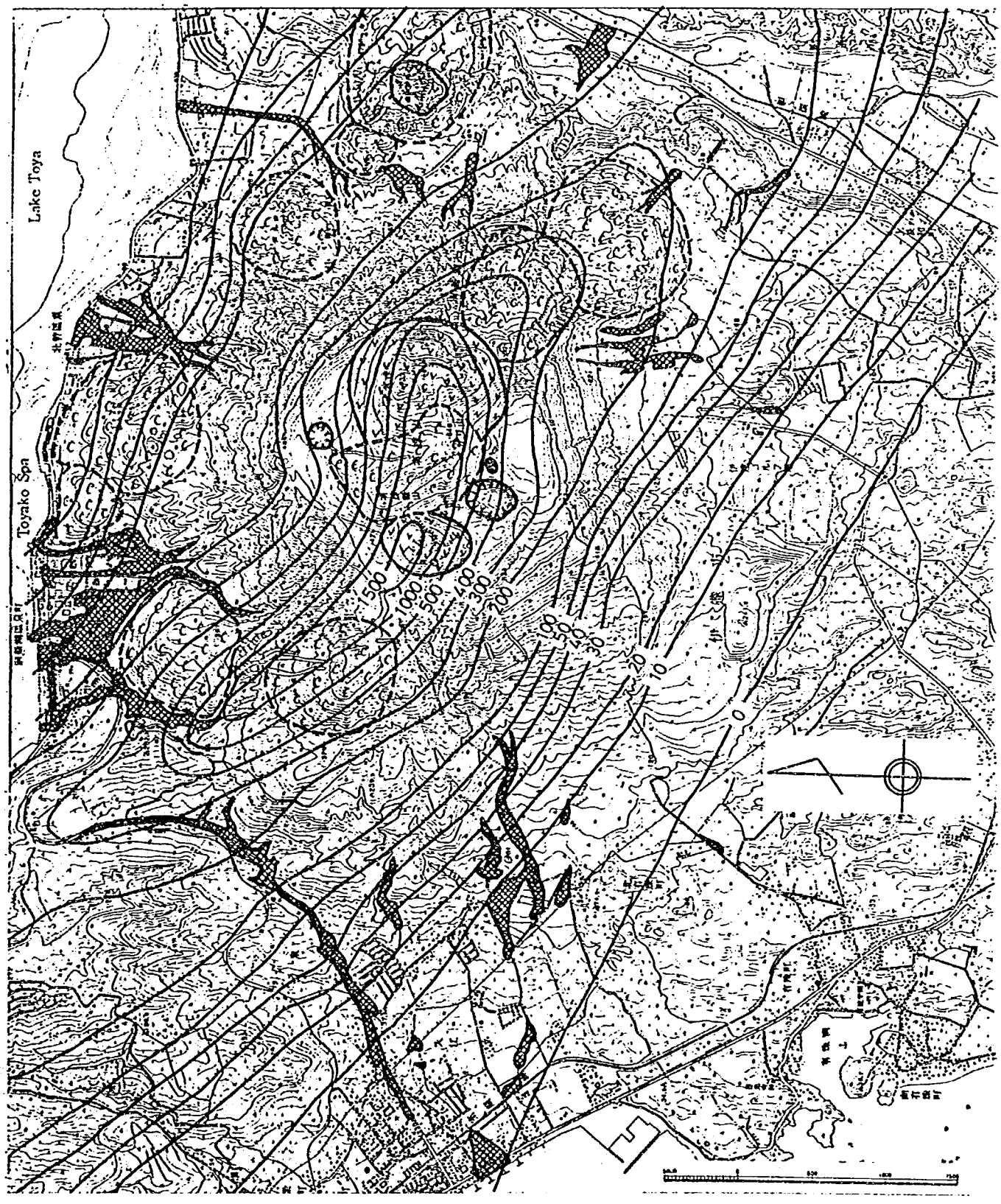


Fig-6 Sequence of the eruption of Uolcano Volcano in August, 1977 (by Katui, 1978)



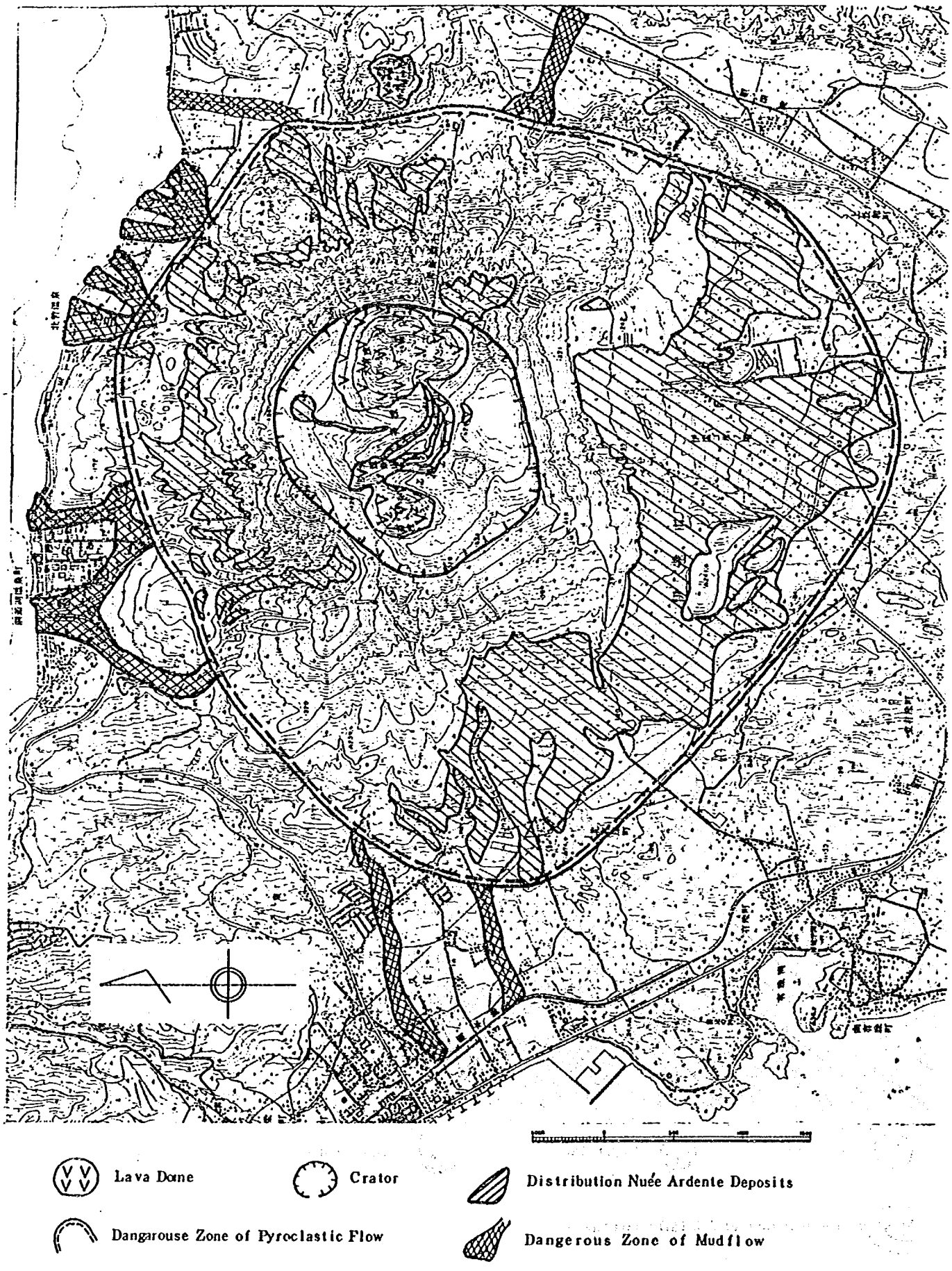
Lava Dome

Cryptodome

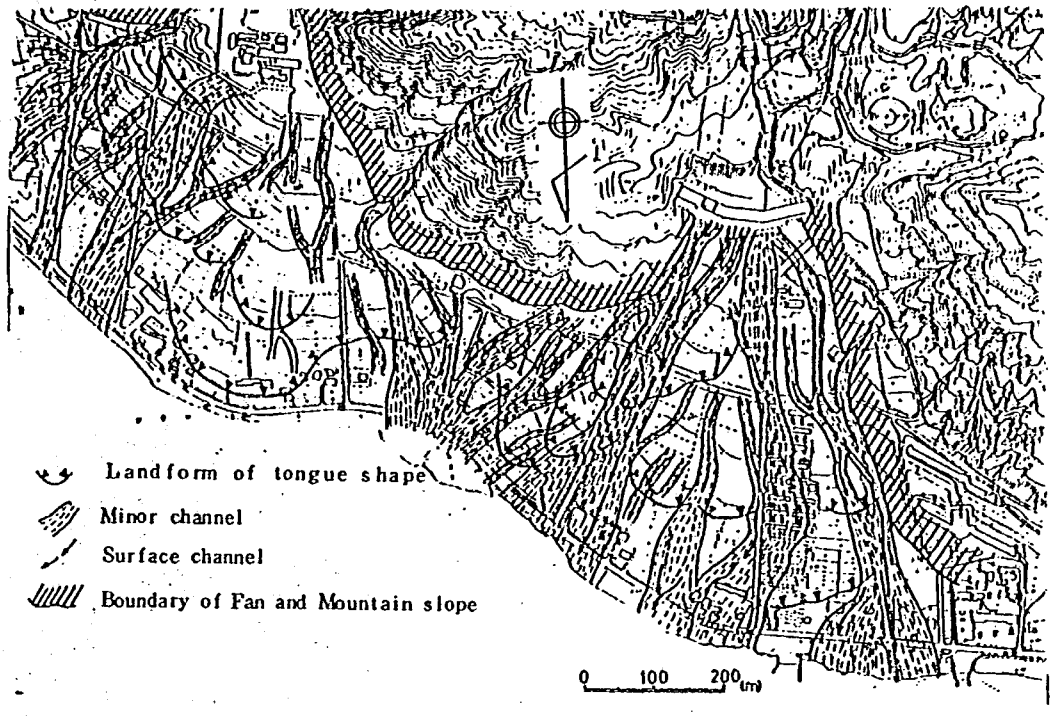
Distribution of Mud Flow

200 Contour Line of Ash Fall (unit : mm)

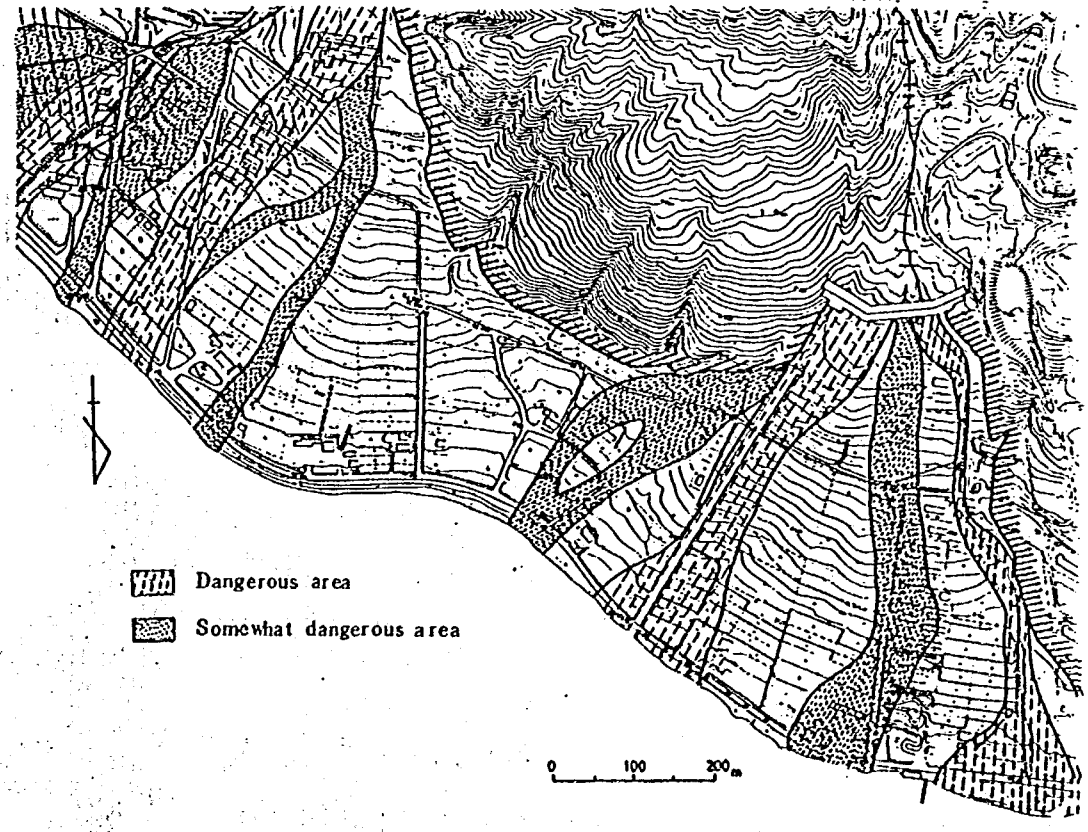
Fig－4 Distribution of Mudflow and Ash fall in the Vicinity of Mt. Usu, Activity in 1977～1978.



Fig－6 Hazard Area to Pyroclastic Flows in the Vicinity of Mt. Usu



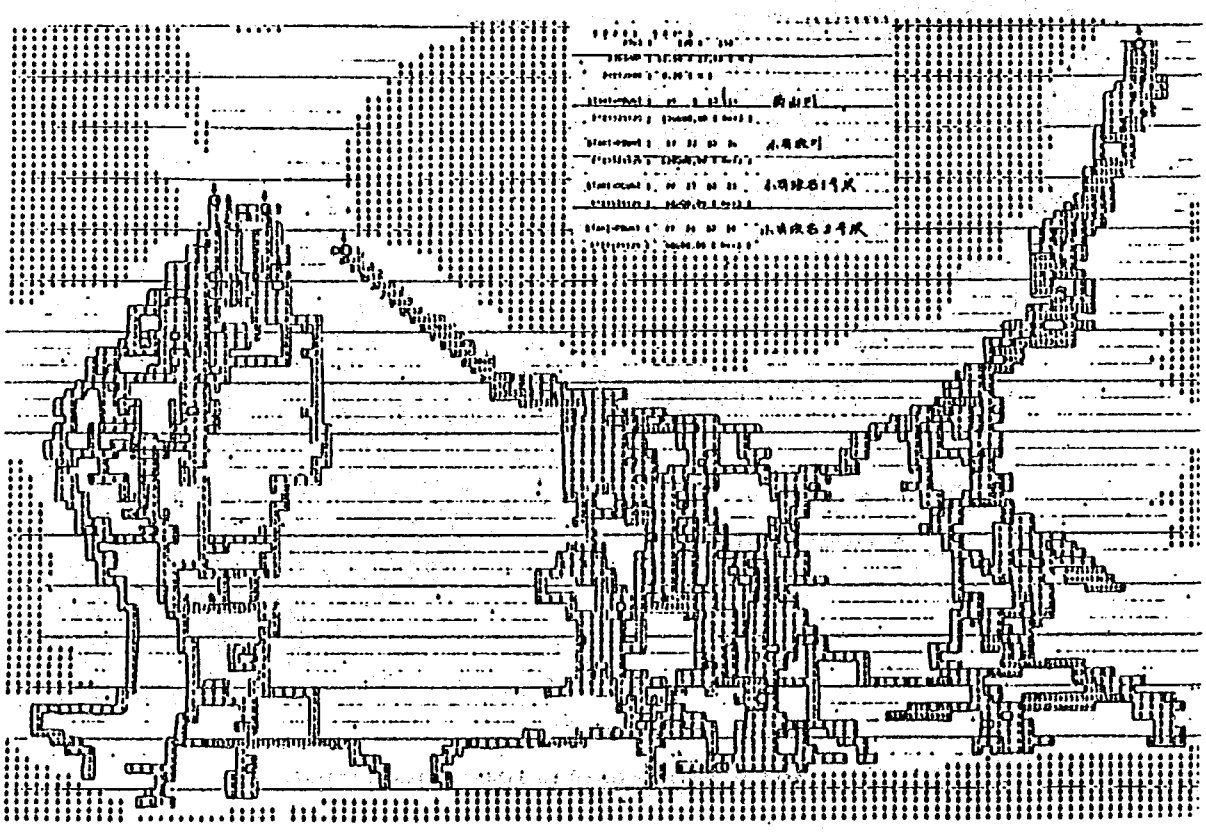
Fig－7　Land Form Classification Map in Sobetu Area



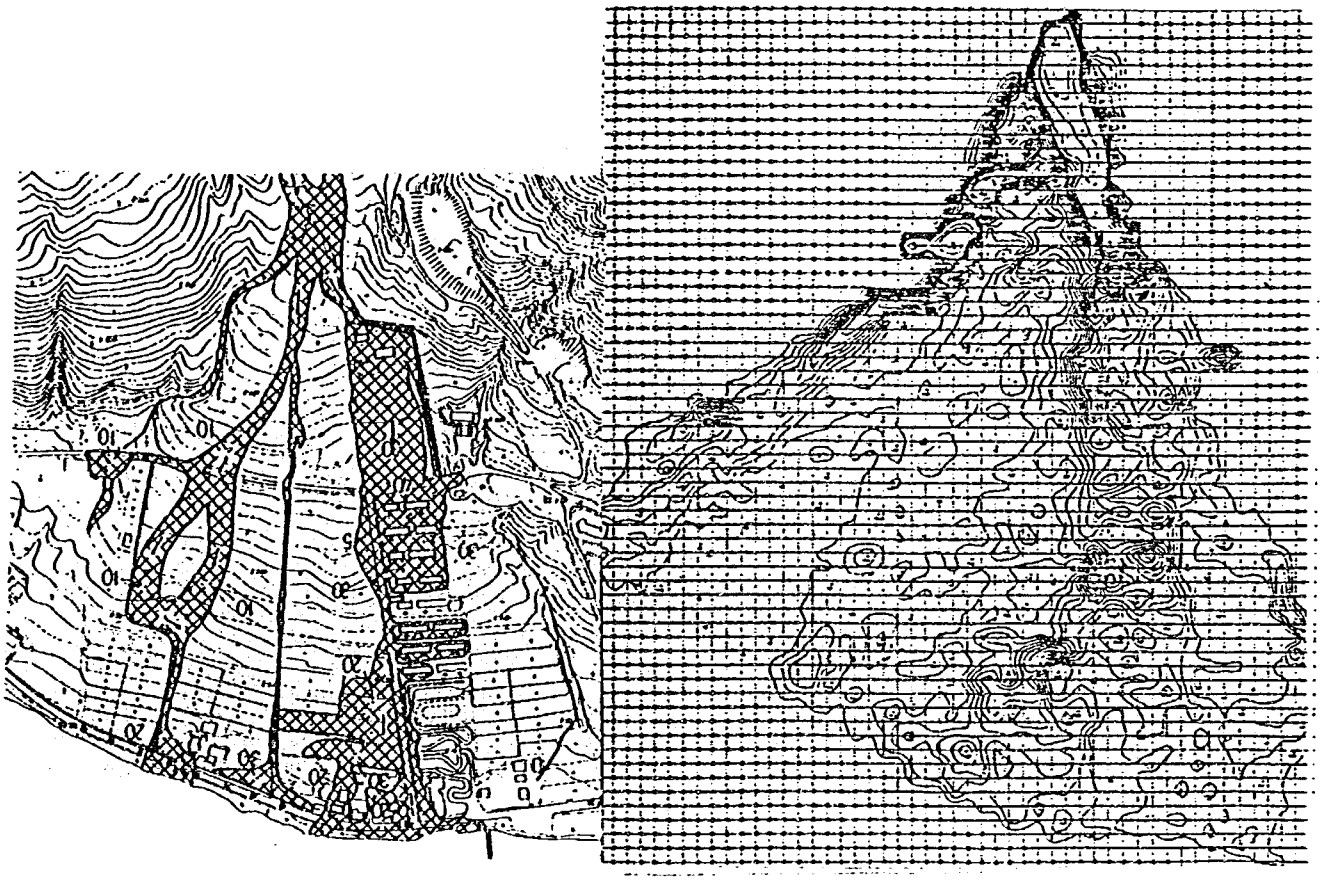
Fig－8　Hazard Area to Mudflow based on Topographical Analysis



Fig－9　Distribution of Mudflow in October, 1978, Toyako Spa

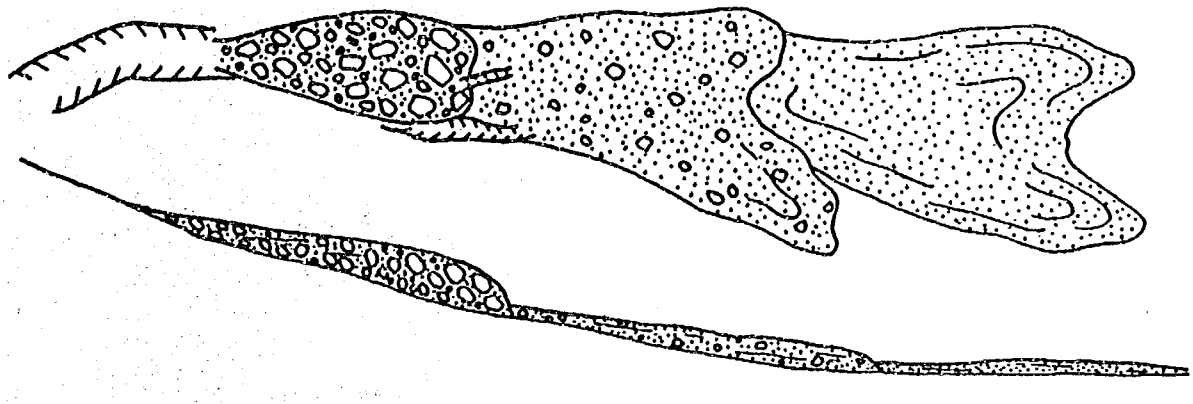


Fig－10　Reproduction Map of Mudflow used by Random Walk Model



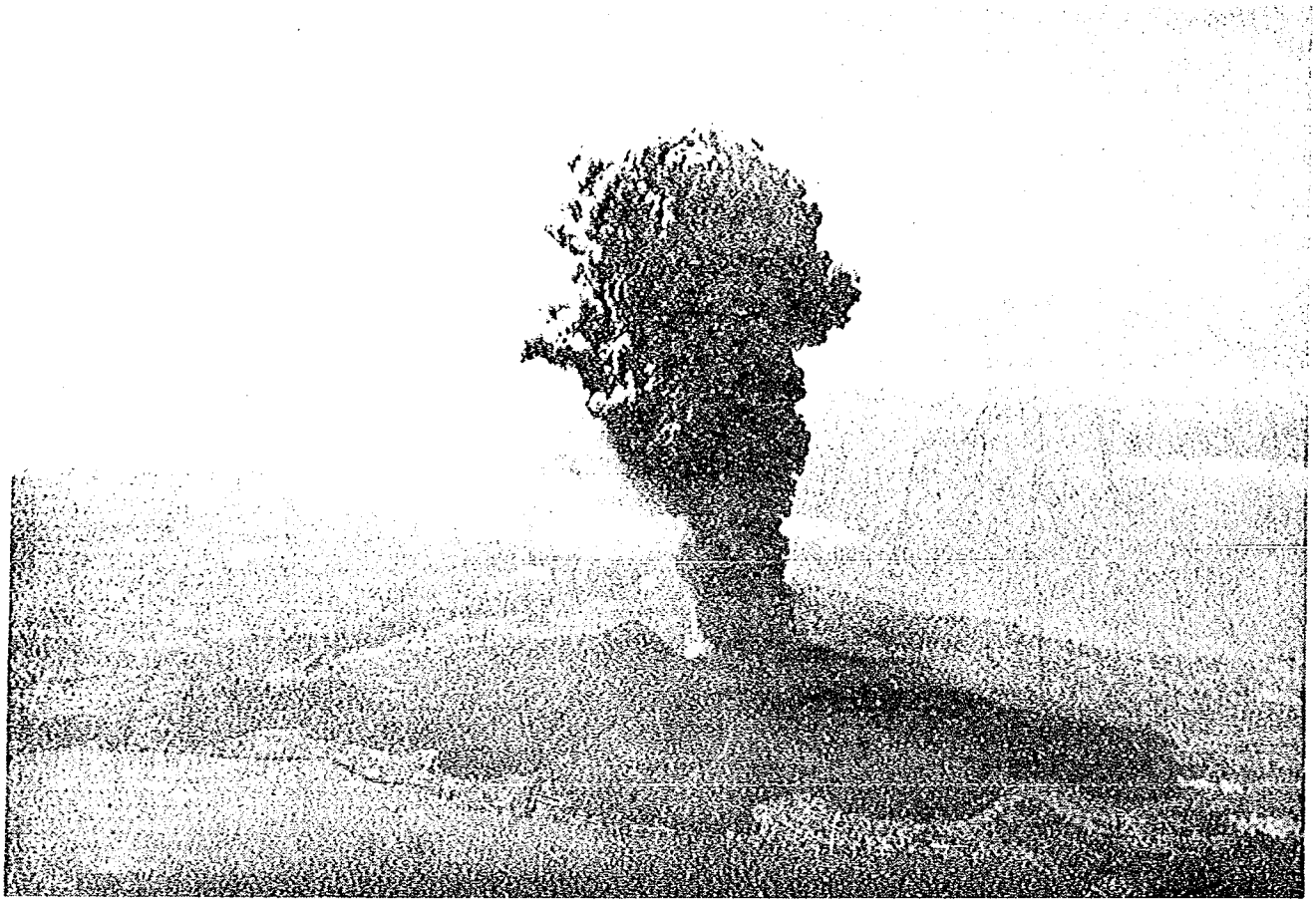
Fig－11 Distribution of Mudflow in October 1978, in Sobetu Area

Fig－12 Simuration Map, using Eight－direction Randon Walk Model, in Sobetu Area



Classification	debris flow	sediment flow (a broad sense)	
		sediment flow (a narrow sense)	flood flow
site of accumulation	maximum ϕ= 3~4m average ϕ= 0.2~0.5m	maximum ϕ = 1m average ϕ = 0.1~0.05m	maximum ϕ= 10~20cm average ϕ= 05cm
depth of sediments	maximum = 4m average = 2m	maximum = 1.5m average = 0.5m	maximum = 10m average = 03m
surface condition of sediments	irregular	mixed to irregular and smooth	smooth
cross sectional condition of sediments	non bedding	partially flow－structure (bedding)	clean flow－structure (bedding)

Fig－1 General Figure of Debris and Sediment Flow in Shoboshima



First Eruption of Usu Volcano, August 7 (9^{h} 12^{m}), 1977



Recent Toyako Spa and Usu Volcano (1982)

DISCUSSION AT THE U.S. - JAPAN SYMPOSIUM

ON EROSION CONTROL ON VOLCANOES

Paper of Janda

Ikeya: Did incision and widening of channels take place throughout the system?

Janda: During the first post-eruption year we observed both incision and widening of channels on the debris avalanche deposit. In the second year, the avalanche deposit widened and filled to various degrees illustrated in the paper. Below the debris avalanche deposit there was both deepening and filling, as well as dramatic widening during the first year, and filling and continued widening during the second year.

Ikeya: Is there evidence of earlier debris flows originating on Mt. St. Helens?

Janda: The stratigraphic record shows that lahars (debris flows) have occurred relatively frequently in the recent geological history of Mt. St. Helens. Deposits from these lahars repeatedly follow the same paths, but have different properties; for example, some consist of more rounded coarse particles than others. The original material may have been angular, but subsequent lahars triggered by lake breakouts may have incised rounded bouldery alluvium in the valley floor.

Ikeya: How was the speed of the avalanche surveyed or calculated?

Janda: Several methods were used:

(i) Measurements of the distance of travel on successive timed photographs;

(ii) The avalanche over-ran the 300-meter high Coldwater Ridge. Use of the equation

$$vel_{min} = \sqrt{2gh}$$

yields a minimum speed of 77 m/s;

(iii) The distance travelled by the snout of the avalanche divided by the seismic signature of the avalanche yields an average speed;

(iv) Balancing the radial acceleration against the super-elevation of the debris flow surface at valley bends leads to the well-known equation

$$\bar{u} = \sqrt{r \cos \alpha \tan \Theta g}$$

* * * *

Paper of Araya and Higashi

Lisle: What is the meaning of the wide and narrow reaches on your last slide?

Araya: The wide zones represent reaches that were sites of deposition while the narrow zones indicate the location of scour or of no net change in sediment storage.

Mizuyama: What controls the location of the narrow zones in your figure?

Araya: They are usually the sites of bedrock control.

Pierson: Is there any relation between erosion and deposition and channel gradient?

Araya: The study reach was 500m, and over that length the gradient varied little.

Dunne: In Japan do you have reliable formulas for predicting the heavy sediment transport rates observed on volcanoes?

Ikeya: A variety of sediment transport formulas are used, including local, empirical formulas. In a particular region, we use the one(s) which experience indicates to be most accurate under the local conditions.

* * * * * *

Paper of Lisle et al.

Shimokawa: Please explain in greater detail the effect of organic matter on flow and sediment transport.

Lisle: Large organic debris disperses the flow of small streams, so that there is no obvious thalweg. There is relatively slow, complex flow through the debris and deposition of sediment occurs between trees that have fallen across the channel. Local scouring occurs under fallen tree trunks or beyond their ends. The flow often divides into several small braided channels at low flow.

Where there is no large organic debris, the channel has a single thalweg incised to a gravel armor layer and there is a bar on one side of the channel.

Janda: There are important differences between channels affected directly by lahars (debris flows) and those channels that were affected only by the lateral blast from the volcano. The lahars flushed out channels up valley and deposited sediment

in the lower valley. Little or no large organic debris was left in the channel and sediment could be flushed downstream efficiently in succeeding years. In the blast zone, large quantities of large woody debris were left in the channel and they caused a rapid attenuation of sediment impacts downstream.

* * * *

Paper of Daido

Dunne: In Japanese debris flows, have you observed any evidence of the behavior that Johnson witnessed which led him to interpret their behavior in terms of the Bingham constituative equation?

Daido: No.

* * * *

Paper of Fairchild and Wigmosta

Nolan: Isn't it possible that the trees may have been broken by logs floating on the debris flow?

Fairchild: Video films show that both log jams and single logs oriented perpendicular to the flow broke trees in the central part of the lahar. We confined our attention to those channel reaches and channel margins in which we were confident that floating logs did not break the trees, either because the fallen trunks did not show gashes or splintering, or because they were distributed through stands in which larger trees survived.

* * * *

Paper of Shimokawa and Taniguchi

Janda: On what are your sediment yields based?

Shimokawa: Volumes and density of dated deposits.

Dunne: How accurate are Japanese methods for predicting sediment yields and sediment transport rates in streams on active volcanoes?

Shimokawa: The first step is the accumulation of data on sediment yields and we find large variations between sites. On the basis of these data we can make rough estimates of sediment yields following eruptions of the same form as those affecting the basins that we have studied.

* * * *

Paper of Swanson et al.

Shipley: Does the density of the tephra vary with time?

Swanson: Our repeated measurements of the bulk density of the tephra have not revealed any changes since a few weeks after the eruption.

Shipley: How does the surface crust on the tephra affect runoff and sedimentation?

Swanson: In the early months after the eruption, the surface of the silty airfall tephra from the May 18, 1980 eruption formed a thin crust of exceedingly low conductivity. The sandier airfall tephra from June 12, 1980 developed a more permeable crust. The origin of these crusts is not known, and it would be interesting to us if any of the Japanese participants could provide any information on this feature. The low infiltration capacity of the crusts resulted in abundant overland flow, sheetwash, and hill erosion. Changes in the crusts during the first post-eruption year increased infiltration and decreased the erosion rate.

* * * *

Paper of Tsukamoto et al.

Dunne: What is the annual expenditure on Sabo works around Mt. Nantai?

Tsukamoto: Approximately 0.25 billion Yen per year.

* * * *

Paper of Stockton

Ikeya: How did you design the cross-section of the spillway on the Debris Retaining Structures to pass the debris flows?

Stockton: The Probable Maximum Flood was calculated and then doubled as a safety factor. The estimated recurrence interval of the design event was 500-2000 years.

Ikeya: How do you calculate the impact force of debris flows on a dam?

Stockton: We use the formula

$F = \rho h \bar{u}^2$,

where F is the impact force, ρ is density, h is thickness, $\bar{u}$ is the vertically averaged flow velocity.

Ikeya: We use empirical relationships.

* * * *

Paper of Anyoji et al.

Janda: Have any controlled experiments been done to measure the effectiveness of Sabo dams in controlling sediment discharge?

Ikeya: No controlled experiments have been conducted, but there have been many informal comparisons of sediment yield (especially in pictorial form) in adjacent torrents with and without Sabo dams during and after large rainstorms.

* * * *

Paper of Newhall

Ikeya: Do landowners object to your estimates of hazard on their land because of any change in value or restriction on use?

Newhall: They object, but we simply define the hazard zone, and pass that information on to the politicians, who define the zone in which land use will be restricted.

Ikeya: Who is responsible for the prediction of an eruption?

Newhall: It is the joint responsibility of scientists from the University of Washington and the U.S. Geological Survey.

Mizuyama: How do you predict when the volcanic activity of Mt. St. Helens will decline?

Newhall: In the nineteenth century, the volcano continued to erupt for 57 years. Earlier periods of activity involved relatively frequent eruptions during a period of 100 years. Therefore, it is likely that (probably small) eruptions will continue for many years. During the next several years eruptions will probably involve mainly dome-building, and should not significantly affect erosion. Over a time-scale of decades there will probably be explosive eruptions, and even small eruptions can melt snow and trigger lahars, as on March 19, 1982

* * * *

Summary of Final Discussions
Symposium on Erosion Control in Volcanic Areas

The fourth and final day of the Symposium on Erosion Control in Volcanic Areas was devoted to discussion of erosion control efforts at Mount St. Helens and selected sites in Japan. The American delegation was particularly interested in getting impressions of Japanese scientists and engineers who have had a long history of work on erosion problems in volcanic areas. Discussions dealt with three topics: effectiveness of existing measures, possible future mitigation measures, and research needs.

Much of the discussion centered on the North Fork Toutle River basin (Fig. 1), because of its position above populated areas and high potential for additional mudflows and continued extreme rates of sediment production. Erosion control on the debris avalanche that inundated about 60 km^2 of the upper North Toutle valley (Fig. 1) was a crucial issue, because it supplied about 75 percent of sediment leaving the upper basin during June 1980 - May 1981 (Lehre et al. 1982).

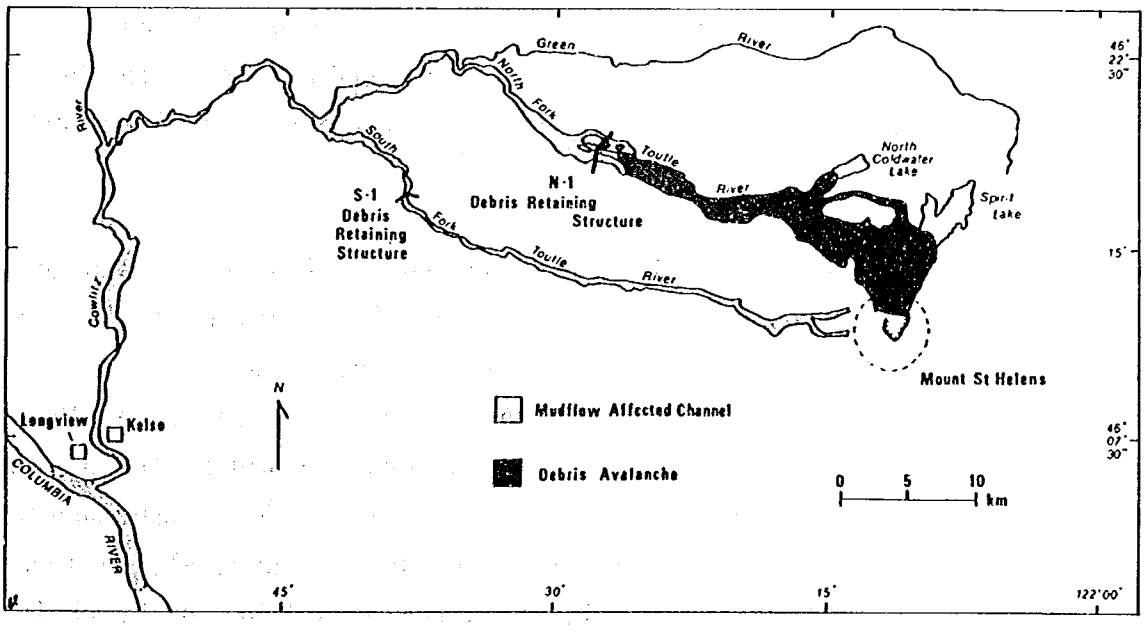


Figure 1. Map of area near Mount St. Helens, State of Washington, U.S.A.

American Discussion of Erosion Control at Mount St. Helens

The U.S. Army Corps of Engineers has assumed primary responsibility for attempting to control possible flooding and sedimentation problems resulting from the 1980 eruptions of Mount St. Helens. S. Stockton began the discussion of existing and possible future engineering means of reducing problems along the Toutle, Cowlitz, and Columbia Rivers. To date, nothing has been done to control similar problems along other streams draining the volcano because sediment loads, and the immediate adverse social consequences there, are not as great.

Stockton indicated that channel excavation work has effectively restored navigation on the Columbia River and flood protection along the Cowlitz River. However, suitable spoil sites for future excavation are quite limited because of prior commitments to other productive uses of the land. Additionally, channel excavation has been quite expensive, therefore, it is now hoped that equally successful, but more cost effective, sediment control can be implemented in upstream areas. Initial channel excavation efforts on the middle reaches of the Toutle River were not effective because subsequent streambank erosion entrained much of the spoil. On the other hand, good potential exists for effective dredging along the lower Toutle River, in part because satisfactory spoil sites are available at reasonable cost. In the future, rock riprap may be emplaced to protect spoil areas from bank erosion.

Two debris retention basins have been constructed (one on the North Fork Toutle River and one on the South Fork, Fig. 1). Stockton indicated that these basins slowed the initial flush of sediment from the eruption-impacted area, but that the long-term effectiveness of these structures was minimal because they were undersized and a lack of funds prevented effctive maintenance dredging. The South Fork structure was removed in fall 1982. The North Fork structure was severely damaged by flood discharges on February 20-21, 1982, and by a lahar on March 19, 1982; the future of this structure is a matter of active discussion.

Stockton also indicated that the Corps of Engineers constructed outlet channels for lakes dammed by the debris avalanche deposit. This was done to prevent disasterous fill-spill floods from two large lakes impounded in the lower valleys of Coldwater and South Castle Creeks. The controlled outlets are safe at present, but the long-term stability of these impoundments is still of some concern because of headward erosion, changing groundwater levels, seismic events, and other site conditions. Spirit Lake poses a more challenging problem because of the potential size of the lake and the extremely erodible nature of some of its impounding materials. Shortly after this symposium, construction of a buried pipeline and barge-mounted pumping system was started to control the level of the lake. Several possible strategies for attempting to construct a permanent, controlled outlet for this lake are still under consideration.

At present, no funds are available for routine sediment control in the Toutle-Cowlitz River system. Measures under study for possible implementation in the future include (1) excavation of the lower three kilometers of the Toutle River, (2) excavation of sediment traps in other areas of expanding flow along the Toutle River, (3) construction of several additional small debris retention structures, and (4) staged construction of a single high dam. Initial economic analysis suggests that a high dam would be the most cost effective of these alternatives. Although it is generally desirable to control sediment as close to the source as possible, the Corps of Engineers can see no vaiable means for controlling the rapidly eroding North Fork Toutle debris avalanche deposit because of persistent extreme instability.

Rock riprap has been successful so far in presenting stream bank erosion that could jeopardize the interstate highway and railroad bridges near the mouth of the Toutle River. However, the chances for future success are unclear if aggradation continues. Aggradation could similarly make proposed revetments around spoil areas ineffective. In the open discussion that followed Stockton's presentation, there was general consensus between the Japanese and American delegations that, despite present difficulties, sediment control along the middle and upper reaches of the Toutle River will be cost effective over the long-term.

H. Ikeya asked what time scales are considered in planning engineering activities and what are the geographic trouble spots. Stockton replied that initial planning focussed on a 5- to 10-year time period, but the Corps is now looking at a much longer time frame. The principal trouble areas extend from the mouth of the Toutle where a major highway and railway cross the river, along the Cowlitz River where many poeple live to the Columbia River where ship passage is critical (Fig. 1). As sediment moves further downstream, disposal of spoils is increasingly expensive because of limited sites. A particularly critical spot is Horseshoe Bend on the Cowlitz River where a potential meander cutoff could increase the local slope, causing instability and jeopardizing levees.

J. Winjum and F. Swanson reviewed vegetative approaches to erosion control and effects of salvage logging and contour scarification. These physical treatments of sites have mixed 1980 deposits and exposed pre-1980 soils, thereby increasing infiltration rate and reducing rates of surface erosion. Seeding with a mixture of grasses and legumes met with mixed success depending on elevation and thickness and texture of deposits from the 1980 eruptions. About 8000 ha of the blast zone were seeded and fertilized from helicopters. Areas of coarse pumice at elevations above 750 m experienced poor establishment. Lower elevation sites with silty and sandy surface deposits had moderate establishment, but in localized sites of good establishment, small mammal populations flourished and damaged conifer tree seedlings. Establishment of grass from some of the seeding operations may have also been limited by the late date of planting. Plantings of conifers for timber production and black cottonwood (Populus tricocharpa) for stream protection have had generally good rates of establishment.

Japanese Discussion of Erosion Control at Mount St. Helens

T. Mizuyama pointed out that papers on erosion studies at Mount St. Helens dealt with small scale problems, but that the overall erosion problem is occurring on a large scale. For example, excellent data are available on channel changes measured by repeated surveys of channel

cross sections, but there is great need for monitoring changes in the longitudinal profile. He also suggested that channel changes might be predicted by use of sediment transport equations.

K. Tanaka began his discussion of the Toutle River sedimentation problem by citing an example from an Indonesian volcano where a debris avalanche of 0.2×10^9 m^3 (Mount St. Helens debris avalanche = 2.5×10^9 m^3) caused downstream aggradation for only 5 years. He felt that check dams on the Toutle River would be rapidly flooded with sediment and that it was necessary to reduce sediment inflow from upstream. Even a high dam would not contain the volume of material in the debris avalanche. Furthermore, a high dam must be designed to withstand the impact forces of mudflows. Tanaka suggested that streamflow in the Toutle River could be reduced by diverting water through a tunnel to another drainage. The debris avalanche deposit might be stabilized with riprap and gabions.

Sediment movement through the Toutle would continue even if the debris avalanche were stabilized. Sabo dams on the order of 4 m high might be of value on the Toutle River below the confluence of the North and South Forks. However, scour below dams would necessitate many such structures.

K. Tanaka also commented that new lakes "may not be so dangerous". Some Japanese lakes have breached gradually, but there are also many examples of disasterous failures of landslide dams such as on the Aritagawa River in 1953.

A. Daido indicated that sediment discharge is a function of particle diameter, depth and width of flow, and channel gradient. In attempting to control sediment discharge, attention is usually focused on either physically trapping the sediment or on reducing channel gradients. These are the functions of sabo dams. Unfortunately in the case of the Toutle River, the gradient is already quite low. Therefore, it might be desirable to attempt to reduce the depth and width of flow. Because channel dimensions are a function of water discharge, sediment discharge could possibly be slowed to manageable rates by diverting some water from the Toutle River into a tunnel that would discharge directly into the Cowlitz River. This suggestion is parallel to that of Tanaka. Daido

suggests that the appropriate volume of diverted flow might be about equal to the sustained low flow of summer. This flow could possibly be used to generate electrical power (thereby partially offsetting the cost of the project) and would still be available to flush sediment through the Cowlitz River. Storm discharges, that according to Corps of Engineers and U.S. Geological Survey spokespersons account for the majority of sediment transport, would still flow down the natural channel.

With regard to Stockton's comment that a possible meander cutoff at Horseshoe Bend could signficantly increase the local gradient of the Cowlitz River and cause it to assume a braided channel pattern. Diado suggested that as long as the sediment grain size remains relatively constant, it is equally plausible that the meander will migrate downstream. He was favorably impressed with the apparent stability of rock riprap along stream banks, but pointed out that meander migration could adversely affect that stability.

A. Takei emphasized the point made many times during the Symposium that the Japanese erosion control specialists found volcanic and erosion phenomena at Mount St. Helens to be occurring on a very large scale. The debris-avalanche deposits present very important but difficult problems of control. He commented that the Japanese had different opinions about the type and timing of construction and potential success of structural controls on the debris-avalanche deposit. His personal view is that structures might be effective on the debris avalanche in 3 to 4 years after channel changes and volcanic activity settle down some more. Now it is important to continue efforts in downstream areas, particularly maintenance of the existing, but damaged, North Toutle debris retaining structure. A series of small (4 to 6 m high) structures in the lower and middle sections of the North Fork Toutle may be helpful. The outlet for Coldwater Lake appears quite stable, but must be maintained carefully.

N. Anyoji pointed out that the events at Mount St. Helens on March 19, 1982, were similar to those initiated by a 2×10^6 m^3 debris avalanche at Mount Tokachidake, Hokaido, on May 25, 1926. The hot avalanche deposit rapidly melted snow and triggered mud and debris flows

that scoured 0.5-1.0 m into the pre-existing valley floor, destroyed much valuable timber, and killed 144 villagers before coming to rest 20 km from its source area. Anyoji indicated that the lahars were examples of high velocity Bingham flow. Initial velocities were 40-50 m/s, and at the base of the cone flow depths were still 10 m and velocities 10 m/s. Large boulders were transported well beyond the base of the cone. Janda pointed out that the small flows initiated by the April 4-5, 1982 partial collapse of the north flank of the Mount St. Helens dome may have been more simiar to the 1926 Mount Tokachidake flows than the March 19, 1982 blast- and snow-avalanche induced flows at Mount St. Helens.

Anyoji indicated that attempts to control erosion at Mount Tokachidake were started only a few years ago, and that control measures were not placed in headwater areas in order to preserve the natural slopes of the volcano which has been set aside as a national park. Protection is afforded primarily by a "staircase" of three large dams (10-15 m high, and 200-300 m long) on the Furano River. The uppermost dam is allowed to remain full whereas attempts are made to keep the two downstream structures free of sediment. Disposal of material excavated from the Furano River dams is a costly problem similar to that associated with dredge spoil disposal along the Cowlitz River.

C.-L. Chen questioned the effectiveness of sabo dams to reduce sediment discharge, because they could potentially be full of sediment during critical flow events. Ikeya responded by saying that the role of the sabo dams is not only to trap sediment but also to reduce channel gradients, and thereby reduce tractive force. These structures are more effective in controlling coarse-grained bedload than in controlling fine-grained material. However, fine sediments generally cause few problems related to changes in channel geometry as they pass through a river system. Chen then asked whether the heights of sabo dams are ever increased after they fill. Ikeya indicated that was indeed the case when staged construction was included in the original plan. More commonly, however, attempts are made to use repeated excavation to prevent the initial dams from filling.

J. Kataoka discussed approaches to grass seeding for erosion control in Japan. Seeding is usually done in spring before the rainy season or in

the fall at the end of the typhoon season. Each time has special problems: spring planting may result in good germination followed by mortality in the hot, dry summer and establishment from fall seeding may be limited by cold weather. J. Winjum pointed out that, based on studies by Weyerhaeuser Company, seeding at Mount St. Helens might have been more effective if carried out earlier in the year.

Kataoka reported that the Japanese use Kentucky blue grass, clovers, and other species from the United States. As found in the case of Mount St. Helens, seed of native species were hard to get in large volume. Seed is sometimes applied in a mixture with mud, but this must be done from roads. Aerial seeding in volcanic area has not been very successful, because fertilizer and water may be needed also.

T. Araya described vegetative erosion control efforts at Mount Usu where the 1977 eruption heavily damaged vegetation over 200 km^2. Tephra 40 to 100 cm thick covered over 10 km^2. Vegetation establishment was attempted by applying grass and willow seed and willow branches from the air and planting of willow and Abies spp. Steps were formed on hillslopes using sheet metal, wood pilings, and willow wattles (bundles of willow shoots laid across slope) in an effort to stop rill and gully erosion. Erosion was measured under conditions of bare ground, 50% plant cover, and 100% plant cover. A maximum erosion rate of 1 to 2 cm/yr occurred in the bare ground plots.

Discussion of Research Needs

R. Janda identified needed research in two categories: theoretical research of general applicability and research specific to a particular situation. In the case of Mount St. Helens additional analysis of the role of the debris-avalanche deposit as a source of sediment is urgently needed. The sediment budget by Lehre et al. (1982) for the North Toutle River for June 1980 - May 1981 identifies this deposit as the major sediment source in the basin. In the following year, however, the relation between channel width and cross-sectional areas, used by Lehre et al. to estimate erosion from the debris-avalanche deposits in 1980-1981, may over-predict actual erosion. The relation appears to have

changed significantly as channels widened and backfilled in response to a rising groundwater table.

A more general need is for bedload transport equations that are applicable under conditions of very high concentrations of suspended sediment and wide ranges in size gradation of bed material. The Meyer-Peter Mueller equation pertains to conditions of low suspended sediment concentration and other equations were developed for finer, better sorted bed material than that in the Toutle River. It is unfortunate that bedload transport and deposition are major causes of channel change and flooding problems, because that is the element of fluvial sediment transport that is most difficult to measure and predict. We urgently need to improve our ability to predict sediment yield and channel changes. Attempts to link rainfall-runoff models to sediment transport models could be rewarding. Moreover, predictions of future channel behavior could benefit from having some stochastic elements imbedded in the largely deterministic models now in use.

J. Winjum, F. Swanson, and R. Janda commented that, although hillslope erosion has decreased substantially, we will continue to monitor erosion by sheetwash, rills, gullies, and landslides. We need to better understand effects of vegetation on each process and ways to use vegetation in controlling erosion rates. Changes in rainfall/runoff relations and effects of volcanic events, such as pyroclastic flows, and altered plant cover on snow melt, are additional important topics for further research, because these factors affect potential for floods and mudflows.

Additional Discussions

Daido pointed out that effective design of sabo dams and other sediment control measures requires reasonable prediction of total sediment yield. This can be done by direct measurement, by use of hydraulic equations, or by study of drainage basin parameters. Sediment yield was successfully predicted for proposed reservoir sites on the Pemali and Comal Rivers in north central Java using an equation relating volumes of sediment trapped in 40 Japanese reservoirs to the product of the square of the average

gradient of eroding areas and the ratio of actively eroding area to total basin area (Daido 1975). Further development of this type of predictive formula is desirable because predictions based on other method are most costly and time consuming.

Tsukamoto questioned the use of repeated measurement of height of erosion pins above the ground surface to measure hillslope erosion. He and Mizuyama emphasized that this method was used in Japan mainly on small plots and for measurement of sheet erosion only. Swanson replied that University of Washington and U. S. Forest Service scientists also measured rill and gully cross-sections along lines of erosion pins crossing hillslopes. At Mount St. Helens these lines of pins were located along contour lines at various positions extending from near the ridge line to the valley floor, so it was possible to estimate sediment production by sheet and rill erosion from large hillslope areas of different gradients and lengths.

Tsukamoto also suggested that landslide erosion will peak about 10 years after trees were killed in the 1980 eruption, because that will be the time of minimum root strength. Residual roots will have decayed substantially and roots of invading vegetation will not yet be well developed in many areas of the blast zone. (The paper by Swanson, Collins, Dunne, and Wicherski in this Symposium provides additional discussion and data on this subject. They report that a large component of tree root strength was lost immediately when the lateral blast uprooted trees. Consequently, the period of major landsliding may occur earlier than it would if root decomposition alone determined the timing of changes in root strength.)

The discussion pointed out that the sediment control problems at Mount St. Helens are substantially greater than those usually dealt with in Japan. However, the differences in scale are not as striking as the similarities in process. This discussion period provided a chance for important exchange of information and many additional topics could have been profitably discussed. The extensive experience of Japanese erosion control specialists working in volcanic areas was very valuable to U. S. scientists beginning to deal with erosion problems at Mount St. Helens.

It was reassuring for U. S. scientists to hear the Japanese delegation comment on the extensive and difficult nature of erosion problems at Mount St. Helens.

We look forward to future good cooperation.

References Cited

Lehre, A. K., B. Collins, and T. Dunne. 1982. Preliminary post-eruption sediment budget for the North Fork Toutle River drainage, June 1980 - May 1981. In Proc. Mount St. Helens: Effects on Water Resources. Washington State Univ. Press, Pullman, Wash., p. 215-234.

Daido, A. 1975. On the estimation for sediment yield in the Pemali and Comal Rivers: Memoirs of the Research Institute of Science and Engineering, no. 29, p. 50-72.

Reported by:

F. J. Swanson
R. J. Janda

(Appendix) List of the Symposium Participants

NAME	AFFILIATION AND MAILING ADDRESS	SPECIFIC FIELD OF INTEREST
Amada, Takaaki	Department Faculty of Agricultural Engineering University of Tsukuba Tsukuba Science City Ibarakipref JAPAN	Lahars, Volcanic mudflows and other valcanic disasters
Anyoji, Nobuo	Sabo Technical Center 3-4, Ichigaya-Sadohara cho. Shinjuku-ku, Tokyo 162 JAPAN	Erosion control planning
Araya, Tohru	Hokkaido University Kita-9, Nishi-9, Kitaku Sapporo Hokkaido Prefecture JAPAN	Erosion control (debris) Channel and forest change
Bradley, Jeff	U.S. Army Corps of Engineers Portland District P.O. Box 2946 Portland, OR 97208	Channel sedimentation
Chen, Cheng-lung	U.S. Geological Survey Gulf Coast Hydroscience Center NSTL Station, Miss. 39529	Fluvial processes and river mechanics, especiall mudflow mechanics
Collins, Brian	Department of Geological Sciences University of Washington Seattle, WA 98195	Hillslope and fluvial processes
Daido, Atsuyuki	613 Yodoshimozu Fushimiku, Kyoto, JAPAN	Debris flows
Do, Shoichi	Kokusai Kogyo Co. Ltd. 3-8, Komeicho, Takarazuka JAPAN	Geomorphology and erosion control
Dunne, Tom	Department of Geological Sciences University of Washington Seattle. WA 98195	Sediment budgets and debris flows.
Fairchild, Lee	Department of Geological Sciences University of Washington Seattle, Washington 98195	Debris flow mechanics

NAME	AFFILIATION AND MAILING ADDRESS	SPECIFIC FIELD OF INTEREST
Gallinatti, John	Department of Geological Sciences University of Washington Seattle, Washington 98195	Channel morphology
Glicken, Harry	Department of Geological Sciences University of California Santa Barbara, CA 93106	Geology of volcanic deposits
Hirano, Masashige	Quaternary Research Center University of Washington Seattle, Washington 98195 Department of Geography Osaka City University Sumiyoshi-ku, Osaka, JAPAN	Mathematical modelling of slope development
Iida, Osamu	Department of Agriculture University of Nagoya Nagoya, JAPAN	Soil and Water conservation
Ikeya, Hiroshi	Sabo Dept. of Ministry of Construction Kasumigaseki 2-1-3, Chiyoda-ku Tokyo JAPAN 100	Debris flows and mudflow dynamics
Janda, Richard	U.S. Geological Swrvey 5400 McArthur Boulevard Vancouver, WA 98661	
Juvigné, Etienne	Quaternary Research Center University of Washington AK-60 Seattle, WA 98195	Tephrostratigraphy
Kataoka, Jun	Department Forestry Faculty of Agriculture, Soil and Water Conservation Nagoya City Furocho-Chikusa-ku, 464	Soil and water conservation
Kobayashi, Fukuzo	Azatsu University 1-1-4 Kamishida, Kofu City 400 Yamanashi Pref. JAPAN	Weathering geology
Lisle, Tom	U.S. Forest Service 1700 Bayview Dr. Arcata, CA 95521	Post-eruption channel change

NAME	AFFILIATION AND MAILING ADDRESS	SPECIFIC FIELD OF INTEREST
Martinson, Holly	U.S. Geological Survey 5400 MacArthur Blvd. Vancouver, WA 98661	Fluvial and hillslope processes and geo-morphology
Meyer, David	U.S. Geological Survey 5400 MacArthur Vancouver, WA 98661	Unstable channels and channel pattern
Mills, Hugh H.	Box 5062, Tennessee Tech. Cookeville, TN 38501	Debris flows
Mizuyama, Takahisa	Research Engineer Sabo Division Public Works Research Institute Ministry of Construction Tsukuba Science City Ibaraki Pref., 305 JAPAN	Sediment transport in steep channels incl. debris flows, channel morphology & erosion control engineering
Nagaoka, Shinji	ASIA AIR Survey Co., Ltd. 13 Nurumizu Atsugi-City Kanagawa JAPAN	Aerial survey
Nakasuji, Akito	Kokusai Kogyo Co.; LTD. 4-2, Kitaku, Sapporo Hokkaido, JAPAN	Lahars, Volcanics, Mudflows and other volcanic disasters
Newhall, Chris	U.S. Geological Survey 5400 MacArthur Blvd. Vancouver, WA 98661	Eruption hazards, pyroclastic flows
Nolan, Mike	U.S. Geological Survey 345 Middlefield Rd. Menlo Park, CA 94025	Channel dynamics
Ohira, Masahito	Aomori Prefectural government Sabo Section Nagachima H-1 Aomori 030 JAPAN	
Omura, Hiroshi	Department of Agriculture University of Shizuoka Ohya 836, Shizuoka City JAPAN	Landslides; Fence effect of forest against debris flow

NAME	AFFILIATION AND MAILING ADDRESS	SPECIFIC FIELD OF INTEREST
Ono, Shigeru	Asia Air Survey Co. LTD. 2-16, Tsurumaki 5 Setagaya-ku, Tokyo JAPAN	Erosion control Forest protection (Soil conservation)
Onodera, Hiromichi	Department of Africulture Hokkaido University Sapporo, JAPAN	Mass-movement and snow avalanche erosion
Pierson, Tom	U.S. Geological Survey Cascades Volcano Observatory 5400 MacArthur Blvd. Vancouver, WA 98661	Dynamics of mudflows/ debris flows, landslides
Reid, Leslie	Department of Geological Sciences University of Washington Seattle, WA 98195	Sediment budgets, sediment transport processes on hillslopes
Roseth, Bob	University of Washington Graduate School, AG-10	General
Shimokawa, Etsuro	1140 Kamoike-cho Kagoshima-shi, 890 JAPAN	Slopes failure
Shipley, Susan	Quaternary Research Center University of Washington Seattle, WA 98195	Tephrostratigraphy
Slaymaker, Olav	Department of Geography University of British Columbia Vancouver, V6P 5S8 CANADA	Sediment sources and yields in mountains
Smith, Rick	Department of Geology Oregon State University Corvallis, Oregon 97331	Sediment movement and routing on hillslopes and in channels
Stockton, Steven L.	U.S. Army Corps of Engineers Prot and District P.O. Box 2946 Portland, OR 97208	Sediment stabilization

NAME	AFFILIATION AND MAILING ADDRESS	SPECIFIC FIELD OF INTEREST
Swanson, F.	U.S. Forest Service 3200 Jefferson Way Corvallis, Oregon	
Sweet, Randy	Box 328 Kelso, WN 98626	Fluvial geomorphology, water quality, Basin Management
Takei, Aritsune	Dept. Forestry, Faculty of Africulture Kyoto University Kitashirakaw, Sakyo-ku Kyoto 603	Debris flows and Land slides. Planning of countermeasures
Tanaka, Kiyoshi	Japan Conservation Engineers Co. Ltd. 30-7 Sihome Minato-ku Tokyo, JAPAN	Erosion control planning
Tanaka, Takafumi	Dept. of Forestry Nagoya University Furocho-chikusaku Nagoya 464 JAPAN	Landslides, Soil physics
Tsukamoto, Yoshinori		
Tubbs, Don	GeoEngineers, Inc. 2020 124th Ave. NE P.O. Box 6325 Bellevue, WA 98007	Landslides, engineering geology
Voight, Barry	333 Deike Bldg. Penn State University University Park, PA 16802	Mass slides and flows
Wigmosta, Mark	Department of Geological Sciences University of Washington Seattle, WA 98195	Mudflow dynamics
Winjum, Jack K.	Weyerhaeuser Co. P.O. Box 420 Centralia, WA 98531	Forest rehabilitation

PROCEEDINGS OF THE SIMPOSIUM ON EROSION CONTROL IN VOLCANIC AREAS

PWRI TECHNICAL MEMORANDUM
No. 1908
Feb. 1983
Public Works Research Institute

Key Words:
Debris Flow, Volcanoes, Mt. St. Helens,

Synopsis:
This publication contains the papers and discussions presented at the US-Japan Symposium on Erosion Control in Volcanic Areas, held at Seattle and Vancouver, Washington USA, on July 6–9, 1982.

郵 便 は が き

Postage stamp

3 0 5 – □ □

茨城県筑波郡豊里町旭１番地
建設省土木研究所砂防研究室

Phone 0298-64-2211
Sabo (Erosion Control) Division
Erosion Control Department
Public Works Research Institute
Ministry of Construction, Government of Japan
Tsukuba Science City
Ibaraki Prefecture, 305
JAPAN

No.

No.

配布先氏名

配布先住所

I received copy(ies) of

PWRI technical memorandum No. 1908

Address:

Name _____